AE3200 Design Synthesis Exercise

Delft University of Technology

Preliminary Design
BirdPlane

Team:
J.S. van der Burgt
K.J.M. Hameeteman
J. Harms
S.H. Lee
I.A. Mkhoyan
D. Risseeuw
W.J. Schoneveld
B. Telgen,
N.A. Voogt
W. Westbroek

Supervisors:
Dr. S.J. Garcia Espallargas
Dr. ir. H.G. Visser
Dr. G.C.H.E. de Croon

TU Delft

BirdPlane

"The desire to fly is an idea handed down to us by our ancestors, who—in their grueling travels across trackless lands in prehistoric times—looked enviously on the birds soaring freely through space at full speed, above all obstacles, on the infinite highway of the air."

Wilbur Wright (1867-1912)

PREFACE

The *Design Synthesis Exercise* (DSE) is the concluding project of the Bachelor Aerospace Engineering at the DELFT UNIVERSITY OF TECHNOLOGY. With a group of 10 students, we have worked on the very challenging *BirdPlane* project. In just over 2 months, we have created a preliminary design of a unique flapping wing aircraft that can fly alongside real geese in order to get more insight in the wonders and beauty of bird flight. With the goal of having a range of over a hundred kilometers, the mission range goes beyond the capabilities of any existing ornithopter design. The project pushed us beyond the limits of our aerospace knowledge and forced us to think outside the box. This report is the result of 10 weeks of hard work and marks the last and final milestone of the *BirdPlane* project.

The purpose of this report is to give the reader an overview of the project and a look into the preliminary design stage of *BirdPlane*. The report is meant to be a standalone document. However, for detailed reasoning and explanation of the design choices, the reader is asked to refer to the previous reports of the project. The concurrent systems design process requires many interrelations between the subsystems and can not be presented entirely chronologically, which is also reflected in the report. The report offers guidance with references where needed.

We would like to express our sincere gratitude and regards to Dr. S.J. (Santiago) Garcia Espallargas, the project tutor, for bringing the *BirdPlane* project to existence and the extensive amount of feedback given during the design process. We thank Dr. ir. H.G. (Dries) Visser for showing enthusiasm about the project and identifying legitimate concerns relating to the mission and technical aspects which allowed us to get a solid design. Thanks also to Dr. G.C.H.E. (Guido) de Croon for offering comprehensive advice in the design process of the electronic subsystems and encouraging us to use a high level of artificial intelligence in the design.

Recognition also goes out to Thomas Lameris, PhD. candidate on the topic of migration timing of Arctic breeding Barnacle Geese at Netherlands Institute of Ecology, for giving insight in the goose researcher needs, his project and providing us with possible research goals for the first mission of *BirdPlane*. Lastly, our special thanks are given to Nico Nijenhuis, Co-founder & CEO of Clear Flight Solutions, for his inspirational guest lecture on our request. We are grateful for the discussions and insight into his products, allowing us to learn directly from successful flapping bird prototypes.

We want to invite the reader to follow our foot steps in the preliminary design process of *BirdPlane*. Sit back and enjoy our report that is meant to be easily accessible. Questions or recommendations are very welcome and can be sent to *info@birdplane.nl*.

CONTENTS

List of Figures

List of Tables

List of Symbols

Arabic

A	Amplitude	[m]
A	Availability	[-]
A_f	Angle scaling factor	[-]
AR	Aspect ratio	[-]
b	Wingspan	[m]
$\bar{c}$	Mean aerodynamic chord	[m]
c_Γ	Flight phase constant	[-]
C	Cost	[euro]
C_a	Overall lift force coefficient	[-]
C_{l_β}	Roll stability due to sideslip	[rad^{-1}]
C_{n_β}	Yaw stability due to sideslip	[rad^{-1}]
C_D	Drag coefficient	[-]
C_{D_0}	Drag coefficient at zero lift	[-]
C_L	Lift coefficient	[-]
C_M	Moment coefficient	[-]
C_T	Thrust coefficient	[-]
C_{Y_β}	Sideforce coefficient	[rad−1]
D	Diameter	[m]
D	Drag force	[N]
e	Oswald factor	[-]
E	Endurance	[min]
f	Frequency	[Hz]
g	Gravitational acceleration	[m/s^2]
G_r	Gear ratio	[-]
h	Altitude	[m]
I	Current	[A]
I	Moment of inertia	[kg m^2]
k_v	Speed constant	[rpm/V]
k_{Γ_N}	Scaling factor	[-]
K	Gain	[-]
K	Spring constant	[N/m]
l	Length	[m]
L	Lift force	[N]
m	Mass	[kg]
M	Gear module	[m]
M	Moment	[Nm]
M	Maintainability	[-]
MTBF	Mean time between failure	[hr]
MTTR	Mean time to repair	[hr]
N	Number of gear teeth	[-]
P	Power	[W]
r	Yaw rate	[rad/s]
$r_{u/d}$	Up- and downstroke ratio	[-]
R	Reliability	[-]
R	Resistance	[Ohm]
R	Turning radius	[m]
s	Half wing span	[m]
S	Planform area	[m^2]
S	Safety	[-]
t	Time	[s]
T	Thrust	[N]
T	Period	[s]
V	Velocity	[m/s]
V_1	Upstroke velocity	[m/s]
V_2	Downstroke velocity	[m/s]
V_{fw}	Forward velocity	[m/s]
W	Weight	[N]
x	Distance in x-direction	[m]
y	Distance in y-direction	[m]
y_Γ	Jones factor	[-]
Y	Sideforce	[N]
z	Distance in z-direction	[m]

Greek

α	Angle of attack	[deg]
β	Sideslip angle	[deg]
Γ	Circulation	[m^2/s]
Γ	Dihedral angle	[deg]
δ	Deflection angle	[deg]
η	Efficiency	[-]
θ	Span-wise twist angle	[deg]
λ	Failure rate	[1/hr]
Λ	Wing sweep angle	[deg]
ξ	Flap angle	[deg]
ρ	Air density	[kg/m^3]
τ	Torque	[Nm]
ϕ	Roll angle	[deg]
Φ	Phase difference	[deg]
ω	frequency	[Hz]
ω	angular velocity	[rad/s]

1 Summary

This report concludes the *BirdPlane* DSE project. It has been preceded by the Project Plan, Baseline Report and Mid-Term Report. The activities of the preliminary design phase are discussed and the result is presented and evaluated. The final mission need statement of *BirdPlane* is defined as follows:

The *BirdPlane* mission is to autonomously follow and study a migrating Barnacle Goose flock with a remotely controllable, bird-inspired flapping wing aircraft.

From this, a detailed analysis of the mission is derived. *BirdPlane* should be able to cruise for 100 min at 18 m/s while doing measurements of several defined study goals. These goals and required sensors and electronics have been established. The *BirdPlane* mission consists of three segments: the aircraft itself, a portable ground station and the base in Delft.

For the mission profile, five stages have been specified: standby, take-off, rendezvous, in-flock and landing. The necessary functions and requirements for each phase are defined and presented in functional flow diagrams. To get a clearer picture of the different flight phases and the interaction between the ground equipment and *BirdPlane*, a software prototype has been developed to simulate the *BirdPlane* mission profile. An outline of the simulation framework is given and features are explained in this report.

A detailed analysis of flapping wing aerodynamics resulted in a set of required parameters for the flapping motion. The optimal combination of flapping angle, wing twist, wing folding and speed of the up- and downstroke motions were obtained. The required control surfaces are discussed and it has been shown that *BirdPlane* is lateral and longitudinal stable.

Subsequently, mechanisms were designed such that they could provide the control and motions required for the different flight modes. Speed and climb rate are controlled by directly changing the RPM of the electric motor, thus changing the flap frequency, and by changing the wing twist, actuated by a servo. The tail is actuated by three servos for pitch, roll and fanning to change the tail surface area. A simple but very efficient spring mechanism is designed in the form of a goose neck to stabilize the camera that is mounted in the front, such that the rapid oscillation due to the wing flapping is damped.

The wings will be driven by a Hacker A20-12 XL EVO electromotor, powered by a 217 Wh, 435 g Li-S battery. The communication systems is designed for continuous contact during take-off, rendezvous and landing, while in the flock *BirdPlane* will fly autonomously. The communication link is established utilizing a combination of ground antenna and cellular network. Precision in-flight bird tracking is realized with help of a stereoscopic thermal camera setup. The autopilot is constantly fed with information from environment and attitude and controls *BirdPlane* autonomously. New inner control loops were developed to account for the unique flight dynamics. All systems are combined in the embedded system with help of the Lisa /M board.

The final preliminary design is the result of an iterative process in which theoretical optimizations had to be realized in practice. The mass and power budget have been updated continuously throughout this process. In the performance analysis, it was evaluated whether lift generated equaled the mass and mean power required during the mission matched the available power and energy. The relatively complex flapping mechanism increased the weight, but thanks to the high wing flapping efficiency, the battery mass could be reduced. The result is a *BirdPlane* aircraft with a mass of 1.4 kg and a mean power of 130 W for a mission of 100 min, with electronics on board for communication, (auto)control and scientific measurements and data storage, by which it complies with all requirements.

The results of the preliminary design phase have to be worked out in a detailed design before it can be built according to the Manufacturing, Assembly and Integration plan. Future versions of *BirdPlane* can be improved by integrating techniques that were considered too far-fetched for this design, and implementing more features or improve flight capabilities.

2 Introduction

More than a few great minds of the past have been intrigued by the way birds maneuver their wings along apparent airflows in order to dynamically change their position. The several attempts of mimicking the seemingly infinite motions which these avian species have incorporated within their wing mechanisms, have unfortunately proven unfeasible for the current state-of-the-art. Therefore, the well-known fixed wing aircraft are the primary kind which have been adapted to fulfill operational standards. Current developments in manufacturing and operational techniques however prove to be promising for the creation of a sustainable bird-like UAV, which is not only operating with a dynamic wing design but also nears the performances reached by real birds. More recent designs of aircraft that incorporate bird-like aerodynamics have shown that it is possible to not only design, but also operate a dynamic wing UAV. Excellent examples for the latter are the Festo Smartbird and the RoBird designed by Clear Flight Solutions. Nevertheless, none of the current designs have been capable of performing sustained flight over a range of more than a few kilometers due to their endurance of only several minutes.

The current mission proposed to the design team of *BirdPlane* is aimed to go again one step further than any earlier designed ornithopter. This described mission is to create a flapping wing UAV capable of performing a sustained flight within an actual flock of geese for over a hundred kilometers. For approximately ten weeks, continuously more detailed analyses and designs have been performed in order to meet the mission requirements and technically desired performances. In the scope of this time-period, a full aerodynamic model capable of analyzing the apparent dynamic wing model has lead to a wing design capable of operating within the bounds predefined by the customer. Primarily due to the ongoing iterations between possible mechanical systems and possible aerodynamic force generations, the final *BirdPlane* system has been realized.

From the final conceptual design, provided in the *Midterm Report* [1], all the individual sub-system designs were worked out in detail. The results show that according to the pre-operational investigations *BirdPlane* will perform on the level of the predefined mission specifications. The function of this *Final Report* therefore is to provide all the additional research and physical investigations which have been performed in order to elaborate on the conceptual design, generating the final design of *BirdPlane*. This report contains the preliminary designs related to the wing mechanisms and aerodynamic performances, creating a specific set of finally required wing motions comparable to the capabilities of the birds. Also all the electronics required to design and operate *BirdPlane* are presented. An entire mission simulation software program is created enabling the general public to foresee what the mission consists of and how exactly *BirdPlane* performs within it.

The structure of this report is as follows: from this introduction first the Project Synopsis is given in Chapter 3 which provides a brief overview of the objectives of the opposed mission and team structuring. Then, the requirements for each aspect of the *BirdPlane* system are identified in Chapter 4. By providing what is specifically expected from the requirements, the mission analysis is built in Chapter 5. Consequently, the fully known mission profile is realized within the software tool indicated in Chapter 6. What follows are the listing of expectations related to final market. By knowing the precise mission capabilities, *BirdPlane* is expected to lie within the current and future market indicated in Chapter 7. Prior to the treating of the conceptual and preliminary designs, the systems design is indicated in Chapter 8. Since at this stage all design constraints and leading requirements are set, the designs are set within bounds for the more elaborated designs in subsequent Chapter 9 and Chapter 10. Knowing what the final investigations have led to, the Chapter 11 provides the overall evaluation of the final design compared to the prescribed (stakeholder) requirements. Then, after the mission and system risks are analyzed in Chapter 12, the expected follow-up of future operations are prescribed in Chapter 13. Finally, the report ends with a conclusion and future recommendations in Chapter 14 and Chapter 15.

3 Project Synopsis

The purpose of this chapter is to give a quick overview of the DSE project and the background of the report. A more detailed look into the project planning can be found in previous reports of the *BirdPlane* project. First, the objective of the project will be given, followed by a brief look into the project outline. Finally, a summary of the project organization is given.

3.1 Objective

The *Design Synthesis Exercise* (DSE) is the final and closing project of the bachelor *Aerospace Engineering* at the Delft University of Technology. For this project, students are required to make a design in the field of aviation, space, earth observation, wind energy or another field closely related to aerospace engineering.

This design project provides students an opportunity to obtain design experience. It covers a complete design process, from creating a set of requirements and selecting a suitable concept to the presentation of a preliminary design. This is all done in a structured and iterative manner. The team experiences the difficulty of making well-motivated design choices and taking conflicting demands into account. They must demonstrate the basic knowledge and skills necessary to accomplish a successful preliminary design of an aerospace system.

BirdPlane is a DSE project performed by a group of 10 students. The main objective of the project is to design a bird-like plane to study the in-flight behavior of birds, a task many researchers are struggling with. Other objectives are to enhance skills in designing, communication and applying knowledge.

3.2 Outline

The DSE is performed in a time frame of 10 weeks. An engineering approach is taken for the project, where the design activities are divided over several milestones (Figure 3.1). Each milestone is met with a result, which is presented to the customer in the form of a report and review session. What follows next is a short summary of the activities performed in each phase.

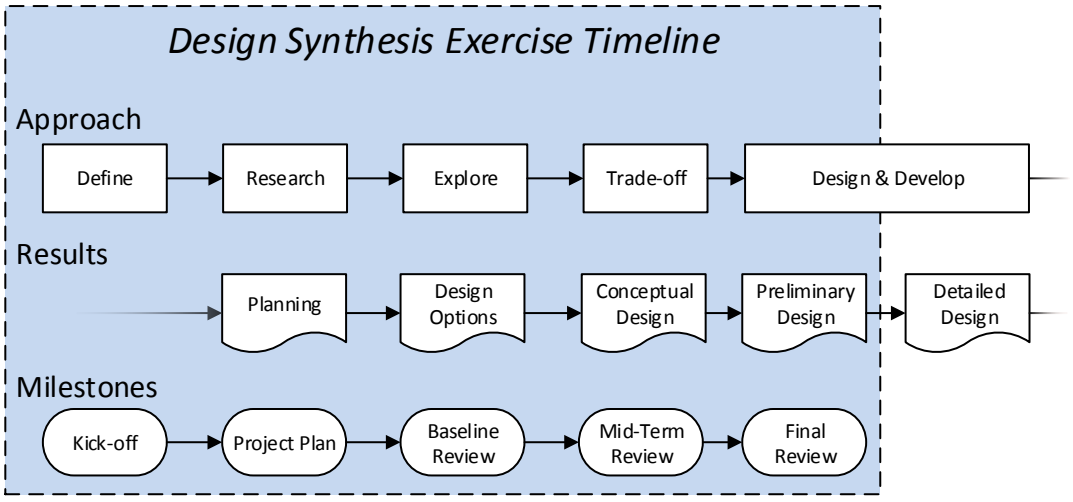

Figure 3.1: Project outline

During the first phase of project the assignment was presented and the kick-off milestone was set. The team focused on defining the *BirdPlane* mission and the planning of the project. Preliminary research was performed in order to come up with a work flow diagram and a sustainable development approach. The result of this phase was the *project plan*.

The second phase was focused on more extensive research and the exploration of different design options. The *BirdPlane* mission was analyzed as well as the functional flow. An initial draft of the requirement specification was set up and five conceptual configurations were created. Additionally, a detailed technical risk analysis was established.

In the third phase of the project, previous work was reiterated and refined. A market analysis was performed and a system definition was given. The electronic system concept was presented and a trade-off between different control strategies was performed. Each of the conceptual configurations has been explored into detail and from a trade-off emerged a conceptual design, which was then presented in the mid-term review.

This report is the result of the final phase of the *BirdPlane* project. In the following chapters, all the work to get to the preliminary design, and eventually the design itself, will be presented . Furthermore, the design will be evaluated based on the performance and compliance to the requirements set within the previous mission analysis and stakeholder communications. Finally, post-DSE activities will be described.

3.3 ORGANIZATION

The integrated engineering design process requires a detailed organizational planning. Ten team members are working concurrently on the *BirdPlane* project, which is why clearly defined responsibilities are essential to avoid conflicts or double work in the collaboration. The *Project Plan* defined a project organogram, in which the organizational structure was defined. Table 3.1 presents a summary of the project organization.

Table 3.1: Project organization

TEAM MEMBER	MANAGERIAL FUNCTION	TECHNICAL FUNCTION
W.J. Schoneveld	Project manager	Mission engineer
D. Risseeuw	Chairman	Propulsion engineer
J.S. van der Burgt	Secretary	Production engineer
B. Telgen	External communications	Electrical engineer
I.A. Mkhoyan	Knowledge manager	Materials engineer
S.H. Lee	Quality assurance and control	Power engineer
W. Westbroek	Planning control	Structural engineer
J.G. Harms	Risk manager	Robotics engineer
N.A. Voogt	Systems engineer	Aerodynamics engineer
K.J.M. Hameeteman	Mission manager	Stability & Control engineer

4 ASSIGNMENT

The previous chapter defined the environment in which the *BirdPlane* is designed, which gives an idea of the level of detail that could be expected from this work. Next it is important to access the scope of the assignment, which is given in this chapter. It gives a global overview of the assignment and the research required to define the *BirdPlane* mission. This chapter has been included into the report for completeness. Readers familiar with the project may decide to skip this chapter, since the content is very comparable to that of the *Midterm Report* [1].

4.1 OVERVIEW

First an overview of the structure of this chapter will be given as to keep clear track of the way this report is constructed. A brief look into the background of the project will be given first. The customer provided requirements are discussed next. Finally, the section ends with a definition of the mission need statement.

4.1.1 BACKGROUND

Birds take-off and land by themselves. They gain lift and thrust by flapping their wings. Constantly changing the shape of their wings and airfoil they increase lift and decrease drag, thereby improving the flight efficiency. Specifically Barnacle Geese, tend to fly in specific formations when migrating whilst searching for air temperature differences.

The customer has expressed a desire for a bird-like UAV to study Barnacle Geese flight behavior. More specifically, the aircraft should be designed with as many bird-inspired concepts as possible and necessary in order to follow a flock of Barnacle Geese migrating across The Netherlands.

Current aircraft are designed following the track of the very first successful airplanes. Every once in a while, a new promising concept arrives as a result of out-of-the-box ideas and multi-disciplinary work. The new aircraft, *BirdPlane*, should make use of the lessons learned from bird flight as well as the advantage of new material developments. *BirdPlane* will be used to study bird flight as never before, flying along with a real flock of geese.

4.1.2 REQUIREMENTS

A list of requirements was provided by the customer. These top level requirements are very important because they mostly determine the constraints and boundaries of the design. The following list gives a short analysis of each of the requirements to identify the impact on the *BirdPlane* mission and discover design limitations. The reader should bear in mind that the following list only gives an interpretation of the requirements, and is not part of the formal set of requirements, which determines the *BirdPlane* design.

- *Unmanned aircraft for daylight operation*: Because of this requirement the *BirdPlane* aircraft will be classified as a *UAV*. *BirdPlane* will require a form of long distance remote control and be capable of autonomous flight.
- *Follow a Barnacle Goose flock from the north to the south of The Netherlands*: This requirement sets the mission of *BirdPlane*. A brief study on Barnacle Geese is done in Section 4.2, in order to formally translate this into a top level requirement.
- *Device should take-off and land with no human help*: The design of self take-off and landing with flapping wing aircraft is almost fully unexplored territory. Few tried-and-true concepts are available, but overall little is known.
- *Detection of bird flock to follow*: Locating a Barnacle Geese flock can be done on the ground or in-flight. To follow the flock, *BirdPlane* should be able to get information on the precise location and exact heading of the flock.

- *Flapping wings*: This requirement is the main design driver. Flapping wing aircraft have been built before, but it is still a new field of research and are highly demanding in terms of aerodynamics and structures.
- *Bird-like aerodynamics with passive and active drag reducing methods*: Birds use a variety of techniques to reduce drag and increase flight efficiency. Passive drag reduction could be materialized with wing feathers. Active drag reduction could be realized with in-flight warping of the wings while flapping.
- *During cruise flight following the flock no propellers can be used*: This requirement puts a constraint on the design options. It does not mean however, that a propeller can not be used during other phases of flight. For cruise, either the aircraft is limited to flapping wings or other propulsion methods have to be considered.
- *Camera incorporated to record flight and send information during whole flight to base in Delft*: An on-board camera will be mounted on the *BirdPlane* to provide visual coverage of the flight. A live camera-feed could be added, but this might require too much of the communication and power budget. Also, *BirdPlane* should send regular flight data to the base in Delft.
- *Non-existing materials can be used as long as they are described based on requirements needed to make the aircraft complete its mission*: This requirement opens up a whole new field of options to look at. Usage of non-existing material will, unfortunately, severely delay the date of product launch.
- *Maximum wingspan 150 cm*: This requirement is a design constraint on the dimensions of *BirdPlane*. The main purpose of this requirement is to give *BirdPlane* similar dimensions as an average Barnacle Goose. Larger wings will generate more lift, but also require a heavier structure. Thus, this requirement is not necessarily a target design value.
- *At least 90% of the structure must be re-usable or recycled at the end of the aircraft service-lifetime*: This requirement will contribute to the sustainability of *BirdPlane*, but will also set constraints on the choice of materials.

4.1.3 STAKEHOLDERS

Before defining the mission need statement, it is important to identify the stakeholders of the project. Table 4.1 gives an overview of the most important parties involved in the development of *BirdPlane*. A more extensive look at the stakeholders can be found in the *Mid-Term Report*.

Table 4.1: *BirdPlane* mission stakeholders

Stakeholder	Description
Scientists	Scientists studying the behavior of bird flight and in particular, Barnacle Goose performance.
Dutch Airspace Management	The party that sets legislations on operations of unmanned aerial vehicles. They are responsible for safe and efficient use of the Dutch airspace.
Bird protection organizations	May be concerned about the well-being of the migrating flocks and the influence of *BirdPlane* following the birds.

4.1.4 NEED STATEMENT

Section 4.1.2 has shown that the mission of *BirdPlane* is mainly defined by the customer in the form of a set of requirements. A mission need statement is a short sentence which gives a better overview of the *BirdPlane* mission. The mission statement of *BirdPlane* is defined as:

The *BirdPlane* mission is to autonomously follow and study a migrating Barnacle Goose flock with a remotely controllable, bird-inspired flapping wing aircraft.

The primary elements of the *BirdPlane* mission can be elaborated as follows:

- *Bird-inspired flapping wing aircraft*: *BirdPlane* will make use of flapping wings to provide lift and thrust. The majority of the design aspects will be based on bird-like flight mechanics and bio-inspired structures.

- *Study a migrating Barnacle Geese flock*: *BirdPlane* will study the flight behavior from a flock of Barnacle geese. Data about the migration path and flight conditions will be gathered in-flight and transmitted back to the base. The study goals are discussed in Section 4.2.2.
- *Remotely controllable flight*: The *BirdPlane* aircraft will be partially controllable from the ground station such that it can safely perform the mission. *BirdPlane* will also incorporate a level of autonomy in the form of an autopilot and in-flight tracking of the birds.

4.2 BARNACLE GOOSE

The first mission of the new *BirdPlane* aircraft is to gain information of the flight of Barnacle Geese migrating through The Netherlands. It is very important to gain insight in the Barnacle Goose itself before further mission analysis can be performed. The next section therefore provides information into the Barnacle Goose characteristics. After that, the *BirdPlane* study goals will be defined.

4.2.1 CHARACTERISTICS

The Barnacle Goose (*Branta Leucopsis*) of the genus *Branta* belongs to the true geese and swan subfamily *Anserinae* [3]. The Barnacle Goose is a medium sized goose easily identified by its black neck and chest. It has a pure white small head, gray striped back and pale belly. The characteristics of Barnacle Goose vary widely between individuals. In the following paragraphs, different features are discussed and average values are given. Figure 4.1 shows a group of Barnacle Geese in The Netherlands.

Figure 4.1: Barnacle Geese in Zeeland, The Netherlands [2]

SIZING

The mass of a Barnacle Goose typically ranges from 1.4 kg to 2.2 kg with an average value of 1.9 kg [4]. The wingspan is often found to be between 1.30 and 1.45 m, averaging at 1.41 m. The length of a Barnacle Goose has a mean value of 0.64 m. The aspect ratio of a typical Barnacle Goose wing planform is 8.13 [5]. The wing area used for calculating the aspect ratio includes the part of the body between the wings, because it attributed to the zone of reduced pressure in normal gliding flight.

POPULATION

Barnacle geese are migratory birds that travel between their breeding and overwintering grounds in the spring and fall [4]. The species consist of three main populations of tens of thousands of birds. Other smaller populations have been identified but these number only in a few thousand.

The *Greenland population* consists of about 45,000 individuals. Their breeding grounds are located in east Greenland. In the winter, they head to Scotland. The *Svalbard population* consists of about 25,000 birds and breed on the (surrounding) islands of Svalbard archipelago. Their wintering grounds are located in the west coast of England. The *Russian population* consists of over 100,000 bodies. They breed in the northwest coast of arctic Russia and Novaya Zemlya. This population winters in western Germany and coastal regions of The Netherlands.

Figure 4.2 shows the typical migration route from the *Russian population*. The shaded area shows the migratory corridor reconstructed from accurate positions and direct observations. Common stopover sites are encircled in the figure. Via the White Sea and the Baltic region the geese fly to The Netherlands and settle in the coastal provinces and Southwest Friesland [6]. The stopover times range from several hours to several days, but the majority of Barnacle Geese migrate from the northern regions to their wintering area within 1-3 days.

Figure 4.2: Positions from satellite tracked Barnacle Goose. [7]

Agonistic behavior has been identified within Barnacle Goose flocks to be ordered according to the number of individuals within social units [8]. Unit size is the best predictor of dominance. Aggressive behavior has only been identified on the ground during grazing and breeding.

FLIGHT

Migrating waterbirds fly at different altitudes depending on the time of day. Typically, these birds fly at a relatively lower altitude over land than over water. During the day, Barnacle Goose fly over West Estonia with a mean altitude of 45 m [9].

Two Barnacle Goose were specifically trained to fly behind an open-topped truck. The normal range of airspeed at which the geese fly is between 16 and 22 m/s [10]. The average cruise velocity is around 18 m/s. The lowest speed the geese will fly is 15 m/s, and peak velocities are around 26 m/s for short periods of time.

Barnacle geese fly, turn and twist as a flock [4]. The flocks are closely packed and have been observed to fly in line- or V-formations. The average wing beat frequency of Barnacle Goose was measured to be around 287 beats per minute. During take-off, the wing beat frequency increased up to 356 bpm [10].

A study has been performed to monitor a group of Barnacle Geese during their migration from Ny-Alesund to Scotland [11]. The results showed a maximum endurance of 14 hours of non-stop flying. The most active bird flew 49 of the total 59 hours without considerable energy intake in terms of food. At beginning of the migration an average Barnacle Goose had an oxygen intake of 300 ml per minute, which corresponds to a metabolic power of approximately 100 W.

SUMMARY

An outline of the discussed parameters is shown in Table 4.2, along with the average values. The values come from different studies and Barnacle Goose populations, so a correlation is not guaranteed. Nevertheless, the values are representative for an average Barnacle Goose.

Table 4.2: Parameters for an average Barnacle Goose

Parameter	**Value**	**Parameter**	**Value**
Mass (m)	1.9 kg	Cruise velocity (V_{cruise})	18 m/s
Length (l)	0.64 m	Cruise altitude (h_{cruise})	45 m
Wingspan (b)	1.41 m	Maximum velocity (V_{max})	26 m/s
Mean chord ($\bar{c}$)	0.173 m	Wing beat frequency (f_w)	4.78 Hz
Wing area (S)	0.245 m^2	Endurance (E)	14 h
Aspect ratio (AR)	8.13 m	Power (P)	100 W

4.2.2 STUDY GOALS

Barnacle Geese are unique animals who have enormous performance during their migration and can sustain flight for a very long time. Especially their migration behavior above The Netherlands is still not fully studied and understood. Detailed studies during the migration wintering were not possible in the past. *BirdPlane* will give new insight in the geese's behavior and performance during this stage of their migration.

In discussion with PhD-candidate Thomas Lameris from University of Wageningen, who is working on the *"migration timing of Arctic breeding Barnacle Geese"*, a number of study goals were defined. A list of the goals is given next. For each study goal, the measurements that the *BirdPlane* should perform are stated in a short description.

SG-1 Barnacle Geese formation patterns. *BirdPlane* should be able to determine the position of individual birds in the flock. With this information, typical formation patterns can be found and flight behavior can be identified.

SG-2 Flight efficiency during Barnacle Geese formation flight compared to free flight. Cyclists ride behind each other to experience reduced drag, in a similar way how birds fly in formations to increase flight efficiency. Measurements of power consumption during and outside formation flying could help determine the amount of power saved. This can be of big interest to commercial aviation since significant fuel savings might be possible.

SG-3 Barnacle Geese social behavior. It is interesting to look at the social behavior in a flying flock. Observations can be made about the leading geese, and the frequency of changing positions within the flock. Camera footage provides this information as well as insight in agonistic behavior. Audio recordings will give an understanding of communication between the birds.

SG-4 Barnacle Goose flight mechanics. The geese use their wings for both lift and propulsion, and depending on the stage of flight different flapping patterns are used. The geese also use other means to control their flight attitude, such as changing the center of gravity with their feet. High quality, in-flight camera footage gives the opportunity to study the flapping motion and flight mechanics in great detail. This footage is in turn directly applicable for further improvement on the final system design and operations.

SG-5 Usage of air-currents and winds. Thermal columns can be used to obtain potential energy. Also flying with tail-wind conditions can be easier to travel large distances compared to head-wind. How the birds utilize the air currents and winds to their advantage can be discovered by measuring the wind vector and vertical speed while flying in the flock.

SG-6 Experimentally lead a flock of Barnacle Geese. *BirdPlane* will try to lead a flock of geese, and test the limits in changing their course. This could be interesting for airports, where bird collisions are a big problem. *BirdPlane* could lead the flock away from dangerous areas. For this, *BirdPlane* should obtain a clear an overview of the positions of the birds to determine if they follow the aircraft.

SG-7 Barnacle Geese migration path. There is little information known about the flight paths of the Barnacle Geese in The Netherlands. During their wintering period, *BirdPlane* will gain insight in the flight path of the geese as well as flight velocities and altitudes.

SG-8 Barnacle Geese reaction to obstacles/events. By measuring flight path and capturing audio and video footage, *BirdPlane* can obtain knowledge of the geese behavior with respect to certain events and obstacles. For example, it can be observed how the geese react to loud sounds and how to adjust their flight path around large towers.

SG-9 Barnacle Geese reaction to weather conditions. Birds are known for their apparent ability to predict the weather. Minute changes in the weather conditions can cause the birds to change their behavior. In order to get more insight, *BirdPlane* will measure general flight conditions such as temperature and pressure. Also humidity, luminance, wind and other weather conditions are measured.

This list sets high demands on the functionality of the *BirdPlane* aircraft. The next chapter will be dedicated to further mission analysis and a definition of the mission profile. Also, a functional flow will be required to perform the study goals presented.

5 Mission Analysis

In Chapter 4, the mission statement and study goals were described. This chapter functions as a follow-up of the initial analysis of the assignment, by translating the given requirements into a mission definition (Section 5.1) and profile (Section 5.2). Finally, in Section 5.3, the functional flow is presented in the form of a diagram.

5.1 Definition

In order to follow the flock, the *BirdPlane* aircraft should be able to fly with a velocity equal to the average of that of the Barnacle Goose. Therefore, the cruise velocity of *BirdPlane* is set to **18 m/s** (Section 4.2.1). Barnacle Geese have a peak velocity of 26 m/s, but cannot sustain this velocity for long periods of time. Nevertheless, *BirdPlane* should be able to accelerate to the same velocity if needed. With this in mind, the maximum velocity is set to **150% of the cruise velocity** and *BirdPlane* should be able to sustain it for at least **10 minutes**.

BirdPlane should be able to fly in formation with the flock. During formation flight, scientific measurements are done in order to achieve the study goals as defined in Section 4.2.2. Table 5.1 gives an overview of the measurements to be performed by *BirdPlane* during this phase.

Table 5.1: Scientific measurements during formation flying

Measurement	Involved study goals
Positions of birds	**SG-1**, **SG-3**, **SG-6**
Power consumption	**SG-2**
Camera footage	**SG-3**, **SG-4**, **SG-8**
Sound recording	**SG-3**, **SG-8**
Flight conditions	**SG-5**, **SG-7**
Weather conditions	**SG-5**, **SG-7**, **SG-9**
Flight path	**SG-7**

From Figure 4.2 it is clear that the Barnacle Geese do not migrate through The Netherlands, but that the northern regions of The Netherlands are merely their destination for wintering. Observant readers will note that Figure 4.1 shows geese in Zeeland, which proves that Barnacle Geese do happen to travel as far south. Usually they stay in the northern parts though and due to design limitations *BirdPlane* will, in the first iteration of the design, focus on this region. Later designs could then explore even higher range missions to cover the whole Netherlands.

In order to be able to follow a geese from North to South of The Netherlands, *BirdPlane* would have to fly an approximate distance of 300 km. With zero wind conditions, the flight time would be a little less than 300 minutes. Rough calculations in the early design stage showed that this endurance leads to unfeasibly high energy demands and as a result, the power source would already weigh more than 2 kg. Because of this, the endurance requirement has to be lowered in order to arrive at acceptable values for the power system. A first estimate was set to **100 minutes**, and iterations have shown this number to be feasible. Without winds, this value would lead to a range of 108 km, which covers a great part of The Netherlands.

With the specifications set, it is important to get a grip on the equipment required to perform the mission. On a high level, the *BirdPlane* mission equipment consists of three parts; ***BirdPlane***, the aircraft itself, conveniently named after the project; a **portable ground station**, which includes a close range antenna system and a pneumatic catapult for take-off and the **base station**, a fixed location used for research, development, analysis and maintenance. Division of the tasks between these will become apparent in the next section.

5.2 Profile

The mission of *BirdPlane* is to autonomously follow and study a flock of Barnacle Geese (Section 4.1.4). Before *BirdPlane* is flying between the geese, it should take-off and rendezvous with the flock. The geese should

be detected before-hand, such that *BirdPlane* mission can be planned for minimum energy usage during rendezvous. When the optimal time to take-off is reached, the *BirdPlane* will be launched from a pneumatic catapult. During conceptual design iterations such a system was found to be most feasible for this type of mission.

When *BirdPlane* nears the moving flock, it has to be maneuvered in a rendezvous trajectory, ending up inside the flock formation and attaining exactly the same airspeed, heading, altitude, clime rate etc. as the geese. Thereafter *BirdPlane* should stay in the same flock, trailing the animals or changing its position, requiring extremely precise control and adequate response time. Meanwhile all scientific measurements have to be performed and stored. Finally, when *BirdPlane* runs out of power or the mission is aborted, it should land on a suitable location. Because of this, the *BirdPlane* mission is defined as a combination of 5 phases, each with its own challenges and opportunities. Figure 5.1 displays these phases in order of the mission profile.

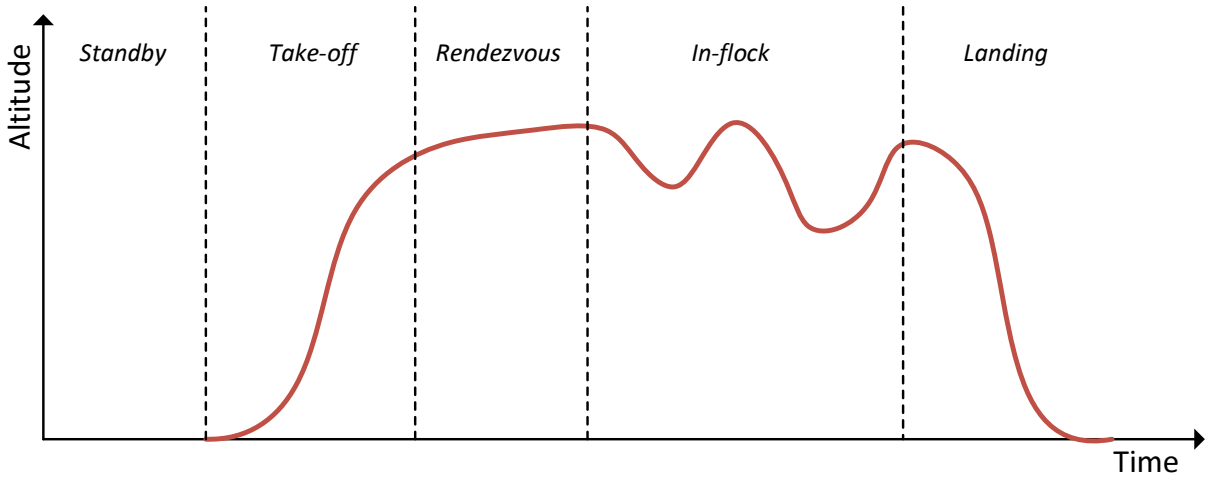

Figure 5.1: *BirdPlane* mission profile

The phases presented in the figure are a result of the high-level division of the mission profile, and each phase may be subdivided into more parts. Each mission phase will be explained in more detail in the following subsections. From the mission profile follows the function flow, which will be addressed in the next section.

5.2.1 STANDBY

The Standby phase spans from the decision a flock might come in range within a certain amount of time until the time to launch. It will be possible to detect flocks of geese all over Europe in the near future (see Section 10.3.4). This allows a *BirdPlane* mission to be planned relatively long beforehand.

Once a flock is expected to cross Dutch airspace, the airspace authorities can be contacted for a flight plan clearance. Depending on the military activities, some airspace restrictions could be lifted for *BirdPlane*. During this phase the trajectory of the flock should be monitored carefully, such that changes in the mission can still be communicated to the authorities in due time.

With the flock approaching and received mission clearance, preparations for take-off can be made:

1. Start-up electronics (autopilot, camera, sensors)
2. Check communication link
3. Check servo and control surface movement
4. Rotate catapult rail against the wind
5. Pressurize pneumatic catapult

5.2.2 TAKE-OFF

The take-off phase starts when the flock is nearing the ideal position for rendezvous. When the airspace in the launch direction of *BirdPlane* is checked for vehicles, the green-light for launch can be given. The catapult

launch will give *BirdPlane* an initial flight speed, from which it is able to climb away. When airborne *BirdPlane* will climb away to 20 meters altitude. At this height *BirdPlane* will change course to the rendezvous trajectory and whilst checking whether the flight behavior matches what is expected from the control input. This is done to ensure no critical parts have been damaged during the catapult launch.

If the launch has been successful the mission can be continued as planned. The *BirdPlane* will continue climbing to a more safe cruise altitude and the rendezvous strategy can be started.

5.2.3 RENDEZVOUS

Once *BirdPlane* has taken off it must find its way to the geese flock. It is desired to have this phase take as little time as possible, but this may not always be the best solution. What follows is a list of trajectory requirements, in order to understand the complexity involved.

- **Power** The *BirdPlane* aircraft should rendezvous with as little power consumption as possible, in order to start the scientific flight phase with maximum energy capacity.
- **Synchronization** *BirdPlane* should arrive at the flock trajectory at the same time as the geese, with the same heading and velocity to ensure a smooth rendezvous.
- **Flexibility** Because of random goose flock behavior, the rendezvous strategy should be flexible and have margins in both directions, that is *BirdPlane* should be able to advance or delay the expected rendezvous time if needed.
- **Awareness** Other factors can influence the rendezvous trajectory such as wind conditions. All these need to be taken into account when defining the strategy.

An appropriate example for existing rendezvous trajectories is the *Parent and Child UAV project* from the MASSACHUSETTS INSTITUTE OF TECHNOLOGY, which uses a very simple trajectory to perform a rendezvous between the parent and child UAV [12]. The parent, a large sized UAV, loiters on a high altitude in a circular motion of fixed radius. The mini sized child UAV receives the position and velocity information of the parent and calculates the optimal rendezvous trajectory. The resulting trajectory consists of very basic geometric shapes, see Figure 5.2. Both UAVs fly with a fixed velocity during the entire phase and the calculated trajectory ensures that the child meets the parent tangentially, about 15 meters behind the parent.

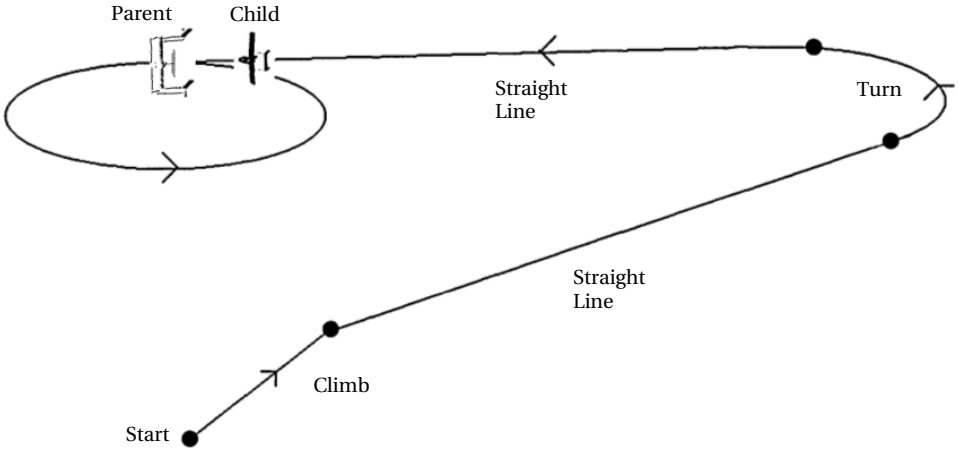

Figure 5.2: UAV rendezvous trajectory

BirdPlane will use a similar strategy in order to rendezvous with the flock. When a flock of geese is detected, its flight path can be extrapolated to a straight line. From basic geometry it follows that the fastest way from the take-off location to this flight path is to fly perpendicular to this line and reach the rendezvous point at the same time as the geese. A schematic representation of this strategy is shown in Figure 5.3.

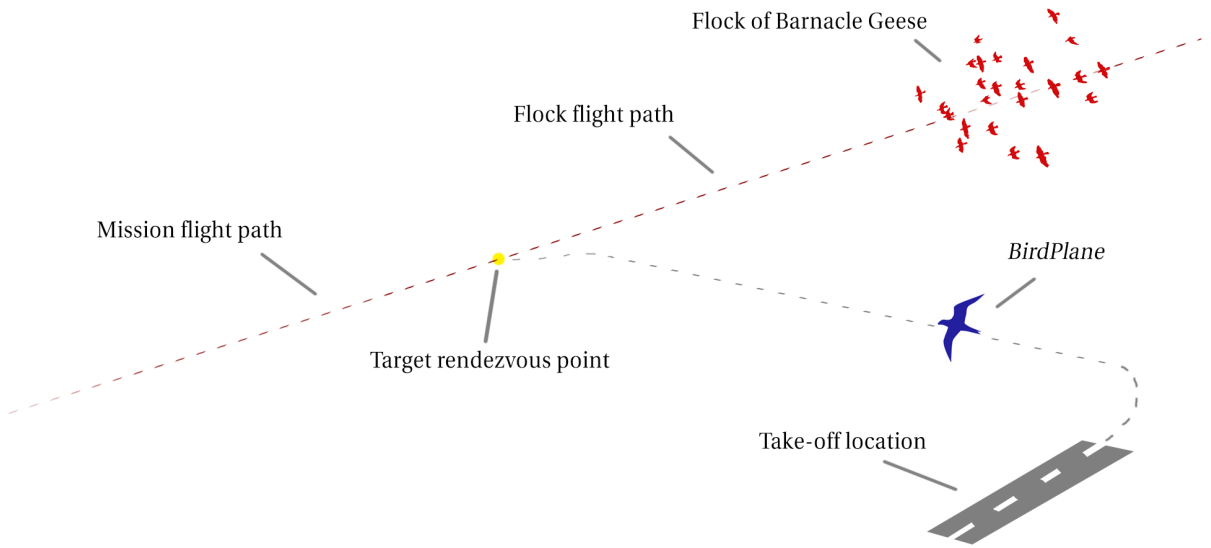

Figure 5.3: *BirdPlane* rendezvous plan

The trajectory can be described with 3 basic shapes. When *BirdPlane* has taken off, it will make a **turn** to set the heading perpendicular to the flight path. Then a **straight** cruise is performed in order to arrive at the rendezvous position with as little power as possible. Right before arriving at the rendezvous, another **turn** is performed in order to synchronize with the flock.

If the flock changes its course the trajectory should be adapted to match the new situation. Throughout the straight cruise the heading can be changed in order to successfully perform the rendezvous with the flock. Also, the target rendezvous point can be shifted forwards or backwards along the geese flight path in order to properly synchronize with the flock. This means that *BirdPlane* will always approach the flock from behind. Should the flock change its direction away from *BirdPlane*'s trajectory, it will need to accelerate to catch up with the flock. If on the other hand the flock happens to steer in the direction of *BirdPlane*, it either needs to slow down or fly an additional turn. *BirdPlane* cannot fly in front of the flock to have it catch up because this would lead to problems when the flock suddenly changes its trajectory or is shy of the alien vehicle.

5.2.4 IN-FLOCK

After the *BirdPlane* has infiltrated the flock, it can start gathering data for the scientific mission. In Table 5.1 the different measurements, required to meet the study goals, are listed. All telemetry sensors will be actively used in this phase.

It will be challenging for the control system to maneuver the *BirdPlane* such that it keeps its relative position in the flock. Especially for the measurements on power consumption, it is required that the *BirdPlane* keeps a certain position to stay in the wake. The ability of the system to follow the semi-random flock movement will be crucial in this phase.

5.2.5 LANDING

When the time has come to end the mission, e.g. due to low battery level, the *BirdPlane* leaves the formation of geese. The system can rely on a database of suitable grass landing sites, ranging from R/C-plane fields to unused agricultural fields, to find a safe landing location. These fields are spaced 10 km apart at maximum. The *BirdPlane* should not only take distance into account, but also the orientation of the field. Landing on private fields will also require the consent of the owner which needs to be obtained beforehand.

When the closest strip with acceptable relative orientation to the wind is found, *BirdPlane* starts cruising towards it. *BirdPlane* will use its GPS-position to perform a glide-in approach, meaning it stops flapping as soon as it is within gliding range. When *BirdPlane* lines up with the strip and has descended below 7.5 m [13] the sonar altimeter will time the commence of the landing flare. The landing maneuver will be done with minimal airspeed to limit the ground impact.

5.3 FUNCTIONAL FLOW

Before the actual design process could start the mission profile needed to be defined which was discussed in the previous section. The functionality that *BirdPlane* needs to provide can be extracted from this profile and the actual study goals. This part of the mission analysis will organize the functions in flow diagrams, one for the whole mission and several smaller ones for each study goal.

5.3.1 MAIN FUNCTIONS

The functional flow diagram depicted in Figure 5.4a is a summary of the functions executed during a typical mission profile. This is a **condensed and updated** version of the one delivered in the **Midterm report** [1].

On a top level the functions required for the *BirdPlane* mission can be divided up between the ground and air segment. As explained in Section 5.2 the mission starts off with *BirdPlane* in stand-by mode. This is not a fundamental function and hence is not mentioned it the flow.

Once a flock of geese is **detected** by the groundstation, the **rendezvous strategy** is calculated and a command is send to **wake** *BirdPlane* out of the stand-by mode. Consequently, *BirdPlane* starts its internal **data and communication loop**, which measures a set of parameters, sends the data to the groundstation, receives data and updates it's mission state. Also it sends a command to the groundstation that *BirdPlane* is **ready** to start the mission.

With the target flock tracked, the groundstation **launches** *BirdPlane* when the rendezvous strategy requests it. The operator on the ground commands *BirdPlane* to **climb** to the rendezvous altitude. During the phase of the rendezvous another loop is executed, **updating the rendezvous** trajectory and leading *BirdPlane* to the new waypoint.

The loop ends when *BirdPlane* is **merged** with the flock, whereupon the switch to **autopilot** is made. At the same instant *BirdPlane* starts to **track** the flock itself. In conjunction with this the main **study loop** is initiated during which the groundstation defines a study goal for *BirdPlane* to performs. Once enough data has been collected or the formation suggests a different study goal could deliver more interesting results the study goal is updated.

At some point the mission ends and *BirdPlane* will determine the closest landingsite and approach it where it will ultimately **descend and land**.

All of the mentioned activities are main functions that *BirdPlane* and the groundstation need to provide in order to cover the mission profile.

5.3.2 STUDY GOAL FUNCTIONS

Each of the study goals further requires their own set of functions. These are on a lower level than the global mission functional flow. Five of the study goals were identified to be actively executed tasks and were analyzed in more detail, the results of which are presented below. Figure 5.4b shows their functional flow diagrams. The **remaining study goals are passively executed** and therefore do not have a functional flow.

As many of the study goals are quite similar, the functions will be shortly summarized.

Formation flight It is required of *BirdPlane* to fly at different position inside the flock which means that it needs to detect the formation and get relative positions of empty spaces inside the flock.

Camera pointing In order to study the flock from different flight positions, the camera needs to be rotatable. Another implication of this is that the pointing vector of the camera with respect to its body frame needs to be known. When trying to lead a flock, the camera will also have to be able to point backwards to observe the reaction of the birds, i.e. whether they follow or not.

Capture & store, audio & video The camera also needs to be able to record and store audio and video data which requires some kind of data storage device.

Measure power consumption In order to study the drag reduction in formation flight, *BirdPlane* needs to be able to measure its power consumption accurately.

The discussed functions are still only the minimum required functions for the *BirdPlane* to succeed. As mentioned above an even more detailed analysis of the functions was provided in the *Midterm report* [1].

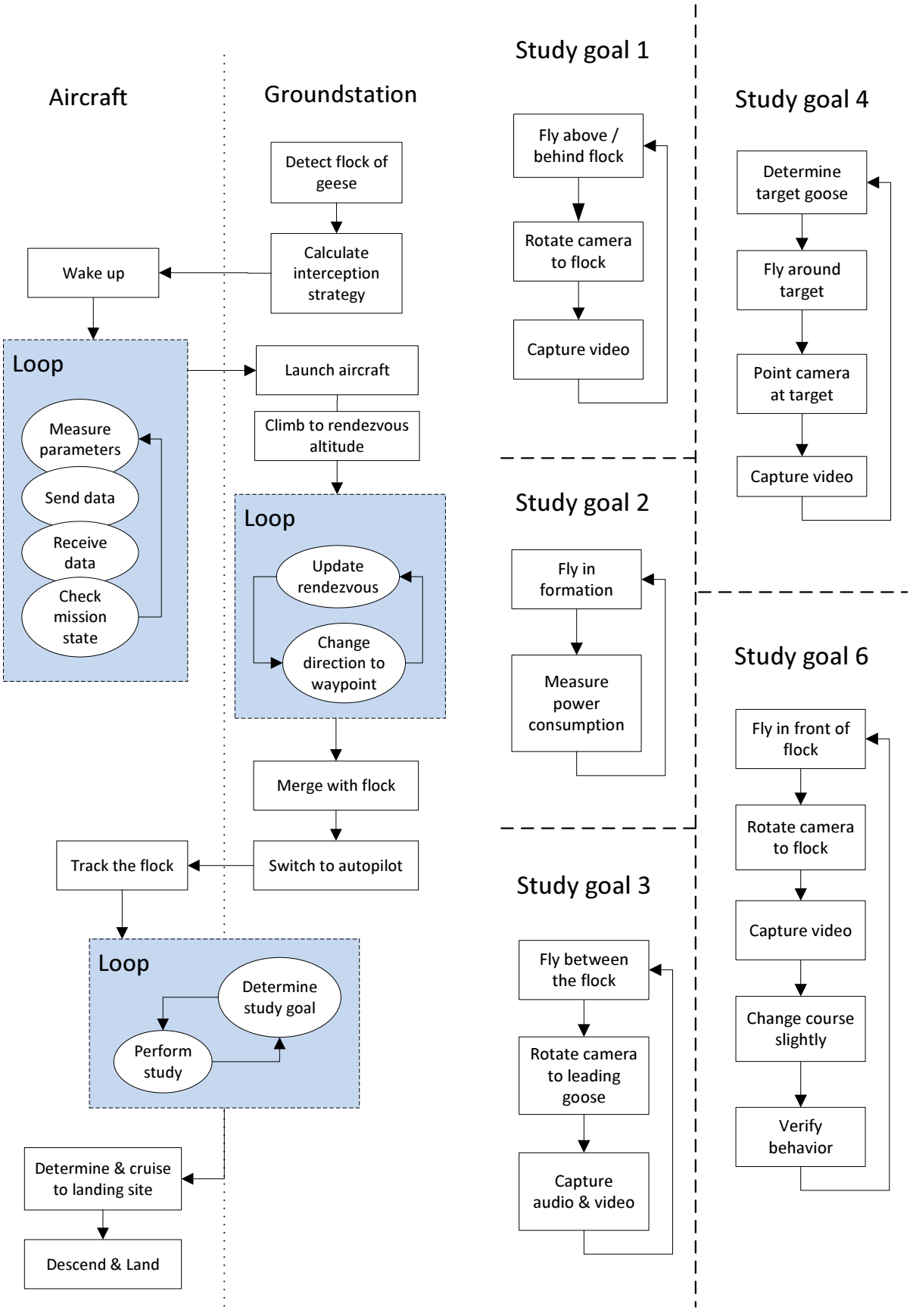

(a) Mission profile

(b) Study goals

Figure 5.4: Functional flow diagrams

6 Mission Simulation

In Chapter 4 an overview of the mission was defined and the requirements were analyzed in more detail. Next the mission was further analyzed in terms of the mission profile and the functional setup of *BirdPlane*. In order to get a clearer picture of the different flight phases and the interaction between ground equipment and *BirdPlane*, a software application has been developed to simulate the *BirdPlane* mission profile.

Due to the limited time that was available for this phase of the project not all the features that were initially intended to be part of the simulation could be implemented. This chapter will give an overview of what parts are completed at this stage and options for the future will be marked as such.

The chapter is divided as follows. First, the intention of the simulation is given in Section 6.1. Section 6.2 presents the simulation framework and discusses the programming. Section 6.3 gives the setup of the simulation mission profile. Following in Section 6.4 is an explanation of the implementation of flock behavior. The map structure and capabilities are discussed in Section 6.5. Finally, in Section 6.6 the results of the preliminary application development are presented and future recommendations are given.

6.1 Intention

The *BirdPlane* mission is not only complicated but also very complex, i.e. there are a lot of factors which can not be controlled, e.g. the Barnacle Goose flock behavior and communication interference. These factors introduce a lot of operational risks in the *BirdPlane* mission and therefore measures have to be taken in order to minimize these risks. This is the purpose of the mission simulation.

Because goose behavior is very unpredictable on a small scale, a mission simulation can help tremendously with event management. Questions that such a simulation could answer are: "What happens when a goose leaves the flock?", "What if the *BirdPlane* experiences loss of communications?" and "What happens when *BirdPlane* has a mid-air collision?". The answer to these questions can be given qualitatively: "*BirdPlane* will return to base." or "*BirdPlane* will land where possible", but exact strategies for these events should be determined in order to guarantee safe and successful operation. Validation with a real prototype is costly and partly impossible. A simulation however is easily adjusted and has no costs which makes operational learning much easier.

It is also a very suitable platform for verification of *BirdPlane* avionics. Different flight strategies can be tested for factors like power consumption and an optimal flock rendezvous trajectory can be determined with ease. Additionally, a fully fledged mission simulation allows continuation of the *BirdPlane* development, tuning and training if actual flight is not possible.

6.2 Framework

It is clear that the simulation can add significant value to the development and operation of *BirdPlane*. Before the actual programming can start, it is important to define a clear framework. This section introduces the simulation world and framework. The time integration method used is discussed next. Finally, the programming language trade-off is performed.

6.2.1 Setup

The simulation has a model of the world containing all objects and entities related to the *BirdPlane* mission. Each entity has a structure with state variables and the system of entities (as a whole) is integrated over time to progress the simulation. A list of the simulation entities is shown in Figure 6.1.

Table 6.1: Simulation world entities

Entity	Description
Ground Station	A static object with a predefined communication range.
BirdPlane	Models the *BirdPlane* aircraft. The most basic form of this entity contains the position, rotation and velocity of the body.
Flock	Contains lists of geese in close proximity of each other.
Goose	An entity representing a single Barnacle Goose with a state vector of position, rotation and velocity.
Landing Site	Another static object representing a feasible landing location.

The simulation is modeled by a single manager containing an overview of all entities in the virtual world. This manager has access to a timer to keep track of the application timing and to update the simulation accordingly. The simulation manager has a camera to give visual insight in the current state of the simulation. Also, an event manager is added to supervise a queue of all events which can then be handled in order.

A detailed street map is used to visualize the mission profile from above and to give a sense of scale. Because the full map of the world is an incredible amount of data, it is impossible to store this data on the disk. The world map is therefore divided into smaller segments which will be downloaded from a remote server while the simulation is running. With the help of multi-threading, this can happen in the background and does not interrupt the simulation. More information about the map can be found in Section 6.5.

In order to display the active simulation to a user, a renderer is created. The renderer is directly linked to the simulation manager and generates images for every object in view. A shader program is then used to display these images to the screen. On top of the simulation view a Graphical User Interface (GUI) is shown, which gives the user information about the current state of the simulation, the *BirdPlane* mission and *BirdPlane* itself.

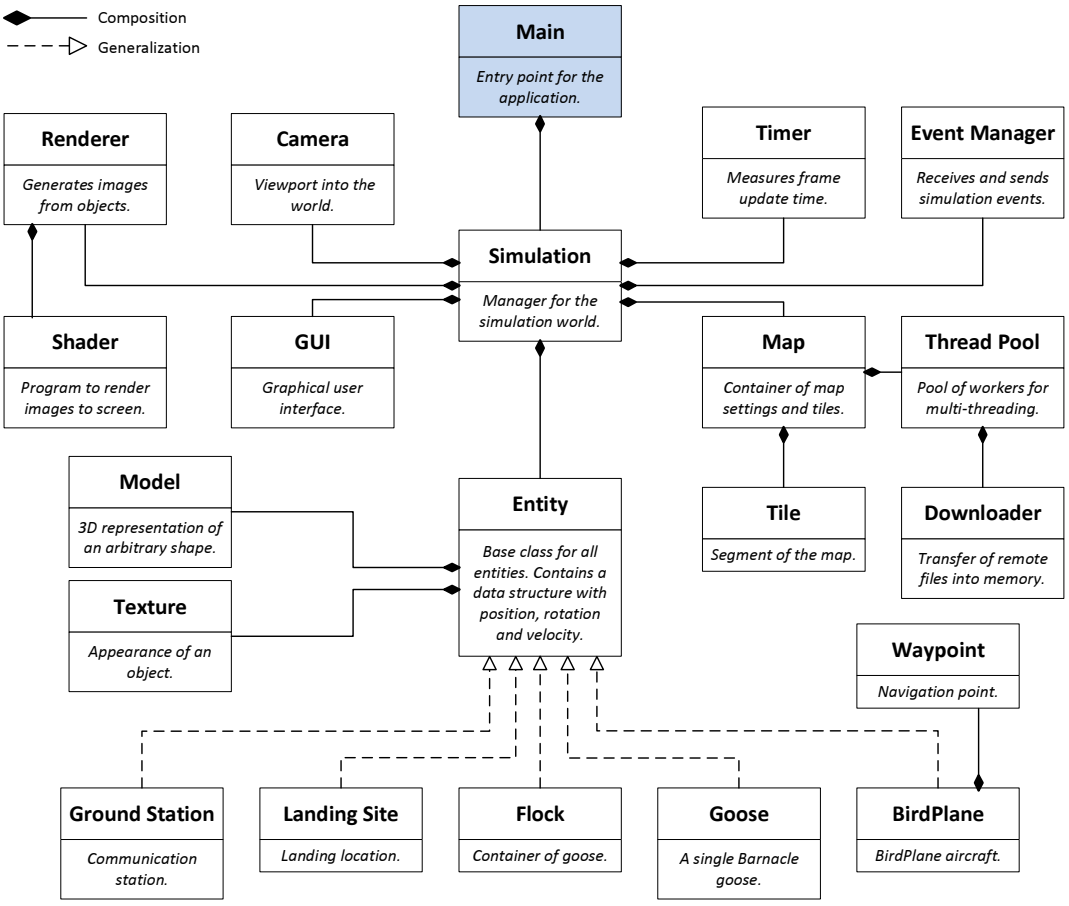

Figure 6.1: Simulation framework as a class diagram

The discussed setup of the framework is shown in more detail in Figure 6.1. Each block represents a class (an element of the simulation) and lines are used to indicate the relationship between the classes. The notation used comes from software engineering, where class diagrams are built using the Unified Modeling Language (UML). Only the basics of UML notation are used in order to keep the framework clear and concise.

Composition is a way to combine simple objects into more complex ones. In the diagram it can be seen that, besides its own data structure, an *Entity* has a model and a texture. On a higher level, the *Simulation* has multiple entities. The *Map* contains a link to a number of distinct tiles, which together make up the map. The generalization relationship indicates that one object (inheriting class) is a special form of the other (base class). The *BirdPlane* class is an entity in its most basic form. The same can be said about the class *Goose*.

6.2.2 TIME INTEGRATION

Many problems in technical sciences can be modeled in the form of ordinary differential equations (ODEs). Bigger problems require more than one equation and can therefore be presented as a system of ODEs. A very common presentation of a system of ODEs is the state space system, as shown in Equation (6.1). In the equation, $\vec{x}$ is the state vector with all state variables. $\vec{u}$ and $\vec{y}$ represent the input and output vector respectively. Matrices A, B, C and D model the system dynamics.

$$\begin{aligned} \dot{\vec{\mathbf{x}}}(t) &= \mathbf{A}(t)\vec{\mathbf{x}}(t) + \mathbf{B}(t)\vec{\mathbf{u}}(t) \\ \vec{\mathbf{y}}(t) &= \mathbf{C}(t)\vec{\mathbf{x}}(t) + \mathbf{D}(t)\vec{\mathbf{u}}(t) \end{aligned} \tag{6.1}$$

In the simulation, each object can have its own state space system which represents the object kinematics. An example is the base *Entity* class with a state vector describing position, rotation and velocity. A future developed version of the *BirdPlane* class, the state space system could describe the full flight dynamics model.

In order to progress the simulation, time integration has to be performed. A very easy method to integrate a system of ODEs is called Forward Euler-Cauchy [14]. The practical application of Forward Euler to a state space system is shown in Equation (6.2).

$$\begin{aligned} \vec{\mathbf{x}}_{i+1} &= \vec{\mathbf{x}}_i + \dot{\vec{\mathbf{x}}}_i \Delta t \\ &= \vec{\mathbf{x}}_i + \mathbf{A}(t_i)\vec{\mathbf{x}}_i \Delta t + \mathbf{B}(t_i)\vec{\mathbf{u}}_i \Delta t \end{aligned} \tag{6.2}$$

In the equation given, $\vec{x}_i$ is the system state at time step t_i and Δt is the magnitude of the time step. The Forward Euler method has a global discretization error of order $\mathcal{O}(\Delta t)$. This means that with a smaller time step, the magnitude of the error reduces with the same rate. More concrete, if the magnitude of the time step is halved, the error is also reduced to 50%. Even though the error can be minimized with small time steps, the global error of the simulation grows with each integration.

Higher order schemes exist such as a 4th order classical Runge-Kutta method [14]. These type of methods require quite a few more evaluations of the state space system per time step, but result in higher accuracy over large intervals. The classical Runge-Kutta method for a state space system is quite complicated but can be implemented quite easily in software [15]. The discussed method is shown in Equation (6.3) for a single ODE of the form $\dot{y} = f(t, y)$.

$$y_{i+1} = y_i + \frac{\Delta t}{6}(k_1 + 2k_2 + 2k_3 + k_4) \tag{6.3}$$

$$k_1 = f\left(t_i, y_i\right) \qquad k_2 = f\left(t_i + \frac{\Delta t}{2}, y_i + \frac{\Delta t}{2}k_1\right)$$

$$k_3 = f\left(t_i + \frac{\Delta t}{2}, y_i + \frac{\Delta t}{2}k_2\right) \qquad k_4 = f\left(t_i + \Delta t, \Delta t k_3\right)$$

A very naive method of integrating a real-time simulation is to capture the screen redraw time and use this value as the time step. With this, the simulation will progress each frame with a single integration. Because a software application will not always run at the same frame rate, this method is known as variable time step integration. The result of this integration is a very smooth result and pleasing for the eye, because the simulation runs at exactly the same rate as the application.

The problem with this approach is that consistent results are practically impossible, because every run has different frame times and therefore different time steps. The result is that the global error is different every time, even with the same initial setup and inputs. As a consequence, a simulation run can never be replicated.

A better approach is to use fixed time step integration. This way, the simulation progresses with a fixed value of the time step and consistent results can be achieved. Additionally, simulation runs could be replicated with identical initial conditions and control inputs. The implementation requires some thinking, because the frame time does not correspond to the fixed time step and could cause visual hiccups in the simulation.

A solution to this problem is to accumulate the total frame time and integrate once the accumulated time exceeds a single time step. After integration, the accumulated time should be reduced accordingly. This procedure can be presented as code, which would be executed every frame:

```
1 time_accumulated = time_accumulated + time_frame * alpha;
2 while (time_accumulated >= time_step) {
3   integrate(time_step);
4   time_accumulated = time_accumulated - time_step;
5 }
```

In the algorithm, `time_accumulated` is the total accumulated frame time. `time_frame` is the (current) frame time and `time_step` is the fixed magnitude of a time step. An extra variable `alpha` is visible in the procedure, which represents the time scale. Setting `alpha = 2` will increase the simulation timing to twice that of the application. This gives the user the ability to speed the simulation up or down depending on the needs, without compromising consistency.

6.2.3 PROGRAMMING

The simulation framework introduced in Section 6.2.1 is complicated and can almost not be realized with procedural programming, where the programming task is broken down into a collection of variables, data structures and subroutines. On the other hand, object-oriented programming is based on the creation of objects that expose behavior and data using interfaces, which is very suitable for the suggested framework. A trade-off of the most applicable programming languages is shown in table Table 6.2. Information in the table is gathered from different sources [16][17].

Table 6.2: Simulation programming language trade-off

Feature	**Fortran**	**C**	**C++**	**Java**	**MATLAB**	**Python**
Type	compiled	compiled	compiled	two-step[2]	interpreted	interpreted
Speed[1]	fastest	fastest	fast	medium	slow	slow
Object-oriented	yes	no	yes	yes	yes	yes
Ease of use	bad	bad	medium	medium	good	good
Extensibility	medium	good	good	good	bad	good

Looking at the table, the most suitable programming language seems to be *Python*; an easy to use high-level programming language which allows for rapid prototyping. Extensibility for *Python* is good which is why it was selected over *MATLAB*.

In order to simulate the full mission time (Section 5.1) in a relatively short interval (5 minutes), up to 20 times more integrations have to be performed per frame. An early prototype of the simulation in *Python* showed that speed quickly became a problem in order to meet these demands. Therefore, it was decided to switch the main simulation programming language to C++, specifically the C++11 standard.

6.3 PROFILE

Section 6.2 gave an overview of the lower level implementation of the simulation and the choice of programming language. The higher-level classes, which the user will be presented with are based on this lower-level setup. This is called the simulation profile and will be discussed in this section.

[1] Speed is related to object-oriented programming where possible and measured using standard expressions instead of optimized routines.
[2] Java uses a two step compilation process. Java source code is compiled down to "bytecode" by the Java compiler. The bytecode is interpreted by Java Virtual Machine (JVM).

6.3.1 OVERVIEW

The simulation is built around the mission profile and therefore covers the different phases of the mission. In the simulation, the mission has a current status which represents one of these phases. Certain events will cause a switch to a new phase.

STAND-BY Initially, the Bird is on the ground at the Ground station, which is the point where the catapult and short range communication antenna is placed. Here *BirdPlane* waits until a flock passes by close enough to be reached without major energy expense such that the scientific part of the mission is large enough. Once a flock is detected, the rendezvous phase starts.

CLIMB Right after take-off, a short climb phase will be started during which *BirdPlane* gains altitude. For now it is assumed that all flocks fly at the same altitude of 45 m. Therefore the climb phase always takes the same amount of time.

RENDEZVOUS During the rendezvous phase, *BirdPlane* will try to decrease the distance between itself and the flock. This is done according to a specific strategy which was discussed in Section 5.2.3. When the bird arrives at the flock, position and velocity should be aligned and the follow phase starts.

IN-FLOCK This is the scientific part of the mission which also has the longest duration. Throughout this part *BirdPlane* can change the position in the flock in order to simulate different study objectives. A couple of events can make *BirdPlane* abort the mission, namely flying above restricted airspace or flying over larger water surfaces. Also if the flock lands, the mission will be ended. In that case the return phase will be initiated.

LANDING *BirdPlane* will set course to the closest Landing site that is available. In case obstacles are in the way, a Waypoint system is used to simulate basic path finding around the obstacle with the landing site as the final destination.

END Once the final destination is reached, the mission state switches to this mode. Then the simulation can be replayed or *BirdPlane* will be picked up and brought back the starting position.

The current stage of the simulation allows the *BirdPlane* to interact with four different classes of objects: the groundstation, a flock, a waypoint and a landingsite. Each of these objects will be explained in the following sections by describing its intended purpose in the simulation.

6.3.2 GROUNDSTATION

While the Home location is in Delft, the groundstation is the place from where *BirdPlane* will mostly operate, a place which is near to bigger populations of geese and has high probability of flocks passing by. Figure 6.2 shows the symbol used for the ground station in the simulation.

Figure 6.2: Image of a groundstation

The groundstation has a radar which is supposed to detect the flocks inside *BirdPlane*'s rendezvous range which is at this point set to 10 km. Once detected, the groundstation spawns an event for *BirdPlane* to take off. Furthermore it posses a communication antenna with a certain range which is used to model the communication data rate.

Finally the groundstation also has a car which picks up *BirdPlane* once it has landed to bring it back to the operation base. In the simulation, there exists only one ground station.

6.3.3 FLOCK

The flock is a dynamically moving association of individual geese. Each of the geese is simulated separately with a model to simulate the dynamic swarm behavior. This aspect of the Flock class will be further discussed in Section 6.4. An illustration of a flock is shown in Figure 6.3.

Figure 6.3: Illustration of a flock

Flocks are not unique in the world and can be spawned at any time during the simulation. Each flock can have different numbers of geese. As long as *BirdPlane* is idle on the ground all flocks are simulated as single objects with a random initial state. Once *BirdPlane* starts a rendezvous trajectory, the target flock will be simulated with the correct flock behavior (Section 6.4).

This method reduces computational power required to run the simulation. While not problematic on a 1:1 time scale, increasing speed manifold will quickly exceed the limits of standard hardware.

Other than the flock behavior, the only other action that is currently implemented is the separation of the flock. The simulation is done within a bound called the radius of influence. Once a bird leaves this area of influence, it is not affected anymore by other birds and therefore separates from the flock.

6.3.4 WAYPOINT

Waypoints are the main method used for the outer-loop control system of *BirdPlane* (Section 10.3.5). For the simulation, implementation has been limited to high-level way point control, which *BirdPlane* uses to determine its flight path. The icon used for a waypoint in the simulation is shown in Figure 6.4.

Figure 6.4: Graphic of a waypoint

For *BirdPlane*, waypoints have a higher priority than their current targets, like the target flock during IN-FLOCK mode or the landing site during LANDING mode. As such they can be used to fly around obstacles during landing or restricted airspace through which the flock flies.

6.3.5 LANDINGSITE

The landing site is the final destination of *BirdPlane* and has little more usage at this point. Once the mission state switches to LANDING mode, the landing site that is closest to *BirdPlane* will be chosen as landing target and once *BirdPlane* reaches it, the mission mode switches to END. Figure 6.5 shows the graphic used for the landing strip.

Figure 6.5: Illustration of a landing site

6.3.6 *BirdPlane*

The *BirdPlane* class is by far the most sophisticated class in the simulation. This is the object where all strings come together and which combines the behavior of all the entities.

FLIGHT MODES

BirdPlane itself also has states describing different flight mode, namely: STAND-BY, CLIMB, CRUISE and ACCELERATION. For each flight mode, different characteristics apply. An overview of the airspeed and power consumption for each can be found in Table 6.3. At this point there is no implementation of a wind model, so the airspeed is equal to the ground speed. More information about the power consumption can be found in Section 10.3.1.

Table 6.3: Characteristics of *BirdPlane* flight modes

	STAND-BY	CLIMB	CRUISE	ACCELERATION
Airspeed [m/s]	0	18	18	26
Power consumption [W]	0	45	40	58

STAND-BY *BirdPlane* is in idle state whenever it is on the ground, as a result it uses no power and has no speed.

CLIMB In the climb phases, which is in the current implementation only during the RENDEZVOUS part of the mission, the cruise speed is assumed to be constant while the power consumption increases in order to increase the altitude.

CRUISE Cruise flight is the most common flight phase as also the flock is assumed to travel at approximate cruise velocity during migration. *BirdPlane* is designed to be most efficient in cruise and as a result the phase has the lowest power consumption.

ACCELERATION Finally, the acceleration mode is entered when during rendezvous the position and velocity are almost fully aligned with the flock but *BirdPlane* is still far behind. In order to quickly decrease the distance, the airspeed is shortly increased. As one might expect, this phase costs the most power.

More detailed differentiation between the flight states is desirable. In the best case continuous coverage of airspeed vs power consumption would be implemented, in the form of a full flight dynamics model. Section 10.1.1 will explore the *BirdPlane* aerodynamics in more detail.

SYSTEM UPDATE

One of the main intentions to write the simulation was to model the internal software of *BirdPlane*. At this point some parts have been implemented which includes the power consumption and battery modeling, flock tracking and landing site tracking.

Apart from the time step integration of *BirdPlane*'s position during each update loop of the simulation, the flocks position is retrieved and all landing sites are tracked. This way the distance to the nearest landing site can be determined which is the target destination once the mission is aborted. Also the energy level of the battery is updated with the current power consumption from the flight mode. Lastly, also the waypoints are tracked.

FOLLOW MODE

Presently the IN-FLOCK mode, the scientific part of the mission, includes the possibility for varying flight positions inside the flock. As true formation flight is not yet fully implemented it is not yet possible to simulate the exact behavior during in-flock flight. In future development stages of the software it should be possible to combine *BirdPlane* flock detection software with the flock simulation, to test the *BirdPlane* internal software against the dynamic formation changes of the flock.

6.4 FLOCK BEHAVIOR

Another main aspect of the simulation is the dynamic simulation of a flock of Barnacle Geese, which is an essential aspect of making *BirdPlane* operate safely in real life. Because a bird flock can show some unexpected behavior which the internal software of *BirdPlane* needs to deal with in real-time, it is of great importance to have a testbed to verify the software. As this simulation is only a proof-of-concept, the implemented model is rather basic with a restricted amount of possible events but already provides a good basis for future extension.

In its most simple form Flock behavior is based on three different influences: alignment with the flock, cohesion of the flock and separation from the flock [18]. Furthermore, for the application at hand, it is useful to also include some random behavior which will lead to more dynamic flock movement. Also all the influences are only valid inside a specific range from the average flock position, called the radius of influence (R.O.I.). In the following sections, this simple technique will be discussed.

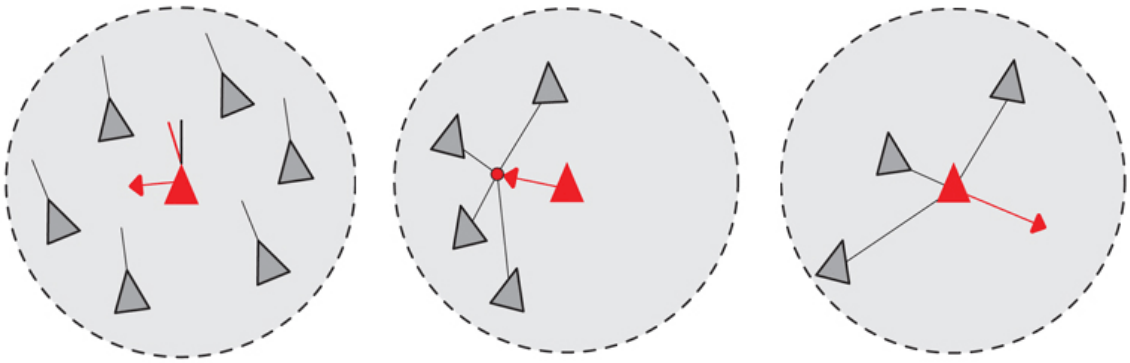

(a) Alignment (b) Cohesion (c) Separation

Figure 6.6: Flocking behavior rules

ALIGNMENT

The purpose of alignment is that all Barnacle Geese inside the flock try to fly in the same direction (see Figure 6.6a). This way, the flock does not separate very easily. The alignment vector can be calculated by iterating through the list of geese in the flock and summing the velocity vectors. Inside the loop there are two checks happening before a velocity is added to the alignment velocity which is whether the goose to be added is equal to the goose for which the alignment is calculated and whether this goose is within the radius of influence.

```
void calculate_alignment() {
  for (goose : geese) {
    if (goose != self &&
          distance_from_self_to_goose < radius_of_influence) {
      alignment = alignment + goose_velocity;
    }
  }
  normalize(alignment);
  return alignment;
}
```

After all relevant velocities were summed up, the vector is normalized and returned. The returned value is simply the average velocity vector of all neighboring geese. This vector can then be used to update every goose and direct it in the same direction. The result of this single technique is already some very basic flocking behavior.

COHESION

Cohesion is the measure of how close the geese fly together in the flock (see Figure 6.6b). The cohesion influence is calculated as a velocity towards the center of mass of the flock. This is calculated from the average position of each goose in the flock. The outer function is the same as in the previous code snippet so only the part inside the loop will be presented.

```
if (distance_from_self_to_goose < radius_of_influence &&
      distance_from_self_to_goose > distance_between_geese) {
  cohesion = cohesion + goose_position;
} else {
  return 0;
}
```

Here another check was added in order to make the geese fly apart from each other. If they are too close to each other, the specific goose is ignored for the calculation of the center of mass. This can be used to further increase realism and make the flock fly in a formation pattern. Expanding this behavior with changing from the center of mass to individual positions in the formation, could make this possible.

SEPARATION

Apart from alignment and cohesion which both make the geese come closer together also movements away from the flock are required to simulate flock behavior (see Figure 6.6c). First the direction of the current goose with respect to the center of mass is calculated and then this vector is inverted to make the goose fly in the opposite direction.

```
if (distance_from_self_to_goose < radius_of_influence) {
  separation = seperation + goose_position - self_position;
}
...
separation = -separation;
```

MERGING OF THE MOVEMENTS

The individual behaviors only provide a correct update on a short interval. The combination of techniques is what makes the behavior work on a long term. The desired behavior can be obtained by introducing weights for each of the influences:

```
for (goose : geese_in_flock) {
  alignment = calculate_alignment();
  cohesion = calculate_cohesion();
  separation = calculate_separation();
  goose_new_velocity = alignment * alignment_weight +
    cohesion * cohesion_weight +
    separation * separation_weight +
    random * fixed_random_weight +
    goose_velocity * fixed_original_weight;
}
```

For each goose in the flock each influence is calculated separately and then combined with the original velocity and a random influence. The current factors used are:

Table 6.4: Overview of the used values for the influence weights of the flock simulation

Alignment	Cohesion	Separation	Random	Original	R.O.I.
0.1	0.1	0.1	0.5	3	1000

6.5 MAP

The simulation objects discussed in Section 6.3 will be rendered to the screen in order to give the user feedback on the current state of the simulation. To give a more detailed visualization, a street map will be used which is rendered on the display background, such that the position and rotation of the entities on screen can be physically interpreted.

Because the software renders to a 2D display, it is needed to project the simulation from a 3D world coordinate frame to 2D screen coordinates. Therefore, it is important to clearly define the used coordinate frames and link them together with a suitable projection method.

6.5.1 COORDINATE FRAMES

The coordinate frame used for the world is the geographic coordinate system (Figure 6.7), which uses *latitude* and *longitude* coordinates. The *latitude* (ϕ) of a point on the Earth's surface is set as the angle between the equatorial plane and a vector from the earth center to that reference point. The *longitude* (λ) of the point is the angle from a reference meridian (set at the Royal Observatory in Greenwich) to a meridian passing through the reference point.

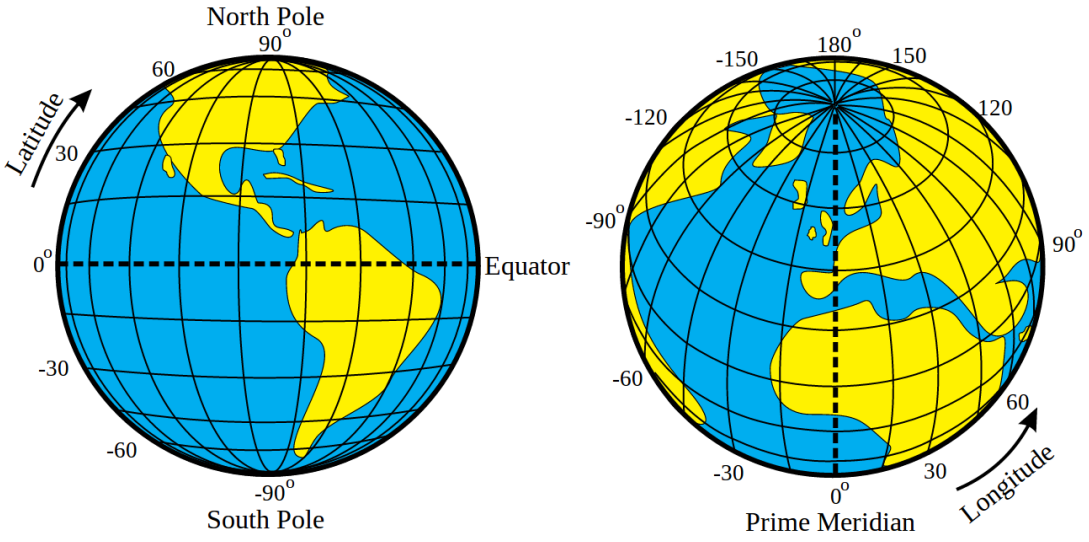

Figure 6.7: Earth reference frame [19]

For the simulation world, an orthogonal Cartesian coordinate frame is used. The x-axis is positive towards the East and the y-axis towards the North. The z-axis is pointed out of frame into positive altitude. Because the mission will be performed with an average range of 100 km (Section 5.1), it is assumed that the covered surface of the Earth is flat, which justifies the use of this world frame. The frame can be seen in Figure 6.8, where the axis are given in unit kilometers. The origin of this frame will be set at the ground station, which means that a position vector of $[0, 1, 0.1]$ is a point 1 kilometer north from the ground station, at 100 meters altitude.

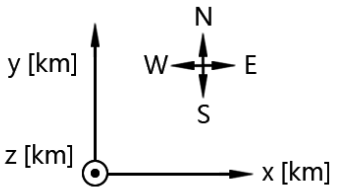

Figure 6.8: World reference frame

Because the world map is defined in the earth reference frame, it is important to find a projection method to transform this frame to the world frame. For reasons explained in Section 6.5.3, it is desired to have a projection method which allows square segmentation of the Earth's surface. For this, the Mercator Projection is used.

6.5.2 MERCATOR PROJECTION

The Mercator Projection (shown in Figure 6.9) projects the Earth's surface onto a rectangle. It is created by folding a piece of paper around the Earth's sphere such that a cylinder is formed. By projecting the surface from the radius of the cylinder onto the paper, the geometry is formed.

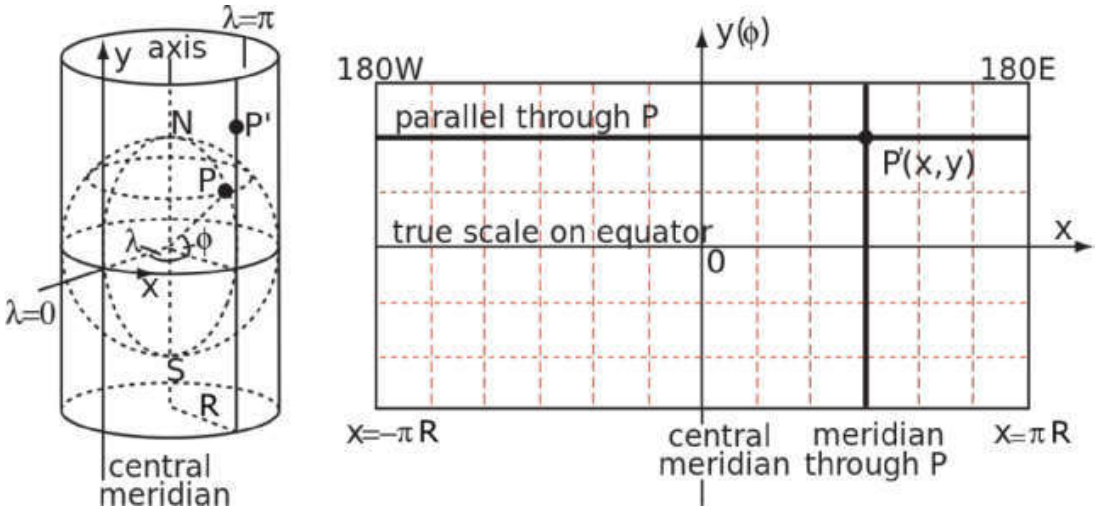

Figure 6.9: Mercator projection geometry

One of the major advantages of the Mercator projection is that constant latitude lines are always parallel to each other and perpendicular to constant longitude lines. Because of this, the world reference frame can be placed directly on a point P with matching orientation. Equation (6.4) describes the transformation of earth coordinates to the world reference frame; Equation (6.5) is the inverse of the transformation.

$$x = R\lambda \qquad y = R\ln\left[\tan\left(\frac{\pi}{4}+\frac{\phi}{2}\right)\right] \tag{6.4}$$

$$\lambda = \frac{x}{R} \qquad \phi = 2\tan^{-1}\left[\exp\left(\frac{y}{R}\right)\right] - \frac{\pi}{2} \tag{6.5}$$

However not all is well, there are some errors related to this projection. First, an assumption is made that the earth can be modeled as a sphere. This results in simplified calculations of the mapping, but will also introduce slight errors in the Mercator Projection. The second error becomes apparent when placing Tissot's indicatrices on the projection. These are circles of a fixed radius distributed evenly along the latitude and longitude grid, see Figure 6.10.

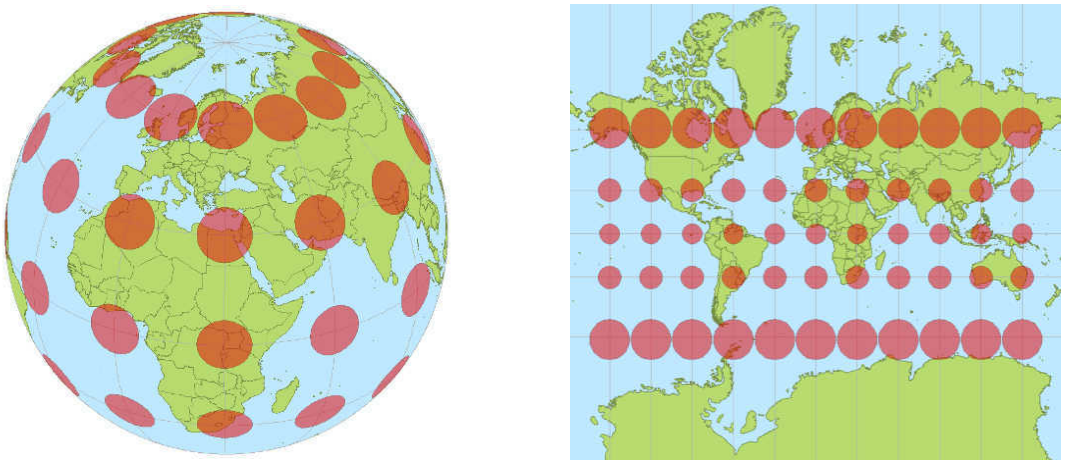

(a) View from space

(b) Mercator projection

Figure 6.10: Tissot's indicatrices [20]

Figure 6.10b shows what happens with the indicatrices when projected, the resulting scale of the map varies widely along the latitude (y-direction). This distortion is also known as "the Greenland Problem" [21]. Even though this is very problematic on a large scale, it does not pose a problem for the mission simulation, which covers distances of only 100 kilometers. Errors are kept to a minimum, and because the projection is described very well, corrections can be made easily.

6.5.3 SLIPPY MAP

With the Mercator Projection in place, it is now possible to display the map behind the simulation rendering. For this, a modern web maps technique called *Slippy Map* is used [22]. A *Slippy Map* divides the world map into a number of tiles (n), depending on the zoom level z. Each tile is a 256×256 pixel image and stored in a database. Depending on the camera position and scale, only a small number of tiles need to be loaded and displayed.

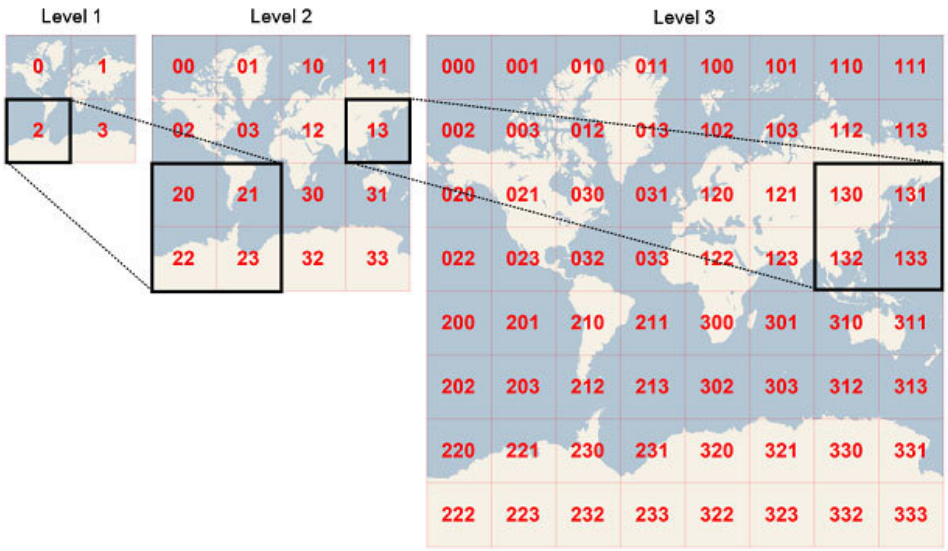

Figure 6.11: World map segmentation [23]

The total number of tiles is quadrupled with every zoom level. In other words, the next zoom level divides a tile in half for both the width and height. The segmentation process is shown in Figure 6.11. There are a number of servers available from which tiles can be downloaded freely. The simulation prototype loads tiles from *MapQuest*, an American free online web mapping service. Three examples of map tiles are shown in Figure 6.12.

(a) Zoom level 0 (b) Zoom level 4 (c) Zoom level 12

Figure 6.12: Slippy map tiles (*MapQuest*)

The tiles needed for display can be determined as follows. First, the camera view boundary is calculated and the minimum and maximum world coordinates are noted. These limits are then converted to Mercator coordinates. The points are then transformed to the tile space, whose size depends on the zoom level. This is described with Equation (6.6).

$$x_{\text{tile}} = \frac{1 + \frac{x}{\pi R}}{2} \cdot 2^z \qquad y_{\text{tile}} = \frac{1 - \frac{y}{\pi R}}{2} \cdot 2^z \tag{6.6}$$

The tiles can be downloaded in real-time and outside the simulation loop. When a tile is fully downloaded, it is loaded into memory, processed and displayed on the screen. Memory can be reclaimed when a tile is outside of view and no longer needed.

6.6 RESULTS

Using the design as discussed in above sections, a proof of concept software package has been developed. Every library used is completely open-source and free to use. The software makes use of *OpenGL* for graphics rendering, *GLFW* for window management and *cURL* for tile downloading. Furthermore, it has been developed with cross-compatibility in mind. As such, the software can be compiled and run on operating systems like Windows, Linux and OS X.

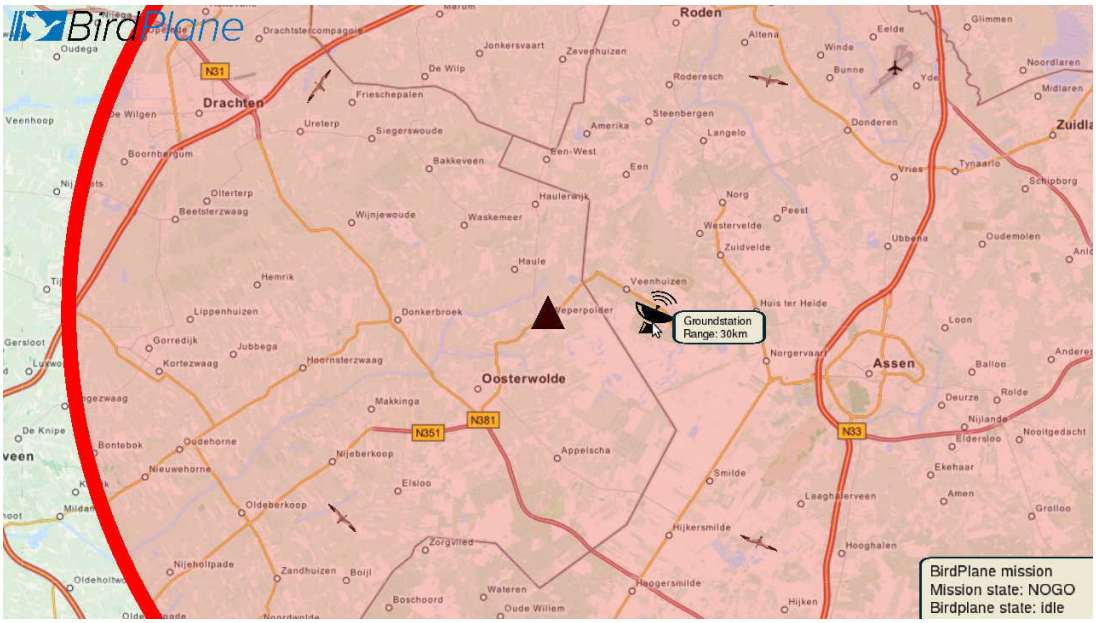

Figure 6.13: Screenshot showing the ground station with range

In the current state, the simulation prototype already has basic functionality to simulate a complete mission. Once further developed, it provides the opportunity to verify various design aspects like the rendezvous trajectory and the internal software of *BirdPlane*.

Figure 6.13 displays *BirdPlane* (black triangle) idle, a ground station with a range of 30 km and a Barnacle Goose flock in every diagonal direction. When one of the flock is within reach and the go signal has been given, *BirdPlane* will start the take-off and rendezvous phase. In the prototype, this event triggers the actual flock behavior of the birds. Figure 6.14 shows *BirdPlane* flying within the flock in cruise mode.

Figure 6.14: Screenshot demonstrating formation flight

Usability, reliability and responsiveness have been key aspects of the preliminary development. The user of the application can speed up and slow down the simulation in real-time and smoothly pan and zoom around the map. Also, the user can edit the world on the fly, by adding random new flocks or landing sites where desired. Furthermore, the user can create waypoints and direct the *BirdPlane* aircraft to desired locations.

The developed framework is built up in a object-oriented and modular way, such that new features can be added with ease. Because of time limitations, it was impossible to implement all the desired functionality in the prototype. Some recommendations for the near future of the simulation development are:

- Basics of a *BirdPlane* flight dynamics model.
- Weather conditions model with wind vector field.
- More extensive behavior of flock, such as landing and merging.
- A simulated pickup of the *BirdPlane* aircraft after landing.
- Implementation of restricted airspaces.
- Full bird flock detection by ground station.
- Virtual communication link with interference.

7 Market Analysis

With the knowledge of the mission definition as discussed in Chapter 4 and the functions that *BirdPlane* can perform, discussed in Chapter 5, it is possible to analyze the market. The current planning of the mission suggests a ground station from where the mission is controlled and one *BirdPlane* which will be assigned different missions. For this market analysis a different approach is chosen to find out whether *BirdPlane* could also be sold as a product. As such this analysis stands apart in *BirdPlane*'s suggested applications but all considerations are based on the capabilities of *BirdPlane* that will be further developed during this project.

The first step of a market analysis is the identification of the market, which means its locality, size and competitors. Factors like these can have great influence on the design and resource allocation of the product. In order to estimate the achievable performance on the market it is further important the predict the future development, which includes market growth and new market opportunities. Combining the results of the two previous steps a prognosis of the sales volume can be made and thus the required infrastructure of the production line deduced. Further this will introduce the option the assess the required sales price to make a specific profit.

In this following sections each of these points will be discussed in detail and finally a conclusion will be drawn on whether *BirdPlane* could be a profitable competitor on a real market. All estimations will be made for a period of **5 years** after the first introduction of the product on the market.

7.1 Identification

The primary mission goal of the *BirdPlane* mission is to study migrating Barnacle Geese. As such *BirdPlane* is intended to be used by bird researchers, who want to find out more about their migration and in-flight flock behavior. This will be called the primary market in the following analysis.

Apart from this, other potential markets can also be identified. In general the UAV market, civil as well as military and the RC model aircraft market seem the most promising candidates with more tentative options in research projects of larger general aviation and transport aviation companies. These markets will be referred to as secondary markets in the following sections.

7.1.1 Primary Market

As stated in the mission need statement, *BirdPlane* is set to "follow and study a migrating Barnacle Geese flock" and therefore will be designed for this purpose.

There are currently only very few methods to accurately study birds in-flock. One possibility is that a couple of birds are imprinted on a person such that they follow them. If the person then drives in a convertible car or flies in a para-glider, the birds start flying to keep up. In this way studies on the flight speed and videos of the movements of the birds could be done. This also means though that the birds are trained from hatching onwards and therefore were **not raised in nature**. This could have an impact on the results as the birds might not displaying natural behavior. Also measurements on the drag reduction through formation flight are not yet possible and flight behavior in the formation has not been monitored over longer distances. By having continuous video footage, biologists would be able to watch the geese behavior and communication inside the flock throughout the whole flight. Other UAV aircraft can not be used to study the birds as the birds fear the artificial objects and try to avoid it. *BirdPlane* will therefore provide in-flight formation flying data, which accurately displays flight behavior and airflow measurements, which is impossible for today's competitors.

Initially the intent is to study Barnacle Geese, migrating in **The Netherlands** which makes the market very narrow and local. These birds also migrate in other countries though, and therefore, for the future use of *BirdPlane* not only Barnacle Geese in The Netherlands could be researched, but especially also those in other countries that house Barnacle Geese during winter or summer. During contact with Barnacle Geese researchers it was indicated that in all of Europe about 5 groups work on Barnacle Geese research.

Furthermore, *BirdPlane* should also be able to fly with other birds which migrate in similar altitudes and at similar speeds. This way *BirdPlane* could serve a higher percentage of the birds researchers. Still, even it would

be possible to fly with other birds the current field of interest will be small.

Therefore it can be concluded that the current market of bird research UAV is very narrow and that *BirdPlane* will be in some ways a unique product.

7.1.2 SECONDARY MARKET

As mentioned in the section's introduction, two main secondary markets can be identified, namely the general UAV market and the RC model aircraft market. Furthermore, it can be argued that large aircraft manufacturers could be interested in the use of flapping wing aircraft for manned flight. Even at NASA studies have been performed on the use of flapping wing aircraft for use on earth and also other planets. Finally, the fact that *BirdPlane* is designed to analyze the overall power consumption reduction due to formation flight within flocks, general aviation is expected to show interest into the benefits of formation flight provided by *BirdPlane* data. These options will be discussed in the following sections.

UAV MARKET

BirdPlane will be designed for an endurance of 100 minutes of cruise flight which corresponds to a range of 108 km Section 8.3.2 during no-wind conditions. With this it is comparable to other small size UAV that are currently in use at the military.

Since the first approval of unmanned aircraft in 1990, the sector of UAV has grown significantly. In 2010, a total of 41% of aircraft of the US Department of Defense were unmanned. This shows the huge market size of UAV. [24].

BirdPlane is not in competition with all UAV. Small size UAV have a much lower share of the market, but it will still be considerably high. Possible competitors could be the following:

- Orbiter from Aeronautics [25]
- SWAN III from ELI Military Simulations [26]
- UAS: RQ-20A Puma AE by AeroVironment [27]

The above examples are UAV meant for military missions and have ranges of about 100 km which is the target of *BirdPlane*. The ranges are however **limited by the communication** link and their endurances are mostly range from a few, up to 10 hours.

Apart from the military missions, UAV are also used for civil purposes for inspection of buildings, bridges, pipelines and other objects that are difficult to inspect directly. Furthermore, traffic control, meteorology, animal herd tracking and various other tasks can be performed well by UAV. Often times these applications require hovering flight though, which *BirdPlane* cannot do. Possible customers in this case could be governments, the police, airports and researchers from various fields.

It can be concluded that the UAV market is huge and even with the limitation of the range and endurance, possibilities are still wide spread. This proves to be promising for *BirdPlane*.

RC MODEL AIRCRAFT

As one of the requirements for *BirdPlane* is for it to be remote-controllable, the RC-model aircraft market could be another option to sell *BirdPlane*. Model aircraft of any many kind already exist although flapping wing aircraft are still rare.

Basically this market again needs to be divided into two sections, one for toy RC models and one for larger more serious and realistic models. The main difference between these two markets is the price paid for the model and the size. While the toy market is huge, the price for each model is small (in the order of €100). On the other hand the larger models are not sold in high frequency but have prices in the thousands of Euros.

The current design of *BirdPlane* will probably place it in the latter market section, suggesting a lower quantity to be sold. Nevertheless, a user-friendly ornithopter such as *BirdPlane* is rare and should perform well within the market.

RESEARCH MARKET

Apart from the obvious markets where *BirdPlane* could be sold, flapping wing flight is still an area which is not well understood in terms of aerodynamics. Also the mechanics of the birds are subject to ongoing research. Projects have been initialized to develop flapping wing aircraft, some of which have been commercialized, thus the research market could be seen as another opportunity to sell knowledge acquired during the design of *BirdPlane*. The list of such projects includes but is not limited to:

- SmartBird from Festo
- Robird from Clear Flight Solutions
- Robo Raven III by Maryland Robotics Center

(a) Robo Raven from University of Maryland [28]

(b) Robird from Clear Flight Solutions

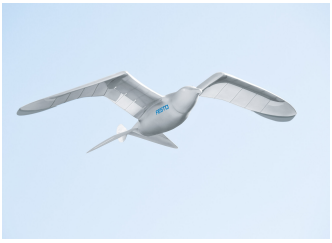

(c) Smartbird from Festo [29]

Figure 7.1: Current research projects

SmartBird SmartBird (shown in Figure 7.1c) is a flapping wing robotic robot which is inspired by a gull. It was developed by Festo, a German control and automation company, in the context of the Bionic Learning Network. The latter is an ongoing cooperation Festo has with universities to develop bio-inspired robots. SmartBird is has a wing-span of 2.00 m, a light-weight carbon fibre structure and uses an electric motor to drive the flapping mechanism. It further uses active wing torquing to increase aerodynamic efficiency. It is able to sustain flight at low velocities for a couple of minutes with a weight of 450 g. [30]

Robird Robird (shown in Figure 7.1b) is the name for a series of flapping wing, predator bird inspired UAV, developed by Clear Flight Solutions. The development of these birds started as a research project at University of Twente and was later commercialized. Birds of different sizes have been built and shown to fly with masses between 750 g and 2 kg with endurances of 10 minutes. The birds are used to scare away birds from landfills, airports and productive land. Throughout the course of the project, the team has been in contact with this company and used demonstrations of the birds to learn more about these robots. [31]

Robo Raven III Robo Raven (shown in Figure 7.1a) is a research project by the University of Maryland Robotics Center. It is smaller than the other presented birds but uses solar power as well as batteries to power the main mechanism. [32]

More studies on flapping wing aircraft have been performed also by bigger organizations like NASA. These could be interested in projects like *BirdPlane* to gain knowledge about flapping wing aerodynamics and the flapping mechanics.

GENERAL AVIATION, FORMATION FLIGHT

One of the primary research topics embedded within the *BirdPlane* system, are the measurements performed on the overall aerodynamic performance of *BirdPlane* in mid-flight. The expected performance improvement on the induced drag force whilst operating in formation flight, is already an important field of research. Airline companies such as the Royal Dutch Airlines, British Airways and American Airlines have already displayed open interest on the possible benefits of formation flight. Therefore, with the data opposed by *BirdPlane*, a few to many unknowns may be solved.

7.2 TREND & OPPORTUNITY

While it is important to analyze the market in its current state, it is even more important to anticipate the future development of the market situation in order to estimate the market performance of the product once it has

been introduced. In this section, the expected changes in market size for the primary and secondary markets mentioned in the previous section are discussed and an analysis of the advantages and disadvantages that *BirdPlane* has over the currently existing products is made.

7.2.1 PRIMARY MARKET

The market that was identified as the primary market is the bird research market. The Barnacle Goose has been researched for a long time already and as these birds are not very high in the public focus, the number of research teams will most likely not greatly increase in the near future.

One reason for the increase in bird research could be the increasing air traffic density. As aircraft are endangered by flocks of larger birds, it could be of high value to steer away geese flocks from airports. The increasing density makes the bird problem more evident and thus could increase the need for this function. As explained before, the current methods to fly inside the flock are rather limited and compared to using para-gliders, *BirdPlane* has the following advantages:

- Lower operation costs
- None or very little infrastructure needed
- Autonomous operation
- Better in-flock positioning (drag measurements)

As *BirdPlane* runs on electricity, the operation cost should be lower, also it can start and land anywhere, provided that the communication antenna and catapult can be built up at that location. It follows the flock in different positions and is able to also measure drag reduction effects as its size is comparable to real Geese.

The disadvantages are that *BirdPlane* needs to be picked up after it landed and as it is a new system, there are some increased risks of software bugs and technical problems.

As mentioned before, *BirdPlane* could also be used to study birds other than Barnacle Geese, which would greatly increase the quantity. This will be possible with birds which fly at approximately equal speeds in the range of 16-26 m/s and fly at low altitudes. Bird researchers that were contacted throughout the course of the project mostly suggested that small birds(<250 g) are posing a larger opportunity for a device like *BirdPlane* as they are extremely hard to follow by other methods. Also it was pointed out that it is not uncommon for research teams to spend €20,000 on transmitters. This gives a good idea of how much money would be available for these teams to buy *BirdPlane* as it actually provides much more data than transmitters can.

7.2.2 SECONDARY MARKET

The secondary markets were identified to be the UAV market, RC model market and research market. Their prospect for the future will be discussed in this part.

UAV MARKET OPPORTUNITY

UAV industry is a very fast growing sector of the aerospace industry with great market demand, high opportunity and profitability in the near future [33]. This is because the mission capabilities of UAVs in performing high risk/threat task has been increasing (and expected to continue this way), whilst the costs have been decreasing.

According to the recent market analysis of UAV industry (Lucintel 2011), the global UAV expenditure has shown a growth of more than 12% from 2005 to 2010, where approximately half of the expenditures are spent for research and development activities [33]. This growth is concentrated in the following sectors/trends:

- Growth in Unmanned Combat Aerial Vehicles (UCAV)
- Increase in endurance limit
- Increase in mission capabilities of UAVs
- Increase in awareness of UAVs
- Increase in HALE (High Altitude, Long Endurance) UAVs

Among these trends, the increase in the demand of the long endurance and long range UAV suggests that successfully designed *BirdPlane* will gain high competitiveness in the market. Although the majority of the UAV market has been led by U.S. so far (particularly U.S. Military Air Force), the trend shows an increase of UAV market in many different segments (e.g. civil, commercial, science) and diverse regions, including Europe and the Asia-pacific region.

While *BirdPlane* is not intended for military use in the first place, its purpose could be extended if it is found that it works flawlessly. It could, in this field, have the following advantages:

- Camouflaged, due to birdlike looks
- Low noise
- Very lightweight, easier transportation

Having a flapping wing UAV could add a camouflage aspect if considered for military purpose, particularly espionage. Especially, since flapping wing UAVs will have a less distinctive noise output as conventional propeller driven UAVs. As *BirdPlane* was not primarily designed for military missions, there are at this point some disadvantages as well.

- Lower endurance
- Lower payload
- Lower top speed

In order to be successful on this market, these points need improvement. Especially the endurance has to be increased as opposing threats are generally some distance apart and the distance will be subtracted from the actual possible mission duration. About 4 hours should be the minimum required endurance.

With the longer range and the on-board cameras, *BirdPlane* could also be used for other civil applications as mentioned before. Options are among others traffic surveillance, to find missing persons, as helper for rescue teams in regions that are hard to access and also animal herd tracking. For such missions the above mentioned advantages are very important, for example lower operation costs than helicopters which are often used with rescue teams. The thermal camera (discussed in Section 10.3.4) that will be part of *BirdPlane* makes it a very good options for these missions, as well as herd tracking. The sophisticated object recognition software of *BirdPlane* could also be used to recognize cars in traffic.

MODEL FLYING

The market of RC model aircraft has shown some growth in the past decades. As micro-electronics get better and smaller, new cheap remote-controlled flying vehicles have appeared on the market. Examples are helicopters, quadrocopters (recently developed) and even smaller drones. Especially with the advent of smart phones, new possibilities of remote controlled devices arise. Quadrocopters, controlled by smart phones and tablets using constant video streams are already available. This could also be an option for *BirdPlane* as it will also be equipped with a camera. However, this connection has limited range and therefore the long range deployment of *BirdPlane* can not be fully exploited using this technology.

One possibility would be to also make a cheaper version of *BirdPlane*, with less range and thus lower weight and cost. As such it could be more attractive to fans of model aircraft.

Furthermore, growth from emerging markets like China and Brazil is to be expected. Currently, wages are rising quickly in these countries and thus more money is available for “toys” and hobbies. Therefore, if overall sales of RC planes rise, also *BirdPlane* could be sold in higher numbers.

RESEARCH PROJECTS

Bio-robotics is a growing field and it can be expected that research will continue to increase. Flapping wing aerodynamics is not very well understood yet so knowledge in this field is highly appreciated. In order to sell *BirdPlane* to other research teams or companies, it’s advantages over the other existing projects need to be pointed out.

- Longer range and endurance
- More measurement systems available

- Highly sophisticated flapping mechanism

These advantages could make *BirdPlane* a wanted project, also for future development of larger and at some point maybe manned flapping wing aerial vehicles.

7.3 PERFORMANCE

Based on the previous market identification and the established opportunities it should now be possible to roughly estimate the sales volume for *BirdPlane*. This will also be influenced by the retail price which is in turn dependent on the materials used, the production process and the additional time needed for design. The exact cost breakdown will be performed in Section 13.2, however in this section will already analyze what the price would need to be to perform well on the market. The retail price needs to leave some room for fixed cost like the production facilities. Finally, a profit margin needs to be taken into account and a feasible break-even point needs to be found.

7.3.1 SALES VOLUME

The sales volume is the number of *BirdPlane* that will be sold annually. As was already indicated in the previous section, *BirdPlane* would need some adjustments to be lucrative on the secondary markets. Therefore a strategy with different versions of *BirdPlane* will be discussed in this section, each tailored to its market's demands. Furthermore it will be assumed that marketing will be done **world-wide** and also world-wide shipping will be possible.

In the primary market currently only 5 groups are working on Barnacle Geese and assuming that each group would buy one *BirdPlane* should be a realistic to optimistic estimation, as some might buy two *BirdPlane*. Still in order to successfully introduce this product and make it profitable its area of application needs to be widened to also support other types of birds. This way a larger set of teams could be reached, in the order of 20-30, probably. This number will correspond to a price in the range of €10,000-15,000 which was indicated by researchers as a reasonable price.

On the secondary market things look slightly different. On the Military UAV market prices usually are in the range of €100,000 or more also for small size UAV [34]. On the other hand only the most dedicated RC model enthusiasts would pay more than €2,000-3,000. So, as mentioned above, small adjustments should be made to the design in order to adapt to the market. On the UAV market more endurance is of importance so a scale up of *BirdPlane* would possible. This would also increase the payload and the price slightly which should not be a big issue as even with a price of €50,000 a good product could definitely succeed on the market. For the RC market a scaled down version of *BirdPlane* would then be appropriate. As model aircraft are usually not allowed to fly outside line of sight a lower range and lower endurance should be enough if this way the price can be brought down considerably.

As the civil UAV market has far lower demand than the military market, there will be no separate model for this market. As high endurance will also something demanded from this market, the military UAV model should fit this market well enough, although the price might be on the high side. For the estimation of the sale volume the civil market will be included.

With the above mentioned prices a sales volume in the UAV market of 20-50 *BirdPlane*'s annually sounds justifiable. Furthermore about 100 RC model versions could be sold annually worldwide. These are only very rough estimations or example numbers for further calculations.

Table 7.1: Overview of annual sale volume estimations

	Primary	**UAV**	**RC model**
Sale volume	10	20-50	100
Price [€]	15,000	50,000	2,000
Total revenue [€]	150,000	1,000,000 - 2,500,000	200,000
Overall revenue [€]	1,350,000-2,850,000		

7.3.2 PROFITABILITY

For a company to be profitable, the fixed and variable cost as well as a profit margin have to included in the sale price. As this company will be built up from scratch and will most probably rely on a loan to cover the initial cost, it is crucial to reach the break-even point as early as possible. The break-even point is reached when the profit covers the initial fixed costs. As a loan is quite big burden for a company to bear, other possibilities such as crowd funding could be considered for during startup of the company.

As the overall sale volume is rather low, the profit margin on the product should be high. An example are expensive sports cars like the new Porsche which has a profit margin 18% [35]. As this is a proven design with a customer base, good reputation and marketing, the profit margin of *BirdPlane* needs to be even higher. Therefore it was decided to opt for a 33% profit margins, which means that after subtracting material and manufacturing cost and any other cost like marketing, 33% of the sale price will be profit.

Assuming an **annual revenue** (R) **of €2,000,000** which is about midrange in the above calculated bounds, and a break-even point after two years (Y), the maximum fixed cost can be calculated (P being the profit margin).

$$C_{\text{fixed}} = R(1-P)Y \tag{7.1}$$

$$C_{\text{fixed}} = 2,000,000(1-0.33)2 = €2,640,000 \tag{7.2}$$

CONCLUSION

From this discussion it can be concluded that there are definitely some opportunities on the market where *BirdPlane* could fit in to be profitable. *BirdPlane* will have some advantages over the current methods used by bird researcher and also over some of the currently used UAV.

The market strategy that was developed is to sell *BirdPlane* in three different versions, shaped to the target market. The basic version that is designed in this project is the one that will be sold to scientific bird research teams with a **target cost** of no more than **€10,000**. For the UAV market a higher endurance and higher payload is required which will be realized in a scaled up version, produced for no more than €33,333. Finally a smaller version will be sold as RC model aircraft, the production of which should stay under a cost of €1,333.

At a later stage throughout the project, a cost breakdown structure will be built to figure out if the goals for fixed and variable cost of *BirdPlane* are reasonable.

8 SYSTEMS DESIGN

At this stage of the project, the *BirdPlane* assignment, mission and simulated mission are fully determined. This section functions as a logical follow-up of the overall requirements which were derived from the investigation on the customer needs and mission analysis.

In this chapter the requirements on *BirdPlane* and the functions it should be able to perform are translated to the corresponding (sub-)systems that are required. First an outline of the approach for of the systems design is given. The six steps are executed and the results are presented in the sections that follow.

8.1 APPROACH

Before the final process of systems design is started, first the primary vision which is striven towards within this section is described. The approach of the systems design is found by its primary meaning, namely that by initial analysis of the mission, (sub-) system requirements are formed. These requirements in turn correspond to additional (sub-)systems which have to be taken into account individually. Continuously verifying the research of the previous chapters, the following method is set:

1. System architecture: As mentioned, the functions of *BirdPlane* have been analyzed in previous sections of this report. From this knowledge, it is directly determined which sub-systems the final *BirdPlane* architecture should contain. Therefore, a primary analysis of the systems is done and the final 'AND-tree' is created.
2. System requirements: From the architecture, the technical requirements related to mission operations are quantified and assigned to the possible sub-systems (iteratively, by using step 1 and 2 more sub-systems are created from the arising requirements). Also, possible 'killer-requirements' are identified and isolated for further inspections.
3. Operations: Now that each sub-system has quantified requirements and specifically assigned tasks, the functional, real-life application of the *BirdPlane* system is taken into account. By means of operations and logistics, the system which is set up to this point is revised for 'common sense', meaning that in real life the system is actually functional.
4. Communication: Once it is known whether the *BirdPlane* system is not only complying with the technical requirements, but also is capable to perform in real-life, the communications system is checked. Once sufficient communications can be realized, the technical, functional and operational requirements are definitively covered.
5. Resource Allocation: At this point, the *BirdPlane* sub-systems have all been assigned specific functions and basic requirements. The following item of systems design constrains the possible design solutions to these functions and requirements. The constraints correspond to the maximum allowable mass and power consumption of each design solution. By means of resource allocation, possible solutions can be checked for the indicated constraints.
6. Sustainability: Finally, out of the possible design solutions to each (functional) requirement, the most sustainable solution is picked. Since *BirdPlane* should be designed according to environmentally prescribed standards (e.g. 95% sustainable material), this final decision making is particularly important.

8.2 ARCHITECTURE

The architecture of the *BirdPlane* system can be visualized by means of a breakdown diagram as shown in Figure 8.1. This architecture corresponds to the initial step provided in Section 8.1, for which is indicated that each prescribed functional requirement is taken up by a specific sub-system.

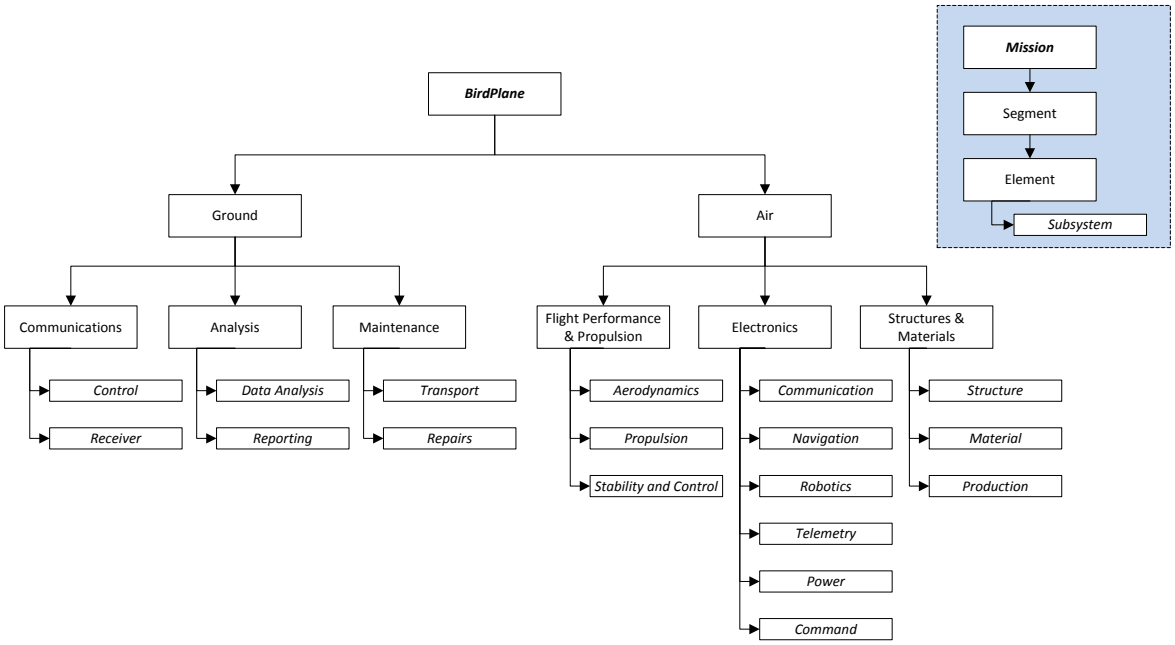

Figure 8.1: Overview of the *BirdPlane* system

The *BirdPlane* mission is divided into a *ground* and an *air* segment. The *ground* segment consists of a 'Communications element', 'Analysis element' and a 'Maintenance element'. The *air* segment contains a Flight Performance & Propulsion element, an Electronics element and a Structures & Materials element. The elements are further divided into subsystems.

8.3 REQUIREMENTS

From the list of requirements provided by the customer (Section 4.1.2), a requirements specification list is derived in the Midterm report [1]. A system with all the capabilities of *BirdPlane* as given in the top level requirements has not been listed before and it is well possible that not all requirements can be met in the final design. Each of the indicated requirements is investigated for feasibility, once proven unfeasible some requirements have to be flexed. In Section 8.3.1 the driving requirements are identified, that are essential for the delivery of a product that corresponds to the customers needs. Other requirements might have to be flexed to be able to find a feasible solution. These corresponding killer requirements are explained in Section 8.3.2. The reader must keep in mind that the term 'flexed' in this context means that the final requirement is adapted such that less demanding *BirdPlane* performance is required.

8.3.1 DRIVING REQUIREMENTS

To determine to which extent requirements can be flexed, driving requirements have been established around which the design process is focused.

- *Flapping wings (**TOP-K-8**)*: *BirdPlane* differs from existing UAVs because it flies with flapping wings. The whole aerodynamic and structural design is driven by the flapping motion of the wings.
- *Flying with a flock of geese (**TOP-K-6**)*: The unique mission of *BirdPlane* is to do research to Barnacle Geese by flying along (possibly in formation) with the flock. Loosening this requirement would nullify the purpose of *BirdPlane*.
- *Range and endurance (**TOP-K-7**)*: Existing flapping wing UAVs have short range and short flight times. To fulfill the mission of flying with a flock whilst conducting measurements on the specific airflow, it is required to develop a product that is different from existing products e.g. a long range and endurance are required.

- *Camera recording flight (**TOP-K-14**)*: From all the possible measurements that are listed in 5, the on-board camera that allows the recording of the flight is a customer need that should be met.
- *Take-off and land without human help (**TOP-K-3**, **TOP-K-4**)*: Most existing flapping wing UAVs are thrown and caught by human help for take-off and landing. The customer explicitly required to eliminate the human help, thus some self take-off and landing system will have to be incorporated in the design.
- *Educational purpose (**STA-1**, **STA-2**)*: The purpose of the design is to let the team of students experience a complete design process in a realistic way. Very detailed design of all the subsystems that would be required to really build *BirdPlane* is beyond the scope of the project. Also not (yet) existing and futuristic concepts can be used, but only with good argumentation the current state-of-the-art can be ignored, and not as an easy way out of difficult design challenges.

8.3.2 KILLER REQUIREMENTS

A killer requirement is a requirement which drives the design to an unacceptable extent [36]. Some requirements can be identified that seem to have this property. These requirements need careful investigation and/or relaxation in order to come up with a feasible design that still performs the mission in an acceptable way.

- *Data link during entire mission (**TOP-K-15**)*: Other than previously implied, this requirement does not mean a continuous data link with the ground station in Delft. Instead, *BirdPlane* will send information during the entire mission, regardless of a present link. This is because analysis of the different design options showed that none of the communication techniques will be able to provide a continuous data link with the ground base in Delft.

  What can also be concluded from this is that no continuous remote control from the ground is possible and *BirdPlane* needs to have a higher level of autonomy. Only in the take-off and rendezvous phase a continuous data transfer will be demanded, for controllability in these critical phases.
- *Self take-off (**TOP-K-3**)*: Ideally *BirdPlane* should be able to take-off and land on water and land multiple times during the full span of the mission, just like real geese do. However, the take-off will either put high demands on the wing aerodynamics or require an additional take-off system, which increases the power and energy needs. By requiring *BirdPlane* to land an take-off with the flock during the mission will therefore be a killer requirement; the overall design modifications are simply to demanding.
- *Range and endurance (**TOP-K-7**)*: The original range was set to 300 km (North to the South of The Netherlands). In an early stage this appeared to be a killer requirement and unnecessary however, because Barnacle Geese do usually not migrate this distance over The Netherlands. Instead an endurance of 100 minutes is specified.

  In no-wind conditions this corresponds to a range of 108 km. A long range and endurance is a driving requirement, but if the current requirements still turn out to be killer requirements, more relaxation is allowed to a maximum reduction in range and endurance of 50%.
- *95% recyclable structure (**TOP-K-12**)*: The many requirements on the structure for stiffness, strength, mechanics and producibility have higher priority than the recyclability. If no recyclable materials can be found which fulfill the general structural requirements, this requirement is flexed. This latter design aspect will not be dropped completely, but most likely a lower percentage of the structure will be recyclable by allowing the critical components to be made of a non-recyclable material.

8.4 OPERATIONS AND LOGISTICS

The operations and logistics are an important part of the system design. The operational flow has major impact on the system design and vice versa. The operational flow of the *BirdPlane* mission is shown in Figure 8.2.

The operations are divided into two major teams. The *Mission Control* team defines the mission objectives and plan, and gives commands to the other team. Mission control is the highest instance. It controls the scientific phase and analyses data and mission outcome. Secondly, the *Ground Control and Operation* team is responsible for the 'field work' throughout the mission of *BirdPlane*. The tasks are mostly of technical nature (e.g. setup launch site, maintenance, retrieve *BirdPlane*), however this team also detects a suitable flock of birds and predicts their flight path.

It should be noted that the division in teams is not completely fixed. It could be that only one team organizes the complete mission from the take-off site itself. Another location for the mission control is not required, but by requirement Delft is given as the main control station. The use of an advanced communication network allows for this flexibility.

8.5 RESOURCE ALLOCATION

Within the chapter of systems design, this section provides the information related to the resource allocation: setting the limitations of the assigned mass and consumption of power. For each indicated subsystem an initial estimation is made in terms of mass and power, such that all concurrently operating design teams can exactly anticipate within which bounds their expected section should remain. The primary part of these estimations originate from the Midterm [1] report, and are adapted to the final chosen conceptual design.

8.5.1 MASS AND POWER ESTIMATION

For the preliminary resource allocation of the mass (and power) systems, the previously computed estimates for specific conceptual designs [1] are revised. As a result, for the finally chosen overall conceptual design Section 9.3 each subsystem is used for this section's resource allocation. The overall estimates can be found within Table 8.1.

Table 8.1: Mass budget

Subsystem Description	**Conceptual Design**	**Total Mass: 1600 [g]**
Wing mechanism	Bio-Inspired	116
Fuselage (additional structures)	Conventional	370
Power storage devices	Conventional	670
Electronics (remaining systems)	Conventional	140
Parasite manufacturing components	'non-specific'	304

The previous estimate Table 8.1 shows the assigned masses to each subsystem corresponding to the previously decided conceptual design. Apart from the mentioned subsystem, once new effect is introduced within this table, namely 'the parasite manufacturing components'. This section corresponds to the unforeseen structural components, which 'unnoticedly' continuously add mass to the *BirdPlane* system.

Table 8.2: Power budget

Subsystem Description	**Conceptual Design**	**Total Power: 225 [W]**
Wing mechanism	Bio-Inspired	150
Electronics (remaining systems)	Conventional	50
Parasite manufacturing components	'non-specific'	25

The power budget, indicated in Table 8.2 shows for which specific subsystems a specific amount of power is assigned. The power storage device will be designed such that is can provide the required power and energy throughout the mission. As for the mass budget, the introduced section 'parasite components' corresponds to unforeseen inefficiencies and added components which consume power.

8.6 SUSTAINABILITY

With current market trends aiming on sustainable products, operations and resources, focusing on this aspect harbors a potential success for the business. In addition, sustainable design normally accompanies an efficient system which in turn will require less resources (power, materials, maintenance etc.). The sustainability of *BirdPlane* can be divided in the sustainable development and operational sustainability.

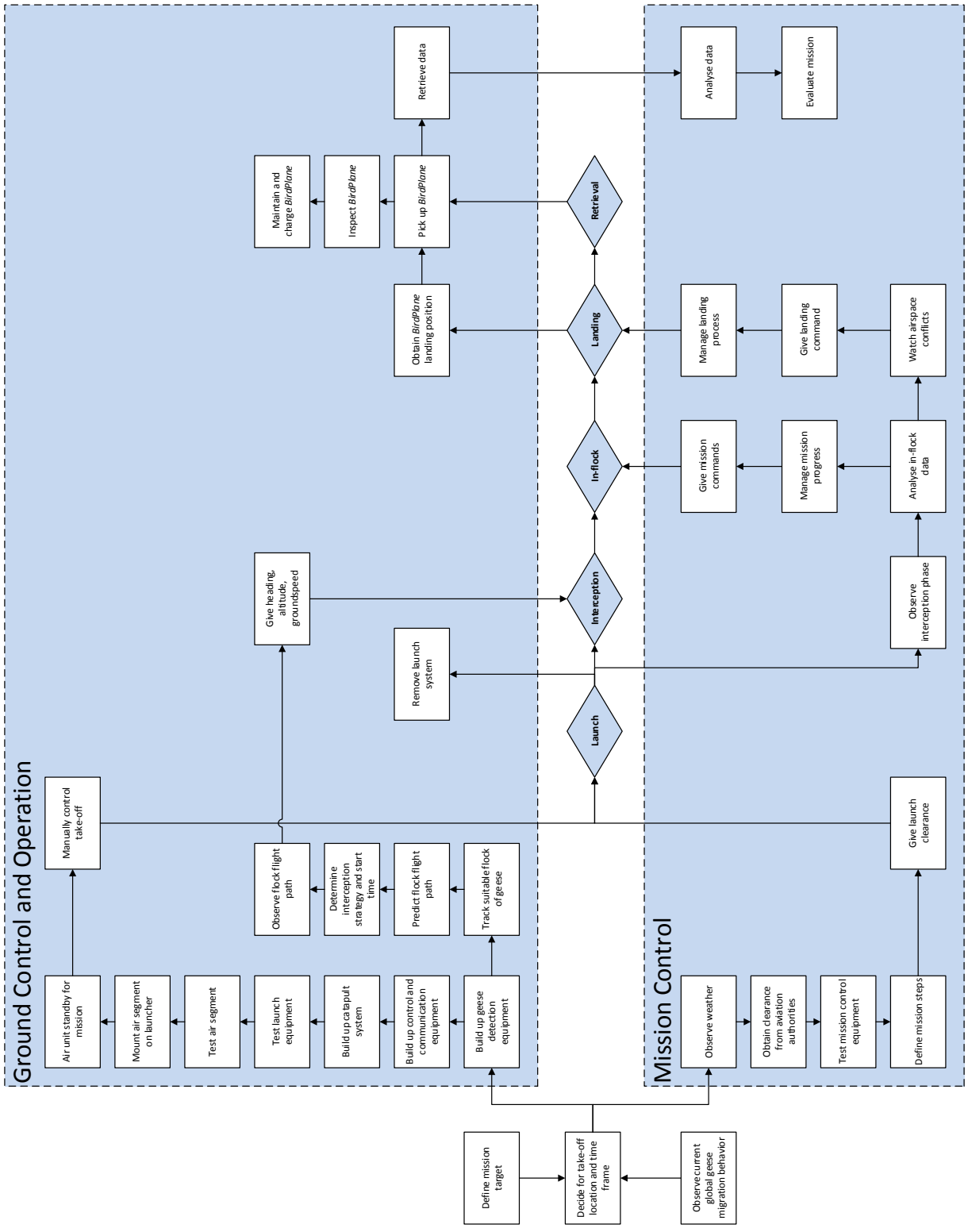

Figure 8.2: Operational Flow Diagram

8.6.1 DEVELOPMENT

For the development of *BirdPlane*, two area's can be elaborated on: efficient use of resources (power, materials, maintenance etc.) and maintainability of the product. Sustainability in the design of *BirdPlane* can be found in the following properties:

- *Smart structuring, weight reduction*:
  - The *BirdPlane* skin is a **0.2 mm nylon 6-6** (Section 10.2.4) and is only used for defining shape.
  - Structural components will be **bird-inspired**. This means that just as bone structures, the load carrying elements are hollow tubes, reducing structural weight and locally reinforced structures.
- *Use of materials*:
  - The *BirdPlane* skin is made from **recyclable nylon**. With the skin covering a significant volume of the final system, the chance of attaining an overall sustainable design is greatly increased.
  - **Self-healing materials** are used for the components that are more prone to non-fatal damages. With minor damages repaired by the material itself, maintenance resources can be reduced: The initial purchase might be more costly, but operations will greatly improve in terms of costs. The self-healing materials are made from an organic source and can be completely recycled at the end of life of *BirdPlane*.
- *Power supply and storage*:
  - **Electric power system** (actuators, motors, etc.) are highly sustainable.
  - Utilizing easily accessible, **reusable electrical power storage devices** allows for an extended use of *BirdPlane*, making it more economically interesting and sustainable.

The previous considerations mainly focused on the possible design options in relation with sustainability. Another important aspect of final sustainability can be found in the ease of maintenance. Even though a design can be considered sustainable, once it is practically impossible to replace or repair any systems, the use of resources will increase beyond initial sustainability. Sustainable considerations in terms of maintenance are: order and method of implementation, moisture and corrosion prevention, accessibility of certain subsystems. In Section 11.4.2 further elaboration on maintainability of *BirdPlane* is provided.

8.6.2 OPERATIONAL

Operation of *BirdPlane* should also be beneficial in terms of sustainability. In accordance with the mission statement described in Section 4.1.4, the possible operating considerations in terms of sustainability are:

- In order to save power, *BirdPlane* should utilize the gliding configuration mode when applicable.
- During cruise flight, *BirdPlane* should sometimes fly in the non-flapping glide mode when necessary or appropriate to save the power consumption.
- The primary wing should constantly allow span-wise folding and span-wise twisting in order to reduce drag and limit power consumption.
- The operational conditions of the *BirdPlane* mission are such that thermal differences can be utilized to the full extent of the mission.
- At cruise velocity (18 m/s) the power consumption is at a minimum due to the wing planform design as explained in Section 10.1.1.

9 Conceptual Design

In the previous chapters, *BirdPlane* has been fully discussed in both technical performance requirements and mission capabilities. From the point of market analysis, the economical 'green light' has lead to the initiation of the possible designs for *BirdPlane*. in the previous chapter, by means of systems design, each sub-system has been assigned a specific set of tasks and design constraints by means of resource allocation. In this section, the conceptual designs which have been the result of mission and requirement analysis, are treated. By first describing the five concepts, then summarizing the trade framework the final concept is chosen.

9.1 Configurations

Selecting a proper configuration for an innovative aircraft design is not a straightforward application. New fields must be explored and different, novel ideas have to be evaluated before any sensible conclusions can be drawn about how the final concept should look like and perform. Extensive literature study and brainstorming preceded the conceptual design phase. Striving to achieve a plausible balance between innovation and credibility, five different concepts were created. In this section, a summarized qualitative overview is given of these concepts.

Bio-inspired Concept is the concept most resembling the features and behavior of a real Barnacle Goose. With an internal structure inspired by the lightweight bird bone structure and a pair of double hinged wings able to perform complex wing kinematics, this configuration combines enhanced flight performance of migrating birds with efficiency. In addition to 3-dimensional flapping motion, a fully rotatable horizontal tail is added for stability and maneuverability. The complex wing kinematics are best actuated by a combination of mechanics and artificial muscles. Together, the wing mechanism enables the continuously varying wing twist, flapping and folding required for most aerodynamically efficient flight. Aided by robotic feet that can rotate the body and wings to achieve the required clearance and desired angle of attack, *BirdPlane* will take off by flapping only. Keel-like shape of the bird-inspired fuselage will support water landing. The fuselage is made of polymers, with a stiff, watertight lower side to absorb landing impacts and provide buoyancy. New manufacturing techniques, such as 3D carbon fiber printing are considered for creating a strong, complex, but lightweight internal structure while minimizing structural weight and production waste. A feather-like covering or flexible skin is used to accommodate the 3-dimensional flapping motion of the wings. The electronic and propulsive power are supplied by a lightweight battery.

Conventional Concept incorporates simplified bird-like features, making it more reliable than the Bio-inspired Concept. Nevertheless, by simplified mechanics, the flight efficiency greatly decreases by absence of fully bird-like motions such as fully equipped wing twist. The structure will be a composite truss of carbon fiber, with non-load carrying ultra-thin foam fairings giving *BirdPlane* its bird-like shape. It has one double hinged wing, however the motions are restricted to simplify the mechanisms and usage of actuators. The gear-and-crank wing mechanism with double linkage ensures flapping, folding and flexing motions of the wing. The twisting motion is achieved by incorporating a servo in the wingtip. For electrical power a separate battery is used next to the combustion engine. This concept is aided in take-off and landing by a spring system.

Three-Wing Concept combines existing flapping wing technology with conventional aircraft wings in a 3 wing setup, two static and one flapping. Although the extra wings create additional drag and add weight, they also generate substantial amount of extra lift and provide stability. Some effective flapping wing kinematics, such as the 'clap-and-fling' used by hummingbirds [37], require a shoulder joint that can at least partially rotate around three axes. This type of flapping provides more flexibility in force vector pointing, but is more focused on thrust generation rather than lift. To accommodate this, the main wing is mounted to the fuselage by means of a ball joint or a three-axis-gimbal joint. The canard and the tail provide sufficient stability and offer room for mounting of control surfaces. Furthermore, this setup has an increased surface area, which can be covered by solar panels for power supply in combination with a rechargeable battery. Take-off and landing is assisted by a wheeled, non-retractable landing gear. The material used for the body and wings is foam; the choice is mainly influenced by the desire to minimize the weight while achieving sustainable and simple production.

Dragonfly Concept has a double-flapping wing configuration, based on the common dragonfly. The two wings are of equal size and situated directly behind each other. During cruise the wings flap in opposite phase. The double-flapping wings generate more lift per effective span, which allows designing for a higher maximum take-off weight, thereby creating room in the mass budget for the power system. Also, the two pairs of wings flapping in opposite phase might make the precise station-keeping easier to achieve, as the fluctuation of the *BirdPlane* body due to the flapping movement can be moderated. All wings are attached to the body by a single hinge and a single spar. The angle of attack of the wings is controlled by active twist, actuated by a servo mounted at the tip of each wing. The additional weight at the wing tips added by the servo fits the anatomy of the dragonfly, which also has a heavy cell in the wingtip. In-flight control is achieved by de-coupling the wing actuation, meaning that each wing can be steered independently. Although this may complicate the control system, requiring more calculation on power output, it also brings in an advantage; as it is no longer required for control and stability, the tail can be eliminated from the design, saving structural weight and reducing aerodynamic drag. Take-off will be realized with a ground based launch system (catapult). The wing material should be thin and lightweight, yet stiff enough to keep the shape without requiring ribs.

Futuristic Concept is the most out-of-the-box concept from the five, since its skin is fully covered in a seemingly, not application proven material. Its feasibility might grow in the near future depending on the rate of technological development of the electro-active polymers (EAP), which have promising properties for advanced wing morphing. The fully EAP-composed wings are connected to the body in a blended wing-body configuration. The polymer needed for this concept should easily adhere to the EAP and be stiff enough to carry the loads. *BirdPlane* will land on its belly; the lower part of the fuselage should be able to withstand impacts. For take-off, *BirdPlane* will be launched by a catapult, inducing other loadings the fuselage has to sustain. The wings are solid because no internal actuators are required, but the fuselage has to be hollow to accommodate the power supply and electronics. Power is supplied by batteries and flexible solar panels covering the entire wings and fuselage. There is a high demand for efficient lightweight solar panels and batteries and developments in this field are going fast. Therefore, improved characteristics for these systems can be assumed to become available in the near future. Ideally, the whole structure should be 3D printed to allow more freedom in the design. Future possibilities for 3D printing of EAP still have to be investigated.

9.2 TRADE SUMMARY

The description in the previous section is rather qualitative. A substantially more detailed analysis was required to be able to make a rational decision about which concept is more suitable than the other. This quantitative analysis was presented in the Mid-Term Report [1].

To be able to select the best design option for the current mission, the five concepts were evaluated, compared and traded-off based on specific trade criteria. To aid this purpose, a trade framework was operated. The trade criteria were chosen such that they directly reflect the *BirdPlane* mission and system requirements. The criteria were categorized into four elements, each subdivided into two criteria. With two additional criteria, the trade framework comprises of a total of 10 trade criteria. Each criterion was weighted in accordance to its degree of criticality. The elements and their respective weights are shown in Table 9.1.

Table 9.1: Categorized trade criteria with respective weights

Category	Criterion	Weight
Flight Performance & Propulsion	Aerodynamics	20%
	Stability and Control	10%
Structures & Materials	Integrity	15%
	Manufacturability	5%
Electronics	Efficiency	10%
	Specific Energy	10%
Mission	Cost	5%
	Reliability	10%
Additional	Sustainability	5%
	Element specific criterion	10%
	Total	**100%**

Each concept was evaluated per criterion and graded according to its performance in terms of satisfying that criterion. The grading is converted from qualitative to quantitative score using the grade conversion in Table 9.2.

Table 9.2: Trade-off grading

Symbol	Grade	Score
−−	Unusable	-2
−	Insufficient	0
+	Acceptable	1
++	Excellent	2

An overview of the trade-off is presented in Table 9.3. The table shows the five concepts, the trade criteria and weight factors per criterion. Below, the concepts are briefly discussed starting from poorest performing concept to the best.

Futuristic Concept has the poorest performance according to the trade method. The available electro-active polymers require high structural mass due to the low power density. Also, these polymers are quite expensive. Unpredictable behavior of the mechanics and the volatile solvent makes the concept unreliable. The fully morphable wings have very low parasite drag. The V-tail provides sufficient longitudinal and lateral stability. The current configuration does not provide self-take-off and is largely dependent on the new developments in the field of electro-active polymers. The score totals to a negative value, as none of the subsystems showed sufficient performance.

Three-Wing Concept scores slightly higher in performance than the *Futuristic Concept*. In this configuration, *BirdPlane* cannot generate enough propulsion to fly with flapping wings only. A large tail area is required to provide static longitudinal stability. Because of manufacturing limits, the structure has to be over-designed, with a relatively large mass as a result. Although the simple flapping mechanism is of low complexity and easy to install, the take-off system with non-retractable wheels has critical disadvantages as an additional thrust generating device is necessary to gain enough speed for take-off. In addition take-off is only possible on pavement. Lastly, the use of solar cells for the power supply has turned out to be inefficient; using the Li-S battery, the same amount of power can be provided with lighter weight, and thus, the added complexity due to the installation of the solar cells is not worth the effort.

The *Dragonfly Concept* has a simplistic and easy to produce construction and scores very well in structural integrity. The aerodynamic performance was average: the wings have limited morphing capabilities and would require operation at very high flap velocities in order to sustain flight by flapping. The fuel cell and available fuel are very expensive in purchase. Refuelling during operation is economically favorable either. Although the fuel system provides sustainable power and the structure is recyclable, the hydrogen fuel cell system is relatively heavy-weight, even with a conceptual low-weight fuel tank.

Bio-inspired Concept seems very promising. Its wing kinematics cover the full range of motion required for enhanced performance and efficiency. If 3D printing carbon fiber is proven to be successful, complex, variable cross-sectional shapes can be created, in which the reinforcement would only be added at maximum stress locations. This would not only result in lightweight, strong structure, but would also help limiting production waste. Unfortunately, the artificial muscles are still very conceptual and inefficient, therefore, impractical for the *BirdPlane* design. Also, the self-takeoff system through robotic feet-aided flapping is not feasible unless the wing is fully morphable and as efficient as the actual Barnacle Goose.

Conventional Concept has the highest score according to Table 9.3. As the concept includes both an elevator and a rudder, stability and controllability are excellent. Flight efficiency is limited, because the configuration only provides twisting at the wing tips. Since the engine is directly connected to the wing by a set of gears - as including a clutch would result in a heavy and complex system - the wing actuation is continuous, unless the engine is shut off. Although the combustion engine is very promising in terms of energy density, continuous wing actuation is not acceptable as the mission relies on flight with varying flap frequency for a great portion of it. It terms of reliability, it is most likely the engine that will threaten the success of the mission. The spring take-off system is not feasible, as it induces high loads and requires a very strong structure.

For the final concept another step is taken in the trade-off: each subsystem is considered separately from its configuration. The highest scoring subsystem in its category is judged upon its integrability into the two highest scoring configurations. This way, if possible the best solutions per subsystem are combined into the *Final*

Concept (Section 9.3) which is a hybrid of the *Bio-inspired Concept* with its bird-like, innovative solutions, and the highly mature and reliable *Conventional Concept*.

9.3 FINAL CONCEPT

The tail of the *Conventional Concept* performs very well with little use of resources. Including the fully movable and fanning tail of the *Bio-inspired Concept* would make *BirdPlane* even more goose-like, which is an essential aspect for sustaining stakeholder needs. The scientific prospect of a fully fanning and rotatable tail is given extra value, which is why it shall be realized for the final concept, on the cost of a more complex control system. The tail arm is relatively short and the fanning mechanism reduces the tail drag considerably. Furthermore, volume reduction is achieved by not having a vertical tail plane. In the worst case scenario where the implementation of the fanning and rotatable tail is infeasible, it can always be rolled back to a conventional tail as a safe solution.

The low-weight mechanics of the *Conventional Concept* perform quite well and will be further optimized during the preliminary design phase. The mechanics of the *Bio-inspired Concept* were deemed unfeasible for their use of artificial muscles. The challenge for the final design process is to implement all required and desired degrees of freedom, without usage of artificial muscles.

The body shape will be based on the *Bio-inspired Concept*, hence goose-like. A goose-like shape increases the acceptance of *BirdPlane* in the flock. Especially the design of the goose neck comprises a number of opportunities and challenges. Since the stabilization of the camera was identified as highly important, the iso-elastic neck mechanism is given a high importance. Especially from a scientific point of view, the implementation of the neck is considered interesting. Since a number of difficulties are included in the implementation, a fixed neck is the fall-back solution.

The power-supply of the *Conventional Concept* is controversial in terms of sustainability. When operated on bio-fuel, the small combustion engine can be CO_2 neutral. Moreover, the environmental impact of e.g. batteries cannot be underestimated. That being said, the internal combustion engine is still discarded as a viable option. The noise and exhaust gases it produces will jeopardize the bird-following mission. Furthermore, serious doubt was raised concerning the reliability of the engine. The engine cannot operate continuously, because of the gliding segments of the mission. In the end, it was decided to switch to Li-S rechargeable batteries and an electrical motor for the *Final Concept*.

The spring system was discarded for the *Final Concept*. It will require to much added structural mass to cope with the fast accelerations. However, the design team still wants to include a take-off/landing system that requires no human help. The vertical take-off of the Bio-inspired cannot be realized for this concept. The mechanics limit infinite wing motions (twisting and flap induces velocities). For these motions, some design parameters which needed to be fixed are optimized for cruise thus limiting self-takeoff. Only the frequency of the flapping can be adjusted, but this will not increase the lift enough, leaving the catapult system of the *Dragonfly Concept* as the only well performing system that can be adapted to the *Final Concept*.

Table 9.4: Design configuration of the Final Concept

Subsystem	**Design**
Wing	A single symmetric flapping wing, double-hinged to the body. Further wing twisting will be evaluated. Structure consist of ribs and a single spar, with a non-load carrying skin.
Body	Goose-like fuselage shape with a skin covered truss structure. Goose-like neck with iso-elastic stabilization mechanism.
Tail	A non-flapping rotatable and fanning tail.
Take-off	Catapult launch.
Propulsion	Slender flapping wings with tip twisting.
Robotics	Mechanical mechanism driven by an electrical motor.
Power supply	Li-S batteries.

Table 9.4 gives an overview of the final design configuration. The design comprises a lot of bird-inspired features and proven mature technology. The implementation of all features will be a challenge. This concept is the result of extensive analysis and trade-off between the different concepts. The range and endurance requirements limit

Table 9.3: Trade-off summary

Element	*Flight Performance & Propulsion*		*Structures & Materials*		*Electronics*		*Mission*			
Criteria	**Aerodynamics**	**Stability & Control**	**Integrity**	**Manufacturability**	**Efficiency**	**Specific Energy**	**Cost**	**Reliability**	**Sustainability**	**Additional**
Bio-inspired	(++) Fully morphable wings with spanwise folding and chordwise twisting. Very likely to reach and maintain efficient cruise flight.	(+) Limited lateral stability due to lack of vertical tail surface. Excellent controllability due to rotatable tail.	(++) Low weight structure of 484 grams. Succesful manufacturing methods could even further reduce the weight.	(+) Productions depends on 3D printing technologies and materials. CFRP printing is a good option.	(--) Efficiency far too low to be feasible, flap frequency not high enough without active cooling.	(+) With only Li-S batteries, 200W can be provided with 670g of mass, 560cm3 of volume	(+) Carbon 3D printing expensive in production and repairs. Artificial muscles production is very economical.	(--) Usage of artificial muscles is still very conceptual. Frequency stability and loading characteristics unknown.	(++) 3D printed gives little waste in production. Recyclable structure	(++) Has biomimicry which could make it easier to fly in formation. High posibility of self-takeoff.
Conventional	(+) No wing twisting capabilities along the entire wing. Relatively inefficient cruise flight.	(++) Longitudinal and lateral stable. Excellent controllability due to rudder and elevator.	(++) Low weight structure. Preliminary analysis puts the mass at 458 grams.	(+) Easy to produce structure. Partly off-the-shelf parts. No high-tech facilities/machines are required.	(-) Efficiency sufficient. Large gear ratio needed to convert to desired frequency. The engine has to turn off during gliding, to save fuel.	(++) With 200W nominal power output and 100 min mission duration, the system has a mass of 425 gram.	(-) Combustion engine not cheap to purchase and operate.	(+) Tried and true wing flapping mechanics. Mechanical complexity in the combustion engine.	(+) Production sustainable. Recyclable structure. Less sustainable without biofuel.	(-) A spring system will allow for self take-off, but induces very high loads. Minimum take-off speed is relatively high.
Three-Wing	(--) Only twist along the chord. Not capable of generating enough aerodynamic force to fly. Cruise barely possible.	(-) Large tail area needed for longitudinal stability. Insufficient lateral stability and controllability due to lack of vertical tail.	(+) The preliminary mass estimate is set at 812 grams. The structure is super overdesigned due to manufacturing limits. Very high yield loads.	(++) Foam covered with carbon fiber cloth. Very easy production technique.	(+) Very efficient energy conversion. Gearbox needed. Inefficient way to mimic movement.	(+) Solar cells and Li-S battery can provide 200W power output with 758g of system mass	(++) Economical structure and repairs. Electrical engine and solar panels are cheap in operation.	(++) Simple flapping mechanism with electromotor. Low amount of complexity increases reliability.	(+) Batteries and solarcells can provide a zero-emision solution. Unfortunately, a lot of material use and waste in production.	(-) Self-takeoff pratically impossible with wing configuration. Multiple wings allow for higher MTOW at cruise velocity.
Dragonfly	(-) Restricted morphing capabilities. Flap velocities are required to be very high. Cruise will be inefficient.	(-) Large tail area. Acceptable lateral stability. Insufficient controllability due to lack of tail.	(++) Simplistic and low weight structure of 317 g.	(++) Simple construction and very managable production technique.	(+) Very efficient energy conversion. Gearbox needed. Inefficient way to mimic movement.	(--) Hydrogen fuel cell system has a mass around 970g even with a very conceptual light fuel tank.	(--) High priced fuel cell. Costs for selected fuels are very high. Carbon fibre structure of average price.	(-) Control system is complex and unreliable. Self-designed fuel tank is conceptual.	(++) Little material used. Recyclable structure. Hydrogen cell provides sustainable power.	(++) Self-takeoff definitely possible. High maneuverability with 4 individually controlled wings.
Futuristic	(+) Fully morphable wings. Significantly lower parasite drag. Optimal cruise capabilities. Limited induced velocities.	(+) Longitudinal stable. Controlability and lateral stability acceptable due to coupling of moments introduced by the v-tail.	(--) Currently available electro active polymers require a minimum structural mass of 5.5 kg. This is due to the low power density of the IPMC polymers.	(+) Extreme cost of the electro active polymers makes the manufacuring process somewhat complicated.	(-) Applications have been studied. Combination of frequency and flap angles too low.	(+) Solar cells and Li-S battery can provide 200W with 713g of total system mass	(--) Electro-active polymers are very expensive, around €10,000/kg. Repairs are costly.	(--) Unpredictable behavior of electro-active polymers. Solvent could dissipate very fast.	(-) Solar cells are sustainable and contain no heavy metals. However, the large mass fraction of electroactive polymers is not recyclable.	(--) Incapable of self-takeoff. Largely dependent on the development of electro-active polymers.
Weight	20%	10%	15%	5%	10%	10%	5%	10%	5%	10%

Trade-off grading: (--) Unusable | (-) Insufficient | (+) Acceptable | (++) Excellent

the design options, but also the scientific value of the design was driving. An impression of what the finalized *BirdPlane* design will look like is given in Figure 9.1.

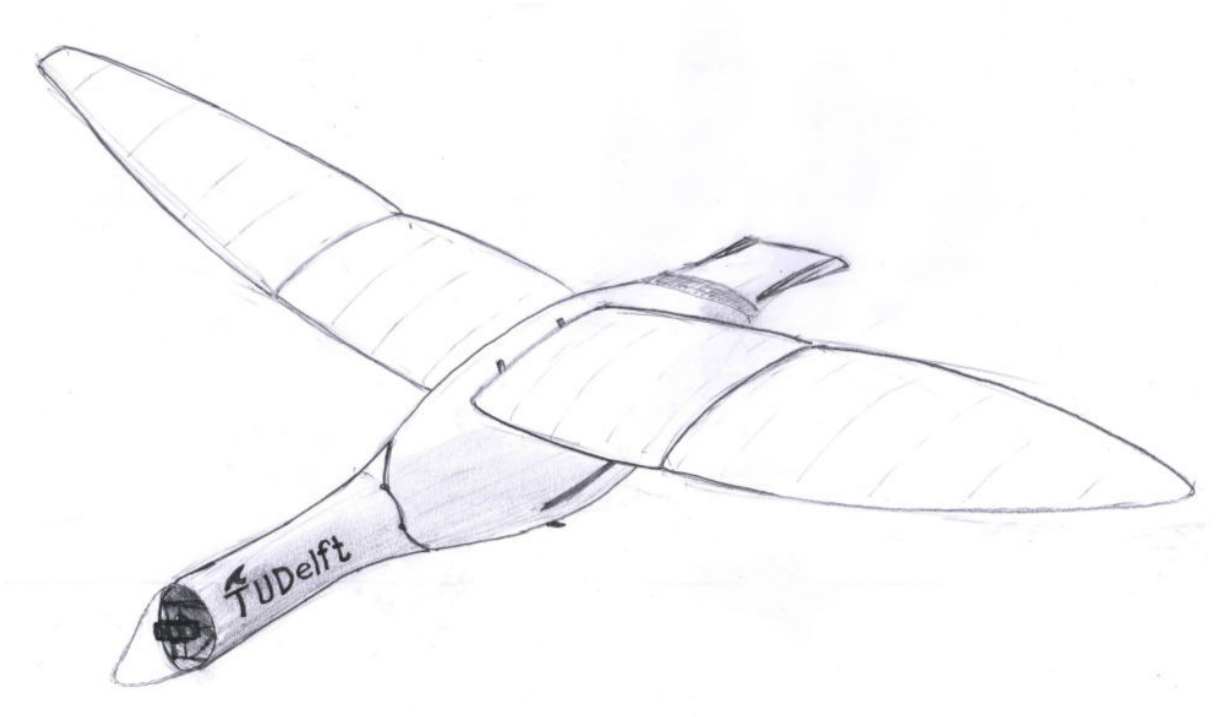

Figure 9.1: Sketch of the final selected *BirdPlane* concept

10 Preliminary Design

The preliminary design is considered as the further elaboration and development of the conceptual design in pursuit of complying with the system and mission requirements. The conceptual design is fully described and fixed within Chapter 9, and the outline of each sub-system has been covered. This chapter provides a more specific view upon how all the requirements are met, and the interrelation between the subsystems are utilized. This chapter comprises the following sections: First, an analysis of the flapping-wing aerodynamics and flight stability (Section 10.1) is given. Then the design of the mechanisms and structures to provide relevant motions (Section 10.2) is discussed and elaborated. This is then followed by the implementation of required electronic system (Section 10.3). Lastly, the final layout of the *BirdPlane* system is provided at the end of the chapter (Section 10.4).

10.1 Flight Performance & Propulsion

In this section, the flight performance of the final design is described and analyzed. First, the aerodynamics of the flapping motion of *BirdPlane* is explained in Section 10.1.1. Thereafter, the stability and controllability of *BirdPlane* is studied from the stability analysis done using XFLR5 (Section 10.1.2). Also, the turning performance and possible effects of implementing feet are stated in this section.

10.1.1 Aerodynamics

One of the outstanding features that *BirdPlane* includes in its design, are the flapping wing aerodynamics. This striking feature will grant the final system to near the bird-like properties which were striven towards from the beginning of the assignment. For this final phase, an overview of all the work that has been performed on the analysis of the aerodynamic performance, is treated. The structure of this section is according to the final programmed product ('Birdplane-aeromech.mat'): Firstly the general ideas derived from real bird flight are treated, secondly the 'Jones-based method' described in the Midterm report is summarized, thirdly the optimization of the *BirdPlane* flight mechanism is clarified and finally the resulting wing design is described completely.

Bird-Inspired Aerodynamics

As mentioned in the Midterm report [1], once starting on the analysis of a relatively new physical phenomenon in the world of engineering, it is always wise to see how the world's most optimal and subtle entity solves this problem. That mentioned entity is of course nature itself; by analyzing birds in flight a general conception of what has to be included in the *BirdPlane* system is created. Summarizing the initial research, the following has been found about bird-like flight:

- The only non-powered phase within flight, indicated by gliding:
  - *Rest phase, Gliding (G)*: Initially, the birdlike wings are situated at rest. This phase is almost fully reproduced by the gliding phase. In this phase no energy is transfered to the flow and therefore no thrust is generated. It is classified as a no-force generating phase related to flight.
- For any flight phase, whether it is cruise, acceleration or climb, two decisive, powered phases within one flapping period can be identified:
  - *Downstroke (2)*: Being the longest of the two primary force generating phases, this phase is determining in providing most of the lift and thrust required for each flapping period.
  - *Upstroke (1)*: Generally, this flight phase is aimed for to be as short as possible. Primarily, birds try to limit their surface area in order to reduce negative lift generated by flapping up. This reduction of surface area can be identified by span-wise folding, which is primarily done by birds for which the wingspan exceeds 1.2 m.
- The primary wing parameters, which are continuously varied by birds are the following:

- *Span-wise twist angles* (θ): By means of full airfoil twist, the total lift-vector can be directed in either lift or thrust preferred direction. Birds generally utilize this feature to switch between flight phases. For example, advancing from cruise to acceleration, the wings are first pushed on to generate more lift. Then the twist is increased to redirect the additional amount of overall lift to generate thrust and thus accelerate.
- *Flap induced velocities* (V_1, V_2): The induced velocities caused by flapping play an important role in the generation of lift, for the case where a general airliner only uses forward velocity
- *Flight velocities, horizontal wing motion*: A specifically small portion of all bird species perform this type of motion. Nevertheless, studies have shown that Barnacle geese actually do utilize the effects of horizontal wing motion. The primary effect again lies in the benefits of the overall wing velocity as well as redirecting the respective lift forces.
- *Flap angles* (ξ): This final wing parameter simply indicates the total angle over which the wings flap from highest to lowest position during the downstroke. In the paragraph Aerodynamic Optimization later in this section, the interrelation between flap angles and induced velocities is clarified by the introduction of $r_{u/d}$.

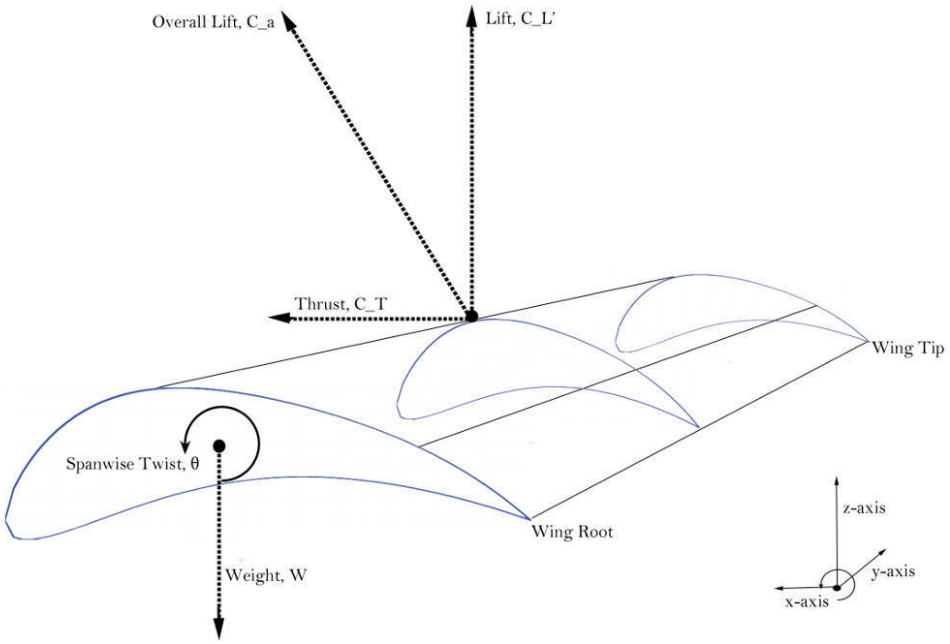

Figure 10.1: Aerodynamics reference frame

AERODYNAMIC FORCE GENERATION

In the first paragraph of this section about bird-inspired aerodynamics, the facts about the utilized wing motions and parameters have been specified. In this paragraph, the expected circulations, forces and angles are indicated. For a full verification of these estimations, the reader is advised to review the section Aerodynamic Analysis and Verification of the Midterm report [1]. For the sign conventions utilized for the force specifications, refer to Figure 10.1:

- *Gliding flight*; characterized by the smallest overall lift force vector (C_a):
  - **Lift**: The primary part of the total lift vector is used to counteract the weight of the bird, limiting the descent rate.
  - **Thrust**: The remaining amount of C_a, is used for thrust, which will almost fully counteract the overall drag component.
  - θ_b: In order to maintain altitude as much as possible whilst limiting deceleration, the span-wise twist angles are directed positively and are relatively small, limiting the angle of attack (α).
- *Downstroke*; portion of flapping with highest effective force generation.

  - **Lift**: As mentioned before, this phase is characterized by the generation of the full amount of lift counteracting weight. Therefore, the primary part of the overall lift is directed perpendicular to the flight direction.
  - **Thrust**: Estimating that 95% of the C_a is directed in opposing weight direction, only a small portion of the lift remains for counteracting drag.
  - θ_b: The span-wise twist angles are positively oriented and relatively large within this flight phase, this is mainly the result of the large induced velocities due to flapping itself.
- *Upstroke*; this short portion of the flapping period is primarily focused upon limiting lift forces.
  - **Lift**: Due to the negatively oriented flow velocity, the C_a is directed downward. It is therefore required to very much limit the general generation of lift itself (which is done by span-wise folding), and by focusing on the thrust component. Expectations are that due to limits in twist and folding, the lift vector corresponds to 35% of the total lift force during this flap phase.
  - **Thrust**: Even though the lift force is oriented downward, the thrust vector is still in opposing drag direction with a magnitude of 65% the total lift force. Therefore, the limits of maximum twist are used to redirect the total lift in thrust direction.
  - θ_b: In order to limit the time spent in the upstroke phase, the flap velocities are the highest for the entire flapping period. This fact directly results in very high twist angles, which are negatively oriented.

COMPUTATIONAL METHOD

The expectations generated from the previous paragraph are quantified by the method explained in this paragraph. Since the Midterm report, the final phase of the project has mainly led to the elaboration and fine-tuning of the aerodynamic model [38] used to quantify the effects of having a flapping wing UAV. The method in which this is done is composed of two parts. Firstly, the equations which have finally led to the verification and application of the Midterm results are treated and secondly the optimization and practical application of the final program.

Jones' Method The generally applied method, which sets a base for the optimization of both utilized induced flapping velocities as well as the choice in aerodynamic angles (θ, α), is shortly discussed. As mentioned in the Midterm report, the wing analysis is based upon the application of the 'Kutta-Joukowski Circulation Theory', which is in turn rewritten for the application of three different flight phases: Downstroke (2), Upstroke (1) and Gliding (G). The distinction between the flight phases is applied in the final computation by utilizing scaling factors, which originate from a theory proposed by R.T. Jones [38]. Combining both methods a slightly simplified, but powerful tool is created to quite accurately predict the generation of aerodynamic forces and finally the power required (P_{req}).
The previously described method can be discussed by means of three blocks, each of which corresponding to an optimization for circulation, computation of specific aerodynamic angles and finally the determination of aerodynamic force coefficients. This first block corresponds to the equations given by Equation (10.1) to Equation (10.6), finalizing the total circulation distributions:

$$\Gamma_{mg} = \frac{m_m g}{\rho V_G b} \tag{10.1}$$

As a first estimate of the circulation value, which is required for the computation of the circulation distribution along the wingspan for each flight phase, Equation (10.1) is used. The specific equation corresponds to the conservative value provided by performance in gliding. Since it is known that birds practically near an elliptical circulation distribution in this flight phase, this initial estimate will result in a conservative one.

$$y_{\Gamma N} = \frac{c_{\Gamma N}}{6\pi} \tag{10.2}$$

Equation (10.2) shows the Jones' factor, which enables the distinction between the three flight phases, corresponding to different polynomials in span-wise circulation distribution in Equation (10.5). The flight phases are indicated by the subscript N. Typical values for these factors are: $C_{\Gamma G}$: 7.0 - 8.0, $C_{\Gamma 1}$: 5.0 - 6.0 and $C_{\Gamma 2}$: 8.5 -9.0.

$$k_{\Gamma N} = \frac{\frac{2-\pi \cdot y_{\Gamma G}}{I_0 C_\alpha} + \frac{270}{b} \cdot (\frac{1}{\pi} - \frac{2}{3} y_{\Gamma G})}{\frac{2-\pi \cdot y_{\Gamma N}}{I_0 C_\alpha} + \frac{270}{b} \cdot (\frac{1}{\pi} - \frac{2}{3} y_{\Gamma N})} \cdot \frac{V_N}{V_G} \tag{10.3}$$

The Jones' factors are finally put to use in the determination of the scaling factors, which allow for the compensation of relative shape of the wings during each flight phase. Due to the increased concave shape along the wingspan, during the downstroke more circulation can be contained thus increasing the overall lift capabilities. By means of this factor, this type of phase shifting is accounted for.

$$\Gamma_{mN} = \Gamma_{mG} \cdot k_{\Gamma N} \tag{10.4}$$

$$\Gamma(y) = \Gamma_{mN}\left[\left(\frac{12}{\pi} - 6y_{\Gamma N}\right) \cdot \sqrt{1 - \left(\frac{y}{s}\right)^2} + \left(18 y_{\Gamma N} - \frac{24}{\pi}\right) \cdot \cosh^{-1}\left(\frac{y}{s}\right)\right] \tag{10.5}$$

$$V_i(y) = \Gamma_{mN} \cdot \frac{9}{s}\left[\frac{1}{\pi} - \frac{2}{3} y_{\Gamma N} + \left(\frac{\pi}{2} y_{\Gamma N} - \frac{2}{3}\right) \cdot \frac{y}{s}\right] \tag{10.6}$$

The two equations (10.4, 10.5) allow for the final determination of the span-wise distributed circulations for each flight phase. Therefore, the resultant from this 'first computational block' are $\Gamma_G(y), \Gamma_1(y), \Gamma_2(y)$ which thus correspond to and are optimized for the corresponding flight phases. The latter equation gives the induced velocity.

With the required circulation values in place, the second phase of computation can be started. For the previous computational block, only two assumptions have been made, namely that the conservative mid-span circulation during gliding is equal to Equation (10.1), and, the wing shape phase shifting is fully taken into account by means of the Jones' factors. The second of the three computational blocks includes additional assumptions related to the final layout of the planform and overall design of the wings. The primary estimates are found by once more analyzing the birds themselves, providing accurate estimates for: Planform corresponding to function for chord length 'I(y)', airfoil estimate directly related to 'C_{a_α}' and the total velocity over the wing 'V_{CN}'.

Setting the initial estimations for the wing design, the overall lift coefficient is computed by using Equation (10.7).

$$C_a(y) = \frac{2\Gamma(y)}{I(y) \cdot V_c(y)} \tag{10.7}$$

The expected shape of the airfoil is used for future calculations in Equation (10.8). Note that this planform estimate simply corresponds to an elliptical wing shape, in the paragraph about optimization later in this section more planforms are investigated to match birdlike properties.

$$I(y) = 2 \cdot \left(\frac{1}{b} \cdot \left(1 - \left(\frac{y}{a}\right)^2\right)^{\frac{1}{2}}\right) \tag{10.8}$$

As mentioned, from the expected C_{a_α} along the wingspan and the estimated airfoil shape, the design angle of attack is determined. From this important estimate, all additional angles of attack can be determined by equations Equation (10.9) to Equation (10.12). Once more, each flap period phase is indicated by means of the factor 'N', corresponding to Upstroke (1), Downstroke (2) and Gliding (G):

$$\alpha_{\text{design}_N}(y) = \frac{2\Gamma_N(y)}{I(y) \cdot V_{c_N}(y) \cdot C_{a_\alpha}} \tag{10.9}$$

$$\alpha_{\text{design}_N} = \alpha_{i_N} + \alpha_{i_{flap.N}} + \theta_N \tag{10.10}$$

$$\alpha_{i_N} = \tan^{-1}\left(\frac{V_{i_N}}{V_G}\right) \tag{10.11}$$

$$\alpha_{i_{\text{flap},N}} = \tan^{-1}\left(\frac{V_{\text{flap}_N}}{V_G}\right) \tag{10.12}$$

The final block of the Jones' method is introduced with the knowledge off all aerodynamic angles along the wingspan for each flapping phase. As an assumption, the prescribed method assumes the existence of three discrete flight phases. In the next section, the computational method is inverted to match real life, continuous flight properties.

Therefore, it is possible to simply utilize the previously computed coefficients and aerodynamic angles within the reference frame. This leads directly to computation of the lift coefficient and thrust coefficient in Equation (10.13) and Equation (10.14).

$$C_{L_N} = \cos(\alpha_{\text{design}} + \theta_N) \cdot C_{a_N} \quad (10.13) \qquad C_{T_N} = \sin(\alpha_{\text{design}} + \theta_N) \cdot C_{a_N} \quad (10.14)$$

The previous lift coefficient is directly related to the lift induced drag. Before application is possible though, the 2-dimensional lift coefficient is converted to the 3-dimensional one applied in Equation (10.15). By using data from Barnacle Geese themselves, the final assumption regarding the parasite drag C_{D_0} is found to vary from 0.008 till 0.016. Assuming that *BirdPlane* will not be as perfectly engineered as a real Barnacle Goose, the initial estimate is set at a conservative value of 0.03 [39].

$$C_{D_N} = C_{D_0} + \frac{C_{L_N}^2}{\pi \text{AR} e_N} \quad (10.15) \qquad C_{D_{dN}} = C_{D_N} \cdot \sin(\alpha_{\text{design}} + \theta_N) \quad (10.16)$$

$$C_{L_{dN}} = C_{L_N} \cdot \cos(\alpha_{\text{design}} + \theta_N) \quad (10.17)$$

With the application of the latter three equations, the initially applied computational method allows for the full computation of:

- *Circulation*: Analysis of bird-like circulation distributions for each individual flight phase, resulting in application of finite-wing estimations.
- *Aerodynamic Angles*: Applying a discrete flight phase estimate (2,1,G), each relevant angle can be determined for each point along the wingspan.
- *Force Coefficients*: All force coefficients are determined with preceding knowledge of the aerodynamic properties of the flapping wings.
- *Total Forces*: The determination of the aerodynamic coefficients along with the discrete knowledge of the velocities enables to exactly quantify the generated forces for the *BirdPlane* mission. For the initial generation of the 'design points', these forces are computed for several induced velocities in order to investigate the 'sweet spots' of operation. In Figure 10.2 the forces are shown, their time of action already normalized with the flapping period.

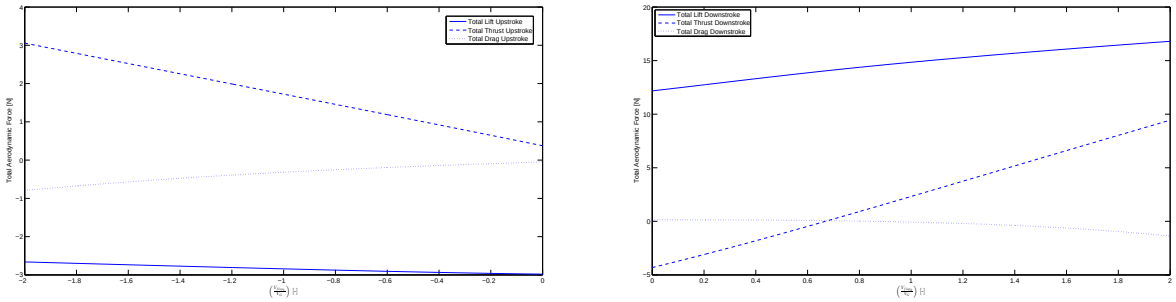

(a) Total Aerodynamic forces Upstroke

(b) Total Aerodynamic forces Downstroke

Figure 10.2: Powered flight phases, varying aerodynamic forces for induced velocities

AERODYNAMIC OPTIMIZATIONS

Initially, the computational method described in the previous paragraph is created to allow an investigatory force determination. By following the method for multiple velocity ratios ($r_{u/d}$) for the cruise flight phase (set by 18 m/s), a preliminary investigation on what range the ideal induced velocities would lie for efficient operation is performed. In this section, an optimization is performed in terms of these induced velocities and different stages along the mission, and the computational method is further emphasized upon by the following steps:

1. The primary cruise phase is first designed for by combining requirements for:
   - $r_{u/d}$: Choosing the right induced velocities for required amounts of aerodynamic forces.
   - *Flapping angle, ξ*: The mechanical operations; limits on the maximum flap angle constrain the operational properties.
   - *Altitude variance, dH*: Constant accelerations in each flapping period cause a sinusoidal altitude variance. In other words flap phase should aim at ending where it started (this is for cruise).

2. The wing design parameters are finalized:
   - *Wing planform*: exact values for $I(y)$, wingspan and therefore the aspect ratio are set.
   - *Airfoil choice*: knowing an expected operational range of $-5° \leq \alpha \leq 12°$, the lift linearly varying with C_{a_α} equal to 4.5.
   - *Wing folding*: investigating the positive effects of wing folding along the wingspan is performed to reduce the generation of negative lift and production of drag.
3. The remaining flight phases are investigated and optimized in terms of limiting flap induced velocities, flapping angle combined with a time-ratio suited for altitude variance (Section 10.1.1).
   - *Cruise*: Higher cruise velocities are optimized for efficiency in operation. The primary mission section (cruise at 18 m/s) is discussed here.
   - *Climb*: Investigations for matching the climb performance of barnacle geese are done here, aiming at around 0.45 m/s climb rate.
   - *Acceleration*: With requirements set by mission capabilities (mainly intercepting the flock), a desired acceleration of 1.0 m/s^2 is looked for.

Even though the enumeration indicated clear distinctions between each block of computation, in real life more iterations have taken place (especially between the first two blocks). Nevertheless, the following paragraphs will be structured equally without extensively emphasizing on the iterations. In other words, the general description below can be seen as the final iteration of the optimization program.

Iterative solver of dynamic constraints By following the prescribed computational layout, initially the dilemma for flapping wing operations has to be explained. To improve the consistency of the computations, the minimum velocity cruise phase is first considered in the explanation. Since the wing planform is created to just match this flight phase (minimum free stream velocity, most demand on planform and airfoil shape), the flow of the computation and design match directly.

As mentioned in the section about the computational method, the primary method of aerodynamic force generation per flapping period follows from creating a surplus of lift in the downstroke (L'_2), whilst equalizing the drag by means of thrust. Also, during the upstroke, the amount of negative lift (L'_1) is limited as much as possible whilst generating enough thrust to cause a net acceleration of 0 m/s^2. On top of these requirements per flapping phase, it is also required to maintain a relative altitude increment of 0 m. Putting these relations within perspective, the following equations hold:

$$L'_2 + L'_1 = m_{\text{design}} \cdot g \tag{10.18}$$

In Equation (10.18) it is shown that the period-normalized, net-lift generated for both upstroke and downstroke should be equal to the design weight of *BirdPlane*.

$$T_2 + T_1 + D_2 + D_1 = 0 \tag{10.19}$$

The equilibrium condition displayed in Equation (10.19), indicates that for cruise the forces parallel to the flight velocities should add up to 0 N.

Noting that Equation (10.18) and Equation (10.19) both consist of terms which are are individually dependent on the utilized induced velocity per phase of a flapping period ($L_2 = f(dV_2), T_2 = f(dV_2), D_1 = f(dV_1)$ etc.), on its own the seemingly independent functions of relative forces are hard to solve. Additionally, the altitude criterion has to be defined, which can be deduced from the altitude changes in down- and upstroke:

$$dH_2 = t_2^2 \cdot \frac{L_2 - m_{\text{design}} \cdot g}{2 \cdot m_{\text{design}}} \tag{10.20}$$

$$dH_1 = -t_1^2 \cdot \frac{L_1 - m_{\text{design}} \cdot g}{2 \cdot m_{\text{design}}} \tag{10.21}$$

The latter equations indicate the relative altitude variation per flight phase, note that during this phase of computation the variance in induced velocities are assumed to vary discretely along the flapping period. This means that once the frequency is set, the specific time that each wing spends in down- and upstroke is computed from the altitude criterion. This new parameter is known as the time-ratio ($T_{d/u}$), and is determined by combining Equation (10.20) and Equation (10.21):

$$dH_2 - dH_1 = \delta H \tag{10.22}$$

The criterion of Equation (10.22) is varied per phase along the mission, but generally *BirdPlane* simply is required to maintain altitude for which δH is equal to 0 m. Therefore by setting the equations of the altitude criteria equal, the time ratios required for sufficient cruise operations are found by:

$$T_{d/u,\text{cruise}} = \left(- \frac{L_1 - m_{\text{design}} \cdot g}{L_2 - m_{\text{design}} \cdot g} \right)^{\frac{1}{2}} \tag{10.23}$$

Equation (10.23) corresponds to the factor indicating how much more time is spent in the downstroke compared to the upstroke within the flapping period. This time ratio is leading when it comes to operations, since the entire wing mechanism has to be modified such that the amount of time spent in the downstroke (t_2) is larger than that of the upstroke (t_1) whilst also varying the induced velocities within the flight phase. The exact time values are found by:

$$t_1 = \frac{1/f}{1 + T_{d/u}} \tag{10.24}$$

$$t_2 = 1/f - t_1 \tag{10.25}$$

At this point, each criterion for cruise flight has been set and are fully computable:

- Aerodynamic forces each of which individually dependent on the induced velocities (creating an independent set of equations all specified by different functions of dV_2 and dV_1, meaning that due to nonlinearity and unpredictability the final system is solved partially by iteration and partially by physical insight in the aerodynamic system.)
- The altitude criterion, for which cruise conveniently corresponds to δH equal to 0 m.
- The specific time ratio, which in turn is dependent on the specific discretely determined aerodynamic forces and δH .

Nevertheless, these computations are based on a mechanical wing system which has no constraints. This latter remark can not be followed through for further optimization computations, since the mechanical system does have constraints for both maximum flap angle (ξ) as well as maximum induced velocities. These constraining parameters will placed fixed limits in both aerodynamic force generation as well as matching the corresponding time ratio. Intermediate estimations on these constraints are provided by the structures department:

- $V_{\text{flap, max}}$ is set to be 10 m/s.
- ξ_{max} is set at a maximum of 60°.

Solving the non-unique system With all the difficulties for flapping wing aerodynamics, it is clear that mainly due to the non-existing interdependence of the generated aerodynamic forces, the way lift will vary during the downstroke due to change in V_{induced} is completely independent of the variance for thrust and drag (also visible in Figure 10.2). This means that in total, there exist six equations (Equation (10.18) and Equation (10.19) each of which dependent and controlled by two flapping induced velocities which also have to comply with the indicated constraints and time ratios:

- Non-unique system of equations:
  - Independent equations: $L_2 = f(dV_2)$, $T_2 = f(dV_2)$, $D_2 = f(dV_2)$, $L_1 = f(dV_1)$, $T_1 = f(dV_1)$, $D_1 = f(dV_1)$.
  - Variable design parameters: induced flapping velocities dV_2 and dV_1.
- Constraints and limitations:
  - δH, for maintaining altitude.
  - $T_{d/u}$, corresponding time ratio.
  - $V_{\text{flap, max}}$, maximum induced velocity. This values is determined from the maximum obtainable angular velocity estimating that the flapping frequency of *BirdPlane* lies around the 5 Hz.
  - ξ, total flap angle. Since a strong, durable mechanism has to be built the total flap angle should be constrained.
- The whole combination of chosen velocity ratios, time variations and constraints should lead to:
  - Right amount of aerodynamic forces to maintain equilibrium.

- A time-ratio which corresponds to the desired altitude change δH.
- Maintaining within the constraints of maximum velocities, meaning that the overall aerodynamic force generation of the downstroke will be limited.
- Staying in the range of maximum overall flap angle, which is directly related to the time spent within each flapping phase and the induced flapping velocities.

From the difficulties stated above, it can be immediately said that by looking at the independence of the aerodynamic forces there will exist no unique solution for any flight situation which will comply with the prescribed constraints. Nevertheless, two values continuously lie at the base of each flight phase and computational constraints, namely dV_2 and dV_1. Since each aerodynamic force is dependent on either value, which determine the altitude criterion. This altitude criterion in turn is used to determine the time ratio, which then corresponds to the finally utilized flap angle for the upstroke and downstroke. Therefore, it is concluded that the two velocity ratios are most important in finding the requested solutions:

1. Apply an estimate for dV_2 and dV_1; the Figure 10.2 allows for different estimates in flap velocity ratios for each phase within the flapping period. These velocities are later on iterated by hand and set a base for the computations.
2. The altitude variance is set, providing the specific time ratio for the required flight phase. At this stage also the actual time spent for each section of the flapping period is known exactly.
3. Since the induced velocities and exact time ratios are known, the flap angle is determined by using a simple relation for the rate of angular rotation.

By initially iterating the first velocity estimates, the estimated value of ξ is obtained. Nevertheless, the prescribed angle of the downstroke has to be matched by the angle during the upstroke. Therefore, the value related to the velocity during the upstroke is set by the required time ratio $T_{d/u}$ and computed flapping angle ξ. Since the mechanics of the wing system of *BirdPlane* are more limited than a real-life Barnacle goose, the previously mentioned design angle of attack and designed twist angles (Equation (10.9) and Equation (10.10)) turn out not to be ideal for the *BirdPlane* aerodynamics. As a result, it is found out that for a sufficient operation, *BirdPlane* should generally decrease the 'optimal twist angle θ' for the downstroke and exactly maintain or increase θ for the upstroke phase. Due to relatively high negative lift velocities of the upstroke, the downstroke is required to generate more lift than initially optimized for. Also the amount of generated thrust should originate more from the upstroke phase than expected. The adaptation of desired design angles is implemented by the integration of two scaling factors:

- Angle scaling downstroke, A_{f2}: typically varying from 0.5 to 0.8. Using Figure 10.1 the following scaling factor corresponds to pointing C_a more towards the vertically oriented $C_{L'}$, utilizing the overall lift as weight counteraction.
- Angle scaling upstroke, A_{f1}: generally shifting the aerodynamic angles by 0.9 to 1.2. Opposite to the downstroke phase, in the case of the upstroke C_a is directed primarily to the thrust vector C_T

These scaling factors are implemented with the overall angles of attack by means of:

$$\alpha_{\text{design}_N}(y) = A_{fN} \cdot \frac{2\Gamma_N(y)}{I(y) \cdot V_{c_N}(y) \cdot C_{a_\alpha}} \tag{10.26}$$

Utilizing the four prescribed design parameters, the user of the finally resulting code ('Birdplane-Optimized.mat') is able to apply the four design variables to finally match each of the four constraints and equilibrium requirements. The final solution to the non-unique problem embedded within the bird-like aerodynamics are iteratively solved and adapted by knowledge about the operations by changing the parameters:

1. dV_2: Velocity ratio applied for the downstroke, directly resulting in a set of aerodynamic forces gathered from the paragraph on computational method.
2. dV_1: Velocity ratio utilized for the upstroke, monitored to remain below the mechanical constraint of 10 m/s.
3. A_{f2}: Correcting factor for lift vector pointing through twist adaptation in downstroke. Preferably used for second iteration.
4. A_{f1}: Correcting factor for lift vector pointing through twist adaptation in upstroke. Preferably used for second iteration.

WING DESIGN

The previous sections have up to now primarily focused upon the description of the aerodynamic phenomena that play significant role within the analysis of the performance of *BirdPlane*. Also the full computational model regarding the quantification of the aerodynamic forces and angles along with the difficultly interrelated flapping wing requirements and constraints are fully noted and solved within the generated code.

This section however contains the real life applications on the preliminarily applied estimations and assumptions regarding the final wing planform and airfoil shape. During computational analysis, the planform was assumed elliptical; the airfoil was assumed to incorporate a C_{a_α} of 4.50 with operating limits $-5^\circ \leq \alpha \leq 12^\circ$. The final wing design is aimed at nearing goose-like shapes and aerodynamic properties. The latter is done by means of an airfoil and planform analysis performed on bird wings by NASA [39].

Airfoil design and Selection The indicated method which has been used by NASA on avian wings has been performed by applying a series of laser scans on many type of avian species. Form the indicated article it is known that by means of a NVISION 3-dimensional non-contact FARO ARM laser scanner, highly accurate measurements have been conducted for the determination of airfoils and exact planforms occurring in nature. The following estimations are the result:

Applying a specific adaptation to the Birnbaum-Glauert rules, a camber line estimation is performed:

$$\frac{z(c)}{c} = \frac{z(c_{\max})}{c} \cdot \eta(1-\eta) \sum_{i=1}^{3} S_N (2\eta - 1)^{n-1} \tag{10.27}$$

$$\frac{z(t)}{c} = \frac{z(t_{\max})}{c} \cdot \eta(1-\eta) \sum_{i=1}^{4} A_N (\eta^{n+1} - \sqrt{\eta}) \tag{10.28}$$

Equation (10.27) and Equation (10.28) correspond to the relative position of the camber line. The equation parameters S_N and A_N are determined by the analysis of the measurements from NASA, and are specific non-dimensional constants for each specific avian species. By combining the equations, the exact chord-wise positions along the airfoil are determined:

$$z_{\text{upper}} = z(c) + z(t) \tag{10.29}$$

$$z_{\text{lower}} = z(c) - z(t) \tag{10.30}$$

For the analysis performed within the article [39], it is clear that the constants regarding the airfoil characteristics of Barnacle Geese the greatest resemblance is found within the airfoil (and planform) of the Seagull. Therefore, for later analysis, the constants regarding S_N and A_N values are copied from the Seagull measurements.

By applying the prescribed method and computation, the chosen airfoil design corresponds to Figure 10.3b. By investigating on proven and true airfoils, it is found that the airfoil S1123 (Figure 10.3a) near perfectly copies the shape and overall performance as the NASA measured airfoils.

(a) Airfoil Description proven and true

(b) Direct copy Seagull/Goose airfoil

Figure 10.3: Comparison between measured Seagull airfoil and proven design S1123

Wing planform design Carrying through the computations of wing design by using the articles measurements on the species of Seagull, the specific chord function is determined and optimized for the lowest cruise velocity given by 14 m/s:

$$\frac{c}{b/2} = \frac{c_0}{b/2}\left[F_{\text{ok}}(\xi) + F_{\text{corr}}(\xi)\right] \tag{10.31}$$

The final primarily Goose imitating planform is extruded from Equation (10.31) by applying the species specific functions indicated by $F_{\text{ok}}(\xi)$ and $F_{\text{corr}}(\xi)$. These two functions correspond to an estimate equation related to

the span-wise chord function (Equation (10.32) and Equation (10.33)) and a correction factor specifically defined for the avian species (Equation (10.34)):

$$F_{\text{ok}}(\xi) = 1.0, \xi = [0, 0.5] \tag{10.32}$$

$$F_{\text{ok}}(\xi) = 4\xi(1-\xi), \xi = [0.5, 1.0] \tag{10.33}$$

$$F_{\text{corr}}(\xi) = \sum_{n=1}^{5} (E_N(\xi^{(n+2)} - \xi^3) \tag{10.34}$$

The final equation contains the non-dimensional factors E_N, which are defined as bird-specific just as for Equation (10.27). Applying these specific functions with the non-dimensional constants defined for Barnacle Geese, the following conclusions can be made:

- The ideal position of the hinge, which is later utilized as initiation point of span-wise folding, is located at 1/3 of the wingspan.
- A production-friendly estimate as approximation of the complex chord function C(y) is set by implication of a leading-edge sweep of 15°.
- Nearing the real bird-like values, the root chord length c_0 is set equal to 0.22 m.
- The wingspan limitation originated from stakeholder requirements, applying a maximum allowable half-wingspan of 0.75 m.

At this stage in the design, each required wing parameter is known and all interrelations are specified with previous equations. Finally, the overall design of a single *BirdPlane* wing is given by Figure 10.4:

(a) Wing planform, view on airfoil

(b) Wing planform, indicated from top view

Figure 10.4: Overall wing design, including the correct airfoil specifications

Proof of planform design The verification of the choice in airfoil and planform layout of the previously designed bird-like wings, follows from analysis in the program XFLR5. Even though this program is created as a simple analysis tool for large aspect ratio wings, even in the NASA article [39] this program is mentioned as accurate estimation tool.

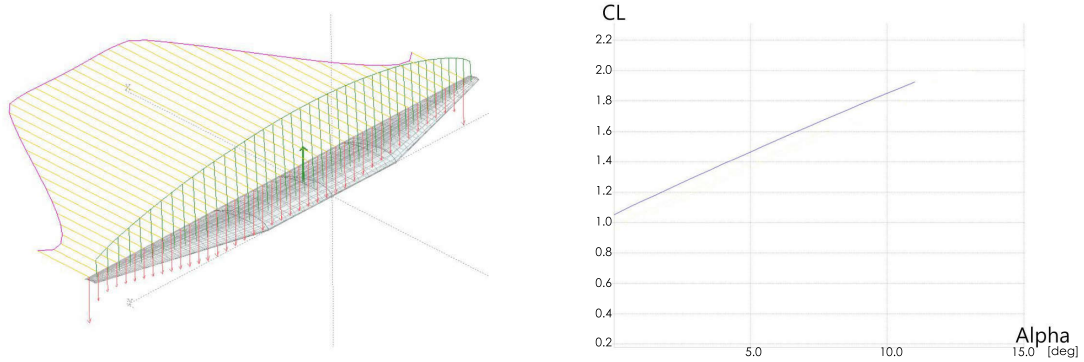

(a) Final wing design, XFLR5

(b) XFLR5 estimate for lift slope curve

Figure 10.5: XFLR5 verification of final wing design

Form Figure 10.5 it can be seen that the rendering of the final wing design corresponds to the previously computed NASA estimates. Also, as important fact regarding the aerodynamic analysis of this rendering at low Reynolds numbers (Re = 240,000), the final choice of the S1123 airfoil has proven to be correct:

- The average C_{a_α} is equal to 4.80 rad^{-1}, which is slightly over the initial requirement estimate. Still, this slight occurrence of over-design will function as a safety factor.
- The operational limits of the airfoil exceed the initial requirement of $-5° \leq \alpha \leq 12°$, since this airfoil remain out of drag divergence range due to operational limits of $-10° \leq \alpha \leq 15°$. This latter fact again allows operations to be safer.

FINALIZING OPTIMIZATION FOR MISSION FLIGHT PHASES

The previous paragraphs on the computation model, aerodynamic optimization and wing design have completely described the required computational methods regarding the aerodynamic forces, angles and additional operational requirements. Finally, the aerodynamic computations have been matched in terms of final wing design which has been analyzed within the XFLR5 environment. In this section, all prescribed knowledge is combined to fulfill the reproduction of force generation within the additional flight phases:

- Cruise: Primary design phase, to which the wing design has been adapted for. This flight phase distinguishes itself by overall equilibrium for each flapping period, meaning that the forces both parallel and perpendicular to the flight velocity exactly oppose each other. This flight phase is investigated for the forward velocities: 14 m/s, 18 m/s and 27 m/s.
- Climb: For future analysis, it is clear that this flight phase is most demanding on the lift generation. This is primarily due to the effect that during the downstroke, even more lift should be generated in order to create $\delta H \geq 0$. Especially at stall speed, this requirement is limiting. The investigated climb rates are the following: 'pull out' (c.r. ≥ 0) at stall speed of 14 m/s and goose-like climb rate in cruise (c.r.=0.50 m/s).
- Acceleration: This flight phase is very important for the mission performance, since by being able to independently accelerate during each cruise velocity immediately allows *BirdPlane* to continue its pursuit of the geese flock. The limit of acceleration is set to 1 m/s^2, which should only be reached once $V_{\text{fw}} \geq 0$. The following cases are quantified: $\vec{a} \geq 0$ at V_{fw} = 14 m/s, $\vec{a} \approx 1.0$ at V_{fw} = 18 m/s, $\vec{a} \approx 1.0$ at V_{fw} = 24 m/s.

Generally, the described program explained within the paragraph on computation method is continuously adapted for each apparent flight phase summarized in this section. Briefly, the wing motions (chord- and span-wise) which are assumed to be continuously variant and incorporated within the final design are the following:

- Span-wise twisting: This continuously varying design parameter directly relates the wing leading edge and basic airfoil shape to $\theta(y)$.
- Span-wise folding: From the hinge point towards the tip, the wing is assumed to operate with perfect folding limiting the amount of negative lift during the upstroke. In Figure 10.6b, the effect of this motion is shown with respect to Figure 10.6a.
- Vertical flapping motion: A primary feature of flapping wing design, the capability of inducing a vertical flapping motion. Note that during aerodynamic analysis, there has been touched upon the incorporation of an additional horizontal motion. This has proven to be a non-beneficial introduction of mechanical difficulty for the relative increase in efficiency ($\Delta\eta \leq 2\%$).

From Figure 10.6b, reducing effect on unwanted lift production for wing folding is clarified. From previous circulation distributions is it known that from hinge to tip, the amount of produced lift is primarily located at the wing tips. By folding the wings, the negative $C_{L'}$ is directed horizontally. Therefore the negative effects of the lift in the upstroke phase are reduced, whilst till maintaining the positive effects of the thrust during the upstroke. The estimated amount of increased efficiency in terms of negative lift is $\geq 75\%$.

Finally, the effects of the folding along the wingspan by means of redirection of the overall lift vectors is indicated by means of Figure 10.7. This latter figure shows that the computations corresponding to the increase of efficiency due to span-wise folding are proven by additional analysis in XFLR5.

Mission specific flight performance

In this section the final expected performance of *BirdPlane* wings is summarized per flight phase, which were briefly mentioned at the introduction of Section 10.1.1. For each flight mode, the utilized values for the four primary design parameters (A_{f2}, A_{f1}, dV_2 and dV_1) are indicated such that with the application of 'Birdplane-Optimization.mat', all aerodynamic properties opposed in this report can be reproduced. As a final remark,

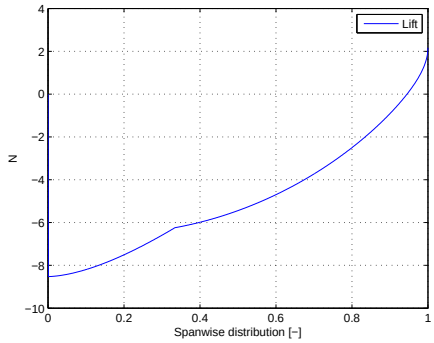

(a) Vertical lift production during upstroke, without span-wise folding

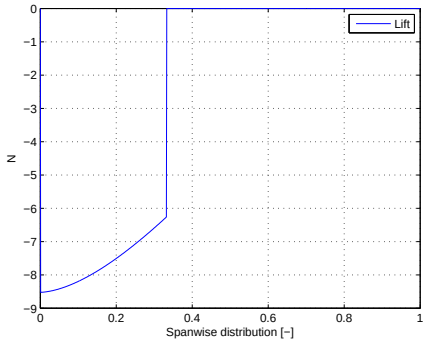

(b) Vertical lift production during upstroke, including the effects of span-wise folding

Figure 10.6: Aerodynamic performance of a span-wise folding wing

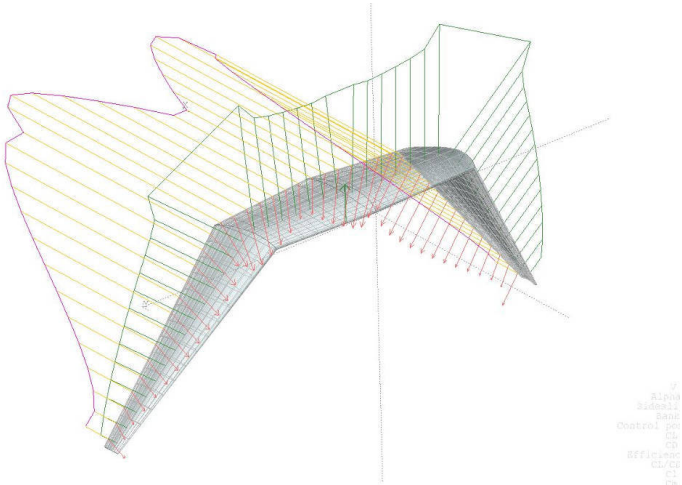

Figure 10.7: Visualization of the upstroke phase.

these computations have been performed using a total m_{design} of 1.4 kg. This limit originates from the climb rate requirement, which has proven to be most demanding.

From Table 10.1 it can be concluded that the overall expected *BirdPlane* mission can be fully performed when looking at the indicated flight phases. The maximum lift which is produced by both wings, generated during climb, is equal to 12.54 N. The only remark which has to be made, is that *BirdPlane* will not be able to start a Gooselike climb rate from any of the indicated cruise velocities. Only once the V_{fw} is equal to the predetermined 18 m/s, the wings are capable of climbing with bird-nearing performances. *BirdPlane* is thus only limited when it comes to climb rate below certain cruise velocities. For the remaining parts of the mission, each flight phase is fully covered by the final wing design.

10.1.2 STABILITY AND CONTROL

Stability and controllability are closely related to each other, and there is always a trade-off between the two. An aircraft can be highly stable, therefore making it hard to control, as it wants to stay in the stability position. On the other hand, too high controllability can make the aircraft unstable due to the big influence of a slight change in force and/or its direction.

Stability in birds is provided by three types of effects; drag-based (e.g. dart), lift-based (e.g. tailplane) and pendulum effect (e.g. paraglider) [40]. *BirdPlane* does not make use of the wing motions that provide considerable shifting in c.g. location (Section 10.1.1). Therefore, the only contributors to stability are based on drag and lift. In this section, the analysis for longitudinal and lateral stability is described along with the control forces. Furthermore, the turning performance that is required to follow the flock of Barnacle Geese is discussed.

Table 10.1: Mission phase specific aerodynamic performance, per wing

Mission section	$A_{f.2}$ [-]	$A_{f.1}$ [-]	dV_2 [m/s]	dV_1 [m/s]	$\alpha_{2.av}$ [°]	$\theta_{2.av}$ [°]	ξ_{total} [°]	$P_{\text{req.avg}}$ [W]
Cruise [14 m/s]	0.85	1.0	7.0	9.71	8.5	−15	47.3	20.64
Cruise [18 m/s]	0.78	1.0	6.3	7.48	5.9	−12	42.4	20.01
Cruise [27 m/s]	0.57	1.0	4.05	4.45	3.0	−32	29.5	15.72
Acceleration [14 m/s, $\vec{a} = 0.25\, m/s^2$]	0.52	1.0	7.28	10.0	9	−32	59.4	26.83
Acceleration [18 m/s, $\vec{a} = 1.0\, m/s^2$]	0.8	1.0	8.64	9.86	3.2	−32	50.8	26.01
Acceleration [24 m/s, $\vec{a} = 1.1\, m/s^2$]	0.52	1.1	7.28	10.0	9.1	−32	48.2	20.43
Climb [18 m/s, $c.r = 0.25\, m/s$]	0.78	1.0	6.3	9.92	3.0	−32	60.0	39.25

LONGITUDINAL STABILITY

Longitudinal stability is determined by the moment slope, the parameter C_{m_α}, which should be negative for stable flight. A large negative value for this parameter will result in a very stable aircraft, though hard to control. A small negative or even positive value will give a aircraft which is prone to react more to the applied control forces. Also, a low pitch value of the tail is required which is beneficial for decreasing the drag. Hence, it was chosen that the moment slope is slightly negative for good stability, controllability and drag performance.

For longitudinal flight, the moment on an aircraft should be zero if no pitch change is demanded. A highly cambered airfoil, similar to that of birds, has a relatively high pitching moment around its aerodynamic center. This has to be balanced by shifting the center of gravity backwards, or by constructing a counteracting moment by the tail.

In flapping flight, the moments which are formed by the wing are merely amplified. Thus, if an aircraft possesses a stable mode, it will possess even greater stability in flapping flight [41]. Therefore, in this chapter gliding flight will be considered since this flight mode is the most critical.

XFLR5 For stability analysis, *BirdPlane* can be modeled as a conventional aircraft: a body, wing and tail. However there are critical differences. Firstly, the body has no cylindrical part, and the cross-section is not circular. Moreover, the wings have a highly cambered airfoil combined with a varying twist and taper. Also, the tail is mounted partly in the body at a small distance from the wing. At last, the tail is rotatable in two axis. All these complications have as an effect that it is not possible to make a descent approximation using analytical estimation methods only. Therefore, the program XFLR5 was used to perform a stability analysis on *BirdPlane*. This analysis may provide more insight in the flight behavior of *BirdPlane*.

The criterion for longitudinal stability is a small negative moment slope as stated earlier. Also, the elevator should be as small possible while providing still sufficient stability and controllability. This was done by first defining the three elements of *BirdPlane*. The wing was formed according to Section 10.1.1 in which the wing configuration was determined. XFLR5 provides a function to determine the inertia and center of mass as a function of the total input mass and the given geometry by assigning each panel element a certain weight. The same was done for the tail in fanned-out condition, since this will be used in gliding flight for stability. The tail uses a slightly negatively cambered airfoil. At last the body was added. At this point in the design stage, no accurate model of the body was present so a cone-like shape, similar in appearance to a goose, was created to perform analysis. This body too, was assigned a mass. The batteries and wing mechanism were simulated as a point mass which was used to control the position of the center of gravity.

The positioning of the center of gravity and sizing the tail was a highly iterative process in which the tail area and center of gravity location were constantly updated. The following parameters are preliminary estimates based on the actual goose shape (which is expected to be optimal); The body has a length of 0.70 m with its thickest point at 0.40 m, the wing is located at a distance of 0.31 m from the nose, and the tail is partially embedded at the end of the body. The root of the tail is embedded at an estimated 0.63 m. At this distance, space for control (e.g. servos and struts) is reserved.

The combination of center of gravity positioning and tail sizing was found to have desired values for the center of gravity location (≈0.433 m), which can be obtained by shifting the battery pack. In this case, the tail must have a chord length of 0.17 m and a width of 0.34 m, which is a result of several manual iterations (XFLR5). The Figure 10.8a shows the tail configuration and Figure 10.8d its incorporation in the body.

Although the wing has a very high camber, and thus, high pitching moment, *BirdPlane* is longitudinally stable.

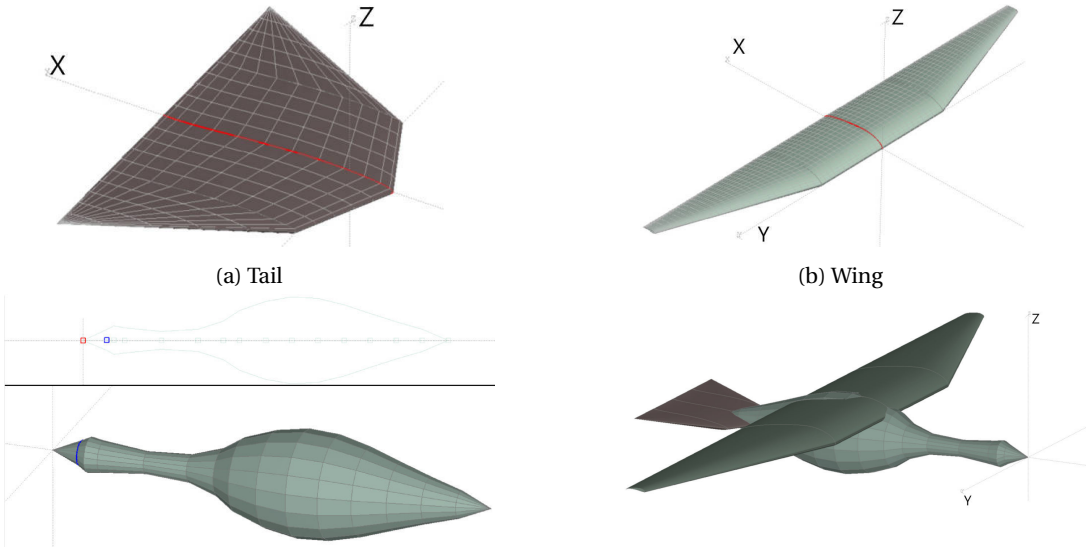

(a) Tail

(b) Wing

(c) Body

(d) Total configuration

Figure 10.8: Different parts of the *BirdPlane* model

The center of gravity is placed as far back as possible, and the tail has sufficient area to counter the rest of the moment of the wing. The resulting moment can be seen in Figure 10.9, given by the lower graph. This is a line drawn for a certain elevator setting and shows that C_{m_α} is negative. In fact, the value is on average about -0.45 rad^{-1}, which is close to that of the Cessna Citation which has a moment coefficient slope of -0.43 rad^{-1} [42].

The second line at the horizontal axis shows the points at which zero moment could be achieved by tail deflection, as calculated by XFLR5. At these angles of attack steady flight is possible. Outside of this range, the tail deflection becomes too high for attached flow. The impact of the deflection of the tail can be seen in Figure 10.10. For a certain tail setting, a lift over drag as high as 17 can be achieved. However, for steady flight an greater elevator deflection is required, thereby increasing the drag. As a result, the maximum lift over drag in steady flight is a bit under 15. Note that these values are an inviscid approximation by the panel method used by XFLR5 on a model. For more trustworthy results, more elaborate numerical calculations or windtunnel tests have to be performed.

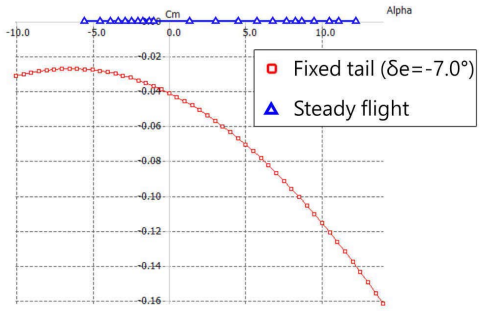

Figure 10.9: Pitch moment in Fixed Tail and Steady Flight

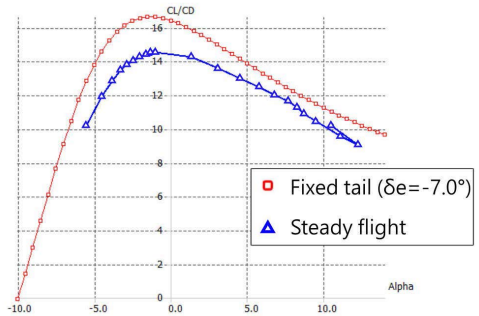

Figure 10.10: Lift over Drag Ratio in Fixed Tail and Steady Flight

(a) Phugoid motion

(b) Short period motion

Figure 10.11: Longitudinal stability modes [41]

Stability Modes In aircraft, two types of longitudinal modes can be distinguished when a disturbance occurs; a very slow *phugoid*, and a fast, highly damped *short period*.

Phugoid (Figure 10.11a)

This motion consists of an interchange between kinetic and potential energy, resulting in a periodic gain and drop in altitude. It is usually a poorly damped and slow oscillation. The angle between the velocity vector and the body X-axis as shown in Figure 10.11a is assumed to be constant during this motion [41][42]. From these assumptions and by neglecting compressibility effects, the period of the phugoid can be approximated as [43]:

$$T_p = \frac{2\pi}{\omega_p} = \pi\sqrt{2}\frac{V}{g} \tag{10.35}$$

From Equation (10.35) it can be seen that the only variable to determine the period is the forward flight velocity. For *BirdPlane* this value is 18 m/s, resulting in a phugoid period of 8.15 seconds.

Short period (Figure 10.11b)

A fast periodic pitching oscillation, which is usually heavily damped in conventional aircraft is called the short period. It can be seen in Figure 10.11b that the flight path can be assumed to be a straight line (i.e. vertical motion is zero). Also flight velocity can be assumed to be constant [41][42]. The frequency of the short period is approximated by Equation (10.36) [43]. By assuming that the vertical motion is zero [41], an approximation for the period can be found in a similar fashion as for the phugoid (Equation (10.38)). Here, M_α is determined by Equation (10.37).

$$\omega_{sp} = \sqrt{\frac{Z_\alpha M_q}{V} - M_\alpha} \tag{10.36}$$

$$M_\alpha = \frac{\partial M}{\partial \alpha} \Big/ I_y = \frac{C_{m_\alpha} \rho V^2 S \bar{c}}{2 I_y} \tag{10.37}$$

$$T_{sp} = \frac{2\pi}{\omega_{sp}} = \frac{2\pi}{\sqrt{-M_\alpha}} \tag{10.38}$$

The derivative C_{m_α} and moment of inertia I_y are estimated using XFLR5, resulting in -0.5 rad^{-1} and 0.0169 kg m^2 respectively. By inserting all values and combining Equation (10.37) and Equation (10.38), a value for T_{sp} of 0.41 s is obtained.

The estimated periods for both longitudinal modes above are also estimated in XFLR5 by simulating the motions. From this simulation, similar periods have been found for the two modes and therefore the values can be verified.

Control Forces In order to keep *BirdPlane* in level flight, a certain tail deflection is needed to counteract the wing's moment contribution about the center of gravity. In Section 10.1.1 it was found that the maximum lift produced by the wing is 12.54 N. In order to counteract the moment produced by this force around the center of gravity, a force of 1.8 N (normal to the tail surface) is needed. This normal force on the tail causes a certain torque on the 'pitching' servo that it has to maintain in level flight. This moment is equal to 0.1381 Nm and should be constantly delivered by the servo during level flight.

LATERAL STABILITY

Lateral stability can be expressed best in the yaw stability and roll stability as an influence of sideslip, respectively C_{n_β} and C_{ℓ_β}. The former, also called weathercock stability, must be positive, hence counteracting a induced sideslip angle. Conventional aircraft use a rudder for this purpose, while birds and small aircraft can fly without [40]. It is beneficial in terms of drag to have no vertical fin, and therefore this is also first investigated for *BirdPlane*. The wing normally has a small positive contribution while the fuselage of a conventional aircraft is destabilizing. For yaw stability the horizontal tail is slightly positive in known configurations. The latter control derivative is also called the effective dihedral, and should be negative for desired motion. As the name suggests, a dihedral can assure a big stabilizing factor. Further stabilizing can be reached by the sweep and high mounting of the wing.

XFLR5 Both for the weathercock stability and the effective dihedral coefficients there is no reliable analytical method. Therefore the best option to analyze these two stability parameters was applying a stability analysis on the model in XFLR5. The result of this analysis was that both coefficients have the desired sign. A very small positive weathercock stability was found as was expected from bird references. Probably due to the high

mounting and the partly sweep of the wings the sign of the effective dihedral coefficient is negative. Also the rest of the coefficients was determined by XFLR5, and with this, the eigenmodes were investigated.

Stability Modes For lateral stability, two motions can be distinguished which are combinations of rolling, yawing and sideslipping motions. Those motions are the *Dutch Roll* and *Spiral mode*.

Dutch Roll

A Dutch Roll is a periodic interchange between yawing and rolling motion which are coupled with a slight phase difference.

In order to estimate the period of the Dutch Roll, stability derivatives have to be known, which can be approximated by XFLR5. Those values may differ from the real values however, because simplifications are implemented in the software. By neglecting the rolling moment (thus, primarily sideslipping and yawing motion), the following expression can be found [43].

$$\omega_{DR} = \sqrt{\frac{Y_\beta N_r - N_\beta Y_r + V N_\beta}{V}} \tag{10.39}$$

Where the four stability parameters in the numerator are calculated as following:

$$Y_\beta = \frac{QSC_{y_\beta}}{m} \qquad Y_r = \frac{QSbC_{y_r}}{2mV}$$
$$N_\beta = \frac{QSbC_{n_\beta}}{I_z} \qquad N_r = \frac{QSb^2C_{n_r}}{2I_zV}$$

Where $Q = \frac{1}{2}\rho V^2 S$.

Results of the simulation show that $C_{Y_\beta} = 5.6468 \cdot 10^{-3}$ rad^{-1}, $C_{n_r} = 5.2303 \cdot 10^{-4}$ rad^{-1}, $C_{n_\beta} = 2.4912 \cdot 10^{-3}$ rad^{-1} and $C_{Y_r} = -7.9796 \cdot 10^{-3}$ rad^{-1}. The analysis is performed at an airspeed of 11.77 m/s instead of the desired 18 m/s. This is due to limitations in the usability of XFLR5 and more (detailed) analysis has to be performed in order to estimate those values for 18 m/s. Performed analysis showed however, that the coefficients do only change slightly at different airspeeds, but overall stability remains the same. Usual periods are in the order of 3 to 15 seconds [43]. From Equation (10.39) a period of 3.94 seconds is obtained. Note that this estimation method is very rough, as the simulation in XFLR5 shows a period of around 2.7 s. Moreover an increase of period was noted for an increasing speed. A rough extrapolation showed an anticipated period of 3.3 seconds for 18 m/s.

Spiral mode

This motion is an aperiodic motion introduced by a disturbance, in which the spiral gets tighter and steeper over time. This can be justified by the small positive, real only eigenvector which can be seen in the rootlocus plot in XFLR5. Althought instable, the spiral mode is a very slow mode and therefore, "a certain degree of instability can be accepted" [44], and might even be desirable for controllability.

TURNING PERFORMANCE

For turning performance, little to nothing is known about birds' performance (Barnacle Geese in particular). For the minimum turning radius, not much literature is available for consultation except for some small birds with a mass ranging from 0.015 kg up to 0.083 kg. In the book EVOLUTIONARY BIOMECHANICS [45], flight performance of soaring birds is available for 2 types of birds: Procellariiformes (seabirds such as albatross, petrels, etc.), Accipitriformes (raptors such as hawk, eagle, etc.). Figure 10.12 shows the turning performance for those two types of birds.

As there is no data available on the turning behavior of geese, analysis is based on the data obtained from the seabird category (black dots in Figure 10.12). It can be seen that at a gliding speed of 16 m/s, at which *BirdPlane* will glide, a turning radius of 15 m is found.

The equation of motion for turning in aviation can be found by equation the force in radial-direction to the centrifugal acceleration, hence:

$$L \sin\phi = m\frac{V^2}{R} \tag{10.40}$$

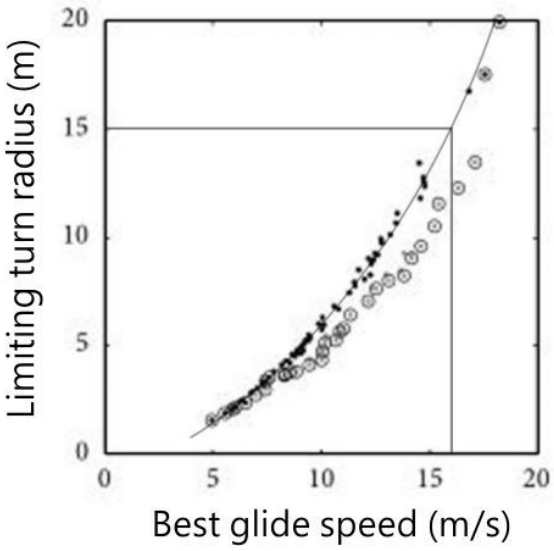

Figure 10.12: Turning performance for Procellariiformes (black dots) and Accipitriformes (grey dots) [45]

Where ϕ is the roll angle and R is the turn radius. Lift L can be written in dimensionless form C_L and be rearranging the terms, the radius can be described as in Equation (10.41).

$$R = \frac{mg}{S} \frac{2}{\rho g C_L \sin\phi} \tag{10.41}$$

The only unknown in Equation (10.41) is the roll angle. By filling in 15 m for the turn radius and by filling in all other parameters, a roll angle of 20° is found.

During gliding, the minimum time to turn is found using Equation (10.42).

$$T_{2\pi} = \frac{2\pi R}{V} \tag{10.42}$$

Here the subscript means a rotation of 2π radians, which comes down to one complete rotation. For a turn radius of 15 m and a gliding velocity of 16 m/s, it takes 5.9 seconds.

The question is whether *BirdPlane* is capable of providing such a turn radius in order to be able to follow the Barnacle Geese in case they adapt their flightpath. With basic analysis, this question is hard to answer, because several stability derivatives have to be known that can be obtained only by for example wind-tunnel tests. However, the method shall be used for this is described below.

Turning by *BirdPlane* is achieved by rotating the tail such that *BirdPlane* rotates, introducing a sideslip angle β. Due to a positive sideslip angle, more lift is produced by the right wing in comparison to the left wing as, because the velocity component perpendicular to the leading edge is larger for the right wing as seen in Figure 10.13.

The derivative that is involved in this coupling between β and rolling moment is C_{l_β}, usually indicated as 'effective dihedral'. The two main contributors to this moment come from the wing and the vertical fin. *BirdPlane* does not have a vertical fin, instead it makes use of the rotatable tail surface to create a force in Y-direction. This force is assumed to act through the X-axis, therefore no rolling moment is created due to it (i.e. no vertical arm between the c.g. and the tail). For the wing there are two parameters that affect the rolling moment namely: wing sweep (Λ) and wing dihedral (Γ), as shown in Equation (10.44) and Equation (10.43) respectively [46].

$$C_{l_\beta} = -C_L \frac{\bar{y}}{b} \sin(2\Lambda_{c/4}) \qquad \text{(Sweep)} \tag{10.43}$$

$$C_{l_\beta} = -\alpha_w \sin(\Gamma) \frac{\bar{y}}{b} \qquad \text{(Dihedral)} \tag{10.44}$$

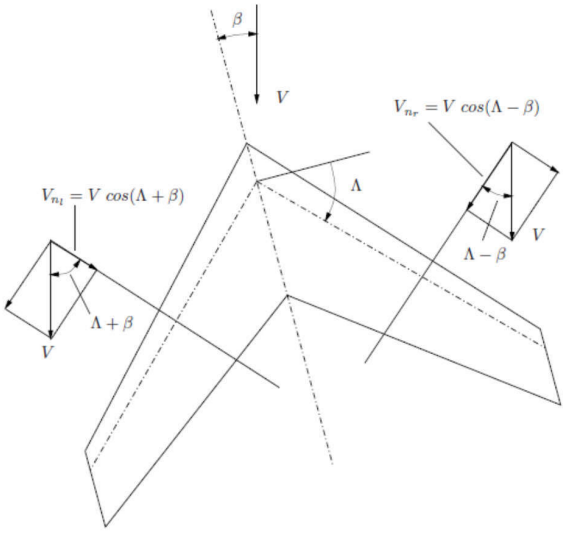

Figure 10.13: Swept wing in sideslipping flight, causing difference in velocity over the wing halves [42]

The latter of the two is variable for *BirdPlane*, because the dihedral angle of the wing can be positioned as desired at any point in time throughout the mission. The sweep of the wing is fixed for *BirdPlane*, therefore the contribution of Equation (10.43) can be estimated. The sweep of the wing is only present in the outer section ($0.33 < \frac{\bar{y}}{b} < 1$), meaning that the difference in lift between the two wing halves only comes from the outer section. By assuming an elliptical lift distribution, the centroid of the lift is located at $\frac{\bar{y}}{b} = \frac{2}{3\pi}$, which is at 42% of one wing half. As mentioned earlier, only the outer section of the wing will produce the lift difference and therefore the centroid of the lift of this section is required, which is estimated to be at 61% of the wing (1/3rd of the wing half plus 42% of the remaining tip-section). The ratio of the lift of the outer section ($0.33 < \frac{\bar{y}}{b} < 1$) divided by the total lift is found to be 58%. By inserting a lift coefficient of 0.3 (found by Equation (10.13) during gliding) multiplied by this 58%, and by inserting the centroid location and wing sweep of 15°, Equation (10.43) yields

$$C_{l_\beta} = -0.053\ \text{rad}^{-1}$$

A stability analysis in XFLR5 showed similar results. At small angles of attack the effective dihedral is around -0.05 rad^{-1}. For a larger tail deflection this coefficient becomes larger, thus the influence of the tail on roll control. When desired, this value can be altered by introducing a dihedral angle.

In conventional aircraft, the turning is done by the ailerons as this is the most effective to introduce a rolling moment. No ailerons are considered for *BirdPlane*, therefore a different method has to be used for this analysis. Aircraft are capable of making horizontal turns with the rudder only, which is comparable to the function of the rotatable tail. In horizontal steady asymmetric flight, equilibrium equations can be derived (according to AE3212-I FLIGHT DYNAMICS [42]) presented in Equation (10.45), Equation (10.46) and Equation (10.47).

$$C_L\phi + C_{Y_\beta}\beta - 4\mu_b\frac{rb}{2V} = 0 \tag{10.45}$$

$$C_{l_\beta}\beta + C_{l_r}\frac{rb}{2V} + C_{l_{\delta_a}}\delta_a = 0 \tag{10.46}$$

$$C_{n_\beta}\beta + C_{n_r}\frac{rb}{2V} + C_{n_{\delta_r}}\delta_r = 0 \tag{10.47}$$

By applying $\delta_a = 0$ (no aileron deflections) to Equation (10.46) and Equation (10.47), the rudder angle variation, roll angle variation, and sideslip angle variation with respect to the yaw rate r is derived:

$$\frac{d\delta_r}{d\frac{rb}{2V}} = -\frac{1}{C_{n_{\delta_r}}} \frac{C_{l_\beta} C_{n_r} - C_{l_r} C_{n_\beta}}{C_{l_\beta}} \qquad (C_{n_{\delta_r}} < 0,\ C_{l_\beta} < 0) \tag{10.48}$$

$$\frac{d\phi}{d\frac{rb}{2V}} = \frac{4\mu_b + C_{Y_\beta} \frac{C_{l_r}}{C_{l_\beta}}}{C_L} > 0 \qquad (\text{for } C_L > 0) \tag{10.49}$$

$$\frac{d\beta}{d\frac{rb}{2V}} = -\frac{C_{l_r}}{C_{l_\beta}} > 0 \qquad (C_{l_r} > 0,\ C_{l_\beta} < 0) \tag{10.50}$$

Measurements on the North American 'Harvard II B' using the rudder only during steady flight has been performed and the results are shown in Figure 10.14. Similar measurements have to be done for *BirdPlane* as soon as a model is manufactured. With the measurements, the rudder deflection (rotatable tail in case of *BirdPlane*) that is needed to maintain a certain roll angle can be found. For the case of the 'Harvard II B' it can be seen that in order to achieve a roll angle of 20°, a rudder deflection of about 0.15° is needed. For the rotatable tail of *BirdPlane* this value will probably be in a higher order of magnitude, because it has no contribution to the rolling moment as the line of action is assumed to intersect with the X-axis. Rotation of the tail will only alter the sideslip, introducing the roll as explained earlier.

In this stage of the designing phase, it can thus not yet be concluded whether the turning radius (15 m) and turning time (360°/5.9 s) can be achieved, and further analysis to the stability derivatives described above has to be performed.

Control Forces As explained above, turning of *BirdPlane* is achieved by introducing a certain sideslip angle. The force that is needed to achieve this angle is determined by Equation (10.51) [42].

$$Y = C_{Y_\beta} \beta \frac{1}{2} \rho V^2 S \tag{10.51}$$

Where C_{Y_β} is negative. This sideforce is mainly driven by the fuselage and rotatable tail (vertical tailplane in conventional aircraft). Similar to the $\phi - \beta$ relation described above, tests have to be performed in order to find the quantity C_{Y_β}, after which the force that the tail has to produce can be determined. From this force, the torque on the servo can be calculated as done for the pitching control.

FEET FUNCTION AND PERFORMANCE

At this point, the quantitative analysis on the *aerodynamics* and *stability and control* of *BirdPlane* is completed and possible future implementations can be considered. The analysis stated earlier does not discuss the possible implementation of feet and the benefits/drawbacks of that. Therefore, this section will elaborate on the feet consideration for *BirdPlane*.

The functions of birds' feet on the ground is similar for all birds, namely to be able to stand, walk and run. During flight however, the feet position differs a lot among birds. Some position their feet in the front, some in the back, sometimes both feet (or one of them) are (completely) drawn up and concealed by the breast feathers. It is even observed that both feet are positioned in opposite direction.

(a) Barnacle Goose positioning its feet backwards during cruise flight [47]

(b) Barnacle Goose using its feet as airbrake during landing [48]

Figure 10.15: Barnacle Goose feet positioning

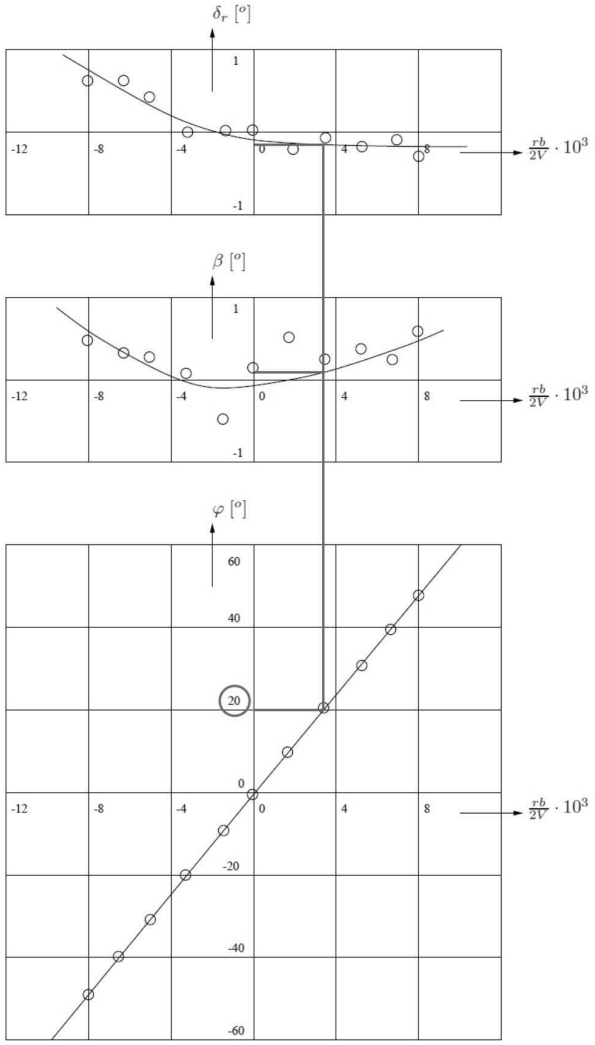

Figure 10.14: Steady turns using rudder only, North American 'Harvard II B' [42]

In general, birds can be divided into two categories when it comes to the feet position during flight; (1) birds carrying the feet behind them, (2) birds carrying the feet in front of them. All ducks, swans and geese (including Barnacle Geese) belong to the first category as can be easily observed Figure 10.15a.

Feet Functions
Studies to birds' feet in flight have been done, and several functions for the feet can be distinguished [49]:

1. *Object carrying* - Nest material or food can be carried by either the bird's beak or claws.
2. *Fighting* - Spectacular claw fights can be observed among birds by grabbing each other in mid-air.
3. *Heat regulation* - Heat loss can be regulated through the feet of birds, by regulating the blood stream.
4. *Scratching* - Sometimes birds suffer from lice.
5. *Standing/sitting* - This function is obviously present in all birds.
6. *Walking/swimming* - Moving on the ground or through the water is off course done by using the legs. Also take-off is aided by means of running to gain enough take-off velocity.
7. *Airbrake* - During landing specifically, the feet can function as airbrake, by turning them into the airflow such that drag increases.

8.	*Fall breaker/damper*	-	During the landing phase on ground or water, the feet can break the bird's fall. For *BirdPlane*, the feet can function as landing surface, absorbing the loads during landing.
9.	*Feet separation*	-	This function helps the bird to increase their 'tail width'.
10.	*Quick turning*	-	Feet can be used for quick turning. This can be compared to the centerboard in boats, which makes quick turning possible.
11.	*Rudder*	-	By stretching the legs backwards, a rudder function can be achieved.
12.	*Yaw stability*	-	Although Barnacle Geese position their feet primarily in horizontal direction, *BirdPlane* may use the legs as 'vertical tailplane', the so called weathercock stability.

Unless *BirdPlane* all of the sudden feels itchy or has the urge to start a fight, the first 6 functions are not applicable for the feet of *BirdPlane*. In addition, the feet of *BirdPlane* can function as 'hook', which is attached to the catapult to aid take-off.

Some of the remaining functions require movable feet (items 7,10,12). For the current phase, fixed feet will be considered as movable feet introduce more movable parts and new variables. Possible benefits are not expected to compensate for the costs. The implementation of the remaining functions (8, 9, 11, 13) can be considered, as this can be beneficial in some fields namely:

- Increase bio-mimicry
- Increase stability performance
- Increase turning performance

Drawbacks of feet for the *BirdPlane* design are:

- Drag increase (beneficial in case of airbrake)
- Mass increase

Feet Drag

An increase in drag is expected when feet are implemented, because of the additional wetted surface and introduction of turbulent flow. This expectation is validated by tests performed on the drag contribution by feet [50]. According to PENNYCUICK's wind-tunnel study done on a pigeon, the gliding drag is achieved as shown in Figure 10.16. The drag gradually lowers as airspeed increases.

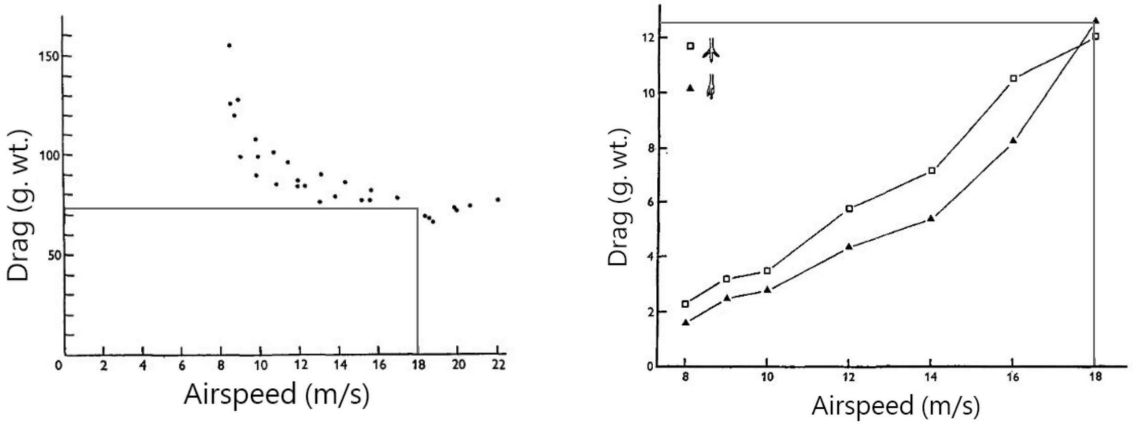

(a) Total gliding drag of a pigeon (feet retracted) versus velocity

(b) Feet drag (1 foot) of a pigeon versus velocity

Figure 10.16: Drag contributions versus airspeed for a pigeon, based on [50]

From Figure 10.16a, the drag of the body of the pigeon with retracted feet is about 75 g. wt., and according to Figure 10.16b the drag of 1 foot is 12.5 g. wt. (25 g. wt. for both feet) at 18 m/s airspeed. Although the study focused on pigeons, the same trend in drag contribution by the feet is assumed to be present in Barnacle Geese. Therefore, at a speed of 18 m/s at which Barnacle Geese cruise, the contribution of the legs with respect to the total drag when the feet are retracted is approximately 25/75 or 33%.

As expected, drag is increased by implementing feet. However, sometimes this is desired as in the case of landing where the feet can function as airbrake. This requires the feet to move into the flow however, and should be investigated in more detail in the future as the tail of *BirdPlane* is also used as airbrake. For now, static feet are assumed and a considerable amount of drag is introduced and thus feet are not implemented in the final design.

10.2 STRUCTURES & MATERIALS

In Section 10.1 the motions required for flapping and control have been analysed. In this section the structural design that provides those motions is explained. First the design of the mechanisms, i.e. all moving parts, is described (Section 10.2.1). This is followed by an analysis of the dimensions and thicknesses required to carry the loads (Section 10.2.3). Next the different materials are described and finally the production methods are defined (Section 10.2.4).

10.2.1 MECHANISMS

In the preliminary design phase the motion of the flapping mechanism was optimized to get the right aerodynamics around the wing. The aerodynamic calculations have resulted in required parameters for the different flight phases. The parameters for which the mechanism is optimized are: The flapping angle ξ, the position of the elbow hinge, the frequency f and the time ratio for up- and downstroke $r_{u/d}$. While optimizing for these parameters at the same time structural integration of the components in the fuselage is considered.

WING FLAPPING MECHANISM

The mechanism is optimized for cruise flight. The position of folding can be adjusted during the design process without influencing the rest of the angles and dimensions, while the speed ratio has to be controlled by the motor. Only the flapping angle is dependent on the design of the mechanism. It flows from the dimensions and relative positions of the driving gear, the crank and the hinge point. A schematic overview of the mechanism is shown in Figure 10.17 with letters indicating the beams and points. In the following description those letters will be used to refer to the components. The initial mechanism made use of a large driving gear which would require a very large fuselage diameter, so the radius of the circle over which the crank moves is shrunk to 24 mm. With the wing span of 1.5 m and the frequency of 5 Hz, the required induced velocity can only be achieved when flapping over a large angle. The shorter the arm left of point O (distance BO), the larger the angle of the spar for the same vertical displacement of B. Changing the radius and distance BO however changes the whole movement. Due to the complex motion of the crank and the large number of variable distances it was impossible to calculate the optimal configuration. By trial and error the motion was optimized.

The initial mechanism with one crank was not capable of reaching large values of ξ. Due to the nature of the motion of the crank (BP), the outer part of the wing had some phase lack compared to the inner part: While the inner part was already moving in upstroke, the outer part was still folding down and vice versa. This resulted in too small induced velocities and *BirdPlane* would not be able to fly. It also gave troubles in controlling the different speeds in up and down stroke, since it was hard to define when the stroke starts. This was solved by adding a cam crank to the driving gear (AP2), to which bar AD is attached that drives the folding. This cam crank also rotates around point O with distance B2O being equal to distance BO and is attached 40° ahead of the first crank, such that the folding and unfolding starts earlier.

For optimal aerodynamic performance the upstroke should be faster than the downstroke, with a speed ratio of $r_{u/d} = 0.8416$, which gives (at a flapping frequency of 5 Hz) 0.1086 s for the downstroke and 0.0914 s for the upstroke. At a constant speed for the driving gear of 5 Hz (31.4 rad/s), the mechanism causes the downstroke to be faster (0.097 s) than the upstroke (0.103 s). This is due to the fact that the downstroke happens over an angle of 2.32 rad of the driving gear and the upstroke over the remaining 3.96 rad. To achieve the right value of $r_{u/d}$ the speed of the driving gear should be 20.8 rad/s for 0.1086 s during the downstroke and 44.0 rad/s for 0.0914 s during the upstroke. The switch between downstroke and upstroke is defined by looking at a point halfway the wing, at 357 mm from the root. Further implementation is discussed in Section 10.3.1. The exact position of this point was chosen as such that the ratio of the mean induced velocity in up- and downstroke corresponds to the value of $r_{u/d} = 0.84$.

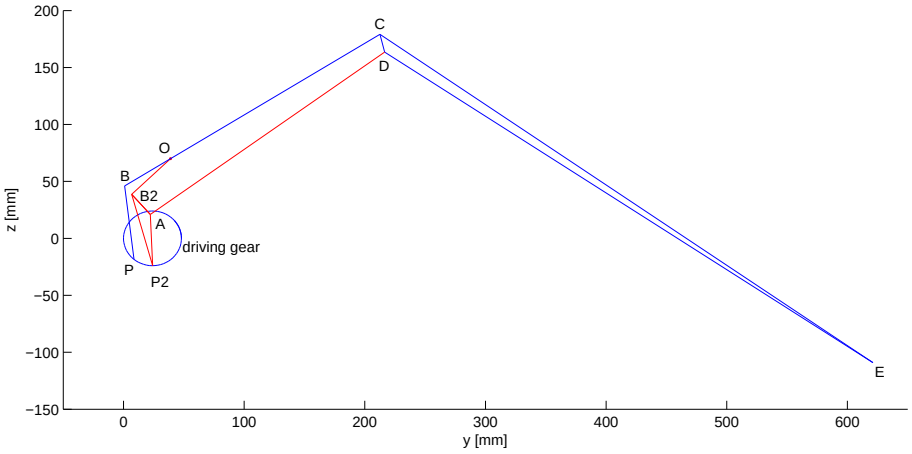

Figure 10.17: Schematic of the wing mechanism with letters to indicate beams and points

WING TWIST MECHANISM

To prevent stall on the wing tips during the flapping motion, the wing has to be twisted into the direction of the flow. Some existing ornithopters use two flapping spars, of which the rear spar has a phase lag to impose a fixed twist as a function of flap angle. A large benefit of this system is the exclusion of servos and wiring in the flapping wings, saving weight and angular inertia. Furthermore, any electronic component is likely to fail under the accelerations in the flapping wing.

Due to the previously mentioned benefits, *BirdPlane* will also use phase lag between the front and rear spars to induce linear wing twist. In contrast to existing Ornithopters, this phase lag will be made variable. Depending on the flight mode, the twist of the wing tip varies between -10° for gliding and -65° for acceleration in the downstroke. The variation in phase lag will be controlled by a planetary gearbox.

During flapping flight the wings should have a positive angle of attack at the root, varying from 5° to 6.5°, while for gliding flight the wings should have a negative angle of attack of -6° because of the highly cambered airfoils. Since the angle at the root cannot be varied with this mechanism, a compromise between gliding and flapping performance was chosen, with a angle of attack of 3° at the root. At zero phase difference between the front and rear spar, the wing twist is -10° at the tip which is optimal for gliding mode. The maximum phase difference can then be calculated using Figure 10.18, from which Equation (10.52) is derived, with $\Delta\theta = 55°$ the maximum change in twist angle, ϕ the phase lag, Δx the distance between the two spars and Δy the vertical displacement of the end of the rear spar. This results in a maximum phase difference of $\phi = 11.7°$.

$$\tan(\Delta\theta) = \frac{\Delta y}{\Delta x} \tag{10.52}$$

$$\sin(\phi) = \frac{\Delta y}{b_{1/2}} \tag{10.53}$$

$$\phi = \sin^{-1}\left(\frac{\Delta x \cdot \tan(\Delta\theta)}{b_{1/2}}\right) \tag{10.54}$$

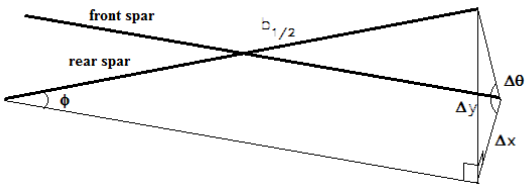

Figure 10.18: Geometry to calculate the required phase lag angle between the front and rear spar.

A fast response time for changes in the phase lag is desired for good control, but changes in the twist angle should not occur too fast, because this might lead to flow separation. Therefore, a response time of 1 s for a

maximum change in phase lag is chosen which is very fast considering the small required phase changes in operation. For the driving gear of the rear spar this means rotating with 11.7°/s or 1.95 RPM faster or slower for one second. In the next section the planetary gear system that will provide this temporary spar-frequency change is explained and the required servo motor speed is calculated.

NECK STABILIZING MECHANISM

In flapping flight the *BirdPlane* body moves up in the downstroke and down in the upstroke according to the conservation of linear momentum between wings and body. Hence, the body describes a periodic motion with a frequency around 5Hz. The neck is used to damp the movement of the head, where sensitive cameras are positioned. Barnacle Geese too, use their neck to stabilize their head. A detailed goose analysis was shown in the Midterm report [1]. The neck structure ensures the camera mounted in the head remains almost unmoved. As the camera will be used by Goose recognition software to command the flight control system, high quality of the camera footage is crucial to the mission.

The forward fuselage , i.e. neck, decouples the head from the body movement using a fully hinged parallelogram with one spring attached to two opposing corners also called an iso-elastic link. The spring is solely used to counteract gravity and keep the head raised. The spring constant should be very low in order to decouple the head movement from the movement of the body. A schematic of this lay-out is given in Figure 10.19.

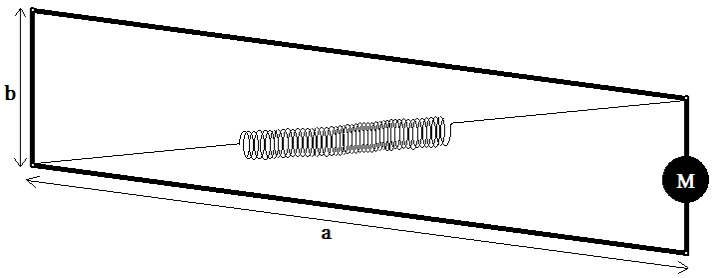

Figure 10.19: Neck spring system: Left connected to *BirdPlane* body, mass (m) right representing the camera

This complex mass-spring system can be described by a differential equation of the form:

$$m\ddot{x} = \sum F_x \tag{10.55}$$

Where:

- m = mass of the head, incl. camera and possibly other sensors
- x = Vertical displacement of the mass around equilibrium

The vertical displacement of the left vertical beam, which will be directly connected to the *BirdPlane* fuselage, is a sinusoidal excitation which is assumed to sufficiently simulating the flapping.

$$u(t) = A \cdot \sin(2\pi f t) \tag{10.56}$$

For the *BirdPlane* the following values of amplitude (A) and frequency (f) are expected:

- A = 0.025 m
- f = 5 Hz

The definition of displacements x and u over time is given in Figure 10.20

The mass spring system is described by the non-linear 2nd order differential equation given in Equation (10.57). The complete derivation of Equation (10.57) is included in the Midterm Report [1].

$$\ddot{x} = \frac{K}{m}\left(\sqrt{a^2+b^2+2b(u-x)} - \sqrt{a^2+b^2}\right) \cdot \sin\left(\tan^{-1}\left(\frac{b+(u-x)}{\sqrt{a^2-(u-x)^2}}\right)\right) \tag{10.57}$$

This differential equation has to be solved numerically, which was done using the *ode45* function in MATLAB. The following values were used as parameters for a possible design of the system:

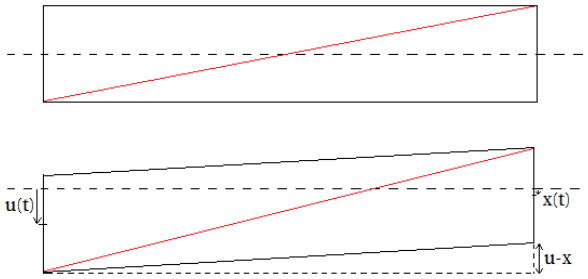

Figure 10.20: Neck displacement definition

- a = 0.16 m
- b = 0.05 m
- m = 0.100 kg
- K = 8 N/m

The decoupling performance of this system is shown in Figure 10.21. The results of this analysis are very promising as the vibrations of the body are weakened by a significant factor. The results were proven with an advanced prototype setup.

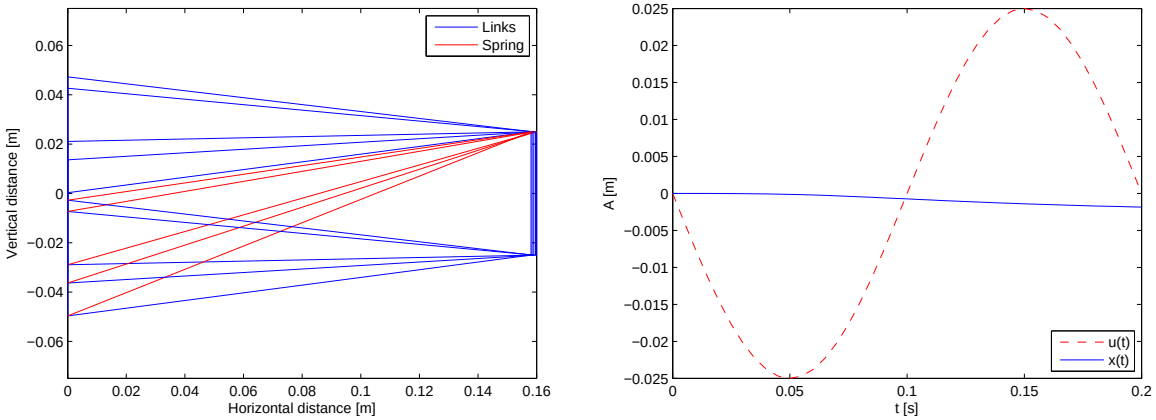

(a) Displacement for one period

(b) Amplitude over time

Figure 10.21: Iso-elastic decoupling of the head

For the final neck design two ribs and four struts are used to form a torsional stiff hinged box structure. The spring will be positioned in the center diagonal. A render of the finalize model is shown in Figure 10.22. The second figure shows the structure for u = 30 mm and x = 0 mm. Due to the spherical shape at the end of the skin, concentric with the hinge line on the rib, the structure remains completely airtight. Gaps in the skin will only show up when u - x exceeds ±60 mm.

The sizing of the Neck is shown in Figure 10.23. The whole skin, i.e. the dome and the cylindrical skin on the neck, will be made of transparent polymer. The dome will be made 0.5 mm thick and the neck skin only 0.15 mm. Both ribs will have an outer radius of 40 mm. The skin of the dome, after attaching it to the front rib will form a fragment of a smooth spherical surface with radius 40 mm. The skin of the neck includes a spherical section with an outer radius of 40.5 mm to allow for the skin thickness. This section can slide over the 40 mm spherical surface in order to maintain a self-contained skin Note that the measurements of the parallelogram are conform to the specified a and b values of 160 and 50 mm respectively.

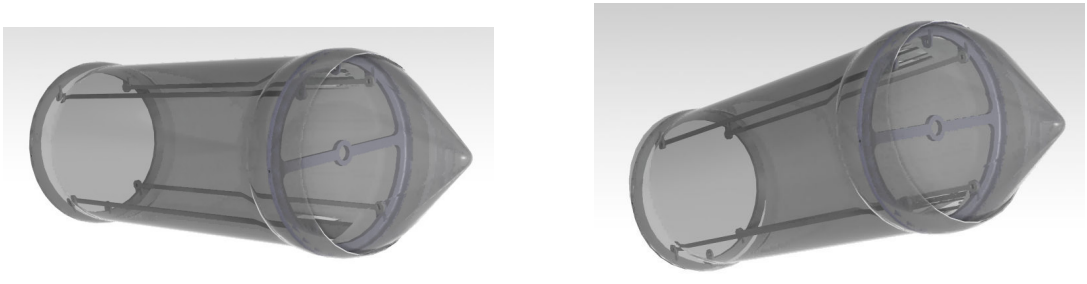

(a) Model at rest

(b) Body displacement 0f 30 mm

Figure 10.22: Model of the Neck design

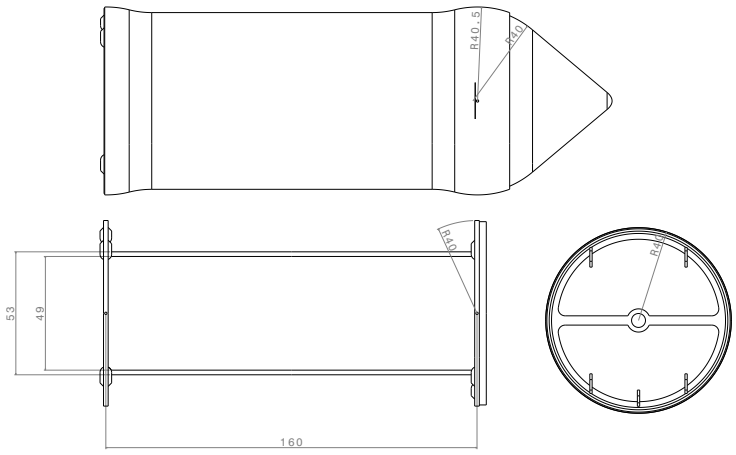

Figure 10.23: Sizing of the neck structure, all dimensions in mm

TAIL ACTUATION

The tail of *BirdPlane* is capable of several bird-like motions. The tail can be rotated completely around the longitudinal axis, pointing the tail lift vector out of the symmetry plane for lateral control. Furthermore the angle of attack of the tail can be adjusted by pitching the tail surface up or down. Lastly, the surface of the tail is variable for optimal performance over the complete flight envelope. An overview of these motions is given below:

1. *Tail rolling:* The complete tail surface is rotated around an axis parallel to the longitudinal body axis (X_b).
2. *Tail pitching:* The, possibly rolled, tail is pitched to change the angle of attack.
3. *Tail fanning:* This motion looks is similar to the (un)folding of a Chinese fan and mimics the folding of the tail feathers seen during Goose flight.

A schematic of the actuation of tail rolling and tail pitching is given in Figure 10.24

A sketch of the rolling and pitching motion of the tail is displayed in Figure 10.24. Two servomotors will be used for this; one will be fixed in the body of *BirdPlane* (Servo 1), actuating a rod providing the rolling motion of the tail, while the second servo serves the pitching control and is fixed to the rod of Servo 1. This setup is most convenient as in this way, Servo 2 (controlling the pitching motion) only has to hold the weight of the tail and does not affect Servo 1 while in rest. If the two were interchanged, Servo 2 would then have to hold the tail as well as the weight of Servo 1, requiring more energy to keep in rest.

The base of the tail of a Barnacle Geese where it is connected to the body is quite broad, which lead to an oval cross section in order to decrease the aerodynamic drag. In *BirdPlane* rotating the tail around an oval cross section will cause discontinuities at the transition from body to tail. Therefore a flexible membrane is implemented for a smooth and aerodynamically efficient transition in rolling control.

The fanning mechanism present in the tail section is shown in Figure 10.25. The fanning is actuated by a string that runs through the structure around a small pulley inside the tail. By reeling in the left end the tail is fanned

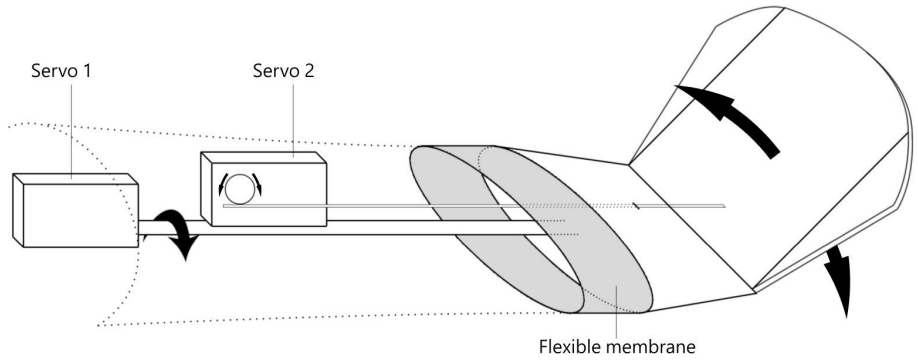

Figure 10.24: Rolling and pitching control of the rotatable tail

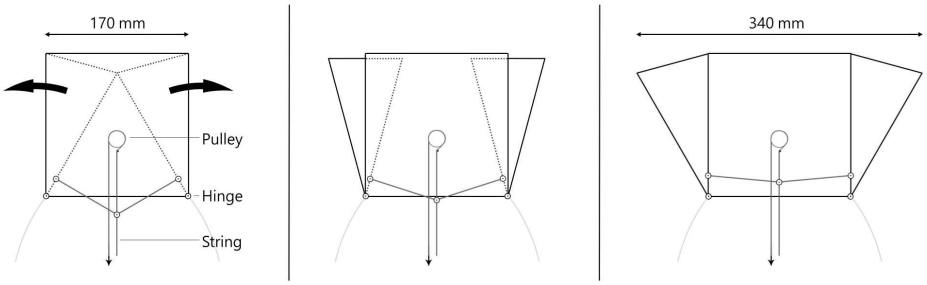

Figure 10.25: Fanning motion of the tail: (left) completely fanned-in, (middle) intermediate position, (right) completely fanned-out

out and by reeling in the right and the tail is fanned in. The advantage of using two ropes is that the rolling and pitching of the tail does not interfere with the ropes and the third servo can be placed inside the fuselage, in front of servo 1 in Figure 10.24.

GEARS

The wing flapping is powered by an electric motor (Hacker A20-12 XL EVO, see more information in Section 10.3.1), rotating at approximately 9000 RPM. As the flapping frequency is in the order of 5 Hz (300 RPM), the frequency has to be reduced significantly between the engine and the wing flap crank shaft. This reduction is done using 2 compound gear engagements, first the RPM is reduced by a factor of 5 to drive a central shaft, secondly the RPM is reduced by a factor of 6 to turn the wing crank shaft. The first reduction, shown in Figure 10.26 is equal for both front and rear spar pairs.

However, the second reduction of 6:1 is done differently for the front an rear spar drive train. The crank shafts of both front spars are attached to large gears with pitch diameters 108 mm and 72 teeth, that engage in the middle. These gears are G1 and G2a respectively. In Figure 10.27 a schematic overview is given of the front gear partial assembly. G1 and G2a drive the front spar through a crank and linkage mechanism.

G1 and G2a form a spur gear train of a gear ratio 1:1 and rotate in opposite directions, which is required for symmetric flapping motion of the wings. Only one of these gears is directly powered by the central shaft through a smaller gear (G3), with a gear of pitch diameter of 18 mm. The gear ratio between G3 and G1 is 6:1, hence the RPM is reduced by a factor of 6. A schematic overview of the gearbox assembly, including gear G3 is presented in Figure 10.29.

The wing twist control is achieved by a planetary gear system with the input on the sun gear and the output on the planet carrier. The serration on the outer surface of the ring gear is coupled to a servomotor with a small gear (G5b), that has a ratio of 5.67:1 to the ring gear. When the ring gear is kept steady this planetary gear set will have a 6:1 gear ratio between the sun and planet carrier respectively. The gears of the planetary gear train are numbered G6 to G9. G6 is the ring gear, G7a to G7c are the planet gears, G8 is the sun and G9 the carrier gear. A technical overview of the gearbox with gear numbers is presented in Figure 10.28 and Figure 10.29. The carrier is coupled to another gear (G10) through a gear ratio of 1:1. G10 directly drives the rear gear G2b which engages G2c in the middle of the rib. G2b and G2c drive the rear spar through a crank and linkage mechanism.

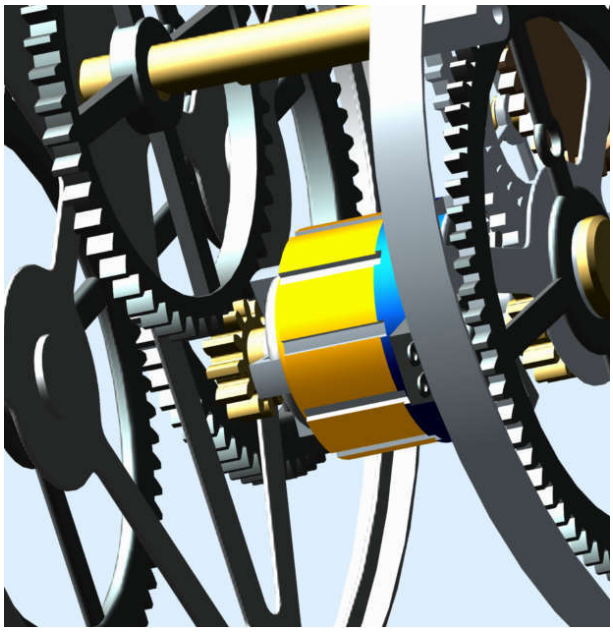

Figure 10.26: 5:1 reduction from engine to central shaft

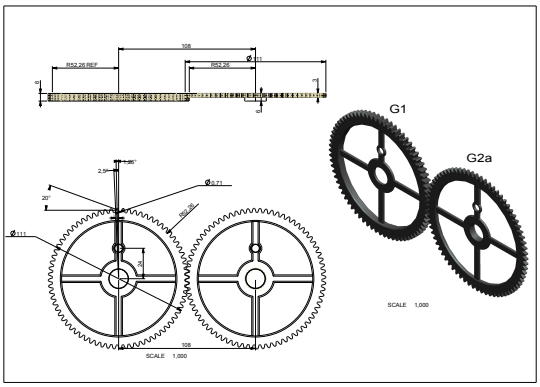

Figure 10.27: Spur gear train assembly drawing, with gears G1 and G2a

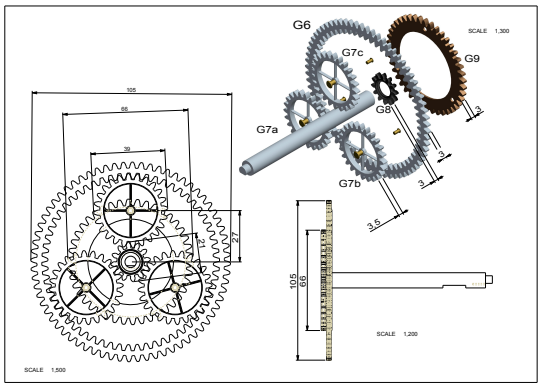

Figure 10.28: Planetary gear train assembly drawing, with gears G6, G7a-G7c, G8 and G9

A data sheet with all gear relevant specifications per gear is given in Table 10.5 in the following section.

The complete wing mechanism will use the two primary fuselage ribs for support. These ribs are placed 100 mm apart and will act as a center wing box for *BirdPlane*. The forward primary rib including the gears of the front spar is shown in Figure 10.30. Note the two spar control gears contain holes to attach the mechanism directly on the gear.

10.2.2 GEARS

Selecting the right gears for power transmission requires quite some iterations. The choice is limited by production, space, mechanism motion and subsequent ratios required to transmit the power from the electric motors with the right reduction rate. On one side the gear couples G1-G2a and G2b-G2c need to be large enough in diameter to engage in the middle of the spar without requiring an additional spur train, yet small enough to fit in the design space. Since only one motor is available to drive the entire system, designing the largest spur gear pairs (G1-G2a and G2b-G2c) in this system requires a trade-off between adding gears or or increasing the size of the gears. Either way, this results in adding mass to the system, however increasing the number of gears increases the complexity of the system, which is not a desirable option.

Moreover, the flapping mechanism in this design can be seen as a type of cam-and-follower mechanism (gear-cranks and spars). Changing dimensions or ratios of the cam, would change the motion of the follower. The

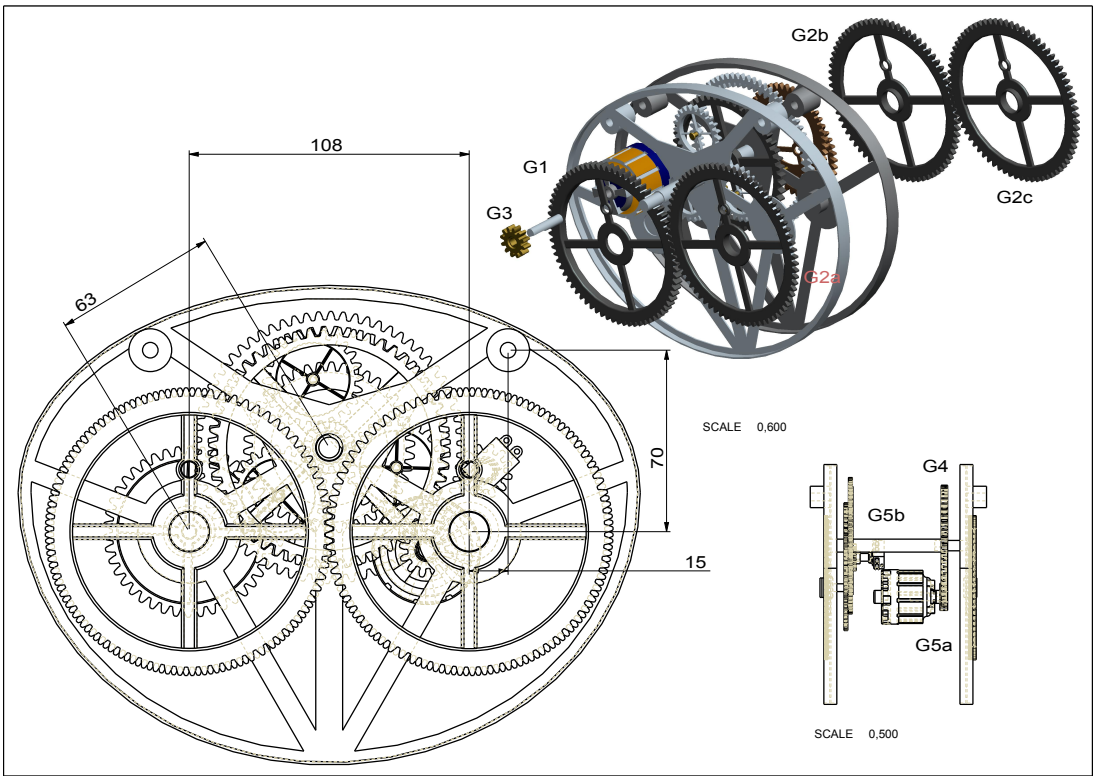

Figure 10.29: *BirdPlane* Gear box

flapping motion is designed to feed the aerodynamic demand of *BirdPlane* as accurately as possible in this stage of design. It goes without saying that the driving mechanism must be designed to preserve the required motion, resulting in a gearbox that is designed around the flapping mechanism, offering little room for full optimization.

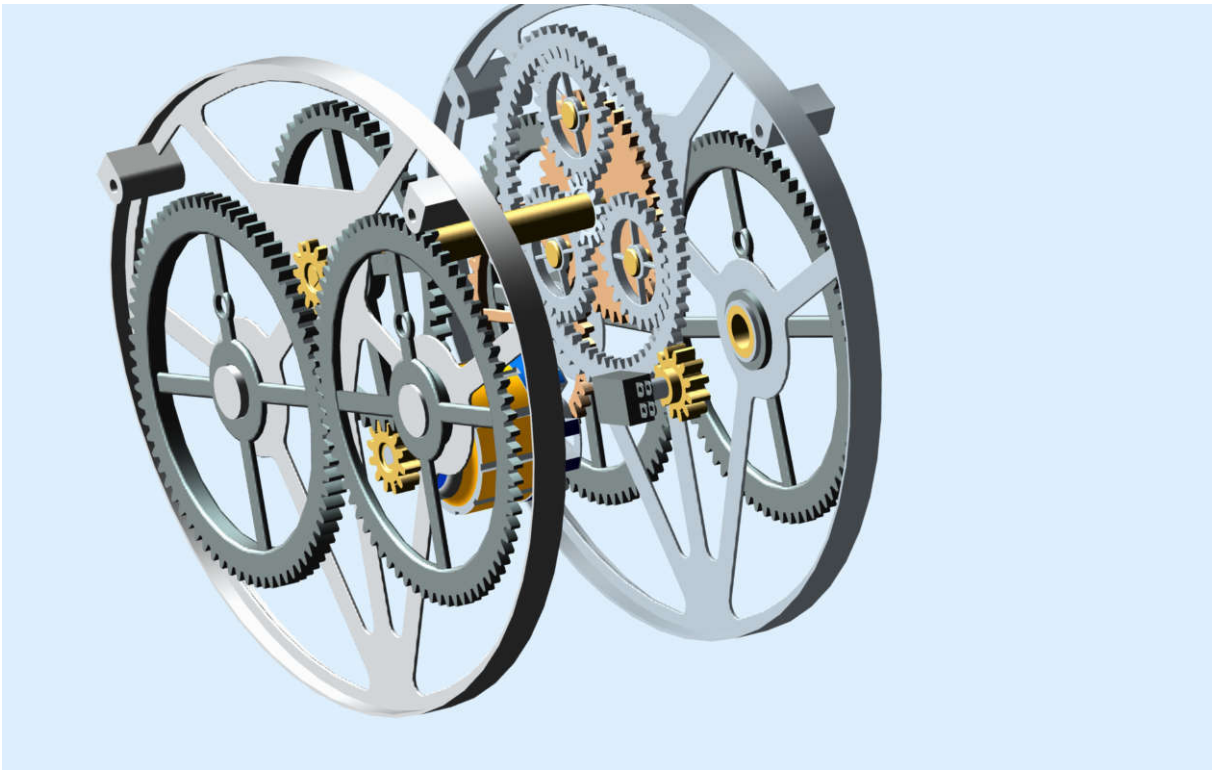

Figure 10.30: Assembled gearbox

Future work, would require detailed analysis and optimization of the cam-and-follower motion of the flapping mechanism in order to open room for gearbox optimizations as well.

Since the system requires quite high reduction ratios, attempts to limit the number of gears used in the system would result in large differences in radii between spur and planetary gear trains. While the size of the largest gear sets G1-G2a and G2b-G2c is already constrained and limited by the flapping motion and available space subsequently, making these sets too small would result in a production impasse regarding the smallest gears in the system.

A compromise between these limitations, constraints and requirements, was achieved by first investigating production limitations of gears offered on the market. The smallest size most companies produce is 18 mm diameter, 12 tooth gears. Then the largest and smallest possible radii for the main spur gear pairs G1-G2a and G2b-G2c were approximated. This result was the minimum and maximum gear size combination of 18mm and 108 mm 1.5 module gears. With these the most critical gears fixed, selection of remaining gears was mainly driven by the need to achieve required reductions for the least amount of gears and lowest weight.

The module of the gears, or the diametral pitch, is a measure of the size of the gear. Large pitch means large amount of teeth per unit pitch circumference, hence smaller teeth. Other relevant gear nomenclature, descriptions and relations are presented in Table 10.3.

Table 10.3: Gear construction relations

Symbol	Nomenclature	Description	Relation/Value
P_d	Diametral pitch	Measure for the tooth size	N/D_p
M	Module	Measure for the tooth size	$1/P_d$
P_c	Circular pitch	Circular distance between two subsequent teeth	π/P_d
N	Number of teeth	-	D_p/M
D_p	Pitch diameter	Diameter of the pitch circle	$N \times M$
D_o	Outer Diameter	Diameter of the outer circle	$D_p + 2A$
D_r	Root diameter	Diameter of the root circle	$D_p - 2B$
A	Addendum	Radial distance between pitch circle and outer circle	$1/P_d$
B	Dedendum	Radial distance between pitch circle and root circle	$1/P_d + c$
c	Clearance	Extra radial space between pitch and root circle	$0.157/P_d$
t_{D_p}	Tooth thickness	Circular width of the tooth (along pitch circle)	$P_c/2$
D_b	Base diameter	Diameter of the base circle	$D_p \times \cos\phi$
ϕ	Pressure angle	Angle between tangents to pitch circle and base through pitch point	$20°$
α_t	Circular thickness angle	Angle between two tooth flanges	$360°/2N$
R_{fill}	Fillet radius	Radius of the rounding at the base of the tooth flanges	$\frac{3}{2}c$
D_f	Tooth face diameter	Circle determining the shape of the tooth face	$D_p/4$
w_f	Face width	The width of the tooth	-
d_c	Center distance	Center-to-center distance between the driver and driven gears	$(D_{p_1} + D_{p_2})/2$
G_r	Gear ratio	Ratio between driver gear and driven gear in a spur gear train	$N_{\text{driver}}/N_{\text{driven}}$

For gear trains to transmit power efficiently, the teeth must mesh with high accuracy. To have perfectly meshing gears, some of the design parameters in Table 10.3 should be equal for gears that are directly connected. For this system, the common parameters are presented in Table 10.4.

Table 10.4: General gear specifications

General geometry	Value	Unit
M	1.5	mm
P_d	0.6667	1/mm
P_c	4.7124	mm
t_{D_p}	2.3562	mm
A	1.5	mm
B	1.7355	mm
c	0.2355	mm
ϕ	20	°
R_{fill}	0.3533	mm

Remaining dimensions are determined using relations from Table 10.3. In Table 10.5 an overview is given of all gears used in *BirdPlane* and their specifications. The last column shows the total mass in case of multiple gears.

Table 10.5: Gear specifications

Gear N°	**#**	D_p [mm]	N	D_o [mm]	D_r [mm]	D_b [mm]	α_t [deg]	D_f [mm]	w_f	**Material**	**Mass** [g]
G1	1	108	72	111	104.529	101.487	2.5	27	6	Nylon	21.6
G2	3	108	72	111	104.529	101.487	2.5	27	3	Nylon	12.3
G3	1	18	12	21	14.529	16.915	15	4.5	3	Steel	4.7
G4	1	90	60	93	86.529	84.572	3	22.5	5	Nylon	11.8
$G5_a$	1	18	12	21	14.529	16.915	15	4.5	6	Steel	10
$G5_b$	1									Nylon	1.78
$G6_{outer}$	1	102	68	105	98.529	95.849	2.65	25.5	3	Nylon	7.6
$G6_{inner}$		90	60	93	93.471	87	3	22.5			
G7	3	36	24	39	32.529	33.829	7.5	9	3.5	Steel	1.72
G8	1	18	12	21	14.529	16.915	15	4.5	3	Nylon	0.49
G9	1	63	42	66	59.529	64.839	4.29	15.75	3	Nylon	3.0
G10	1	63	42	66	59.529	64.839	4.29	15.75	3	Nylon	3.1

PLANETARY GEAR TRAIN FOR TWIST CONTROL

Effective, variable twist is achieved by controlling phase variation of the rear spar pair using a planetary gear train. The rear end of the central shaft rotates the sun gear (G8) which in turn drives the 3 planet gears (G7a,b,c). The planets rotate around their own axis because they are meshed to the sun gear in spur configuration. However, due to the presence of the ring gear the planets cannot rotate without translating. This results in the rotational motion of the planet carrier. In a planetary gear, a combination of any of the 4 elements as drivers in the system is possible. In this figuration, however, the sun and the ring gear are always the drivers. The planets and the planet carrier are the outputs, although the latter is more of interest than the first.

In nominal conditions the ring gear will be fixed ($\omega_R = 0$ rad/s). The amount of teeth on the components of a planetary gearbox has to comply with Equation (10.58)

$$N_R = N_S + 2 \cdot N_P \tag{10.58}$$

The following parameters were used for a fixed ring, 6:1 reduction planetary gearbox. The gear ratio between the sun and the carrier is defined by Equation (10.59)

- $N_S = 12$ (Number of teeth on the sun gear)
- $N_P = 24$ (Number of teeth on one planet gear)
- $N_R = 60$ (Number of teeth on the ring gear)

$$G_r = \frac{\omega_C}{\omega_S} = \frac{N_S}{N_R + N_S} \tag{10.59}$$

The output shaft of the planetary gear box is already rotating at the right RPM to drive the wings. The rotation is transfered to one of the rear spar crank shafts with a 1:1 gear ratio. The pitch diameter of these two spur gears is imposed by the distance between the two shafts. This is fixed by the engagement of the gears turning the front spar, with pitch diameters 18 and 108 mm. Therefore, the pitch diameter of the gears is:

$$D_p = \frac{18 + 108}{2} = 63 \text{ mm}$$

The rotation of the driven rear spar is coupled to the other rear spar by two spur gears with pitch diameter 108 mm.

To vary $\theta(\beta)$, the relation between twist and flap angle, the phase lag of the rear spar is increased/decreased by rotating the ring gear. The maximum rate of phase adjustment is set to 11.7°/s. Using this rate the $\theta(\beta)$ can be adjusted between its two extremes in one second. This entails a variation in rotational speed of the carrier of 1.95 RPM. The sun is still rotating at 1800 RPM, i.e. $6 \cdot 300$ RPM, as this is the nominal speed of the center shaft. The relation between the rotational speed of the carrier as function of sun and ring rotation is given by Equation (10.60).

$$\omega_C = \frac{\omega_S N_S + \omega_R N_R}{N_R + N_S} \tag{10.60}$$

Equation (10.60) can be rearranged to:

$$\omega_R = \frac{\omega_C(N_S + N_R) - \omega_S N_S}{N_R} \tag{10.61}$$

As the nominal rotational rate of the carrier is 300 RPM and the variation is 1.95 RPM, the carrier will rotate at 301.95 RPM to decrease the phase lag and 298.05 RPM to increase the phase lag. Using Equation (10.61) the rotational rate of the ring gear is calculated to be ± 2.34 RPM. These calculations assume instant variation of the rotational rate ($\alpha_R = \alpha_C = \infty$). In reality the time to accelerate and decelerate the mechanism will require a higher ω_R than presented here. As the rotational rate is so low this should not entail any significant problems. In order to keep track of the precise actual phase lag the position of the back spar is continuously tracked with help of a second hall sensor (implementation shown in Section 10.3.5).

Also the ring adjustment will be monitored by an angular displacement sensor on the ring servo. Therefore the exact adjustment rates will not have to be integrated for the wing setting determination.

The servo actuating the ring gear will use a 5.667:1 gear ratio to turn the ring gear. The ring gear itself will have 60 and 68 teeth on respectively the in- and outside and the servo gear 12. (Table 10.5). Using the previously calculated ring rate of 2.34 RPM, the servo needs to rotate at 13.26 RPM.

The complete assembled drive-train is shown in Figure 10.30. The structure supporting the engine and the servo was deliberately left out to improve the visibility of the mechanism.

GEAR CONSTRUCTION (CAD)

All gears were constructed in PRO-ENGINEER according to the specifications in table Table 10.5. First, the outer circle and root circle are drawn with diameters D_r and D_o on disc with diameter D_p. A tangent to the pitch circle, normal to the centerline, is drawn at a point of intersection (pitch point) with the pitch circle. Through the pitch point a line of action is drawn at an angle of 20° to the tangent through the pitch point, this line is the pressure line. D_b is constructed by drawing a tangent circle to the pressure line. Circle A with diameter D_f is drawn around the pitch point. Another circle A with the same diameter is drawn around the intersection point of circle A with the base circle. The right side of the curve represents the right tooth face. The curve is mirrored w.r.t. a line at half α_t from the vertical center line. A fillet with radius R_{fill} is drawn at the base of the profile and mirrored w.r.t. half-α_t-line. All teeth are drawn using this construction method and tested for meshing in a CAD mechanism simulation. Figure 10.31 shows a CAD screenshot of the construction lines.

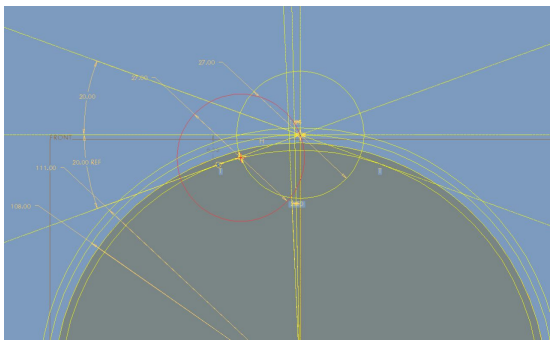

Figure 10.31: Gear construction method

10.2.3 STRUCTURES

The design of the structure of *BirdPlane* is closely related to the mechanisms. The mechanisms as presented in Section 10.2.1, should not only allow for the required motion, but also carry the loads induced by those motions. In addition, the internal structure should give the required aerodynamic shapes of the airfoils inside the wing and tail and the fuselage by means of ribs. Inside the fuselage the internal structure functions as mounting point for the payload and the connection between wings, neck and tail. The structure is covered by a skin that protects the payload and provides the aerodynamic shape.

WING STRUCTURE

Both wings have two spars which are positioned 100 mm apart. Each spar has an upper and a lower rod to drive the wing folding. Since the lift on a wing usually acts around the quarter chord line, which is also roughly the position of the front spar, it can be assumed that this spar carries most of the load. The loads on the wings are highest during the downstroke, in which the bending of the wing loads the upper rod in compression and the lower rod in tension. Rough calculations on the ultimate compressive and tensile strength of carbon fiber rods showed that those are no limiting factors: rods of 1.3 mm diameter would already be sufficient to carry the maximum force generated on the wing. The shear force at the root is even less limiting, requiring rods of less than 0.5 mm.

It is difficult to calculate what the exact loading of the structure will be. Especially the peak loads induced in the flapping mechanism of the wings and the effect of the large number of cycles on fatigue are hard to predict. Therefore, the structure is over-designed for the expected loads on the *BirdPlane* structure. Those margins are also sufficient for impacts at landings and gusts. In a detailed design, using the knowledge that is available about carbon fiber composites an efficient design of the structure can be made for the first prototype of *BirdPlane*.

Since the tubes can thus be very thin, producibility and commercial availability are considered in choosing the dimensions. Carbon fiber tubes of many dimensions and thicknesses are available. The thinnest tubes available have 8.8 mm outer diameter (OD) and 8 mm inner diameter (ID) [51]. These would be very suitable for the front spar. For the tip section of the wing and the rear spars even smaller diameter would be sufficient, so tubes of 6.8 mm OD and 6 mm ID are used.

Besides strength, the stiffness is also a main design concern. The bending resistance will come largely out of the tensional stiffness of the lower links and and also partly from the compressional stiffness of the upper links. These links will be made from CFRP, which has very low failure strain (0.8%). As these parts are loaded far below failure strain, the structure should have adequate stiffness.

The airfoil shape of the wing cross section comes from the ribs on the spars, with 4 ribs on the root section and 4 ribs on the tip section. The ribs are 0.5 mm thick. The wings are covered by a thin, slightly flexible skin, such that the airfoil shape is remained between the ribs, but some deformations are allowed for variable wing twist.

FUSELAGE STRUCTURE

The fuselage will have a total of 4 CFRP ribs, including the rear rib of the neck structure. These ribs will be connected by a truss structure of carbon fiber rods. The fuselage skin will be attached to the outer surface of the ribs. The skin has the sole purpose to make the structure air and splash-water tight. As it has no load carrying function the skin thickness can be set to the manufacturing minimum, i.e. smaller than 0.5 mm.

The ribs are the main support for the subsystems. All the shafts of the wing mechanism will use the two center ribs for support. The main Li-S battery will be mounted outside the two center ribs. It will be attached as low as possible to lower the Z_b-position of the center of gravity.

Forward of the front center rib there will be abundant volume for hardware components of the control system. The 3 servos used for the tail are placed rearward of the rear center rib. This allows the torque required to rotate the tail to be directly transfered to the stiff fuselage-wing section.

The two center ribs will be 5 mm thick with flanges of 10 mm. To save weight 7 large cut-outs remove abundant material. The front an rear ribs will be only 2 mm thick. The loads on this part of the structure are expected to be very low and these ribs are mainly required to support the skin. The catapult attachment will be between forward fuselage section, i.e. between the front rib and the forward center rib. The loads of the launch will be transfered to the center section via the CFRP truss structure connecting the previously mentioned ribs.

For the truss structure OD 6.8 mm, ID 6 mm CFRP tubes are used, equal to the links in the tip and rear spar of the the wing structure. These links are very light weight and versatile enough to flex in a crash landing.

The neck structure consists of two ribs and four links as was already discussed in Section 10.2.1. The rear neck rib doubles as the most forward fuselage rib. Both ribs have a circular cross-section with an outer diameter of 80 mm and circular cut-out of $\varnothing$= 70 mm. The thickness of these CFRP ribs is set to 2 mm.

The four links used for the parallelogram are bar shaped CFRP parts (160X2X1mm) that can be cut out of a 1 mm thick CFRP sheet. At both ends the width is increased from 2 mm to 5 mm in circular end caps, thereby creating enough material for the hinges.

10.2.4 MATERIALS

BirdPlane is made of a load carrying structure of ribs and rods that are covered by a skin, as described in Section 10.2.3. The load carrying structure is subject to several forces and moments and moving parts of the mechanisms suffer high wear from friction. The skin protects the payload of the fuselage, carries some aerodynamic loads and has to absorb impacts. Those different functions and loadings require different materials, of which the design choices are described in this section.

LOAD CARRYING STRUCTURE

The load carrying structure has to have high strength and stiffness. The materials that provide the required mechanical properties for a low weight are carbon/epoxy composites. For *BirdPlane* a composite with 63% fiber volume of AS4 carbon fibers in a 3501-6 epoxy matrix is used.

To enhance the lifetime of *BirdPlane* the structure can be made of a self-healing composite. The NovAM research group is currently developing self-healing fiber composites with compartmented fibers in PMMA [52]. In this bio-inspired composite some of the carbon fibers are replaced by compartmented alginate fibers filled with healing agent of 1,2-diclorobenzene. Upon fracture or cracking of the composite, some of the compartments break and release the healing agent. The large advantage of the compartments compared to the already available self-healing composites with hollow tubes is that only one compartment in a fiber is emptied at a time. One fiber can therefore provide healing agent multiple times. Exact quantitative data about the effect on the mechanical properties of adding those fibers to a composite is not available yet, but the effects seemed to be small. These self-healing composites are thus a very promising material for future development of *BirdPlane*.

BELLY FOR LANDING

BirdPlane will not have any landing gear, but will just land on its belly. This will most likely happen on a rough surface of grass or stones and sand and with some impact. An ideal material for absorbing the impact and recovering from scratches and tears from the landing is the "smart rubber" developed by Ludwik Leibler [53]. The material reconnects at a cut interface within a few seconds at room temperature while keeping the desired properties of normal rubbers of recoverable extensibility of several hundred percents with little creep. At a cut surface there is a high density of non-associated groups that immediately form hydrogen bonds when brought in contact with the other surface. After this first connection the molecules become entangled over time by diffusion over the interface, after which the mechanical properties are recovered nearly completely. One of those mechanical properties is the high damping, which is beneficial for absorbing the impact on landing. In addition this material is produced from renewable resources and easy to produce, process and recycle which makes it a sustainable and cost-efficient choice.

FLEXIBLE SKIN ON MOVING INTERFACES

The wings and tail move and rotate in several directions with respect to the fuselage. To provide good, bird-like aerodynamics at the interfaces a flexible skin will be used. The self-healing polyimide that is currently under development within NovAM by Arijana Susa is a suitable elastomer. The strength and elasticity of this material can be tuned by changing the composition. The required mechanical properties will have to be determined experimentally. The main advantage of using a self-healing material is that small cracks that might be induced due to the high number of cycles or unexpected deformations due to for example gusts will heal themselves over time. Since the material will be applied at the outside, it is easy to provide some extra heat when cracks are detected, by which *BirdPlane* can be repaired quickly for the next flight.

WING AND FUSELAGE SKIN

The remaining parts of the *BirdPlane* skin are made of a non-flexible material to maintain the aerodynamic shape. Apart from keeping its shape under the aerodynamic loads while supported by the ribs there are few requirements on the skin. It should be stiff but not too brittle and light weight. A material that has those properties and is cheap, readily available and easily recyclable is Nylon 6-6. A 0.2 mm thick Nylon skin (with ρ_{nylon}=1,150 kg/m^3 the skin is 171 g/m^2) will be applied on the neck, fuselage and tail. As mentioned before, the skin of the wings should allow small deformations for wing twisting. To allow this and to reduce the wing weight the skin of the wings will be made of Nylon sailcloth of 136 g/m^2. A protective coating will be applied to increase the UV resistance and make the skin waterproof.

GEARS

The material choice for the complete gearbox consisting of 15 gears, is carbon steel and Nylon. The small gear directly mounted on the shaft of the electric motor (G5a) will be spinning with 9000 rpm. Therefore G5a will be made of steel. With a reduction ratio of 5 to the driven gear G4 the forces on the second gear are expected to be higher. The torque increases throughout the system as well, although it is compensated by the fact that gear G4 is 5 times larger than G5a. The next gear after G4 is is gear is G3 and it rotates with the same angular velocity as G4, as it is mounted on the same shaft in parallel. However, since G3 is 5 times smaller than G4, the torque and forces on G3 are more probable to cause wear or failure, which is why also G3 is chosen to be made out of steel. All other gears, including the gears that drive the crank-spar system, the planetary gears and the gear on the shaft of the servo, will be made of Nylon. Nylon gears are widely used in engineering applications and have proven to be efficient enough in transferring mechanical power. Wear resistance properties of Nylon in operation is satisfactory for this design.

10.3 ELECTRONICS

In the previous chapters and sections the Mission (Chapter 5) was analysed and the Aerodynamic (Section 10.1) and Structural (Section 10.2) design of *BirdPlane* were derived accordingly. Now a link between the systems to realize the anticipated performance is necessary. Advanced autonomous control capabilities and measurement equipment is needed to satisfy the mission.

The electronic subsystem has the task to be the interface between the previously mentioned subsystems and the operator to fulfil the mission successfully. It needs to drive the mechanisms (Section 10.3.1), provide the required power (Section 10.3.2), establish the communication links to ground (Section 10.3.3) and provide the required artificial intelligence by means of a sophisticated navigation (Section 10.3.4) and control (Section 10.3.5) system. Furthermore, the electronics system is responsible to gather the scientific data (Section 10.3.6). The large number of subsystems inside the electronics system are connected with an ingenious embedded system (Section 10.3.7).

10.3.1 ACTUATION

After the extensive trade-off on different methods of actuation for the main flapping mechanism during the Midterm phase (Section 9.2) it was finally decided that electric motors will have the best power-over-weight ratio and the best efficiency. Furthermore all actuations of the control surfaces will be done using electric servo motors. This section will discuss the sizing of these components and present a set of available devices.

MAIN MOTOR

As explained in Section 10.2.1, the main mechanism is driven by one electric motor which is connected via a set of gears to two spars per wing. A planetary gear system with an attached servo motor is used to change the phase difference between the two spars which results in the twisting of the wing. The main mechanism therefore consists of two devices for actuation, the electric motor and the servo.

The sizing of the motor is mostly dependent on the gear ratios combined with the flap frequency and the power required during the flight. These values have been determined in Section 10.2.1 and Section 10.1.1. While the flap frequency is 5 Hz on average, it changes between a maximum and a minimum value. These values have been determined to be 20.8 rad/s at peak power of 82.1 W during downstroke and 44 rad/s at minimum power of 0 W during the upstroke.

Combining the knowledge of the required flap frequencies and the gear ratios of the mechanisms it is possible to work out the required minimum and maximum rotations per minute (RPM) of the motor as shown in Equation (10.62).

$$RPM_{\text{motor}} = \omega_{\text{wing}} \cdot G_{r_1} G_{r_2} \cdot \frac{60}{2\pi} \tag{10.62}$$

$$RPM_{\text{motor,min}} = 20.8 \text{ rad/s} \cdot 5 \cdot 6 \cdot \frac{60}{2\pi} = 5958.76 \text{ RPM}$$

$$RPM_{\text{motor,max}} = 44 \text{ rad/s} \cdot 5 \cdot 6 \cdot \frac{60}{2\pi} = 12605 \text{ RPM}$$

With the given peak power and the calculated RPM of the motor, the torques can be determined that will be applied on the motor.

$$\tau_{\text{motor}} = 2\frac{60P_r}{2\pi \cdot RPM_{\text{motor}}} \tag{10.63}$$

$$\tau_{\text{motor,min}} = 2\frac{60 \cdot 0.008}{2\pi \cdot 12605} = 1.212 \cdot 10^{-5} \text{ Nm}$$
$$\tau_{\text{motor,max}} = 2\frac{60 \cdot 82.1}{2\pi \cdot 5958} = 0.2632 \text{ Nm}$$

The lowest torque is approximately 0 so the RPM corresponding to that value can be assumed to be the free running RPM. This allows for the selection of a Motor/Voltage combination.

One difficulty in this application is that the **highest power output is required at the lowest frequency**, which usually corresponds to low voltages in order to also achieve the peak power of the motor at this point. Thus, high currents are required to achieve this power at the low voltage. As a solution to this problem, the peak power of the motor has to be chosen high enough to provide the values required while running below the peak. Larger motors with equal speed constants (k_v) are usually designed for higher currents and therefore will be safe against overheating.

The most important aspect of the motor choice therefore is to estimate the **peak power** of the motor. With a peak value of 82.1 W per wing during cruise flight, a total of 164.2 W needs to be the mechanical output power. As the calculations were done only for cruise flight, the acceleration and climb phase need to be adjusted accordingly and all further calculation will be based on the available data for cruise.

During the midterm phase of the project, it was decided to use a **brushless DC motor** which is the standard for RC model industry mostly due to their advantageous power-to-weight ratios and wide range of available sizes. Strictly speaking these motors are powered by an alternating electric current which comes from an inverter: the motor controller. This controller converts the DC input signal to AC signals, controlling amplitude and waveform. The controller is provided with the desired frequency and torque and then adjusts the output voltage amplitudes. Also the controller needs to be scaled based on the maximum current that will be drawn by the motor.

Firstly the battery voltage will be fixed to a maximum of 12 V which is important for the later implementation of the complete electronics circuit explained in Section 10.3.7. This will mean that the speed constant k_v of the motor needs to be around **1050 RPM/V**(see Equation (10.64)).

$$k_v = \frac{RPM_{\text{motor,max}}}{V} = \frac{12600\text{RPM}}{12\text{V}} = 1050 \text{ RPM/V} \tag{10.64}$$

Based on this value and the requirement on the maximum power a motor was chosen for continuing calculations on the motor controller size. The chosen motor is the **Hacker A20-12 XL EVO**. Table 10.6 shows an overview of the most important data of this motor which is depicted in Figure 10.32.

Figure 10.32: Hacker A20-12 XL EVO, 78 g, 300 W max power [54]

Table 10.6: Overview of the most important aspects of the Hacker A20-12 XL [54]

Parameter	**Hacker A20-12 XL EVO**
Power range	max. 300 W (15 s)
Idle Current @ 8.4 V	1.2 A
Resistance	0.075 Ohm
k_v	1039 RPM/V
Weight	78 g
Diameter	28 mm
Length	40 mm

The peak power this motor can provide seems to be excessively higher than what is required of the motor, but this should leave enough margins for the additional required power during climb and acceleration phases.

In order to chose a controller for this motor, the point of maximum torque during the wing stroke needs to be considered. The target torque (τ) for this part is 0.26 Nm with a corresponding frequency of 5958 RPM (623.92 rad/s). The electric current varies linearly with the applied torque, the proportionality constant being the motor torque constant [55].

$$\tau = k_m I \tag{10.65}$$

The motor constant k_m is directly related to the speed constant of the motor. Equation (10.67) shows this relation and supports it in terms of a unit equality.

$$\begin{aligned} k_m &= 1/k_v \\ \frac{\text{Nm}}{\text{A}} &= \frac{\text{V}}{\text{rad/s}} \\ k_m &= \frac{60}{2\pi \cdot 1039} = 0.0092 \text{ Nm/A} \end{aligned} \tag{10.66}$$

Using Equation (10.65), results in a **maximum current** drawn from the motor of **28.3 A**.

In the interest of finding the maximum current, the idle current needs to be added to the one calculated above. As shown in Table 10.6 the idle current at 8.4 V is 1.2 A which will be assumed constant over the range of the calculated voltage. Thus the total current is found to be **29.5 A**.

In conclusion, the current analysis suggests that the above determined value will - at no phase during the flight - be higher than 30 A. As during flight phases like climb and acceleration, where higher power is required also the flap frequency is increased, less stress in terms of current and overall higher voltages result. As the power of the motor is more than sufficient to also deal with considerable increases in power required, the above calculated values should be the most strenuous requirements.

With this in mind the Hacker Speed Controller X30-Pro with the specifications as shown in Table 10.7 is a suitable choice. The controller is illustrated in Figure 10.33.

Table 10.7: Overview of the most important aspects of the motor controller [56]

Parameter	**Hacker X30-Pro**
Operating voltage	6-12 V
Dimensions	51x24x10 mm
Weight	24 g
Operating current	30 A
BEC load	2-3 servos

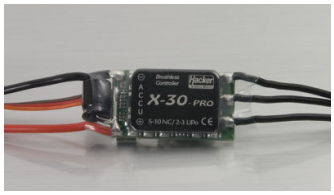

Figure 10.33: Hacker Speed controller X30-Pro with BEC, 24 g, 30 A max current [56]

This controller has the additional advantage to have a Battery eliminator circuit (BEC) for up to 3 servo motors. This feature monitors the input voltage from the battery and shuts of the main motor once the voltage drops considerably due to low energy levels in the battery. This way the aircraft stays operational as the remaining energy is redirected to the control surfaces only (assuming that the micro controller is directly connected to the battery, discussed in Section 10.3.7).

One more aspect of the motor that is of importance for the current stage of the design is the motor efficiency. This will determine how much electrical power is actually pulled from the battery during operation. This efficiency will again be determined at the point of maximum power usage as low RPM of the engine usually entail lower efficiencies.

The output voltage of the motor controller can be calculated with the above derived constants and values for current and resistance.

$$\begin{aligned} V &= \frac{\tau R}{k_m} + \left(\omega \frac{1}{k_v}\right) \\ V &= \frac{0.26 \cdot 0.075}{0.0092} + \left(623.92 \frac{1}{108.7}\right) = 7.859 \text{ V} \end{aligned} \tag{10.67}$$

With the maximum current of 29.5 A as calculated before, the electric input power into the motor is **231.84 W**. The mechanical output power is the multiplication of frequency and torque.

$$P_{\text{mech}} = \tau\omega = 0.26\text{Nm} \cdot 623.92\text{rad/s} = 162.2\text{ W} \tag{10.68}$$

$$\eta = 162.2/231.84 = 0.699 \tag{10.69}$$

The resulting efficiency 0.699 will be in the lower regime of the efficiency compared to the rest of the wing stroke. Thus it is a good, slightly conservative estimation of the motor efficiency.

As the motor is connected to a set of gears and these can also heat up considerably during operation, another factor of 0.9 will be included into the **complete mechanism efficiency**, thus being **0.6288**.

SERVO ANALYSIS

At this stage of the design, most forces have only roughly been estimated and therefore sizing of the servo motors is difficult. Overall four servos will be built into *BirdPlane*: One to change the phase difference between the two actuated spars of each of the two wings and three to actuate the movable tail.

Main wing servo The servo for the main wing mechanism is connected to the outer ring of the planetary gear and will turn it when changes in velocity or the ratio of lift and thrust are required. The forces it needs to work against during this adjustment are mostly friction forces and the aerodynamic forces on the wing, which are very hard to calculate. Since the major part of the aerodynamic forces can be assumed to act on the front spar, and this servo has to cause a rotation around the longitudinal axis the forces can be assumed to be small. The only requirement on this servo that can be identified at this point is that it needs to turn with 14 RPM for an interval of 1 s as described in Section 10.2.1.

Tail servos Overall three servo motors will need to be installed in the rear of *BirdPlane* to actuate the tail: One for the pitch control, one for the roll control and one for the folding of the tail. As for the main wing servo, exact calculations for the torques on these motors go beyond the scope of this project. What can be said is that the roll control and folding will only need to counter friction, while the pitch servo also needs to cope with aerodynamic forces. The torques for the pitch action can very roughly be estimated as the tail forces during cruise are known from the stability analysis. The moment at the hinge-line was thus calculated to be 0.131 Nm. However these are the minimum forces at the hinge and thus on the servo motor. In order to be on the safe side a large safety margin will be included, the torque for the servo motor will be assumed to be as big as 0.5 Nm.

There is a wide range of servos available for a huge range of torques and reaction times. As the exact sizing is not possible one possible option for the servos will be presented here for the sake of weight estimation and the overall implementation of the electrical system.

The type of the servo should be digital. This is currently the standard in robotics and RC models, as these servos provide faster reaction times and constant torques. They do use slightly more power but as the actuation will not be continuous this disadvantage is not big enough to opt for an analog system. Thus one option for the pitch servo would be the Bluebird Midi servo BMS-390. Table 10.8 shows a listing of the most important properties of this motor.

Table 10.8: Overview of the most important aspects of the servo motor

Parameter	**Bluebird Midi servo BMS-390 [57]**
Torque at 4.8 V	0.46 Nm
Actuation time at 4.8 V	0.14 s (60°)
Width	13 mm
Weight	23 g
Servo technology	Digital

This servo has a torque which is just below the mentioned value at 4.8 V which will be the output voltage from the Controller. The weight is 23 g which is a considerable weight for only one servo motor. Further analysis and especially testing will be needed in order to validate the rough estimation and make a more sophisticated determination of the actual torques. Furthermore, a lighter servo has to be found.

SUMMARY

At this point, the main motor, its controller and one of the tail servos have been specified. It is important for the evaluation of the feasibility of the design to make an estimate of the weight of each system. For that a weight for the other three servos needs to be assumed. As explained before, these servos are mostly resisted by friction forces and small aerodynamic turbulences which makes their torque requirements quite small as well. Servos are divided into size classes, the above mentioned servo being in the midi range. It is expected that the other three servos will be one size smaller, thus in the mini range. This usually corresponds to a weight of about 10-14 g. Especially for the fanning of the tail very small torques are expected and even a micro servo can be used, for example the HS-35HD Micro Servo Motor [58] of 4.5 g. The mass of wing and tail actuation are calculated respectively in Equation (10.70) and Equation (10.71).

$$m_{\text{w,act}} = 78\text{ g} + 24\text{ g} + 12\text{ g} = 114\text{ g} \tag{10.70}$$

$$m_{\text{t,act}} = 23\text{ g} + 12\text{ g} + 5\text{ g} = 40\text{ g} \tag{10.71}$$

Because of the average weight of 12 g for the two mini servos, the total actuation system weight excluding cabling, will therefore be **114 g** for the wings and **40 g** for the tail.

While most of the above calculation were done on the most power hungry part of the stroke during cruise flight, the average power requirement is substantially lower, namely 20.13 W per wing, 40.27 W in total. Including the efficiency factor as calculated in this section the power used by the actuation mechanism is 64.04 W. In order to compensate for simplifying assumptions and the sporadic actuation by the servos a **total power of 80 W** will be used for further calculations.

10.3.2 POWER

In the previous Midterm report, four different power supply systems (batteries, solar cells, fuel cell, and internal combustion engine) were explored and compared in terms of specific energy of the system. The conclusion was that the two feasible options were Li-S batteries and 2-stroke micro IC engine with the gear transmission system. Even though the micro IC engine could provide higher specific energy, it had critical disadvantages, such as the production of exhaust gas, noise, and some other operational limitations. Therefore, the Li-S batteries were chosen for the final design of the power subsystem.

LI-S BATTERIES

The highest specific energy of Li-S batteries on record has been achieved by the prototype battery developed by Lawrence Berkeley National Laboratory at 500 Wh/kg. They demonstrated that this particular type of Li-S prototype cell had a significantly high initial discharge capacity of 1,440 mAh/g of sulfur at 0.2 C rate, and an extremely low decay rate of 0.039% per cycle [59]. This ensures the long durability of the cell, as well as the capability to produce enough discharging current. Also, the energy density of the Li-S battery of 500 Wh/kg of specific energy is estimated to be about 600 Wh/L [60]. Therefore, the *renewed* 130 W power supply requirement for 100 minutes of mission duration results in a total energy demand of 217 Wh. This suggests that the battery will weigh around 435 g with the volume of approximately 361 cm^3 (For the complete power budget, refer to Section 11.1). It should be however noted that this certain type of Li-S battery is not yet readily available, as it is still a prototype cell at laboratory scale. Therefore, it is highly likely that in practice the currently available Li-S cell would exhibit specific energy lower than 500 Wh/kg. Nevertheless, the growing trend of Li-S cell capacity suggests that this level of batteries will be available for practical use in a foreseeable future.

In addition to the battery, an electric current monitor, ACS761 from Allegro MicroSystems [61], is also implemented in order to monitor the current and manage the power supply from the battery. This device is chosen as it is capable of handling a wide range of voltage (up to 12 V) that is applicable for the miniature-sized UAVs. By keeping the log of the current and voltage that has been provided by the battery, the energy consumption can be deduced, and thus, the remaining battery level.

While this sensor monitors the current and voltage level supplied by the battery, it may be also desired to know specifically how much of this power is used for driving the main motor, and how much is used for the other electronics. This is in order to investigate the flight efficiency during the formation flight (Item **SG-4**). The power consumed by the main motor may be directly measured by using an absorption dynamometer. However, this is only an optional choice because the power consumption of the electronics other than the main motor is expected to be more or less constant during the cruise flight, and thus, the total power consumption level can be

compared to study the flight efficiency of the formation flight. Besides, the use of an absorption dynamometer will also increase the total system weight. Therefore, this is left as an open option in case the power consumption of the avionics fluctuate significantly during the cruise.

BATTERY IMPLEMENTATION

The battery pack with a total mass of 435 g and a volume of 3.61 cm^3 must be placed in the body. As stated earlier in Section 10.1.2, the battery pack can be used to shift the center of gravity at 433 mm. The body configuration is made such that there are two ribs in the center of the body: 365 mm and 465 mm from the tip, respectively. The battery pack will be split into two, and placed before and behind these two ribs in order to leave the space in between for the gear system. Using the inertia and center of gravity calculations given by XFLR5, it was found that the center of gravity of the battery pack individually should be at 444 mm from the tip in order to achieve stability and maneuverability.

For the position of the battery packs, the cross-section of the batteries are determined first. This is illustrated in Figure 10.34. It was then decided that the far end of the front battery would be located at 300 mm from the tip. At this location, the front battery can shift front- and backwards in the fuselage, which will help fine-tuning *BirdPlane* in the test phase, since the exact center of gravity is difficult to determine. The rear battery is positioned immediately behind the rear spar plus the margin of 15 mm, thus, at 480 mm from the tip. Solving for the required center of gravity, yields a length of 13 mm and 36 mm for the length of the front and rear battery respectively, which corresponds to a mass of 115.5 g and 320 g. The positions are shown in Figure 10.35.

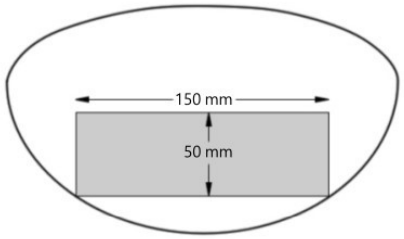

Figure 10.34: Cross section of the body at the battery position

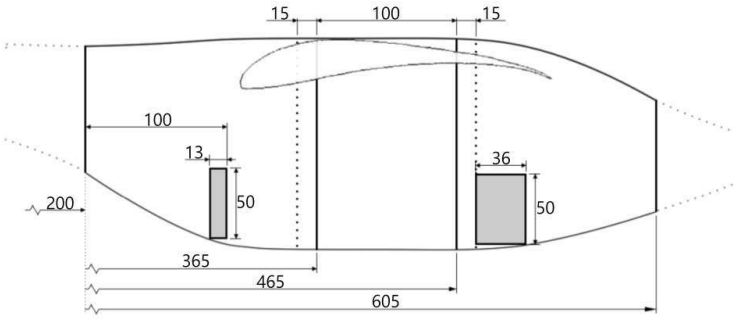

Figure 10.35: Side view of the body at symmetric center. All lengths in [mm]

10.3.3 COMMUNICATIONS

The *BirdPlane* communication system sets the functionalities and constraints of the data flows between ground station and *BirdPlane* on-board systems. Its architecture defines the context in which the communication system must function, the connectivities and interfaces. In the Midterm report the communication system was identified as one limiting and driving factor for the control system design, implying a higher required level of autonomy of *BirdPlane*. An iterative and detailed trade-off between requirements and different communication topologies led to the final implications and communication topology which will be further detailed this section.

In the following section the communication system is presented in a top-down approach. From the system definition (Chapter 8) the global communication system environment and requirements were deduced. Afterwards, the considered communication topology is presented. Lastly, the detailed hardware implementation is shown.

ENVIRONMENT AND REQUIREMENTS

The mission definition (Chapter 5) gives the general outline of the global *BirdPlane* mission. The mission has a great impact on the required communication architecture and formerly also vice versa; In the Conceptual Design Phase the mission requirements were relaxed in an iterative process due to communication system constraints. The relaxation process and the communication system environment and requirements are summarized in the following:

The initial killer requirement was to achieve a continuous communication link with a reasonable effort in the scope of the *BirdPlane* project. After analysing possible network architectures, the requirement for a continuous communication link was relaxed. A continuous communication link is now only required for the take-off and rendezvous phase, because for those phases full autonomy is not considered to be feasible and short-range manual control was favorable for early testing phases. After rendezvous, a discontinuous connection suffices and *BirdPlane* operates generally autonomously with possible mission commands from ground. The connection after rendezvous needs to provide the possibility to transmit the *BirdPlane* status to ground and commands to the *BirdPlane* at least every five minutes. This has a large impact on the control system which will be explored in Section 10.3.5. Furthermore, in the first flight phase a continuous video link is demanded and also in later flight phases frequent visual footage is desired. Lastly, the mean power demand of the communication system shall not exceed 5 W and a maximum power of 10 W.

NETWORK TOPOLOGY

In the conceptual design phase a number of different network topologies were considered, namely a satellite communication network, different mobile relay topologies, fixed antenna setups and the cellular network. A detailed trade-off between the topologies was performed based on performance, reliability and constraints of the different topologies. The mobile relay and the satellite network were identified as infeasible or insufficient in the scope of the *BirdPlane* mission. In order to achieve the highest possible communication performance a combination of ground antenna network and cellular network was chosen as the final network topology.

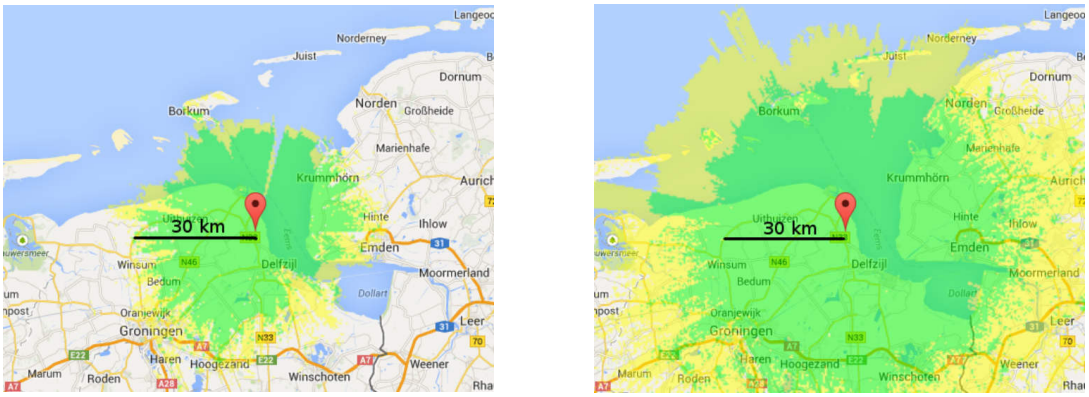

(a) Coverage map for 5.8 GHz video link, Tx=0.5 W

(b) Coverage map for 430 MHz control link, Tx=10 W

Figure 10.36: Coverage maps from potential launch site at Delfzijl (-2 m) by use of a 2 m high parabolic tracking antenna (30 dB) and assuming 2 m high *BirdPlane* (3 dB); receiver sensitivity: -90 dBm; fade margin: >20 dB/ >10 dB (green/ yellow)

In detail, a continuous analogue communication link will be used for the launch and rendezvous phases. Therefore, a parabolic ground antenna is placed at the launch site. Mature FPV technology is used to establish a live video downlink (5.8 GHz) from the *BirdPlane* and a continuous control uplink (430 MHz) to *BirdPlane* during those mission phases. Figures 10.36a and 10.36b show the coverage of the 5.8 GHz video link and the 430 MHz control link respectively. The results were obtained by link budget calculations, including the Fresnel-zone and taking into consideration real earth evaluation data. The marked regions indicates a fade margin of >20 dB which gives a large safety margin. Regarding the required line of sight for electromagnetic wave communication a worst case scenario was assumed - to obtain conservative coverage maps - by taking a launch site below sea level and a *BirdPlane* altitude of only 2 m.

The coverage region of the video stream goes well beyond 20 km which complies with experience from FPV applications. This area is large enough for the rendezvous phase as defined initially in the Midterm report [1]. To increase system safety a smaller and distinct frequency was chosen for the control link. This together with

a higher available transmitter power on ground results into a larger coverage for the control link as seen in Figure 10.36b. Hence, even when the video signal is lost during rendezvous phase, commands can still be given to *BirdPlane* in order to recover into a safe area. Additionally, this link will be used during early test phases and provides flexibility for different missions. When the rendezvous with the flock is completed this communication link will be switched off.

Figure 10.37: 4G cellular network coverage in the northern Netherlands, KPN: marked area [62]

For the complete mission the cellular 4G network will provide the possibility to give commands to *BirdPlane* and receive status data about the current mission state including photos or footage. In Figure 10.37 it can be seen that 96% of The Netherlands are covered by the KPN 4G-network. The data link is digital. No direct manual control will be done using this link. The cellular link is the main communication link that is also used to switch the analogue FPV link and other on-board systems on or off.

HARDWARE IMPLEMENTATION

The hardware implementation of the complete communication system is rather complex and to extensive for this design stage. The preliminary implementation is shown and divided into two parts: The implementation of the analog antenna communication link and the digital 4G data link.

Analog FPV communication link The task of the analog communication link is to transmit the video stream and telemetry data to the launch site and receive the control inputs. Therefore, separate transmitter and receiver are required. The current FPV range records of >50 km were flown with ImmersionRC equipment. The on-board video transmitter and control receiver are shown in Figures 10.38a and 10.38b respectively. Both, transmitter and receiver have their own antennas which need to be placed as far apart as possible to avoid interference. By choosing two very distinct communication frequencies the interference was already minimized. Omni-directional antennas will be used to enable a communication link in all possible flight states.

(a) EzUHF 5.8GHz 600mW Tx, mass=18g, 50 x 23 x 15 mm, 3 W

(b) EzUHF Long-Range RC RX - 8 CH Lite, mass=7g, 67 x 23 x 7 mm, 1W, S/N=-112 dBm

Figure 10.38: On-board analog communication equipment [63]

The video signal is fed directly from the full HD camera to the video transmitter to avoid the impact of failures of other subsystems. Additional telemetry data can be transmitted via the audio channel. The control receiver has

8 channels which are used for either different direct controls of actuators, or communication of commands to the embedded systems to control the subsystems, or feed commands to the auto-pilot.

On ground at the launch site a receiver and transmitter setup with higher power and antenna gains is used. Therefore, a parabolic antenna mounted on a pan and tilt mechanism will be used. Automatic antenna tracking, commercially available, control the mechanism to maximize the received signal strength.

Digital cellular communication link The hardware implementation of the cellular network link can be done with a widely available 4G dongle or with a 4G shield. As an example a 4G shield is shown in Figure 10.39. The communication adapter establishes the connection to the 4G mobile phone network and internet with high data rates.

Figure 10.39: Cooking Hacks 4G cellular network shield, mass 27 g, avg. power 4 W, max. 8 W [64]

The adapter is connected to the embedded systems and transceives control and telemetry data. An online interface can be used to watch the real-time data from *BirdPlane* and give control commands. Hence, this can be done from any internet-ready device. The launch team, but also the bird scientists can use the interface.

10.3.4 NAVIGATION

The Navigation subsystem has the task to determine *BirdPlane*'s position in global coordinates, and specify the target location and path to get to the target. The information about path and target are fed to the control system by the Navigation system. Hence, the control system is strongly dependent on the data given by the navigation system.

On a high control level, waypoint following was defined as the main control method and will be further elaborated in Section 10.3.5. Therefore, the navigation strategy is to define waypoints in all flight phases which will then be fed to the control system. A high accuracy of the navigation system is thus required.

In the following sections first the implementation of the *Global Position Determination* system is discussed and then the target determination and implementation, divided by the flight phases *Launch and Rendezvous*, *In-flock* and *Landing* is shown.

GLOBAL POSITION DETERMINATION

An accurate global positioning system is essential for the control system. The global position is used by the control system to compare its current position with the target position and derive the control inputs from the difference. A number of requirements regarding the global position information were given.

Initially, a number of different options were considered for the position determination including ground Radar tracking, transponder use, radio location and GPS system use. For reasons of cost, weight, accuracy, reliability and maturity, GPS was chosen as the most suitable technique in the trade-off.

The GPS principle is assumed to be known. The system is very mature and widely used in all kind of electronics. It can easily be implemented and is usually already embedded on most of the available auto-pilot boards. Further elaborations on the hardware implementation can be found in Section 10.3.7.

LAUNCH AND RENDEZVOUS

The navigation in the first flight phases is governed by the rendezvous strategy. The rendezvous strategy defines the trajectory to be followed in order to meet and merge the flock smoothly at the right position. It is described in Section 5.2.3 and is visualized in Section 6.3 with help of a mission simulation. Technically, the rendezvous

strategy and also the launch is implemented by feeding continuously waypoints to *BirdPlane* from the launch site. Hence, at the launch site new waypoints are continuously calculated to adjust the flight path for smooth rendezvous between *BirdPlane* and geese flock according to the strategy as presented in the mission simulation. At the launch site also the optimized launch path is defined.

Ground flock detection An essential aspect of the rendezvous strategy is continuous knowledge about the geese flock position. Different methods were considered, including computer vision, human vision, goose equipped with trackers and radar systems. Vision based systems did not deliver sufficient range and position precision, while the tracker systems are expensive and can only be applied for few geese, hence reducing the generality of the system. Therefore, the choice was made to rely on radar based flock detection systems with human vision assistance for identification of the bird species.

A wide range of different bird detection radars were developed in the past to avoid bird-strikes around airports. Those systems are however considered too expensive for the *BirdPlane* mission. A very promising approach was found by the KNMI in 2009 that developed a bird detection system by using operational weather radar (see Figure 10.40). [65] A large scale implementation all over Europe is currently integrated called OPERA. Real-time flock information can hence be obtained directly from KNMI and does not need to be obtained separately.

Figure 10.40: Dual-polarization weather radar [65]

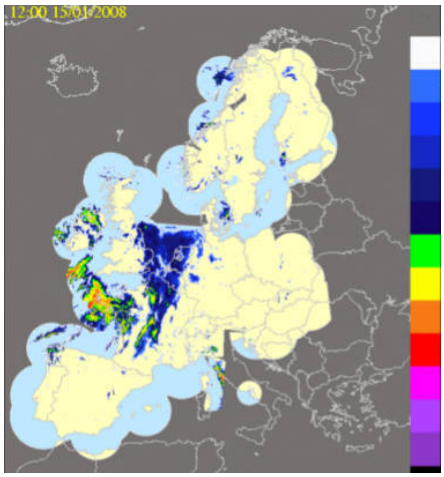

Figure 10.41: Example of European radar coverage [65]

The radar network has mutually full coverage over Europe (see Figure 10.41). The KNMI research showed that single birds can be detected with a certainty up to 99% [65] and information about the bird density inside a flock is obtained as well. With this information a suitable flock can be chosen days before it even reaches the Netherlands. The overall migration paths can be observed exactly and the mission can be planned accordingly. The current flock positions can be mapped by the mission control software that builds up on the simulation shown in Chapter 6.

The disadvantage of the system is that it can not identify the bird species which needs to be done by humans and that the system is still under development. However, the development is in progress and the European system can already be operating by the first *BirdPlane* launch. Additionally, the system is already tested for The Netherlands. Hence, only visual bird identification of the birds is considered to be a remaining issue. This can be done by bird researchers who spot the flocks visually in Germany, or by spotting communities like "waarneming.nl", where bird spotter share information about spotted birds which are then connected to the radar information.

Waypoint determination Given the position of a chosen flock the launch moment and rendezvous path is determined according to the strategy defined in Section 5.2.3 and constantly updated according to the anticipated and actual flock movement. This is done by a computer at the launch site on a tablet or portable computer. Given the desired path, the waypoints are constantly sent to *BirdPlane* to describe the patch during launch, climb and rendezvous phase. The waypoint control is described in Section 10.3.5.

IN-FLOCK

For the in-flight phase *BirdPlane* is equipped with advanced autonomous control capabilities to be able to (re-)merge, follow, lead and observe a flock of Barnacle Geese (Section 10.3.5). The control logics require the *relative position of BirdPlane with respect to the flock*. Therefore, the geese need to be first detected and then their relative position is to be evaluated. These tasks are performed by the *In-flight Goose Tracking System* which will be presented in the following paragraph. This system was identified as sensible and crucial for mission success, for this reason a general proof of concept supported by video analyses is shown in the following section.

Tracking Strategy A number of different options were considered initially for the *In-flight Goose Tracking System*, including on-board radar, echo sounding, tracker-equipped geese and chromatic / thermal cameras (see Baseline report). Based on size, power consumption, cost, accuracy, feasibility and maturity, the trade-off between the different options led to a combined camera solution with a mono high-resolution chromatic camera and a stereo infra-red camera setup. This solution convinces due to low weight and low power, very good availability and maturity of the components and high feasibility. Furthermore, a fourth small camera is used pointing backward. The tracking strategy is built up on this setup.

In general, the tracking process is divided into detection and relative position determination. First, the objects need to be identified on each video frame separately. Next, the relative positions of the objects in respect to the *BirdPlane* is determined with help of the stereo infra-red camera setup. Furthermore, different situations need to be covered throughout the in-flight phase:

As *BirdPlane* approaches the flock the mono high-resolution camera has the task to detect the flock. Due to its high resolution it can possibly detect the flock before the infra-red cameras can. As soon as the flock is detected the line of sight orientation is fed to the auto-pilot. When close enough to the flock, the stereo thermal infra-red cameras are used to detect single birds within the flock and their relative position. Their heat dissipation will give distinct IR-images of the birds. The high-resolution camera is then not used for detection anymore. If *BirdPlane* has to fly above the flock for scientific purposes, the cameras are pointed downwards to have the flock in view and keep a constant relative position above the flock. In leading flock mode, the rearward pointed camera is used to check if the flock follows.

Hardware Implementation The tracking strategy requires the implementation of a combination of different cameras, lenses, mechanisms and processors. The camera output is also partly shared with the telemetry system for scientific purposes, which needs to be adjusted in the design. In the following paragraph the hardware for the different components is addressed shortly.

The mono high-resolution chromatic camera needs to be able to adjust for different light intensities in order to obtain a clear view on sky, geese and ground. To be able to adjust for the different light intensities in one frame a **Full-HD-CMOS** sensor will be used. CMOS sensors are superior to CCD sensors, because every pixel can adjust for the light intensity. Furthermore, their power consumption is much lower. Only its higher sensitivity to vibrations needs to be accounted for. A possible solution with a camera board is shown in Figure 10.42. Additionally, a **wide angle lens** is mounted to the camera. So called fish-eye lenses give view angles up to 180°. However, they also distort the view considerably more. Since the camera footage is also supposed to be used for scientific purposes, a lens with a lower, but still wide view angle is chosen (see Figure 10.43). A large view angle is important to be able to track as many geese as possible.

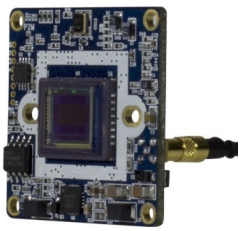

Figure 10.42: V-1290-2MPPCB CMOS Full-HD board camera, mass: 8 g, 2.8 W @ 60 fps, 32 x 32 mm [66]

Figure 10.43: 2.9 mm F2.0-2MP VIS-IR Wide-Angle Lens (ca. 142.9°), M12 mounting [67]

The **stereoscopic long-wavelength infrared (LWIR) camera** is the heart-piece of the in-flight goose tracking system. It is able to detect thermal dissipation of objects and their relative distance to *BirdPlane*. The stereoscopic setup consists of two FLIR Quark 640 with a 6.3 mm lens (Figure 10.44). They deliver a resolution of 640 x 512

Pixels and can sense body temperatures between $-40°C$ upto $+160°C$. With the 6.3 mm lense a horizontal angle of view of 140° is covered. The distance between the two cameras and their pointing needs to be exactly known in order to achieve accurate distance measurements. Careful calibration will be required. FLIR Quark 640 is an uncooled LWIR camera which has superior low-power performance for short range applications. [68]

Figure 10.44: FLIR Quark 640 with 6.3 mm lens, mass: 18.3 g, 1.0 W @ 30 fps, 22x22x12 mm, 640 × 512 pel [69]

Figure 10.45: Fiberglass camera tilt mechanism, mass: 8 g, 42x40 mm [70]

The three cameras are mounted on a **tilt mechanism** as shown in Figure 10.45 in the head of the goose. The mechanism is driven by a small servo enabling the three cameras to tilt 90° up and down which is needed to observe the flock when flying above or below. The Full-HD CMOS camera is mounted in the center and the other two FLIR Quark 640 sensors are mounted left and right of it.

A fourth **backwards camera** is used to keep track of the geese behavior behind *BirdPlane*. As relative position determination is not required, a simple and light-weight solution could be chosen. A small single chip camera was selected, equipped with a fish eye lens for maximum view angle (see Figure 10.46).

Figure 10.46: V-XA095-5V-PCB-3.6 Single Chip Color CMOS, mass: 2 g, max. 0.1 W @ 30 fps, 21 x 21 mm [71]

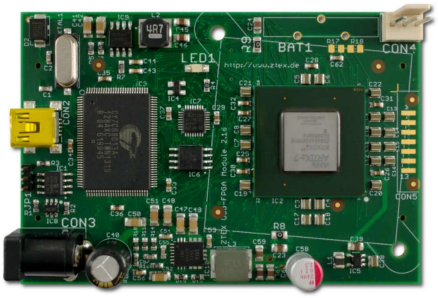

Figure 10.47: Artix 7 XC7A200T FPGA Board, mass: 8 g, max. 6.6 W, 57x84 mm [72]

A strong processor is required to process the visual information coming from the four different cameras and analyse them in order to obtain information about the position of the flock. Therefore, a **Field Programmable Gate Array** (FPGA) is an efficient solution. FPGAs are very efficient for video processing. They deliver high computational power while demanding little power. The XILINX Spartan 6 FPGA, initially developed for automotive applications, proved to enable real-time visual feature tracking and processing in a setup with 5 cameras simultaneously [73]. A possible implementation of the Spartan 6 successor Artix 7 is shown by ztex with the Artix 7 XC7A200T FPGA Board (see Figure 10.47). An interface board will be required to connect the 4 cameras to the board. Furthermore, a storage medium is required to store video footage which will be done on a Micro-SD card. Additionally, an information link to the control system is necessary to feed the geese positions to it.

The schematic of the total setup is shown in Figure 10.48. All visual processing is done within the FPGA board. The cameras and the tilt mechanism are connected to it by an interface board. A Micro-SD storage is connected to store video footage for scientific use. The system can work independently of the control system. It feeds continuously data about the flock and geese positions and the camera pointing to the control system. The control system has the possibility to switch the visual tracking system into different modes and has also influence on the camera pointing.

Chromatic Moving Object Detection The geese and flock detection is done by both, chromatic and infrared cameras. Both camera systems support each other to some extend and add redundancy to a further extend. For

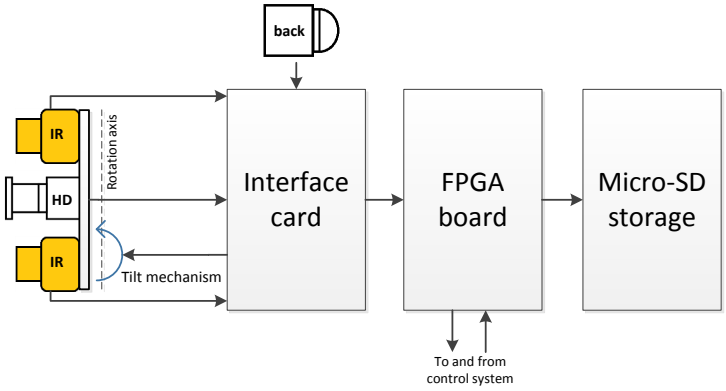

Figure 10.48: In-flight bird tracking system hardware schematic

far distance detection, the chromatic Full-HD camera is primarily used, since it makes use of a superior lens and resolution. For the backward geese detection the chromatic backup camera is used.

Background A lot of research was done in the past and is still ongoing in the field of visual moving object tracking, mainly for virtual reality and UAV applications. However, the *BirdPlane* **motion environment** proves to be especially demanding, which is why the problem is very general and only little assumptions can be done. Due to the movement and vibrations of the camera the background constantly moves within the frame, and therefore, widely used background subtraction [74] or Camshift [75] methods can not be used.

Furthermore, there is always an unknown number of moving objects that need to be tracked which requires a fairly general approach and prohibits the use of methods like HandVu [76]. Indistinct colors of the geese and varying light conditions make it infeasible to use a color thresholding for detection [77]. Additionally, the geese bodies and wings morph constantly during flight, which is why often used cascade identifiers can not be trained to detect the geese [78]. Also, the background texture can vary a lot from very noisy e.g. close to the ground to fairly monotonous at the sea.

Given the challenging detection environment, different approaches were tested and implemented with the real-time computer vision library *OpenCV* in *Python*. Hereunder, tests were made on Barnacle Geese footage with different background subtraction methods, Camshift and color thresholding. As expected none of the methods gave promising results due to the challenging environment explained previously. Therefore, a more advanced strategy based on the relative motion between objects and background was applied. In the following this strategy is further elaborated:

Approach The main assumption of the considered approach is that the observed object movement between two frames is different from the observed background movement between those frames. Hence, a relative movement can be observed which is used to distinguish between different objects. A similar approach was supposed by David Lieb which is used as reference [79].

First of all, the movement between frames need to be analyzed. Therefore, two different methods are compared. In the Lucas-Kanade Optical Flow method so-called features are detected within the frames [80]. Features are small, distinct patches in the frames like corners which can be detected in following frames. After detecting those features in one frame their relative position in the next frame is evaluated. This method is also used by Lieb. The Dense Optical Flow method does not make use of features, but analyses the flow of each pixel separately over two frames [81]. In Figure 10.49 the comparison of the two optical flow methods can be see by means of an analyzed example frame. Four Barnacle Geese can be seen in the example.

Figure 10.49a shows the unfiltered result of the Lucas-Kanade **Optical Flow method applied on Shi-Tomasi features**. It can be seen that a lot of features were detected on the geese and some further on the ground. However, wide areas are without any features, because their texture is fairly monotonous. The movement of each feature is indicated with a line and the color indicates the movement direction. The geese can already be detected by eye, because of their opposed movement direction. In Figure 10.49b the result of the **Dense Optical Flow method** is seen. The background image is extracted, but the result is similar. The main difference was seen

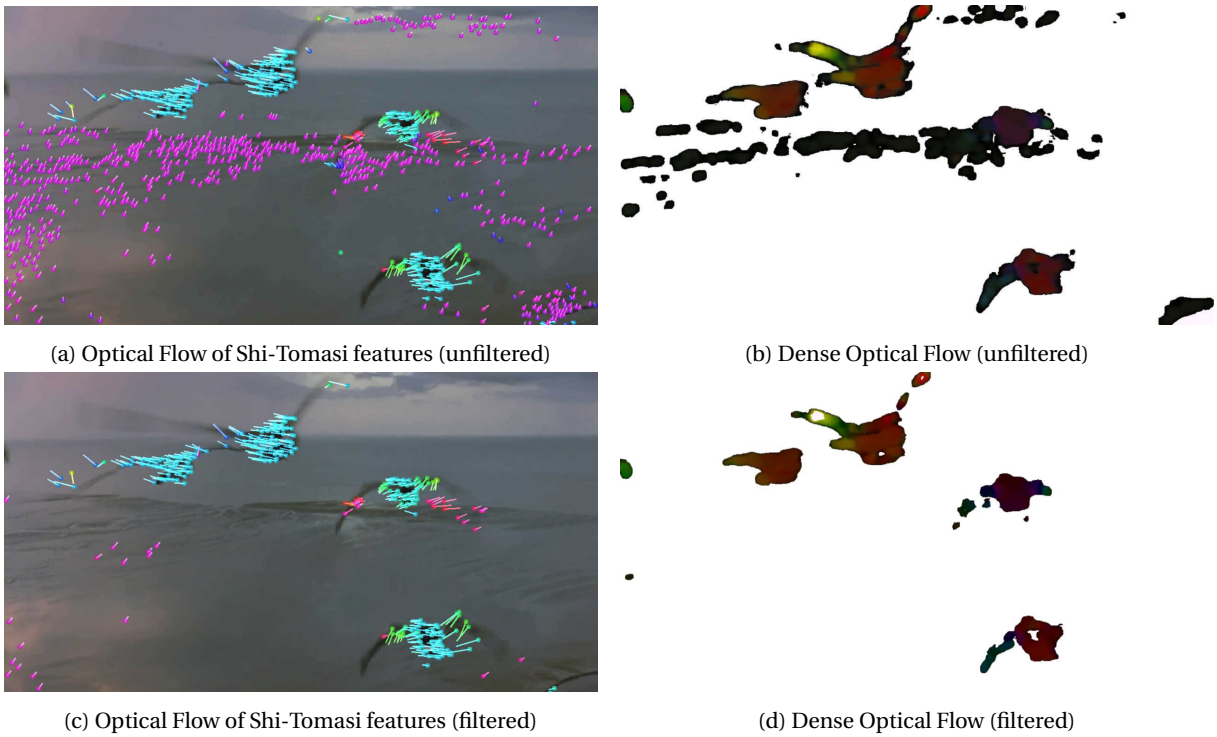

(a) Optical Flow of Shi-Tomasi features (unfiltered)

(b) Dense Optical Flow (unfiltered)

(c) Optical Flow of Shi-Tomasi features (filtered)

(d) Dense Optical Flow (filtered)

Figure 10.49: Example frame of video analysis of in-flock footage: Four Barnacle Geese above the sea

in the computational effort. While the Lucas-Kanade method could be run in real-time, the Dense Optical Flow method was very slow and took around 10 times as long.

In a second step the background motion is filtered out in order to obtain distinct motion images of the geese. Outliers are sorted out first by the developed **filter**. Afterwards, the information about movement direction and velocity are combined in an evaluator (see Equation (10.72)) to make a distinction between foreground and background motion. The evaluator ($eval$) is the product of the deviations of velocity (v) and angle (θ) from their respective medians. The deviations are squared to take the sign differences into account.

$$eval = (v - \tilde{v})^2 \cdot (\theta - \tilde{\theta})^2 \tag{10.72}$$

The evaluator of every point is compared to the median evaluator. If it is outside a set range of median standard deviations the corresponding point is filtered out. The assumption behind this filter is that the background motion is slower than the foreground motion. Hence, the background motion is filtered out. The results of the filter can be seen in Figure 10.49c and Figure 10.49d. With few exceptions only the motion images of the geese pass the filter as desired.

In a final step, the filtered motion image needs to be divided and grouped to find the **distinct goose position** within the frame of every goose. The results are shown in Figure 10.50. The developed algorithm groups features based on their distance to each other and the value of their evaluator as explained above. Hence, features that are close to each other and have similar velocity and direction are grouped and identified as a goose, given that the area is large enough. The results show that all geese are tracked and no false detections were done.

However, the sample frame in Figure 10.50a also shows the limitation: Because the two geese in the upper left corner are very close to each other and describe a similar movement direction the algorithm can not separate them. With help of a stereoscopic setup this problem can be solved, because then also information about the distance is available. In case of following a single bird, the results are already very good as seen in Figure 10.50b.

A few **final remarks** need to be made on the object detection techniques shown. The comparison between the Lucas-Kanade Optical Flow method and the Dense Optical Flow method shows that the results are rather similar if a large number of features is used with small advantages of the pixel based method. However, the feature based method seems computationally much more efficient which is important for the *BirdPlane* implementation.

(a) Multiple Barnacle Geese tracked in sample frame

(b) Single Barnacle Goose tracked

Figure 10.50: Barnacle goose tracked from camera footage: Illustration of two examples

Tests on FPGAs were not conducted yet which could speed up the computations considerably. Additionally, it was found out that backgrounds with a stronger texture are favorable for this approach. Furthermore, it was observed that the quality of the results of both methods vary a lot with the relative motion of fore- and background based on the initial assumption made. By giving the camera a continuous for- and back-movement like chicken, the results could be improved. Alternatively a stereoscopic camera would improve the performance as well. Finally, it should be noted that the analysis made is a proof of concept and shows that goose detection from video footage is possible. Further research is however essential.

Infrared Geese/ Flock Detection In the previous subsection, a proof of concept of the geese detection with help of the chromatic camera was given. However, the heart-piece of the detection system is the stereoscopic infrared camera which gives much better detection possibilities for short distance, e.g inside the flock.

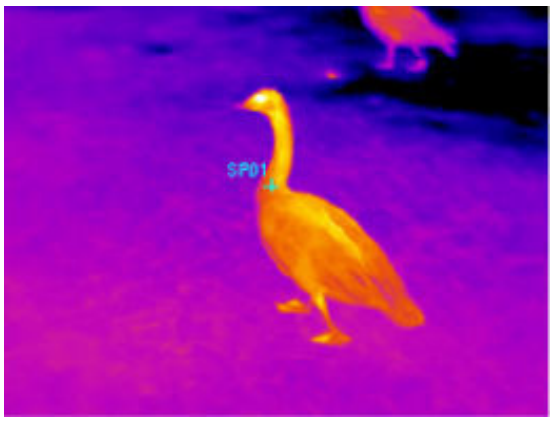

Figure 10.51: Infrared image of a goose on ground [courtesy of Wikipedia]

Thermal imaging is based on the fact that the black-body radiation intensity of every object depends on its temperature. Geese are endothermic animals with a mean body temperature of around $42°C$. This differs significantly from their environment. Hence, geese show up very distinct on thermal images (see Figure 10.51). Therefore, the geese can be detected by simple thresholding, where the temperature range of the outer goose body is filtered out of the images. If this technique is not sufficient it can be complemented by the results of the earlier detection method presented which also applies for thermal images. Furthermore, the distance information obtained through the stereoscopic setup can be used to distinguish the objects. After all, there is a lot of available information which can be used to detect the geese. Further research with the actual setup should be used to develop the detection system.

Waypoint Determination The target of the in-flight Goose Tracking system is to feed continuously the position of the goose or flock to follow in form of waypoints to the control system. So far, the subsection was only about the detection of the geese, but no distance information were obtained yet. This is the task of the stereoscopic infrared camera setup. Similar to human eyes, distance information can be obtained with two cameras being separated by a certain distance and recording the same object.

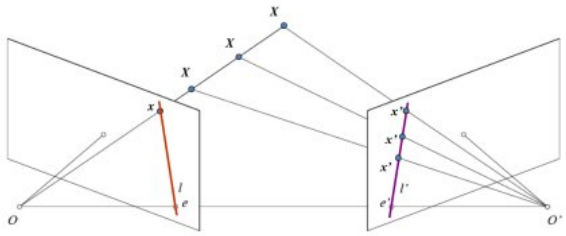

Figure 10.52: Epipolar geometry concept

Figure 10.52 gives the schematic of the object distance determination with stereo cameras. If an object X is detected with the left camera, its location can be anywhere along the line OX. The second camera gives now information about the position of X on the line OX, its 3D position can be triangulated. This is the concept that is used to find the exact relative positions of the geese with respect to the camera.[82]

For the control system, the relative positions need to be translated into global GPS waypoint coordinates which are then fed to the control system. This is done by converting measured relative distance of the goose to a relative longitude, latitude and altitude distance considering the current *BirdPlane* GPS position and heading.

Closing thoughts From the start of the project, the bird tracking system was identified as one of the major question marks. This subsection intended to suggest its implementation and serve as a proof of concept. With the obtained results and the prospect improvement possibilities the bird tracking system is definitely feasible. A stereo camera setup and the use of infrared cameras make it possible.

Further improvements could be made by the use of a stereo chromatic camera which by itself might already be a sufficient solution for the task, being less costly than infrared cameras at the same time. Furthermore, the addition of sonar sensors, or a pointable laser could improve accuracy of the distance determination. Lastly, the use of the tilt mechanism must be accounted for in the analyses. This has not been covered yet. However, the implementation is no major concern and only important for the distance determination, regarding the camera line of sight.

LANDING

In the preceding subsections, the target and path determination from launch to in-flock phase was described, which now leaves only the landing phase navigation. The landing phase is controlled fully autonomously by *BirdPlane*. Hence, after the scientific phase has ended, the navigation to the landing site should be started.

A grid of different safe landing sites within the mission area is defined first. Those landing sites are designated, such that the maximum distance from *BirdPlane* (at the end of its mission) to any of the sites does not exceed 10 km. During the in-flock phase the navigation subsystem continuously tracks the distance to the closest landing site and estimates the required energy to reach the landing site considering the environmental conditions. As soon as the flock lands, or the *BirdPlane* energy level hits the lower bound for the operation, it terminates the flock-following task, and waypoint is given to the control system, such that *BirdPlane* flies to the closest landing site.

The landing site is approached in a way that the final approach is done with head wind. The navigation system is able to set the waypoints accordingly. The wind direction is determined from the difference of ground speed (GPS) and airspeed (Pitot tube). During the approach, gradual descent to the landing site altitude is started. The landing sites are chosen to have possibly no obstacles. For safety, the camera system has the task to detect possible obstacles and the navigation system incorporates the information in its approach strategy. The altitude information is initially used from the GPS measurement. However, these measurements are not accurate enough for the final approach and landing flare. Therefore, an ultra-sonic rangefinder is used as shown in Figure 10.53. The sonar module can sense distances of more than 7.5 m to 3 cm with accuracies of 1 cm. Similar systems are implemented for UAV as well and supported by available UAV autopilots.

In the final approach *BirdPlane* switches into gliding mode and approaches the ground. The sonar senses the distance to ground and sends it to the control system which controls the landing flare for smooth gentle landing. After landing the navigation system stays intact to send continuously the *BirdPlane* position to the ground team for recovery.

Figure 10.53: High Performance Ultrasonic Rangefinder - UCXL-MaxSonar-WRC, mass: 12 g, max.: 0.1 W [13]

10.3.5 CONTROLS

In order to acquire the data which are necessary to investigate the study goals (as stated in Section 4.2.2), *BirdPlane* is required to join the formation flight of the flock, and follow them while precisely controlling its relative position with respect to the flock. This follows the necessity of delicate control strategy of *BirdPlane*. As already discussed in the Section 10.3.3 and Section 10.3.4, an autopilot is to be used partially and/or entirely as a means of the control and navigation of *BirdPlane*; during the climb and rendezvous phase (where the FPV manual control is possible), the trajectory of *BirdPlane* can be set manually by adjusting the successive locations of the waypoints, whereas during the cruise flight, the on-board autopilot would be fully utilized to determine and follow the location of the waypoints at each moment (i.e. outer-loop control). Both autopilot modes have the inner-loop control system which actuates the control surfaces, such that the *BirdPlane*'s attitude and rates can be controlled according to the commands.

In the previous Section 10.3.4, the positioning of the waypoints for the the guidance and navigation has been discussed in detail. To achieve the successful trajectory tracking, both outer- and inner-loop control of the autopilot is necessary. In this section, the basic concept for the outer-loop control is touched upon, and the specific inner-loop control of *BirdPlane* is introduced. First of all, a global view of the autopilot given. Afterwards, analogous to the previous navigation section, the flight phases are divided into three main stages: (1) Initial climb flight phase, (2) Cruise flight phase, and (3) Final descent flight phase. Then three different control strategies are implemented for the three corresponding flight phases. In the following section, these three different control strategies are discussed one by one. For convenience, the cruise flight phase is considered first. Afterwards, the implementation of the filters is briefly explored.

GLOBAL VIEW OF THE AUTOPILOT

As a basis for both hardware and software of the *BirdPlane*'s autopilot, it was decided to use an Open-Source Project, which can be accessed via free license. Besides the high availability and convenience of OSPs, another important reason for choosing OSP is because most of them rely on PID (Proportional-Integral-Derivative) controller for both stabilization and control of the UAVs. PID controller is favored over other control designs for the following reasons:

- It is the most commonly used control algorithm, which suggests its reliability and practicability [83].
- It is simple to use, and does not require the state-space representation of the aircraft dynamics. This is the advantage over the modern control system which is specified as a system of first-order differential equations (i.e. time-domain state-space representation). In other words, the PID feedback control does not require the values of the stability and/or control coefficients for the linearized equations of motion of the aircraft flight dynamics. This makes the PID controller a desirable choice because these stability / control coefficients are generally not available in the current situation for *BirdPlane*.
- It is relatively easy to tune. It is quite common to see that only one or two of the gain terms are used - for example, only using the proportional gain, or only proportional and integral gain [84].
- A number of open-source autopilot projects make use of the PID controller, ensuring high adaptability in many types of aircraft (e.g. fixed-wing aircraft, rotorcraft, quadropter, etc.). Therefore, this type of controller is readily available.

- Since *BirdPlane* does not have a considerably extended flight envelope when compared to a real bird (e.g. *BirdPlane* is not going to hover, or perform unique flight maneuvers), the PID feedback control design for the fixed-wing can be used for the outer-loop control of *BirdPlane*.

The basic working principle of PID controller is given in the next section. Among many open-source autopilot projects which implements PID control, Paparazzi is chosen due to its diverse functionality and capability which is suitable for the mission [85].

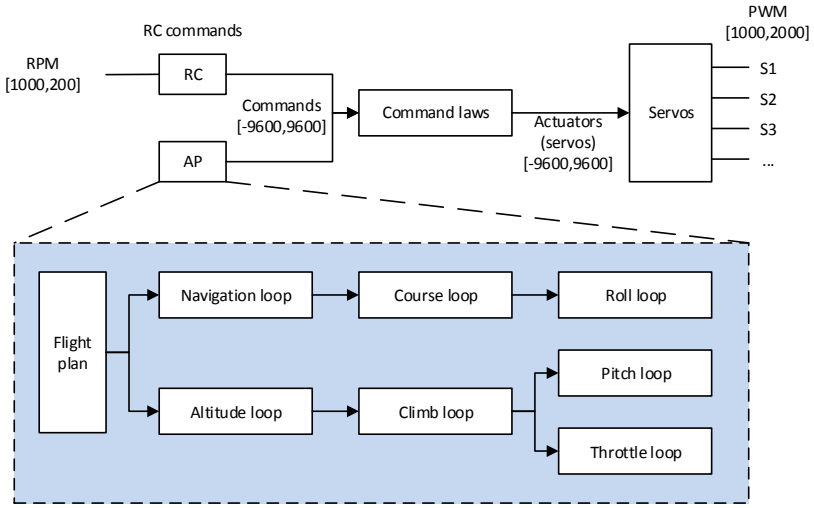

Figure 10.54: Global view of the Paparazzi's fixed-wing autopilot [86]. Note: PPM stands for Pulse-Position Modulation, and PWM stands for Pulse-Width Modulation

A global view of the control loops that are used for the Paparazzi's fixed-wing autopilot is given in the Figure 10.54. From the figure, it can be seen how the outer-loop of the autopilot (navigation, altitude loop) is connected to the inner-loop of the autopilot (roll, pitch, throttle loop) through the course and climb loop. The outer loops are by default based on the proportional control; the error in the course is transformed into the bank set-point by the coefficient of the proportional gain (course K_p), and the error in the altitude is transformed into the climb set-point by the coefficient of the proportional gain (altitude K_p). These set-points are then fed to the inner-loop, which are in this case roll loop for the course following, and pitch and throttle loop for climbing.

CRUISE FLIGHT PHASE

From the moment that the autopilot takes over the entire control and navigation of *BirdPlane* to perform the flock-following task, *BirdPlane* is then said to be in the cruise flight phase. During this flight phase, *BirdPlane* is required to follow the waypoints that the navigational autopilot sets continuously along the desired flight trajectory. Moreover, *BirdPlane* is required to follow the flock of geese at a fixed distance ($\approx$1.5 m) behind the rearmost goose in the formation flight. Therefore, the inner-loop control should consist of attitude control (i.e. heading, roll, and pitch) and throttle control for climb and flight speed regulation.

Attitude Control The heading, roll and pitch control of *BirdPlane* is done by varying the tail settings. Since *BirdPlane* has a rotatable tail, instead of conventional tail with a vertical stabilizer and rudder, the control inputs for the tail are the tail pitch and rotation angle. As already discussed in Section 10.1.2, the deflection of the tail serves the similar purpose as the elevator deflection which governs the pitch motion of the aircraft, and the rotation of the tail serves the same purpose as the rudder deflection, as it tilts the lift vector on the tail, thereby creating the lateral force for the necessary yaw and roll motion. In short, it is assumed that the pitch of *BirdPlane* is mainly determined by the tail deflection, whereas the heading and roll is mainly determined by the tail rotation. It should be emphasized that the tail rotation will initially provide the yaw moment which will correct the heading. This alone may be enough for the slight modification in the heading direction. However, when the flock of geese make a turn to change their flight direction considerably (e.g. 90^o to the left or right) over a long time, the roll at a certain bank angle will be necessary to provide the enough centripetal force to follow the turn. In either case, the tail rotation is controlled to modify the heading, or perform the turn. The detail analysis of the turning performance is given in Section 10.1.2.

In order to match the current attitude to the desired attitude, the PID (Proportional-Integral-Derivative) control loop configuration from Paparazzi OSP is used. PID control is a method of feedback control in which the error value is calculated as the difference between the desired input and actual output, and send to the controller where this error signal is processed using the three different gains (i.e. proportional, integral, derivative gain) in an attempt to generate the appropriate control signal which would minimize the magnitude of the subsequent errors after being processed by the plant [87]. A simple example of unity feedback system shown in Figure 10.55 is used to describe briefly how PID controller works.

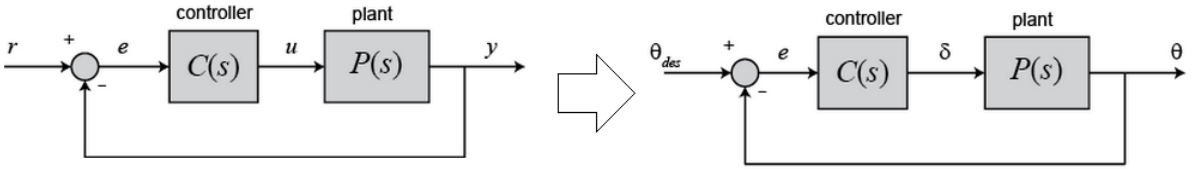

Figure 10.55: Example of unity feedback system [87]. The left diagram shows the general case. The right figure shows how the left diagram can be translated/interpreted as the aircraft pitch control example

The output of the PID controller is the control input to the plant. In case of aircraft pitch example, this is the elevator deflection. This can be computed in the time-domain as:

$$u(t) = K_p e(t) + K_i \int e(t)\,\mathrm{d}t + K_d \frac{de}{dt} \tag{10.73}$$

where K_p is the proportional gain, K_i is the integral gain, K_d is the derivative gain, and e(t) is the error signal. The transfer function of this PID controller can be obtained by using the Laplace transformation of Equation (10.73):

$$K_p + \frac{K_i}{s} + K_d s = \frac{K_d s^2 + K_p s + K_i}{s} \tag{10.74}$$

Applying (or increasing) these terms have the following effects as listed in Table 10.9:

Table 10.9: Effects on the closed-loop response of each controller parameters [87]

	Rise time	**Overshoot**	**Settling time**	**Steady-state error**
K_p	Decrease	Increase	Small Change	Decrease
K_i	Decrease	Increase	Increase	Eliminate
K_d	Small Change	Decrease	Decrease	No Change

It should be remarked that there are many methods to tune those gains effectively depending on the dynamics and the preferred behavior of the aircraft. Therefore, with the limited knowledge on the aircraft dynamics of *BirdPlane*, tuning of these gains are neither possible nor meaningful at the current stage. Also, it should be noted that there are numerous possibilities for the design of the PID control loop; for example, the addition of the airspeed sensor to measure the actual airspeed for better throttle control and aircraft performance in presence of heavy wind, or the method of implementing energy control loop to control the total energy (speed + height) of the aircraft.

However, at this point of design phase, a detailed analysis and comparison of such design options for the PID controller is beyond the scope of the project. Therefore, in this report, the most basic default PID control loop for the stabilization of pitch and roll angle that Paparazzi uses for the fixed-wing aircraft is introduced. One must keep in mind that in order to control the ground and airspeed of the aircraft, the use of airspeed sensor is compulsory. (For reference, read the section "Control Loops using Airspeed Sensor", and "Energy Control Loops using Airspeed Sensor" from [86])

In Figure 10.56 and Figure 10.57, the Paparazzi's default pitch and roll loop is illustrated. These figures are extracted from the users' manual for the Paparazzi fixed-wing autopilot [88]. The pitch loop is a proportional control loop which involves one gain and one neutral. The 'pitch neutral' value ensures that the aircraft is trimmed at the desired airspeed at the zero set-point, and the 'pitch pgain' value can be adjusted to obtain a satisfactory response to a step command in pitch. On the other hand, the roll loop is a P-D loop which involves two gains (K_p and K_d) and one neutral. The 'roll neutral' value ensures the straight flight with zero command

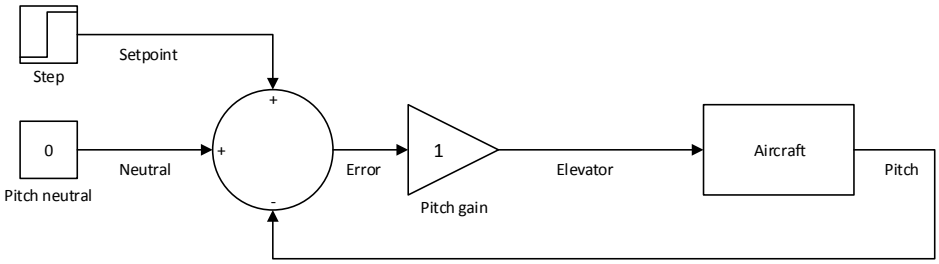

Figure 10.56: Paparazzi's default pitch loop [88]

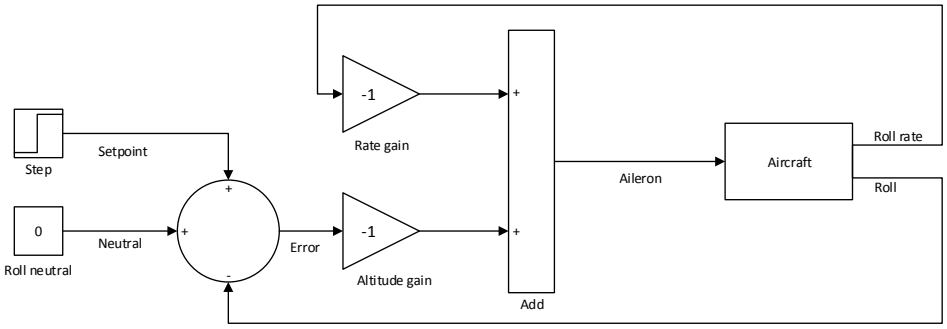

Figure 10.57: Paparazzi's default roll loop [88]

applied, and the two gains ('roll attitude pgain' and 'roll rate gain') can be adjusted to regulate the response time, overshoot, and damping of the osculations [88]. Lastly, one should beware that, for *BirdPlane*, the elevator deflection in Figure 10.56 will be replaced by the tail deflection, and the aileron deflection in Figure 10.57 will be replaced by the tail rotation.

Flight Speed Control Besides the attitude of *BirdPlane*, another important variable that must be controlled during the cruise is the flight speed. If *BirdPlane* was a typical fixed-wing aircraft with the conventional thrust generation system, such as propeller, or engine, it would be then possible to simply use the Paparazzi's preset control loops with the airspeed sensor (refer to [86]). However, *BirdPlane* has a distinct propulsion system which differs from the fixed-wing aircraft, and any other existing flapping-wing aircraft: the upstroke motion should be faster than the downstroke motion, and the wing twist (θ) for each flapping frequency should be controlled in order to achieve higher aerodynamic efficiency. For the detailed aerodynamics analysis, refer to Section 10.1.1.

In order to use the continuous control of the wing flapping actuation using PID controller, the proposed control strategy is to carry out the following actions simultaneously:

- **Control the average RPM of the main electric motor continuously with a fixed ratio of down- and upstroke RPM.**
- **Control the the wing twist (θ) continuously by varying the phase lag (ϕ) between the two wing spars.**

Each of these two actions are conducted in the following manner:

1. *Control the average RPM of the main electric motor continuously with a fixed ratio of down- and upstroke RPM*

This means that the autopilot will control the average RPM of the main electric motor continuously, as if it is controlling a propeller aircraft. The difference is that, in case of *BirdPlane*, the actual RPM of downstroke motion should be different from that of upstroke motion. Therefore, given a target average RPM of the motor, the motor actually rotates faster during the upstroke motion, and slower during the downstroke motion. This is in order to generate the lift and thrust more efficiently, like the actual birds (see Section 10.1.1). The time ratio between the up- and downstroke motion is fixed for the ease of continuous throttle control. As it is shown in Figure 10.58, the RPM during the upstroke motion should 1.38 times the average RPM, and the RPM during the downstroke motion should be 0.68 times times the average RPM.

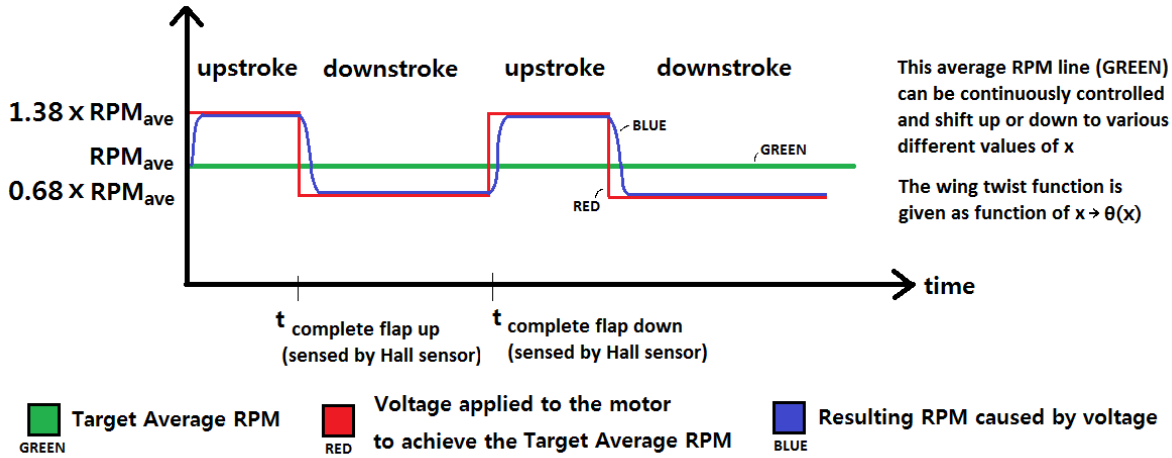

Figure 10.58: Method for the RPM control of the main electric motor

These values (1.38 and 0.68) were derived from the equations below:

$$\text{RPM}_{\text{down}} = \frac{\theta_d}{t_d} \times \frac{60}{2\pi} \tag{10.75}$$

$$\text{RPM}_{\text{up}} = \frac{\theta_u}{t_u} \times \frac{60}{2\pi} \tag{10.76}$$

$$r_{u/d} = \frac{t_u}{t_d} \tag{10.77}$$

$$\text{RPM}_{\text{ave}} = \frac{\text{RPM}_d t_d + \text{RPM}_u t_u}{t_u + t_d} \tag{10.78}$$

where θ_d and θ_u are the angles traveled by the driving gear during the downstroke and upstroke motion respectively (= 2.3248 rad, 3.9584 rad from Section 10.2.1), and $r_{u/d}$ is the time ratio between the up- and downstroke motion (= $dV_2/dV_1 = 6.3/7.48 = 0.84$ from Section 10.1.1). Since there are now four unknowns and five equations, it is now possible to express any three unknowns in terms of the other. In this case, RPM_{up} and RPM_{down} is expressed in terms of RPM_{ave}:

$$\text{RPM}_{\text{down}} = 0.68 \times \text{RPM}_{\text{ave}} \tag{10.79}$$

$$\text{RPM}_{\text{up}} = 1.38 \times \text{RPM}_{\text{ave}} \tag{10.80}$$

In Figure 10.59, it is shown how the variation of the target average RPM would affect the up- and downstroke RPM. Note that the shift of the curve is in fact continuous, rather than discrete - the figure is showing a discrete shift of the curves just to make a clear distinction between before and after the shift. The continuous change in the RPM_{ave} is also followed by the continuous change in the phase lag (ϕ), and thus, the continuous change in the wing twist (θ). For the specific function that relates the average flapping frequency (= $60 \times \text{RPM}_{\text{ave}}$) and required the wing twist (θ), refer to Section 10.1.1, and for the function that relates the wing twist (θ) and the required phase lag (ϕ), refer to Section 10.2.1.

Once the up- or downstroke motion is completed, this is sensed by the Hall sensors installed at the motor, and the on-board processing unit will then send the signal to the motor to either decrease the RPM to RPM_{down} or increase it to RPM_{up}. For this motor control, PWM (Pulse Width Modulation) controller is used, and this is elaborated in Section 10.3.7.

Besides the RPM control of the main motor, another control action that should be done simultaneously is the control of the wing twist:

2. *Control the the wing twist (θ) continuously by varying the phase lag (ϕ) towards the optimal twist angle at each given average RPM.*

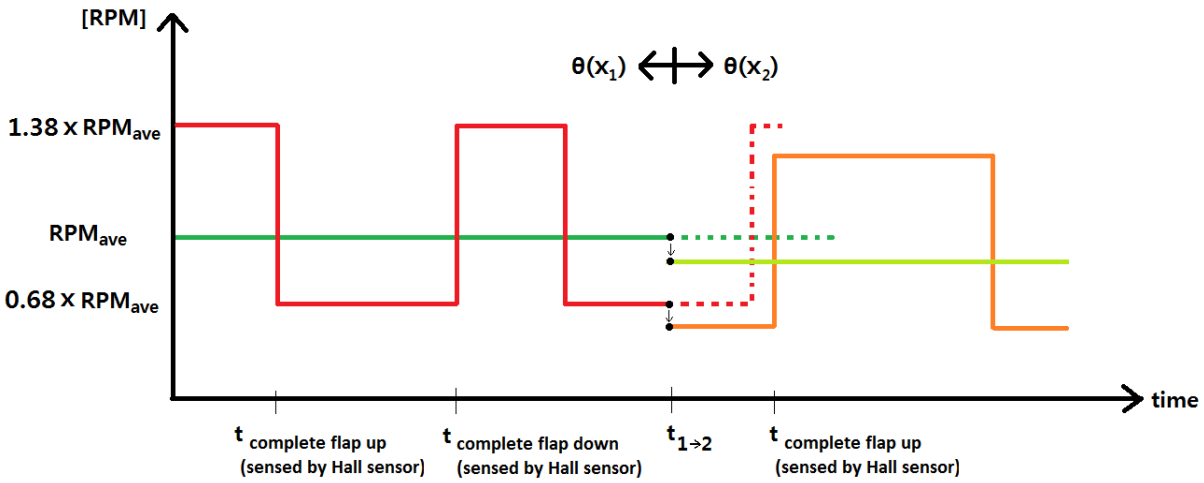

Figure 10.59: RPM control of the main electric motor during the change in the target average RPM

Remember that, for each average flapping frequency of the wing, there is a corresponding value of wing twist which generates the lift and thrust most efficiently - refer to Section 10.1.1. Also, the wing twist (θ) is a function of the phase lag (ϕ) - refer to Equation (10.52):

$$\phi = \sin^{-1}\left(\frac{\Delta x \cdot \tan(\Delta\theta)}{b}\right)$$

Therefore, the target phase lag (ϕ_{optimal}) can be programmed as a function of target average RPM of the electric motor, and it can be reached by continuously actuating the rotation of the ring gear with a PID controller - the wing twist mechanism is explained in Section 10.2.1. For ease of understanding, you can simply compare the ring gear actuation with the elevator actuation for the conventional tail: both of them have a target set-point (phase lag and pitch angle), and the control input through angular displacement (ring gear rotation and elevator deflection) which is provided by the servomotor.

These two control actions of the wing is summarized in Figure 10.60.

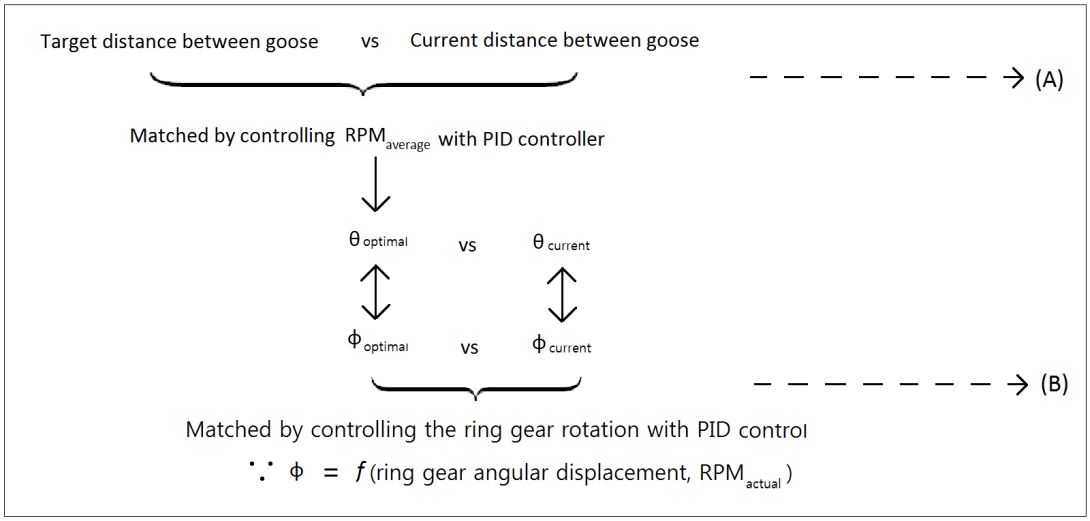

Figure 10.60: Control actions for the wing actuation. (A): Throttle control (RPM_{ave}). (B): Wing Twist control (θ)

The processes illustrated in Figure 10.60 are as follows: first of all, the current distance between the rearmost goose and *BirdPlane* is measured using the stereo-vision system. This value is compared with the target distance between the goose (≈1.5 m), and the error value is generated. By controlling the RPM_{ave} of the main electric motor with PID controller, this error is attempted to minimized. This is defined as the throttle control (A). Besides this control, another control is necessary to match the current wing twist angle (θ_{current}) with the optimal

wing twist angle ($\theta_{\text{optimal}} = f(\text{flapping frequency}) = f(\text{RPM}_{\text{average}})$). Since the wing twist angle is also a function of phase lag (ϕ), instead of matching the wing twist directly, the current phase lag (ϕ_{current}) is matched with the optimal phase lag ($\phi_{\text{optimal}} = f(\theta_{\text{optimal}})$ using PID controller, where ϕ_{current} is determined by the angular displacement of the ring gear, and measured by the hall sensors at the front and rear driving gears. This is defined as the wing twist control (B).

INITIAL CLIMB FLIGHT PHASE

The initial climb flight phase is the flight phase from the start of flapping (after launch) until reaching the target altitude for rendezvous. The control strategy is quite analogous to the cruise phase; given the waypoint, autopilot will actuate the throttle (i.e. RPM of the electric motor) and control surfaces (i.e. tail deflection and rotation), such that the attitude and flight speed is controlled in order for *BirdPlane* to follow the computed trajectory towards the waypoint.

The only differences between the cruise flight phase are:

1. The required trajectory and positions of the waypoints are determined by the computer on the ground at the launch site, and not by the on-board autopilot itself. This process is already discussed extensively in Section 6.3 and Section 10.3.4.
2. A different wing twist function θ_N (from Equation (10.10)) is used, and also, the time ratio between up- and downstroke motion ($r_{u/d}$) now takes value of 0.64 (= 6.3/9.918 from Table 10.1 in Section 10.1.1). This is in order to achieve more efficient lift generation during the climb.

FINAL DESCENT FLIGHT PHASE

At the end of the mission, *BirdPlane* will switch into the glide flight mode until it lands on the ground. Paparazzi also has the landing functionality in the autopilot, which can be used for the outer-loop control of *BirdPlane*. The procedures are as follows [88]:

1. Set the TD (Touch Down) waypoint to the ground level at the desired landing site.
2. Set the AF (Approach Fix) waypoint to the desired location for the start of the glide mode. Since headwind is favorable for landing, the AF waypoint should be set downwind compared to TD waypoint. This can be done by using the displayed estimation of the wind direction.
3. Depending on the last turn direction, choose the landing block - either right-hand or left-hand.

Paparazzi can also enable the users to set the desired glide slope by configuring the navigation modes in the flight plan. The most commonly used approach slope for the conventional aircraft is 3^o, and the longitudinal stability analysis confirmed that this was a reasonable value.

As the wings are static at fixed position during this phase, the inner-loop control of the autopilot for the final descent phase is only present for the tail deflection and rotation, and this is analogous to the previous two flight phases.

CONSIDERATION OF FILTERS

In this section, two types of commonly used filters are explored - Kalman filter and complementary filter.

Kalman filter Kalman filter can be used to predict the position, orientation and speed of *BirdPlane*, based on the prior knowledge of the state. Paparazzi OSP allows for a multi-state Kalman filter for INS (Inertial Navigation System) and AHRS (Attitude and Heading Reference System) [89] [90]. For example, there are currently possible INS subsystem types where Kalman filter can estimate the vertical position, vertical speed, and also, the accelerometer bias and barometric offset with an extended version. As for the AHRS subsystem, Kalman filter may be used for the quaternion formulation, but this is considered to be more suitable for rotorcraft, rather than fixed-wing aircraft. Recall that *BirdPlane* does not hover, and its flight envelope is closer to that of fixed-wing aircraft than rotorcraft. Also, Paparazzi offers the versatile use of complementary filter for AHRS subsystem (discussed in the next subsection), which can be computationally less expensive than the Kalman filter [91]. Therefore, Kalman filter is considered to be used only for the INS subsystem of *BirdPlane* for the prediction and estimation of at least the vertical position and vertical speed.

Complementary filter Complementary filter is another feasible option for the AHRS subsystem in terms of compensating the measurement errors [90]. These are:

- Long-term errors in the measurements of the attitude angles, caused by the accumulated gyro bias (i.e. drift). This happens because the attitude angles are not directly measured, but rather estimated using the integration of gyrometers measurements (i.e. angular rates).
- Noise in the accelerometers measurements of angles due to the presence of vibrations in a short-term.

In order to overcome these two limitations and measure the attitude angles more accurately, a complementary filter can be used to apply a low-pass filter on the accelerometers measurements, and a high-pass filter on the gyrometers measurements. Especially, as *BirdPlane* has a cyclic flapping motion where the downstroke causes more lift than the upstroke, the implementation of a well-designed low-pass filter is crucial to properly filter out the noise caused by the fluctuating motion of *BirdPlane* during flight. Therefore, an n-th order Butterworth low-pass filter can be considered, as it is known give the most flat frequency response in the passband, thereby offering uniform sensitivity within the passband [92][93]. A more detailed design of the filters is not covered in this report, as it would require the knowledge beyond the scope of this project, and moreover, the valid experimental data.

10.3.6 TELEMETRY

The main purpose of the *BirdPlane* is to research Barnacle Geese, hence a number of different parameters need to be measured. The term telemetry defines all desired measurement data connected to the scientific purpose of the *BirdPlane* mission. The desired measurements were defined in Section 4.2.2. In the following section the hardware implementation is discussed. It should be noted that some measurements are also used by other systems which will lead to overlap with other sections. The telemetry data will be stored during the complete mission and can be retrieved after landing of the *BirdPlane*. The implementation into the overall electronic system will be discussed in Section 10.3.7.

DATA HANDLING AND STORAGE

A modular approach will be followed to be flexible in case further measurement equipment is to be added. Thus, the system is designed in a way that it is possible to easily add further sensors to the system. The data handling and logging is organized by the open-source TWOGA-LOGGA from Paparazzi UAV [94]. Its implementation into the total setup is shown in Figure 10.65. The logger continuously saves the desired measurement data to a 8 GByte micro-SD card which is sufficient for nearly two missions. The data can be retrieved after completed mission.

MEASUREMENTS

In this subsection the different measurement devices are presented that are required to take the measurements necessary to fulfil the study goals as defined in Section 4.2.2.

Visual footage Visual footage is the main information source for the study goals (**SG-1**, **SG-3**, **SG-4**, **SG-6**, **SG-8**). In order to obtain sufficient data, high quality video is necessary. Furthermore, a large angle needs to be recorded in order to fulfil the study goals. Ideally, 360 degree around the *BirdPlane* are recorded. This main camera will take high-resolution footage. A second smaller camera is mounted on the fuselage for rear view. This camera is used to observe the in-front of flock phase. High-speed footage can be interesting for investigations on the geese flight mechanics. The considered Full-HD camera solution which fulfills those requirements was supposed in Section 10.3.4 and is shared with the navigation subsystem.

Audio recording To investigate on the Barnacle Geese social behavour and their reactions to noise pollution (**SG-3**, **SG-8**) a microphone is mounted in the front of the fuselage (near the camera). This way the microphone is mounted as far away from the engine and gears as possible. The sound data will need to be filtered afterwards to improve on goose-sound audibility. Similar to a mobile phone a small hole in the case is used to allow sound waves to reach the microphone. A 0.2 g solution with negligible power consumption was chosen.

Wind speed and direction The wind speed and direction (**SG-5**) can be determined by measuring the airspeed and ground speed (see Figure 10.61). The ground speed is determined from the GPS data provided by the control system and the airspeed can be measured with a Pitot tube. The Pitot tube is positioned in the nose of the *BirdPlane*. It is important that it points exactly in flight direction. An example is shown in Figure 10.62.

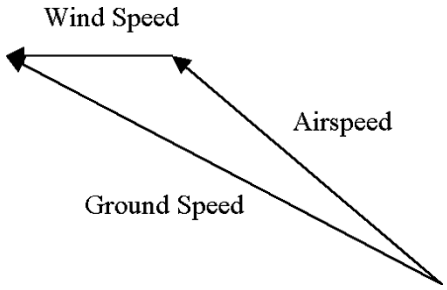

Figure 10.61: Wind vector determination from ground and air speed

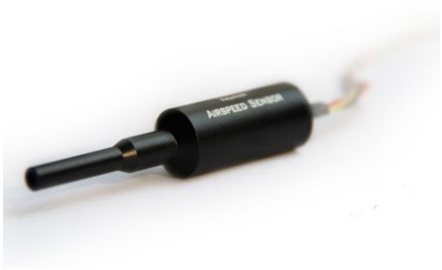

Figure 10.62: Pitot airspeed meter (9 g) [95]

Pressure and Vertical Speed Vertical air currents (**SG-5**) can be measured with help of a very precise pressure altimeter. Small pressure changes give insight about the altitude change, hence vertical velocity. GPS system are to inaccurate to measure the small differences. Furthermore, also the pressure itself can be logged. A possible solution is the use of the *openaltimeter* [96]. Weighing only 3 g it already provides more features than needed. This is also called an electrical Variometer.

Temperature and Humidity A wide range of temperature sensors is available with weights lower than 0.1 g. Humidity sensors are a little bit heavier. (Item **SG-9**) Combined solutions weigh about 10 g. An example can be seen in Figure 10.63. Instead of on-board measurements also data from weather institutions in The Netherlands can be used. The KNMI measures and predicts many weather parameters with high accuracy and a lot of this information is public available. However, to accurately measure small temperature changes on-board equipment is preferred regarding the very small size and power consumption.

Figure 10.63: DHT22 Humidity and temperature sensor (10 g) [97]

Figure 10.64: Photo-conductive resistor (<1 g) [98]

Luminance The luminance (**SG-9**) can be measured with an photo-conductive resistor. The resistor needs to be mounted on the outside of the *BirdPlane* and needs to be calibrated before usage. An example is shown in Figure 10.64.

Power consumption The power in an electrical system is given by the product of voltage and current. Therefore, the power consumption (**SG-2**) is determined by measuring voltage and current at the battery. The detailed implementation is explained in Section 10.3.2.

Migration path To determine the Barnacle Geese migration path simply the GPS data is used and logged. (**SG-7**)

10.3.7 EMBEDDED SYSTEMS

At this point almost all subcomponents of the Electronic System have been discussed, so this section will enlarge upon the actual implementation and connection of these systems. The missing part is the connection between the components, the mainboard and microprocessor that runs the autopilot system, logs the data and steers the servo motors.

This section will thus first discuss the computational mainboard and then give an overview of all built-in systems of the electronics. Finally the communication between the systems is discussed and finally the electronics section will be summarized.

AUTOPILOT BOARD

Section 10.3.5 already discussed the low level control loop which will be implemented as a software on the main microprocessor of *BirdPlane*. Apart from that also the outer loop, that is the waypoint steering, as well as data management and other functions need to be implemented on this processor. Fortunately, there are autopilot systems available that combine all these features.

At this point multiple autopilot boards are available, some of which were taken into consideration, specifically the Arducopter, Paparazzi (Lisa/M) and Pixhawk. Table 10.10 gives an overview of the capabilities of different autopilots.

Table 10.10: Comparison of different autopilot boards [85]

Parameter	**Arducopter**	**Lisa/M**	**Pixhawk**
Size [mm]	60 x 40.5	51 x 25	40 x 30.2
Weight [g]	23	10.8	8
Processor	ATmega2560	STM32F105RCT6	LPC2148
Additional features	Attitude estimation algorithm, GPS-based waypoint navigation, Altitude hold, Hardware in the loop simulation, Support of other multirotor airframes, GCS provided, Camera stabilization	Attitude estimation algorithm, GPS-based waypoint navigation, Altitude hold, Hardware in the loop simulation, Support of other multirotor airframes, GCS provided, Camera stabilization	Attitude Hold, Support for Computer Vision, GCS provided

From the table it can be seen that Arducopter and Lisa/M include the most features while Pixhawk is the lightest option with included Computer Vision support. The data is from 2012 and Pixhawk has ongoing opensource community support which continuously adds new features but the system is quite new and therefore might be less reliable than the Paparazzi system which is being developed since 2003. Lisa/M however is light as well, includes a powerful microprocessor and GPS-based waypoint support which the system at hand depends on. It does not provide internal computer vision but as explained in Section 10.3.4 it was decided to use a separate micro-processor to process the video data. Besides other research teams at TU Delft have experience with the system and have applied it in multiple UAVs already. Hence, Lisa/M from Paparazzi is the chosen Autopilot system. The following lists the connection ports and on-board systems:

- Pressure sensor BMP085 (optional as of 08/2012)
- 7 x Analog input channels
- 3 x Generic digital in-/out-puts
- 2 x 3.3V TTL UART (5V tolerant)
- 8 x Servo PPM outputs (only 6 if second I2C (I2C1) bus in use)
- 1 x CAN bus
- 1 x SPI bus
- 1 x I2C bus (2 x when using only the first 6 Servo PPM outputs)
- 1 x Micro USB
- 4 x status LEDs with attached test point
- 10.8 grams (0.4 oz) (with Aspirin IMU mounted)
- 34mm x 60mm x 10mm
- 4 layers PCB design
- 3 Axis Gyroscope
- 3 Axis Accelerometer
- 3 Axis Magnetometer
- Barometer MS5611 (as of Aspirin v2.1)

On-board the Lisa/M there are two pressure sensors (one inside the optional IMU), a gyroscope, an accelerometer and a magnetometer. The further connection scheme will be discussed next.

OVERVIEW & CONNECTION

Throughout this electronics section a lot of design options have been made with specific hardware which is to be built into *BirdPlane*. Table 10.11 lists the devices with their masses and power requirement. In order

Table 10.11: Compilation of all electrical systems

	System name	Mass [g]	Power required [W]
Communication	EzUHF 5.8 Ghz (Transmitter)	18	3
	EzUHF RC Rx-8 CH Lite (Receiver)	7	1
	Cooking Hacks 4G cellular	27	4
Navigation	V-1290-2MPPCB CMOS Full-HD camera	8	2.8
	2x FLIR Quark 640	2x 18.3	2x 1
	V-XA095-5V-PCB-3.6 (backward camera)	2	0.1
	Artix 7 XC7A200T FPGA Board	8	6.6
	UCXL-MaxSonar-WRC	12	0.1
Telemetry	Microphone	0.2	0.1
	Airspeed meter	9	N.A.
	Altimeter	3	N.A.
	Humidity and temperature	10	N.A.
	Luminance sensor	1	0
Actuation	Hacker A20-12 XL EVO	78	80
	Hacker X30-Pro	24	0
	Bluebird Midi servo BMS-390	23	N.A.
	HS-35HD Micro Servo Motor	4.5	N.A.
	2 Servos	2x 12	N.A.
Total		295.3	≥ 100

to make sure that the system can be connected, the interfaces of some of the parts shall be explained in the following.

Transmitter & Receiver The high resolution camera is connected directly to the transmitter which also powers the camera. The receiver gets its power through the mainboard which outputs 5 V instead of 12 V from the battery. The receiver needs to actuate the servos and therefore is connected through a conversion of its PPM output channel to the RX channel of UART1. This way input commands can be forwarded through Lisa/M while still retaining the auto-pilot functionality.

Dual camera setup As already explained in Section 10.3.4 all four cameras will be connected to an intermediate board which hands over the data stream to the Artix 7 micro processor. The processed data will be sent to Lisa/M via the UART2 connector which allows asynchronous data communication which comes in handy as the two processors are not clocking at the same speed. The Artix 7 board supports up to 12 V as input voltage and therefore can be connected directly to the battery.

Motor controller The motor controller converts the batteries input voltage and input torque and frequency from the autopilot to the correct output of the motor, based on PWM (Pulse Width Modulation). Although the motor controller provides a Battery eliminator circuit, this is not needed as the mainboard also supports high input voltages of up to 16 V. This way all servos can be connected to the mainboard, which could only lead to problems with the maximum current. This needs to be determined by testing.

INTER-SYSTEM COMMUNICATION

Communication between the different elements and subsystems is essential for mission success. The Communication Flows are visualized in Figure 10.65. There are communication flows within the air and ground segment and between those two segments. The communication flows are divided into data flows (black arrow) and command flows (white arrow).

Within the air segment a modular setup is used. The segment is divided into a **telemetry, a control and a storage module**. The internal computation unit is the central device that processes the data coming from the

different modules. The communication between the air segment and the ground segment is handled by the communication module. An analog and a digital cellular link are used, both having an uplink and a downlink. The data rates and command links can be seen in the Communication Flow Diagram (Figure 10.65).

Apart from the communication between the internal systems, additional contact takes place between the ground segment and the air segment. The ground segment is divided into a launch system and scientific ground system. In the launch system the operator organizes the *BirdPlane* take-off and goose flock rendezvous. The scientific ground team has the overall mission control. This team gives commands to *BirdPlane* regarding its mission based on the mission status. *BirdPlane* in turn sends information on weather, telemetry data and even live video streams back to the ground. The mission control can be performed from any place, since the mobile phone network is used. The division into operator and scientific team originated from the requirement of a ground station in Delft (***TOP-K-15***).

SUMMARY

This section on the electronics of *BirdPlane* should have unraveled how the highly ambitious communication range, remote-controllability, efficient actuation and intelligent three-dimensional bird detection system act together in one system.

The system is built up around Paparazzi's Lisa/M Autopilot which works in symbiosis with an Artix 7 FPGA processor for video processing. Different subsystems interconnect with this core, namely the Navigation and Telemetry subsystem. The main motor provides the necessary power for the actuation of the wings with servos for the control of the tail, which are all governed by the microcontroller. Communication will be provided by two independent systems, the FPV solution for mid-range live streaming and direct control and 4g cellular network for long range, command transmission and status updates.

At this point some parts need more refined design which would be part of the next design phase. Especially more in depth study of the exact interfacing of the subsystems need to be made as only the main systems connection was considered until now.

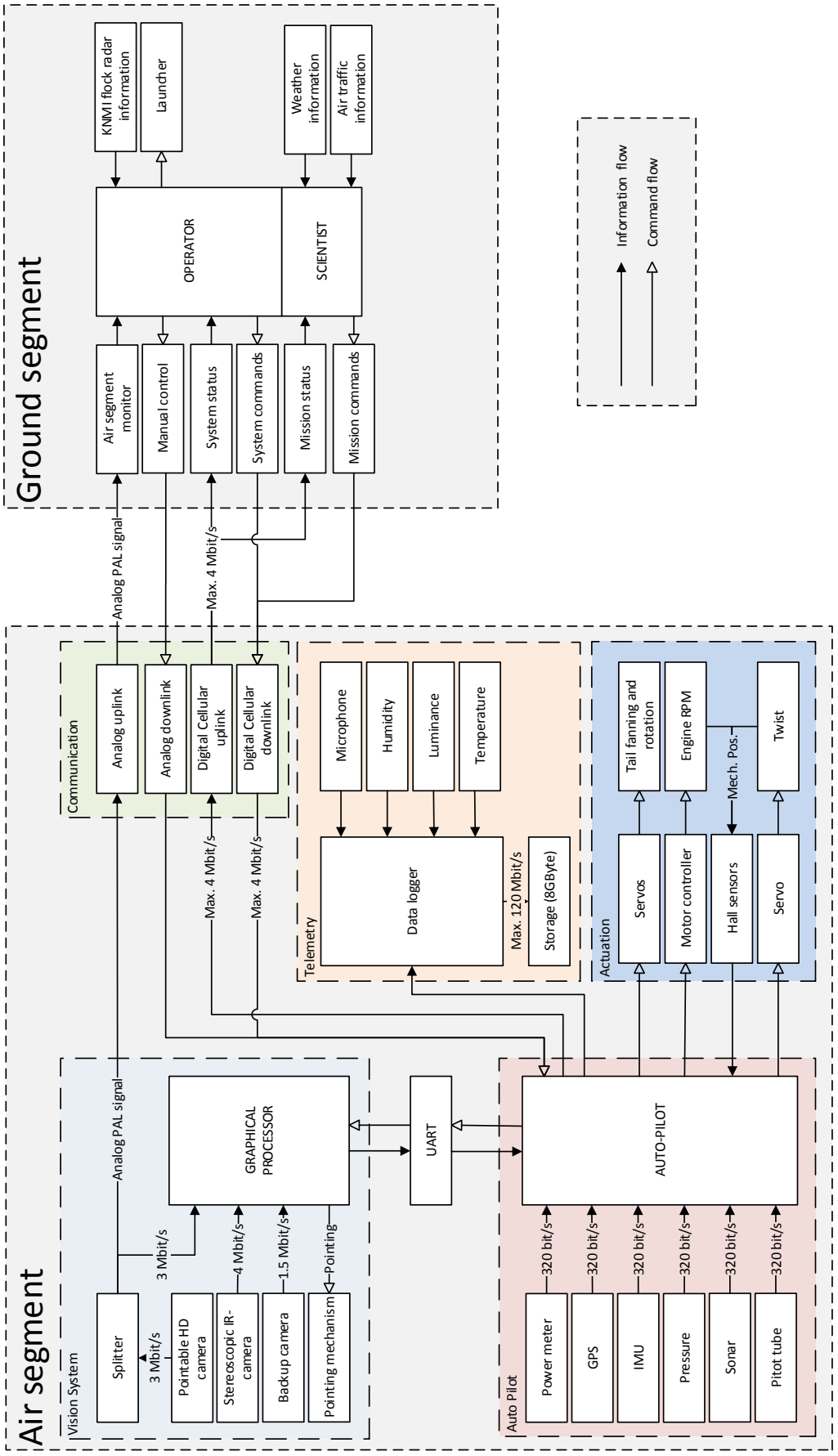

Figure 10.65: Communication Flow Diagram

10.4 FINAL LAYOUT

In this section the final design features of *BirdPlane* are summarized and concluded with a representation of the design. A rendering of the final assembly is shown in 10.66.

The *BirdPlane* wing mechanism is designed to preserve a broad range of flapping motions, including folding and twisting. Wing flapping is actuated through one central shaft, fed by a single electric motor, and translated to the spars through a set of spur, compound and planetary gears, a (cam)crank and a double set of 2-bar linkages.

Twist control is achieved by actuation of a ring gear which is part of the planetary gear set. When the ring gear is kept stationary, both front and rear spar sets are flapping with equal rotational velocities. Slight rotation of the ring gear, causes the planet carrier in the planetary gear train to change its velocity, and acceleration accordingly. As the front and rear spars are now flapping with different angular velocities, their angular displacements differ from the initial condition as well. The resulting phase shift directly affects the rate of twist.

Figure 10.66: Finalized preliminary design

11 Design Evaluation

In Chapter 10 the preliminary design of the subsystems of *BirdPlane* has been performed. In this chapter the characteristics of the complete design with all the subsystems put together will be evaluated. Firstly, it is analyzed how the subsystems perform in the integrated system in Section 11.1. After this analysis, compliance with the requirements can be checked and the feasibility is evaluated. The sensitivity analysis in Section 11.3 evaluates the effect of small changes on the final design. Next to all technical aspects this chapter concludes with the RAMS characteristics on the design.

11.1 Performance Analysis

The subsystems of *BirdPlane* have been designed with a certain goal in mind of what they should be capable of doing. In this section the actual performance of the integrated subsystems are evaluated. First the aerodynamic performance of the flapping mechanism is evaluated. Then the final weight and power budgets and the impact of the weight and power on the performance is presented.

11.1.1 Wing Mechanism

The aerodynamic analysis (Section 10.1.1) had resulted in a set of ideal parameters for the flapping wing to perform all flight phases at maximum efficiency, as summarized in Table 10.1. The mechanism was designed to allow for this ideal flapping as well as possible, but a trade-off had to be made between simplicity and a low weight versus accurate motions. To evaluate the actual performance of the flapping mechanism, the aerodynamics program was rewritten to calculate the aerodynamic forces resulting from the flapping motion prescribed by the mechanism. It was evaluated how big the impact of certain deviations from the ideal motion were on the aerodynamic performance and the mechanism was adjusted accordingly.

The flapping induced velocities at each span-wise position of the wing for each moment in time were calculated when the mechanism ran in the correct RPM. This was used as an input for the aerodynamics program, from which the lift, thrust and drag at each moment in time could be calculated. The resulting maximum and average forces could then be used for the next design iteration of the mechanism and the structures. In addition, the lift and thrust distributions over time could be used to verify the model. By plotting those values it was checked visually whether the forces were induced as expected. It could be concluded that the wing mechanism performs as it should and is capable of generating the lift and thrust required for all flight phases.

11.1.2 Weight Budget

The sizes and values attributed to the components and subsystems in Chapter 10 were the result of an iterative design process. The maximum allowable and the actual total weight have varied throughout this process and iterations and design changes were made until the two values were equal.

The initial estimate of the design mass for *BirdPlane* was set at 2 kg. The aerodynamic analysis showed that at this mass it would be impossible to achieve sufficient flight performance with the limited wingspan of 1.50 m. To be able to reach the climb rate of 0.4 m/s required to follow the geese, the maximum mass was reduced to 1.2 kg. After the first phase of the preliminary design the weight of all components and subsystems was estimated and including an additional mass of 5% for finishing (screws, wires etc.) the total weight was 1738 g, as shown in Table 11.1.

The found mass proved too high or a viable *BirdPlane* design, so an iterative design process was commenced. In the course of this process all departments had to give in a bit on their performance. The consecutive iteration showed a reduced total mass of 1362 g. Most profit was made by reducing the mass of the battery. The initial power requirement of 200 W was updated based on a more recent estimation of the subsystems power requirements, and the new power required was reduced to 150 W, by which the battery could be scaled down with a factor 0.75. The complex but efficient flapping mechanism caused the power requirements of the motor

to be lower than initially estimated, by which the weight added by the mechanism was compensated for by a smaller battery.

The mean power consumption of 150 W included still a large safety margin, since the calculated power required is only 118 W. This safety margin was desirable because of the large uncertainty in some of the calculations and the unknown powers for some flight cases and electronic components. However, combined with the small additional mass margin this resulted in very limited safety margin for the total mass, which should not exceed 1400 g.

Therefore one more iteration was done, in which the power requirement was further scaled down. The battery power was reduced to 130 W, resulting in a battery mass of 435.5 g. Including a higher margin of 10% for additional mass of screws and wiring (instead of 5%) this resulted in a new total mass of 1349 grams. So in total this leaves 50 g as a margin for unforeseen design mishaps.

Table 11.1: Initial weight budget estimation and final weight budget after iterative design process

Structural components	**First estimate [g]**	**Final value [g]**	**Subsystems in fuselage**	**First estimate [g]**	**Final value [g]**
Wing spars	57.4	45.3	Battery	670	435.5
Wing ribs	40	33	Wing actuators	116	114
Wing skin	90	71	Gear box	293	223
Fuselage skin	48	36	Tail actuators	51	40
Neck	40	22	Navigation	66.5	66.5
Tail	30	19	Telemetry	50	23
Rubber belly	35	25	Communication	52	52
Flexible skins	10	10	Internal computer	11	11
Total	**350.4**	**261.3**	**Total**	**1309.5**	**965**
Total first iteration (350.4 + 1309.5) * 1.05 = 1738 g			**Total final iteration (261.3 + 965) * 1.10 = 1349 g**		

Many load carrying structures were over-designed, as explained in Section 10.2.3. By reducing the dimensions of the components the safety margins have been reduced and testing of the prototype will have to show if these necessary weight reductions are allowable. With a mass of 1400 g the climb rate is reduced to 0.25 m/s at cruise speed, which is lower than the climb speed of Barnacle Geese, but considered to be sufficient. This is because climb speeds comparable to geese can be reached when flying faster.

11.1.3 POWER BUDGET

All electronic components with the power they consume power are listed in Table 10.11. For most of the components for navigation and telemetry the exact power consumption is known, however for some low-power components the exact power consumption is unknown. Also for the actuators, for which the mean power consumption is also strongly dependent on how often they are active, these values have to be estimated. In Table 11.2 the estimated mean power consumption of each subsystem are summarized. Including a safety margin of 10% for unexpected power consumptions the resulting total power available is **130 W**.

Table 11.2: Estimates of the power budget available for the electronic subsystems

Subsystem	Mean power [W]
Communication	8
Navigation	12
Telemetry	7
Embedded Systems	1
Actuation	90
Total power required	118
Total power available (Safety factor of 1.10)	**130**

For all electronic components either a known value or a conservative estimate for the power consumption is used, so together with the safety margin sufficient power should be available for all components to perform as

required. With the battery mass of 435.5 grams it is able to deliver 130 W continuously for 100 minutes, which was the required endurance. Any deviation of the actual mean power from the expected mean power will in the end increase or decrease the endurance of *BirdPlane*.

11.2 COMPLIANCE & FEASIBILITY

This section presents the verification of the requirements stated in the Baseline Report [99]. The Requirement Compliance Matrix is given in Section 11.2.1. In Section 11.2.2 the reasons for exceeding certain requirements will be given.

11.2.1 COMPLIANCE MATRIX

The Requirement Compliance Matrix is presented in Table 11.3. The requirement identification (ID) and description were taken from the *Baseline Report* [99]. For quantified requirements, the 3rd column restates the target value, for some cases in more convenient units. The last two columns are related to the final design, i.e. whether it actually meets the requirement. A tick mark can relate to a what output is required or can indicate when a certain requirement is met.

The Requirement Compliance Matrix presented below does not contain all requirements. However, all top level requirements are included. Furthermore the quantified system requirements are verified. It was deemed insensible to incorporate requirements containing <tbd> values.

ID	REQUIREMENT DESCRIPTION	REQUIRED OUTPUT	FINAL DESIGN OUTPUT	
TOP-K-1	*BirdPlane* shall be an unmanned A/C	✓	✓	✓
TOP-K-2	*BirdPlane* shall operate during daytime	✓	✓	✓
TOP-K-3	*BirdPlane* shall be able to take-off without human help	✓	✓	✓
TOP-K-4	*BirdPlane* shall be able to land without human help	✓	✓	✓
TOP-K-5	*BirdPlane* shall be able to detect a flock of migrating Barnacle Goose	✓	✓	✓
TOP-K-6	*BirdPlane* shall be able to follow a Barnacle Geese flock	✓	✓	✓
TOP-K-7	*BirdPlane* shall have an endurance of 100 min (108 km range without wind)	100 min	100 min	✓
TOP-K-8	*BirdPlane* shall have flapping wings	✓	✓	✓
TOP-K-9	*BirdPlane* shall have use passive drag reduction methods	✓	✓	
TOP-K-10	*BirdPlane* shall have use active drag reduction methods	✓	✓	✓
TOP-K-11	*BirdPlane* shall have a maximum wing span of 1.50 m	1.50 m	1.563 m [1]	✓
TOP-K-12	*BirdPlane* shall have a structure of which 90% is recyclable at the end of lifetime	90%	62%	X
TOP-K-13	*BirdPlane* shall not make use of propellers during cruise flight when following a flock	✓	✓	✓
TOP-K-14	*BirdPlane* shall incorporate a camera to record during the entire flight	✓	✓	✓

Continued on next page

[1] This span is only attained in a very small fraction of the flap cycle. During gliding the wingspan will be less due to the dihedral angle.

Table 11.3 – continued from previous page

ID	REQUIREMENT DESCRIPTION	REQUIRED OUTPUT	FINAL DESIGN OUTPUT	
TOP-K-15	*BirdPlane* shall send information to the ground during the entire flight	✓	✓	✓
TOP-M-1	The *BirdPlane* mission shall allow communication between the ground station and the aircraft	✓	✓	✓
TOP-M-2	*BirdPlane* system shall allow long range (>10 km) flock detection	10 km	2000 km [2]	✓
TOP-M-3	*BirdPlane* system shall allow close range on-board flock detection	✓	✓	✓
TOP-M-4	*BirdPlane* shall be remote controllable at all time during the mission [3]	✓	X	X
TOP-M-5	*BirdPlane* shall be able to autonomously follow a flock of Barnacle Geese during cruise	✓	✓	✓
TOP-M-6	*BirdPlane* shall be able to measure airspeed during flight	✓	✓	✓
TOP-M-7	*BirdPlane* shall be able to determine flight attitude	✓	✓	✓
TOP-M-8	*BirdPlane* shall be able to determine position during flight	✓	✓	✓
TOP-M-9	*BirdPlane* shall be able to measure static temperature during flight	✓	✓	✓
TOP-M-10	*BirdPlane* shall be able to measure static pressure during flight	✓	✓	✓
TOP-M-11	*BirdPlane* shall be able to measure humidity during flight	✓	✓	✓
TOP-M-12	*BirdPlane* shall be able to measure wind characteristics	✓	✓	✓
TOP-M-13	*BirdPlane* shall be able to measure power consumption during flight	✓	✓	✓
TOP-M-14	*BirdPlane* shall be able to record video during flight	✓	✓	✓
SYS-G-COM-3	The command link lag shall not be larger than 250 ms	250 ms	100 ms (Analog) or 150 ms (4G)	✓
SYS-A-ELE-COM-3	The Communication subsystem shall provide a data link with a data rate of 4000 kbit/s	4 Mbit/s	50 Mbit/s (4G)	✓
SYS-A-ELE-COM-6	The Communication subsystem shall have an average power consumption under 5 W	5 W	4 W	✓
SYS-A-ELE-COM-7	The Communication subsystem shall have a maximum power consumption under 10 W	10 W	8 W	✓
SYS-A-ELE-COM-8	The Communication subsystem shall have a mass below 0.05 kg	50 g	52 g [4]	✓
SYS-A-ELE-NAV-1	The Navigation subsystem shall determine its global position with a minimum accuracy of 10 m	10 m	5 m	✓

Continued on next page

[2] Weather Radar coverage of Europe
[3] This requirement was dropped officially during the Midterm review
[4] Since the required value has only one significant number, the extra 2 grams are a justified deviation

Table 11.3 – continued from previous page

ID	REQUIREMENT DESCRIPTION	REQUIRED OUTPUT	FINAL DESIGN OUTPUT	
SYS-A-ELE-NAV-2	The Navigation subsystem shall determine its global position with a minimum sampling frequency of 1.9 Hz	1.9 Hz	10 Hz	✓
SYS-A-ELE-NAV-5	The Navigation subsystem shall detect a flock of birds within a radius of 20 m	20 m	To Be Verified	
SYS-A-ELE-NAV-6	The Navigation subsystem shall determine the relative position of each single bird in the flock with an accuracy of at least 0.1 m at a distance of 1.5 m from the rearmost goose in the flock	0.1 m	0.1 m	✓
SYS-A-ELE-NAV-7	The Navigation subsystem shall have an average power consumption less than 3 W	3 W	9 W [5]	✓
SYS-A-ELE-NAV-8	The Navigation subsystem shall have a maximum power consumption less than 6 W	6 W	11.5 W [5]	✓
SYS-A-ELE-NAV-9	The Navigation subsystem shall have a mass lower than 0.05 kg	0.050 kg	0.062 kg [5]	✓
SYS-A-ELE-TEL-1	The Telemetry subsystem shall determine the power consumption of the motor with an accuracy of 0.1 W	0.1 W	0.0148 W	✓
SYS-A-ELE-TEL-2	The Telemetry subsystem shall determine the power consumption with a frequency of 20 Hz	20 Hz	20 Hz	✓
SYS-A-ELE-TEL-3	The Telemetry subsystem shall determine the airspeed with an accuracy of 0.25 m/s	0.25 m/s	0.28 m/s	X
SYS-A-ELE-TEL-4	The Telemetry subsystem shall determine the airspeed with a frequency of 20 Hz	20 Hz	20 Hz	✓
SYS-A-ELE-TEL-7	The Telemetry subsystem shall determine the acceleration with an accuracy of 0.5 m/s^2	0.5 m/s^2	0.49 m/s^2 (0.05 g_0)	✓
SYS-A-ELE-TEL-8	The Telemetry subsystem shall determine the acceleration with a frequency of 20 Hz	20 Hz	40 Hz	✓
SYS-A-ELE-TEL-9	The Telemetry subsystem shall determine remaining battery energy with an accuracy of 10 J	10 J	>> 10 J	X
SYS-A-ELE-TEL-10	The Telemetry subsystem shall determine remaining battery energy with a frequency of 1 Hz	1 Hz	20 Hz	✓
SYS-A-ELE-TEL-11	The Telemetry subsystem shall provide visual observation of the front view with at least 24 fps	24 fps	60 fps	✓

Continued on next page

[5] The camera is moved to the Navigation subsystem. Therefore the power and mass budget of this subsystem has been increased, to the detriment of the Telemetry system

Table 11.3 – continued from previous page

ID	REQUIREMENT DESCRIPTION	REQUIRED OUTPUT	FINAL DESIGN OUTPUT	
SYS-A-ELE-TEL-12	The Telemetry subsystem shall provide visual observation of the front view with at a resolution of 1920X1080p	1920X1080p	1920X1080p	✓
SYS-A-ELE-TEL-13	The Telemetry subsystem shall determine the air temperature with an accuracy of 1 K	1 K	0.2 K	✓
SYS-A-ELE-TEL-14	The Telemetry subsystem shall determine the air temperature with a frequency of 20 Hz	20 Hz	20 Hz	✓
SYS-A-ELE-TEL-15	The Telemetry subsystem shall have an average power consumption under 10 W	10 W	< 3W	✓
SYS-A-ELE-TEL-16	The Telemetry subsystem shall have a maximum power consumption under 15 W	15 W	< 5W	✓
SYS-A-ELE-TEL-16	The Telemetry subsystem shall have a mass lower than 0.1 kg	100 g	25 g	✓
SYS-A-ELE-IC-5	The Command subsystem shall have a mass lower than 0.05 kg	50 g	26.8 g	✓
SYS-A-FPP-AER-4	The Aerodynamics subsystem shall provide flight capability at an altitude of 50 m	50 m	0-2900 m	✓
SYS-A-FPP-PRO-2	The Propulsion subsystem shall provide a flapping frequency range from 240 to 320 beats/min	4 - 5.33 Hz	4 - 6 Hz	✓
SYS-A-FPP-PRO-3	The Propulsion subsystem shall provide a range of cruise velocity from 15 to 26 m/s	15 - 26 m/s	14 - 27 m/s	✓
SYS-A-SAM-STR-5	The Structure shall not fail under a $1.5g_0$ landing impact	$1.5g_0$	To Be Verified by FEM	

Table 11.3: Requirement Compliance Matrix

Another request from the customer was to implement as many bird-like features as possible Section 4.1.1. Many options were analyzed throughout this project, among others wing flapping, a movable tail, an iso-elastic neck and feet. As mentioned in the above table, a flapping wing mechanism was one of the top-level requirements. At this point, it should be clear that flapping wings can be realized on different levels of complexity. The more complex, the nearer to the real flapping of the goose. A trade-off between complexity and efficiency was done and it was found that the imitation of three different movements, namely flapping, twisting and folding, results in the best overall performance. This kind of trade-off had to be done for all bird-like features as they all have advantages for the flight performance, but on the other hand, add complexity. The preliminary design implements, except for the feet, all analyzed bird-like features and thus bears a **high similarity to an actual Barnacle Goose**.

11.2.2 FEASIBILITY

In total 4 requirements are not met by the final design. These requirements are listed below:

1. *BirdPlane* shall have a structure of which 90% is recyclable at the end of lifetime (**TOP-K-12**)
2. *BirdPlane* shall be remote controllable at all time during the mission (**TOP-M-4**)
3. The Telemetry subsystme shall determine the airspeed with a frequency of 20 Hz (**SYS-A-ELE-TEL-3**)

4. The Telemetry subsystem shall determine remaining battery energy with an accuracy of 10 J (**SYS-A-ELE-TEL-9**)

In the following paragraphs the reasoning is given individually for each missed requirement.

TOP-K-12 The final structure is only 62% recyclable, whereas 90% was the design goal. This is mostly due to the use of CFRP parts for the structure. This is the only material that provides the required specific strength and stiffness to comply with the mass budget. Furthermore, this requirement has been classified by the main stakeholder as a soft requirement. Not satisfying a soft requirement has no direct implications for verification of the final design.

TOP-M-4 In the early stage of the design process, a system has been developed to remotely control the *BirdPlane* over the required range, using an analog system. High gain antennas had to be placed at large-altitude existing telecommunication masts. However before the Midterm review expert consultancy gave the design team a new view on the mission operation. The doubtful reliability of complete remote control was the basis of this sea change.

SYS-A-ELE-TEL-3 Of all requirements not met, this is the most minor. Although a determination of the airspeed with an accuracy of 0.25 m/s proved to be not feasible, a slightly less accurate sensor can be used. This difference has little to no impact on the final design.

SYS-A-ELE-TEL-9 The ability to determine the remaining battery level with an accuracy of 10 J has been softened. First of all with a power consumption exceeding 100 W, this amount of energy will be used in less than 0.1 s. Moreover the energy in a filled battery cannot be determined with that accuracy. Therefore the required accuracy has been increased to 1% of the total capacity, i.e. 14.4 kJ.

11.3 SENSITIVITY ANALYSIS

During the entire design process and also in the later product life certain system parameters will be subject to changes, due to smaller or larger design/mission iterations or maintenance. There are many dependencies between the components and a change in one of them will therefore have an impact on other components. In order to assure that these changes do not drive the final design to an unacceptable extend and to evaluate the design feasibility, a general sensitivity analysis of the preliminary design is carried out. More specific, the sensitivity of the design for a change in one of the major system parameters is to be determined.

The major system parameters are those that are important for many subsystems and have therefore a large influence on the final design. For the global sensitivity analysis the following system parameters are considered to be of major interest:

- **Total weight (W)**: The total weight of *BirdPlane* is very prone to increase slightly during rest of the design process and operation. To prevent that the weight increase leads to severe design changes or even makes a design entirely impossible the sensitivity with respect weight is analyzed.
- **Power (P)**: Although the power has been determined with a reasonable margin, an in- or decrease of the power must be evaluated for the rest of the design process.
- **Communication link**: the amount of data that can be sent during cruise has a large impact on all the electronics.

In the following the sensitivity analysis is conducted for the preliminary design.

Total weight *BirdPlane* is designed close to the edge of the maximum weight boundary which is implied by the aerodynamic capabilities of the flapping wing and the power system. It is very unfavorable to exceed the maximum weight, because further lift improvements are very difficult if not infeasible to attain within the given dimension constraints. Furthermore, those adjustments imply further weight increase resulting into a snowball effect.

Power and energy In general, a change in required power and energy over the mission duration can be responded with an up- or down-scaling of battery and/or electric motors which by itself causes only little problem. However, the implication by means of weight change can cause severe problems as seen before. Caution has to be taken with regard to the size of the power system: a power increase of 30 W would mean an augmented weight of 100 g.

Communication link The communication link was found to be one of the most limiting factors in the complete system design. Especially, the data rate, latency, range and continuity of the communication link are sensible parameters. If the mission is changed to a different setup requiring more manual control or higher downlink rates the communication system might be insufficient with large impacts. A completely new communication architecture might be required, which might also affect the power and weight. However, in general the communication system has a relatively large flexibility due to the use of cellular network and analog FPV link.

In conclusion, changes in the major system parameters can have severe impacts on the design and limit the feasibility. Especially, the weight was found to be very sensible to keep within the bounds. Therefore, strict contingency management is essential.

11.4 RAMS CHARACTERISTICS

Four characteristics that are of importance to the design of any system are the Reliability, Availability, Maintainability and Safety (RAMS), because they influence the profitability of the system. Therefore in this section the RAMS characteristics for *BirdPlane* are clarified. First the terminology is explained in Section 11.4.1 and after that, the RAMS analysis for *BirdPlane* is presented in Section 11.4.2.

11.4.1 RAMS TERMINOLOGY

In order to be able to characterize the *BirdPlane* system in terms of RAMS, a clear definition of what the characteristics mean is necessary. The definition of each term is stated below:

- RELIABILITY (R) - The ability of a system or component to perform its required functions under stated conditions for a specified period of time. [100]
- AVAILABILITY (A) - The degree to which a system or component is operational and accessible when required for use. Often expressed as a probability. [100]
- MAINTAINABILITY (M) - (1) The ease with which a software system or component can be modified to correct faults, improve performance or other attributes, or adapt to a changed environment. (2) The ease with which a hardware system or component can be retained in, or restored to, a state in which it can perform its required functions. [100]
- SAFETY (S) - The condition of being free from undergoing or causing harm, injury, or loss to people and the environment. [101]

11.4.2 RAMS ANALYSIS

The definitions on the four characteristics of RAMS stated above can be applied on the *BirdPlane* system. The characteristics are treated individually in this section in order to clarify which non-technical aspects are affected by the *BirdPlane* design.

RELIABILITY

The reliability of the *BirdPlane* system can be expressed in two ways: The design- or the operational reliability. The former means that the product is able to function as intended. The latter denotes that the *BirdPlane* system is able to function in operation during its total lifetime. In most cases reliability is a result of the safety of the specific system. The reliability of a system can be predicted by using the following relation between reliability and failure rate λ [102]:

$$R_{\text{system}} = e^{-\lambda t} \tag{11.1}$$

This failure rate depends on the implemented subsystems and their interrelation. A typical value for this failure rate for small UAV is approximately 0.001. The failure rate of small UAV with respect to conventional aircraft is in the order of 100 times larger. *BirdPlane* makes use of flapping wings, which require moving parts in the mechanisms and this will most likely increase the probability of failure, and therefore the failure rate is approximated to be increased in the same order of magnitude as for small UAV. Thus for a flapping *BirdPlane*, λ is assumed to be 100 times larger, hence $\lambda = 0.1$ (note that this is a rough approximation as no failure statistics

are available for ornithopters). When this value along with a mission duration of 100 minutes (1.67 hours) is inserted in Equation (11.1), it results in an R_{system} of 85%.

AVAILABILITY

Availability of a system depends on the operational time between system failures, and the time it takes to repair this failure. For the latter, maintainability is of importance which will be elaborated upon later in this section. The availability can be predicted by means of Equation (11.2) [102].

$$A = \frac{\text{MTBF}}{\text{MTBF+MTTR}} \tag{11.2}$$

Where MTBF is the 'Mean Time Between Failures' and MTTR denotes the 'Mean Time to Repair'. For constant failure rate systems, MTBF is calculated by the relation

$$\text{MTBF} = \frac{1}{\lambda} \tag{11.3}$$

By implementing the failure rate found earlier, this comes down to a MTBF of 10 hours. The mean time to repair on the other hand is estimated to be 3 hours. Therefore the availability of *BirdPlane* will be approximately 77%.

MAINTAINABILITY

As mentioned in Section 11.4.1, maintainability is linked to the ease of modifying or restoring components (or software) and it is beneficial for maintenance procedures (and thus availability of the system) to improve on this. Maintainability is related to sustainability (Section 8.6.1), as efficient use of resources is desired. The considerations that contribute to the maintainability are found to be:

- **Production should start around the power delivery system**. Assuming that this system is very reliable and will not require constant access, it can be embedded deep inside the structure.
- Most **sensitive** components (e.g. measuring devices, actuators, complex hinge systems) are **implemented last**, which provides easy accessibility when maintenance is required.
- The fuselage (bird-defining shape), is designed such that all structural components can be **slid-in** from the respective tail section of *BirdPlane*. Firstly, having only one opening for access will keep parasite-drag sufficiently low. Secondly, easy disassembly of *BirdPlane* fuselage allows for quick and regular maintenance if required.
- Data storage devices are implemented in a location **easy to access** as this is a component that should be removed/replaced after each mission.
- Maintainability can be increased by implementation of **access points** in such a way that all components can be easily accessed without removing other obstructing subsystems.
- Each maintenance **access point** is provided with a **seal**, minimizing moisture problems.
- Before assembly, those structural elements sensitive to corrosion are treated with specified **coating**.

SAFETY

It is necessary to keep *BirdPlane* as hazardous-free as possible to human, the environment and the equipment itself. The harm, injury or potential system loss is related to the technical risks of *BirdPlane* which are further evaluated in Chapter 12. For these risks, reduction techniques can be applied in order to increase safety. In defining the safety of a subsystem only the severity of failure is considered, not the likelihood of it happening. It can be seen that subsystems that score poor on safety, are in the small risk segment of the risk map because of their catastrophic failure modes, though combined with a small likelihood of happening. Therefore the total risk imposed by these subsystems is still small.

Furthermore, safety of the environment is related to the top level requirement that *BirdPlane* shall have a structure with 90% recyclability (**TOP-K-12**). The target of this requirement is beneficial for the environment, because efficient choice of materials will be considered (e.g. no toxic materials).

12 Technical Risk Analysis

Next to the evaluation of the design, it is also essential to analyze the technical risks related to it. This chapter introduces possible technical risks which may be confronted with during operation of *BirdPlane*. As these risks can potentially endanger the successful completion of the mission, a comprehensive plan for the management of each risk at each different level of threat must be deliberated and established. In this chapter, a list of potential technical risks are first identified for each element and subsystem of *BirdPlane* (Section 12.1). Subsequently, these risks are evaluated in terms of their level of threat, using a risk map in which the consequence and likelihood of each risk are graded (Section 12.2). Finally, in the last section (Section 12.3), the minimization and mitigation plans are discussed and addressed for each risk.

It should be stressed that the risks addressed here are the 'operational risks', rather than 'development risks'. Development risks are defined as the risks which occur during the product design process, including the verification and validation of the design with respect to the product requirements. They are distinguished from the operational risks which are the risks that occur during the actual operation of the mission. In other words, the development risk can be considered as the risk which result from the imperfect design (e.g. unfitting simplification made during the design process, oversight/neglect of the factors of significance, error in the calculation, etc.), and thus appear in the prototype of *BirdPlane*. In this report, the risk analysis will not cover such development risks, and assume that the design is verified and validated under the standard operational conditions.

12.1 Risk Identification

In this section, possible risks are addressed for each one of the four elements in the *BirdPlane* system (Mission, Electronics, Flight Performance & Propulsion, Structures & Materials). Responsible subsystems for each of these risks are identified between brackets behind them. As the list given here is an updated version of the previous list in the Baseline and Mid-term reports, refer to these reports for more elaborate explanation of each risk.

12.1.1 Mission

Mission-related risks which are not directly related to the *BirdPlane*'s subsystems, but affects the general operation of the mission are listed below.

1. Outdoor operation of the mission is deemed as an illegal activity
2. *BirdPlane* enters prohibited airspace
3. *BirdPlane* enters dangerous flight zones
4. Unable to locate migrating Barnacle Geese flock
5. Aggressive Barnacle Geese flock behavior
6. *BirdPlane* scares away the geese
7. Heavy weather conditions
8. Unable to take-off
9. Flock rendezvous fails (first trial)
10. Flock rendezvous fails (multiple times)
11. Geese land too early before the sufficient data acquisition

12.1.2 ELECTRONICS

The possible risks are identified for the Electronics element (Communication, Navigation, Robotics, Telemetry, Control, Command, and Power) and listed below.

12. Data link lost temporarily during cruise (Communication)
13. Data link lost permanently during cruise (Communication)
14. Main motor failure (Robotics)
15. Main wing twist servo failure (Robotics)
16. Malfunction of the detection of individual geese (Telemetry, Navigation)
17. Wing mechanism blockage (Robotics)
18. Tail mechanism (control surface) blockage (Robotics)
19. Malfunction of the mechanism sensors (Robotics)
20. Telemetry sensors issue(s) or measurement data partially lost/corrupted (Telemetry)
21. Geese split up / separate during cruise (Navigation)
22. Losing sight of the geese during cruise (Navigation)
23. Neck mechanism broken (Robotics)
24. Malfunction of the internal computer (Command)
25. Insufficient power level supplied (Power)
26. Insufficient duration of power supply (Power)
27. Sudden power shutdown (Power)

12.1.3 FLIGHT PERFORMANCE & PROPULSION

The risks that are relevant to the FPP element (Aerodynamics, Propulsion, Stability & Control) are stated below.

28. *BirdPlane* enters deep stall (Aerodynamics)
29. Wing damage (Aerodynamics, Stability & Control)
30. Wing broken (Aerodynamics, Stability & Control)
31. Tail damage (Aerodynamics, Stability & Control)
32. Tail broken (Aerodynamics, Stability & Control)
33. Insufficient lift and/or propulsion to keep up with the geese (Aerodynamics, Propulsion)

12.1.4 STRUCTURES & MATERIALS

In this section all risks that come from production, structures and materials are listed. The possible failures influence the structural integrity. Depending on which part of the structure breaks down, it can influence any of the incorporated subsystems. Note, that some of the risks related to the wing and tail damage are already listed in the previous Section 12.1.3, and not stated here.

34. Materials imperfections (Structure)
35. Fatigue (Structure)
36. Resonance (Structure, Telemetry)
37. Corrosion/degradation (Structure)
38. Water leaking (Structure, Electronics)
39. Plastic deformations/creep (Structure, Aerodynamics)

12.2 RISK EVALUATION

This section contains a risk map (Figure 12.1) which accounts for a qualitative and quantitative risk evaluation.

Catastrophic failure	24, 30, 32	17			
Abort mission, damaged		5, 14, 18, 27	3, 29, 31		
Abort mission, safely	2, 7, 11	10, 13, 23, 28	33, 16	6, 15, 25, 35, 38	
Perform majority of mission			19, 20, 37	36	26
Negligible severity		39		12, 9, 21, 22	34
Consequence, **Possibility**	**Very unlikely**	**Unlikely**	**Moderate**	**Likely**	**Very Likely**

Figure 12.1: Risk Map: Note, that Risk 1, 4, and 8 are not included here because their occurrence simply means that the mission cannot be realized from the start.

The risk map contains references to the risks stated in Section 12.1. Each of the referenced risks is placed in the cell which corresponds to its likelihood and level of severity. As can be expected from the gradient, the closer a risk is positioned to the top right corner (black section), the higher the threat of the risk.

The definitions of the *Consequence* classifications in the risk map are as follows:

- *Negligible severity*: A risk which generally causes no difficulty for the general operation of the full mission.
- *Perform majority of mission:* A risk which does not require the mission to be aborted, nevertheless part of the mission can not be performed.
- *Abort mission, safely:* A risk which is mainly related to the altitude maintaining devices. Such a risk will require the mission to be aborted, although (through fail-safe gliding mode) *BirdPlane* can still be recovered safely.
- *Abort mission, damaged:* A risk which requires the *BirdPlane* mission to be aborted. Control and/or lift devices experience such difficulty that it is likely that *BirdPlane* will be damaged before recovery is possible.
- *Catastrophic failure:* A failure which will harm *BirdPlane* beyond possible refurbishing or recovery.

12.3 RISK MANAGEMENT

In order to achieve a reliable design, the risks of high threat must be dealt with throughout the entire design phase and process. In this section, possible minimization and mitigation methods are discussed for each risk, presented in Table 12.1.

Table 12.1: Risk management methods summarized

Risk No.	Minimization method	Mitigation method
1	Contact the authority/legal institute beforehand to avoid the risk of legal issue	-
2	Obtain the information about regulations and prohibited airspace	Abort mission by performing 180° turn [1]
3	Identify potential areas of risk in the vicinity of the expected flightpath (e.g. airports, tall buildings, etc.)	Abort mission by performing 180° turn [1]
4	Investigate the Barnacle Geese migration path	Cancel or postpone the take-off
5	Sufficient study on the Barnacle Geese behavior [2]	Immediately abort the mission safely
6	Sufficient study on the Barnacle Geese behavior [2]	-
7	Use weather forecast information	Abort the mission if considered as potential threat [3]
8	Perform tests and verification using the actual catapult [4]	Launch team stand by, and assist the take-off if necessary
9	Increase the margin of the power supply	Generate necessary peak power to follow and catch up the geese again
10	Increase the margin of the power supply	If recognized as an obstacle in completing the mission, abort the mission safely [3]
11	-	Abort the mission safely [3]
12, 13	Establish stronger data link, using more powerful communication devices	Use of autopilot [5]
14, 15	Verify the motor and servo actuation at various design torques	Abort the mission [3]
16	Perform extensive simulation, tests and verification in various possible conditions [6]	Abort the mission safely [3]
17, 18	Limit the complexity of the mechanism to increase the reliability	Abort the mission safely [3]
19	Perform tests and verification in various conditions	Use of redundant sensors
20	Perform tests and verification in various conditions	Use of redundant measuring instruments (if considered necessary)
21	Extensive simulation and tests of the navigational/guidance autopilot	Follow the group with higher flock density
22	Extensive simulation and tests of the navigational/guidance autopilot	Dead-reckoning [7]
23	Perform tests and verification in various conditions	Abort the mission safely [3]
24	Perform tests and verification in various conditions	-
25, 26	Increase the margin of energy storage	Abort the mission safely [3]
27	Perform tests and verification in various conditions	-
28	Introduce wing morphing, or use a safer airfoil	Switch to gliding mode to gain stability or to abort mission
29–32	Perform tests and verification in various conditions	Abort the mission[8]
33	Additional lift-/thrust-generating device, or consideration of various wing planform variation	Abort the mission safely[3]
34	Close inspection of materials to detect fatal imperfection	-
35, 36	Consideration of lower flapping frequency, or more rigid structures	-
37, 38	Consider materials with better corrosion-resistance characteristics, add layers of waterproof material, avoid heavy weather	Replacement of parts through frequent inspection and maintenance
39	Introduce safety margin in the structure stiffness	-

*** Annotations:**

1. The flight should be switched to a risk mitigation mode to revert the flight direction. Preferably, FPV radio control can be used if the data link is established throughout the entire flight course, such that the continuous transmission of the real-time video is feasible. Otherwise, an autonomous flight mode can be implemented in which *BirdPlane* performs 180° turn when receiving a simple signal input from the ground base.
2. In order to minimize and mitigate this risk, the social behavior of the geese should be studied thoroughly and the factors which might make the Barnacle Geese hostile, or scare them away must be considered and reflected in the design of *BirdPlane*. For example, if during the flight the geese distinguish their own kind from other birds by observing the flapping speed, or sound it makes, then *BirdPlane* should be designed to have a similar flapping speed and/or sound production (e.g. playing the recorded sound of geese).
3. Change the flight mode to the fail-safe gliding flight, so that *BirdPlane* can slowly descend until landing. After this premature abortion of the mission, *BirdPlane* can be located (using the GPS signal) and retrieved safely.
4. The take-off may be not possible if there is a defect in the initial launch system, or if there are unfavorable weather conditions, such as the wind speed/direction, or heavy weather. To minimize the risk caused by the defect in the initial launch system, the performance of catapult should be verified, and tested with *BirdPlane* beforehand. Also, it is important to design the structure of *BirdPlane* strong enough to be able to endure the load it would experience during the acceleration for launch.
5. In fact, the communication and control subsystem of *BirdPlane* is already designed such that the on-board autopilot takes over the control of the aircraft during the cruise and landing. Therefore, as long as the data link is established until the rendezvous, the risk of losing this link temporarily is not a serious issue. However, permanent loss of data link would be a serious problem because it will then be very difficult to retrieve *BirdPlane* after landing when GPS data is unavailable. Also, the flexibility of the operation reduces considerably if one entirely relies on the autopilot control, as direct transmission of control commands would not be possible.
6. A possible cause of this risk may be deterioration of the visual data caused by various factors (e.g. too heavy rain/snow/cloud/mist/etc.), or condensation on the camera lens or the *BirdPlane*'s nose. Such risk can be minimized through a thorough verification of the detection system in many plausible scenarios.
7. If *BirdPlane* loses sight of the geese temporarily, the autopilot should enable *BirdPlane* to fly in the same direction as before. This can be done by placing the next waypoint based on the extrapolation of the previous waypoints. However, if this situation continues over a certain period of time, then the autopilot should give the following commands: first, tilt the camera up and down to search for the flock. Second, correct the heading based on the expected trajectory of the geese. If *BirdPlane* still cannot detect the geese, the mission must be aborted safely.
8. Whether the *BirdPlane* mission can be aborted safely depends on the magnitude of structural damage on the wing or the tail. Safely ending of the mission is possible when minor damage occurs, because gliding flight may still be initialized. However, when for example the wing totally breaks, *BirdPlane* will enter an inevitable spiral leading to a catastrophic crash.

13 Project Follow-up

Finally, the future prospect of the project is deliberated in this final chapter. This chapter gives an overview of which design phases still need to be performed for the final *BirdPlane* product. An estimation of the amount of time is made for each phase and task and these are summarized in the Gantt chart.

The rest of this chapter will focus on the cost breakdown of *BirdPlane*, which includes the development, purchase and manufacturing costs. The Manufacturing itself will also be treated together with the assembly and integration planning. At last, the methods and procedures to be used for the verification and validation process is discussed.

13.1 Project Design & Development

In this chapter, the post-DSE project phases are indicated together with a block diagram, describing the logical order of the activities. Also, these post-DSE activities are planned with the estimation of the time required for each activity. This is presented in a Gantt chart.

13.1.1 Design Phases

The following main phases can be considered:

- *Detail design.* Further elaboration of the design has to be done for *BirdPlane* that was not able to be achieved during the ten weeks of the DSE. Detailed computational models can be used in this phase.
- *Design optimization.* Wind-tunnel experiments are performed in order to measure uncertain design characteristics (e.g. stability derivatives) and validate aerodynamic performance (e.g. lift, thrust and drag predictions). By applying this iterative process, the final design can be optimized.
- *Manufacturing prototype.* This phase consists of the production of all subsystems and integrating them to one complete working system.
- *Testing.* The final step before entering the market is to test *BirdPlane* for possible flaws and unforeseen issues which need to be solved.
- *Operations / Service.* Eventually after successful production and testing, the product (and service) can be introduced to the market. *BirdPlane* will be used for an actual operation of the mission.

Table 13.1 shows the phases stated above with their corresponding activities and the estimated time spent on each phase. It can be seen that the total time for the future development phases until the operations phase is 30 weeks. The biggest part is the detailed design, while the manufacturing and testing phases for example do not require as much time.

Each phase with its described activities can be visualized in a flow block diagram as seen in Figure 13.1. Iterative processes can be seen in this flow diagram as well as the development logic.

13.1.2 Project Planning

The timing of the rest of the project can best be represented graphically to show the timescale and interdependence between the tasks. In Figure 13.2, a Gantt Chart is presented showing the activities planned after the DSE in a time-wise breakdown. All remaining design phases are given with their allocated time.

The smallest time scale given in this Gantt chart is a working week of five days. All tasks defined have thus been assigned at least a week. If a certain tasks turns out to require less time, the next one can already be started.

Table 13.1: Post-DSE phases

Phase	Duration (weeks)	Activities
Detail design	15	Perform detailed research Create computational models Perform detailed analysis Finalize design Compose Technical Design Report
Design optimization	5	Manufacture wind-tunnel models Perform tests Analyze data Optimize design Reporting
Manufacturing prototype	5	Manufacture subsystems Subsystem integration / assembly
Testing	5	Perform full scale tests Observe and process performance Optimization if required Documentation
Operations / services	-	Find contractors Setup contracts Start operations
Total	**30**	-

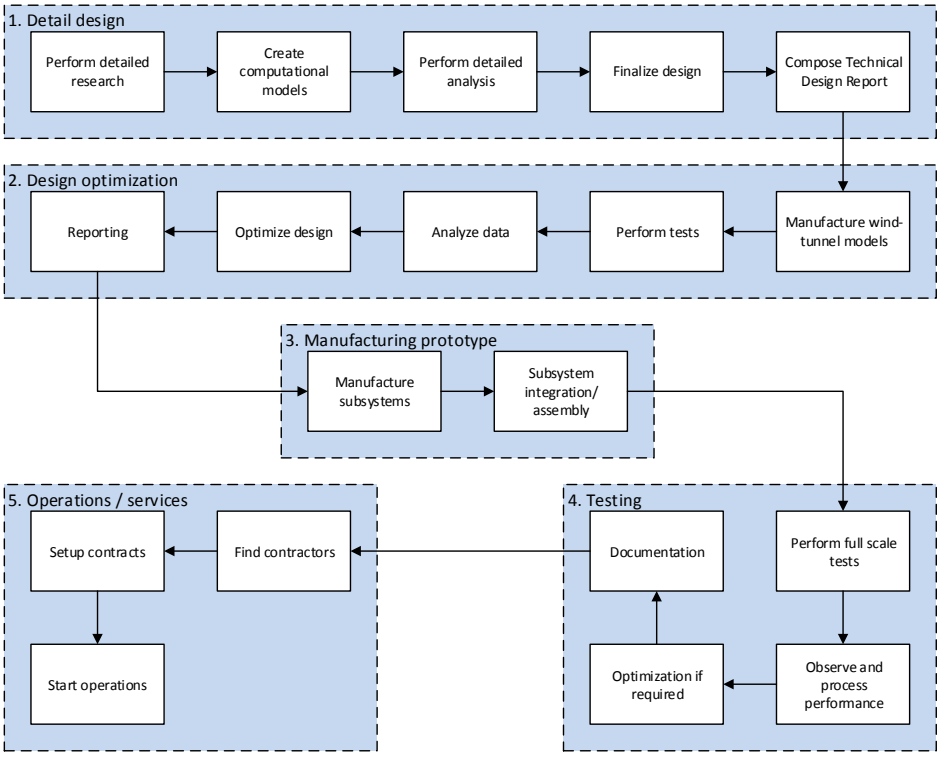

Figure 13.1: Block Diagram of the post-DSE activities

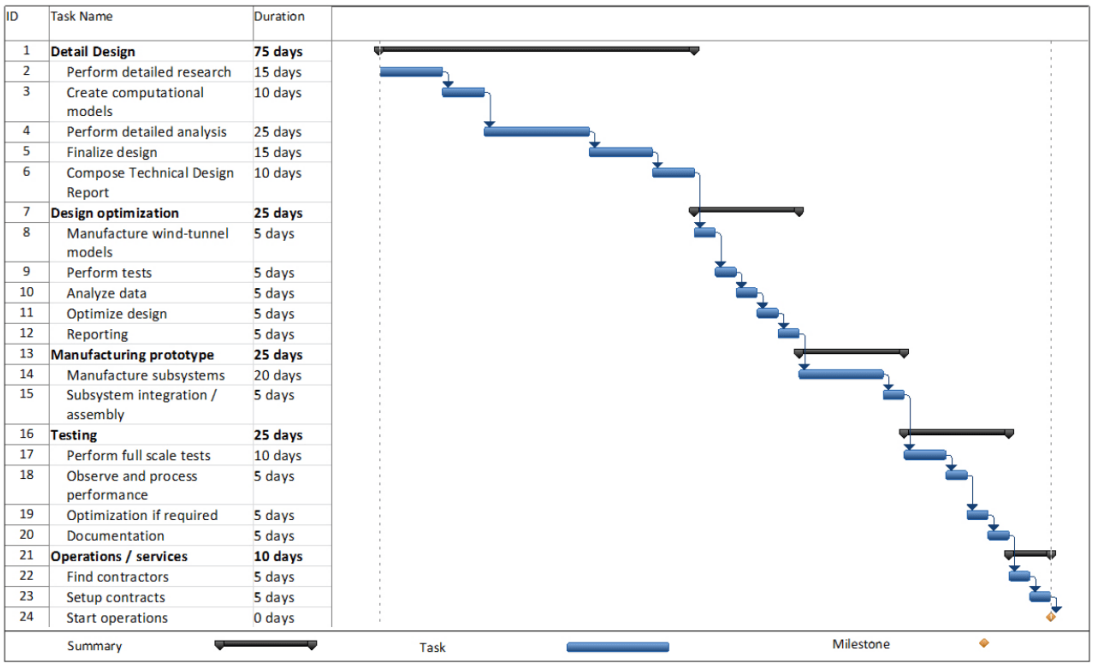

ID	Task Name	Duration
1	**Detail Design**	**75 days**
2	Perform detailed research	15 days
3	Create computational models	10 days
4	Perform detailed analysis	25 days
5	Finalize design	15 days
6	Compose Technical Design Report	10 days
7	**Design optimization**	**25 days**
8	Manufacture wind-tunnel models	5 days
9	Perform tests	5 days
10	Analyze data	5 days
11	Optimize design	5 days
12	Reporting	5 days
13	**Manufacturing prototype**	**25 days**
14	Manufacture subsystems	20 days
15	Subsystem integration / assembly	5 days
16	**Testing**	**25 days**
17	Perform full scale tests	10 days
18	Observe and process performance	5 days
19	Optimization if required	5 days
20	Documentation	5 days
21	**Operations / services**	**10 days**
22	Find contractors	5 days
23	Setup contracts	5 days
24	Start operations	0 days

Figure 13.2: Project Gantt Chart of the post-DSE activities

13.2 COST BREAKDOWN

The tasks that will be needed in order to finish the design and produce *BirdPlane* have been discussed in Section 13.1. All these tasks have costs, and there are many additional expenses that are not directly related to the work flow, but still need to be covered . This section will present a breakdown of the costs by arranging them in different categories. The breakdown is illustrated in Figure 13.3.

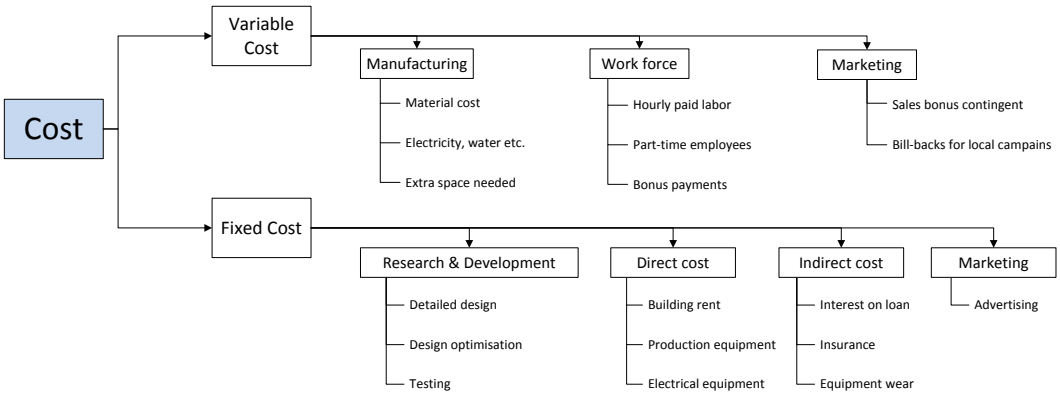

Figure 13.3: Cost breakdown structure

On the highest level, cost can be broken down into fixed cost and variable cost. Fixed cost are the expenses that do not change with the sales volume, i.e. no matter how many items will be sold, these costs are always the same. Variable cost, on the other hand, changes with the sales volume, i.e. selling zero items also makes zero variable cost. This assumes that production only starts once the order is received.

13.2.1 FIXED COST

The fixed expenditures can again be broken down into several components.

Research & Development As mentioned in the previous section, the design of *BirdPlane* has not yet come to an end as the detailed design of all subsystems is yet to be done. Once the design is final and the first prototype is

built, a phase of testing and consequent design optimization will follow. All such activities need to be completed before the first *BirdPlane* can be delivered to the customer which makes these costs fixed.

Marketing Marketing is a part of both variable and fixed cost. The fixed cost part is mostly the advertisement of the product. The product and service should be properly advertised, so as to increase the awareness of the product and initiate the demand.

Next, a distinction can be made between the direct cost, those that directly translate into something of value, and the indirect cost, cost which are unavoidable but do not have any direct real-world value. As marketing and R&D are large factors they were considered outside these categories, but could be classed as indirect cost.

Direct cost In order to be able to design and produce *BirdPlane*, some facilities are required. This includes a building in which work-phases can take place, the manufacturing equipment and other office equipment.

Indirect cost Lastly, some additional indirect costs need to be considered. This includes the interest that is to be paid on the loan which will probably be required to start up the production process. Furthermore, insurances on the building and equipment will need to paid. Additionally the equipment will have wear, and hence, its value will also decrease, which is considered as the depreciation cost.

13.2.2 VARIABLE COST

Apart from the fixed cost, some variable costs could be identified.

Manufacturing The manufacturing cost consists of the material cost, labor costs which is covered as a branch, and the cost for electricity, water and other resource costs. At high volume production, it could be possible that additional space is needed or tasks could be assigned to external companies which introduces additional expenses.

Work force The labor cost is a substantial fraction of the product cost, especially within an European country. At high volumes, additional part-time employees could be needed. Also, the bonus payments to the employees may be considered during the winnings.

Marketing Finally, some marketing strategies could involve variable marketing costs such as discounts for high volume or local discounts to increase sale volume.

13.2.3 ADDITIONAL

Section 7.3 has already proposed numbers for the fixed cost and variable costs that could be tolerated while still being profitable. A more detailed analysis of the exact cost goes beyond the scope of this phase of the project. The following will quickly analyze what would be required to assess the cost.

The manufacturing cost are mostly composed of the material and electrical component costs, as well as the labor cost. A detailed list of materials and components with list prices is thus required, which creates difficulties as some materials chosen are not yet commercially available, like the self-healing rubber or the prototype Lithium-sulfur battery that is used for the design. Furthermore, the production plan needs to define an exact amount of work hours to calculate the labor cost.

As the target markets are global, marketing could most easily done through the internet. Figures on the advertisement prices would need to be compiled to estimate those costs.

From the production plan, a list of equipment could be derived which makes it possible to determine equipment cost. Also, the number of working hours combined with the expected sales volume will give an overview of the number of workers needed which in turn influences the type of building to be rented. A good location in terms of logistics would be desirable, but needs to be weighed off against location rent prices.

At this point many of these figures are still vague, and therefore, a detail cost budget could not be justified sufficiently. However, an estimation for the target cost is justified in Section 7.3, and used as the indicator for the maximum allowable cost.

13.3 MANUFACTURING, ASSEMBLY & INTEGRATION PLANNING

The Manufacturing, Assembly & Integration (MAI) plan of the final *BirdPlane* concept is presented in this chapter. The MAI plan gives a chronological outline of the activities required for production.

The MAI flow diagram is given in Figure 13.4. The production is branched in parallel sub-assemblies. These sub-assemblies can be done simultaneously, speeding up the manufacturing process. Connecting skin to the frame will be the last step of the production process. In this way, everything is still easily accessible until the final assembly step.

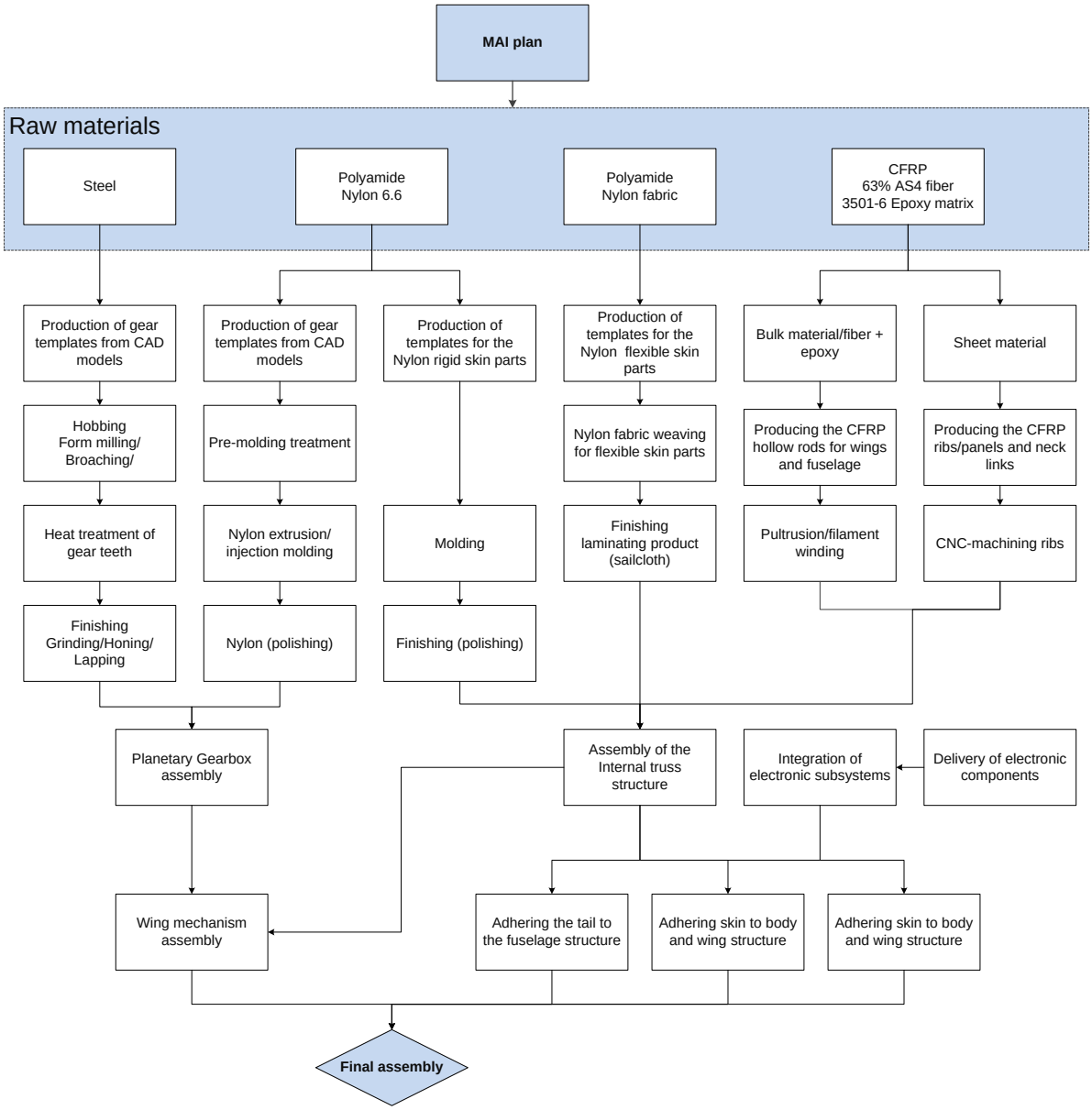

Figure 13.4: MAI flow chart

13.4 VERIFICATION & VALIDATION PROCEDURES

Verification and validation are important steps in a design process to assure that the system can perform the defined mission. Verification refers to the step of proving that the design solution performance complies with the defined requirements. In the validation step, it must be proven that *BirdPlane* accomplishes the intended purpose as expected by the stakeholders. These definitions comply with the official NASA definition.

In the conceptual and preliminary design phase, a number of requirements were continuously checked with the current design parameters for verification as shown in Section 11.2. For the further design and product implementation phases, a more detailed verification procedure is necessary. Furthermore, the validation methods need to be defined. The following subsections will define the procedures to be taken and how verification and validation will be planned. The approach is in accordance with [103].

VERIFICATION PROCEDURES

A large set of requirements were defined for *BirdPlane*. The subsystems need to be verified accordingly. In general, a number of different methods can be used for verification depending on the system and requirement to be verified. In the following those methods are defined and examples will be given how they are or could be implemented:

- **Inspection** - The design is reviewed by inspecting the compliance between design documentation and the requirements. As an example, it can be checked if the wing span of *BirdPlane* does not exceed the initially set maximum span.
- **Analysis** - Some requirements need to be verified by making a mathematical analysis of the subsystem. This can be done in form of direct computations or simulations. An example is the calculation of the forces during a flap cycle which verified the requirement that *BirdPlane* shall be able to fly. In the further design process, more advanced CFD or FEM methods can be utilized. Furthermore, the designed mission simulation will be used to verify and model the complete mission setup.
- **Demonstration** - Often it is not sufficient or possible to verify certain systems theoretically. Then a demonstration setup can be a good way for verification. The wing mechanism concept was for example demonstrated with the help of 3D rapid prototyping or the bird detection with help of a sample detection algorithm. More detailed demonstration of the bird detection is of interest for further stages.
- **Test** - Sometimes a representative model of a subsystem or several subsystems need to be tested under design conditions to verify compliance of certain requirements like power consumption. This is a more detailed verification technique which has not been utilized yet, but will be used in future development.

The choice of the verification strategy per requirement is to be defined in further design stages.

VALIDATION PROCEDURES

Also for the validation procedures, a number of different methods are available. The validation does not regard the requirements, but the actual product performance compliance with respect to the stakeholder demand. In the following different methods are presented:

- **End-to-End Information System Testing** - The compatibility of all information systems is tested in a full set-up. This can be done, when the ground equipment is fully built up and the *BirdPlane* electronic system is fully assembled.
- **Mission Scenario Tests** - The mission scenario is tested in flight-like conditions. This means that each flight phase is executed as realistically as possible. The hardware and software should be demonstrated without real timeline, and certain phases like the launch, or the flock rendezvous is demonstrated separately.
- **Operations Readiness Tests** - The End-to-End Information System Testing already proved the compatibility of all subsystems. Then an electronic mission simulation can be run to validate the interaction between the different systems according to the expectations. This test is done in real-time for the whole mission process.
- **Stress-Testing and Simulation** - In this validation step, the performance and robustness of the system is evaluated by testing fault conditions or long-time use to evaluate fatigue life.

VERIFICATION AND VALIDATION PLANNING

Planning of the verification and validation tasks before start is important to achieve the desired outcome: 1) The verification or validation objective needs to be defined. 2) One of the previously defined methods is chosen to achieve the defined objective. 3) Afterwards, all required inputs and outputs need to be determined that are needed to execute the method or expected from it. 4) The process is planned in detail according to the method. 5) The plan is documented and should be discussed and iterated with others. 6) The Verification or Validation activity is executed. 7) Lastly, the result is documented and the process should be iterated if necessary.

14 Conclusion

Ten weeks ago a group of 10 Aerospace Bachelor students accepted the *BirdPlane* challenge. Confronted with seemingly endless stumbling blocks on their journey, those ten students are now proud to conclude the project as the authors of this report with a cutting-edge design. Countless innovative solutions were found to reach and exceed the expectations and qualify for future tasks.

BirdPlane has the potential to become a milestone in the development of bird-like UAVs. By careful analyses of Barnacle Goose flight behavior, their flight mechanics could be decrypted and modeled with help of an advanced aerodynamic simulation. A sophisticated light-weight mechanism allows to mimic the bird-mechanics in detail by implementing vertical flapping, span-wise folding and variable wing twisting as Barnacle Geese do it in cruise flight. The *BirdPlane* flight mechanism allows for unseen efficiencies and flight durations in this UAV class. Stability and control are guaranteed with a unique fanning and rotatable tail inspired by nature, decreasing drag compared to conventional designs and allowing high maneuverability.

A state-of-the art camera system providing full-HD footage and stereoscopic thermal pictures is used to gather scientific data, but also to implement a precise in-flight bird tracking system for autonomous control. Key to the usability of the video footage is the camera stabilization. Again the geese provided an answer to this problem: by means of an iso-elastic link the motion of body and head are decoupled and hence the camera is stabilized, which was proven by a prototype.

The long mission range induced constraints on the communication link of *BirdPlane*. Artificial intelligence is implemented to provide the *BirdPlane* with sufficient autonomy to cruise by itself. The autopilot is able to perform the whole mission from rendezvous to landing and cope with different scenarios without interaction from ground. Therefore, it makes use of manifold measurements to constantly keep track of its own position and attitude and its environment. The mission control itself is realized in a sophisticated mission software, a first version of which serves for mission simulation at the current stage.

With the detailed performance analysis conducted the design outcome has proven to exceed the initial expectations in many subjects. With existing materials and technologies all important requirements have been fulfilled. Only a few requirements had to be flexed, witch could be done without sacrificing significant performance of the final design. In the iterative process, in which sophisticated functions and performance where traded for their weight and power, the limits of what is possible with state-of-the-art technologies were investigated. This lead to a progressive final design that performs all its functions without exceeding the weight and power budget.

Sufficient weight margins are available and conservative estimates of the power consumption are likely to lead to extra safety margins for the power source. Hence, *BirdPlane* is designed to maximum compliance of the pre-defined expectations as agreed upon with the customers. Furthermore, the market analysis gave insight in the future market possibilities for *BirdPlane* in the fields of research and surveillance with its superior capabilities and performance and the market interest in the *BirdPlane* related innovations.

This concludes the preliminary design of *BirdPlane* and the work of DSE group 6 within the TU Delft Aerospace curriculum. Further design recommendations are given in the following chapter. For the future process the next steps are already planned including the Verification and Validation procedures and a draft of the manufacturing plan is presented. The team is highly motivated to take also the next steps in the realization of *BirdPlane* depending on the success and public perception.

15 RECOMMENDATIONS

In Chapter 10 and Chapter 13 several aspects have already been mentioned that could be addressed during further development of the *BirdPlane*. Of course a detailed design and testing phase for all elements is required before *BirdPlane* can be finalized as a product. Moreover some design options have been discarded during the preliminary design because they were too complex to investigate to a sufficient detailed level. However a detailed analysis might show that they add value to the product. In the following shall give an overview of such potential features for future versions of *BirdPlane*.

Cam crank design The shapes and positions of the different components in the flapping mechanism were primarily obtained by trial and error. A cam crank was added to optimize the motion. Advanced calculation tools are available for designing cam cranks for a prescribed motion. The current mechanism causes the downstroke to be faster than the upstroke, while the opposite is required. This leads to large variations in motor speed. The tools could help to relieve stress from the motor by optimizing the cranks for the correct speeds.

Flapping angle The aerodynamic analysis showed that the angle ξ over which the wings of Barnacle Geese flap varies between the different flight modes for most efficient flight. With the current mechanism this angle is fixed and the only variables in the flapping motion are flapping frequency and twist angle. A mechanism has been investigated that shifts the position of the hinge point on the spar. This way the flapping angle ξ is varied by changing the arm driven by the crank. The mechanism was designed in such a way that both the hinge on the frame and on the spar move the same distance in and out, which results in constant span and no skin deformation. This system was discarded because the maximum achievable value of ξ was already required for cruise and the mechanism would unnecessarily be complicated. Time constrained the further investigation of this option so for the future a more detailed trade of between complexity and efficiency gain is recommended.

Feathers A very bird-like feature that has been investigated only peripherally in the design of *BirdPlane* is the use of feathers. The limited time available did not allow for extended analysis of how feathers could be implemented (several MSc and Phd thesis could be focused merely on this topic). Feathers would impact many subsystems, not only structures and materials, but also the control and the complete aerodynamic analysis. A future design would mean quite some design changes, but could increase efficiency and would definitely increase the bird-like character of *BirdPlane*.

Feet Finally the implementation of static or adjustable/retractable feet is another bird-like feature which can be beneficial for the aerodynamic performance of *BirdPlane*. Birds use their feet for many functions as described in Section 10.1.2. The main advantages of feet are a significant increase in both turning and stability performance. The main disadvantage is the introduction of drag, especially with static feet. It would be more advantageous to implement feet that can be adjusted in a similar fashion as the rotatable tail. That way they could increase controllability and be retracted when not required to reduce the wetted surface. However this requires a mechanism which adds weight and complexity.

Following different birds The current *BirdPlane* is designed with a strong focus on Barnacle Geese. This limits the use of *BirdPlane* for research of other birds. Bird research groups that have been contacted for the mission definition and market analysis indicated that demand would be larger if research could be done on different bird species. Especially the interest in research on small birds is high. To increase the market potential it can be investigated what changes or scaling can be applied to *BirdPlane* to make it suitable for different missions.

Autonomy Currently it is still intended to remote-control *BirdPlane* during the take-off and rendezvous phase of the mission. This requires an operator to be on-site and available whenever a mission opportunity arises due to passing flocks. By making *BirdPlane* even more autonomous, this need could be nullified, decreasing operation costs and increasing mission flexibility.

REFERENCES

[1] van der Burgt, J. S., Hameeteman, K. J. M., Harms, J., Lee, S. H., Mikoyan, I. A., Risseeuw, D., Schoneveld, W. J., Telgen, B., Voogt, N. A., and Westbroek, W., *BirdPlane Midterm Report*, May 2014.

[2] Le, S., "Barnacle Goose population from Nova Zembla in winter quarters, Zeeland, Netherlands," 2010, http://ibc.lynxeds.com/photo/barnacle-goose-branta-leucopsis/population-nova-zembla-last-weeks-winter-quarters, retrieved on 23-05-2014.

[3] Planet of Birds, "Barnacle Goose (Branta leucopsis)," http://www.planetofbirds.com/anseriformes-anatidae-barnacle-goose-branta-leucopsis,retrieved on 21-05-2014.

[4] Ekin, U., "Branta leucopsis, barnacle goose," Animal Diversity Web, University of Michigan, http://animaldiversity.ummz.umich.edu/site/accounts/information/Branta_leucopsis.html, retrieved on 13-05-2014.

[5] Pennycuick, C. et al., "A trial of a non-statistical computer program for monitoring fuel reserves, response to wind and other details from GPS tracks of migrating geese," *Journal of Ornotholigy*, 2010.

[6] Nijland, D., "Overwinterende ganzen in Nederland," 2010, Vogelbescherming Nederland.

[7] Eichhorn, G. et al., "Tracking Fall stopovers in Russian Barnacle Geese: When, Where and How Long?" Conferene poster, http://www.antarctica.ac.uk/engineering/posters2.php, retrieved on 20-05-2014.

[8] Black, J. and Owen, M., "Agonistic behavior in barnacle goose flocks," *Animal Behavior*, Vol. 37, 1989, pp. 199–209.

[9] Kahlert et al., "Factors affecting the flight altitude of migrating waterbirds in Western Estonia," *Ornis Fennica*, Vol. 89, 2012.

[10] Butler, P. and Woakes, A., "Heart rate, respiratory frequency, and wing beat frequency of free flying Barnacle Geese Branta Leucopsis," *Journal of Experimental Biology*, Vol. 85, 1980, pp. 213–226.

[11] Butler P. J., W. A. J. and M., B. C., "Behaviour and physiology of Svalbard Barnacle Geese Branta leucopsis during their autumn migration," *Journal of kah Biology*, Vol. 29, 1998, pp. 536–545.

[12] Jourdan, D., *Trajectory Design and Vehicle Guidance for a Mid-Air Rendezvous between Two Autonomous Aicraft*, Master's thesis, Massachusetts Institute of Technology, 2003.

[13] MaxBotix, "I2CXL-MaxSonar-WR/WRC Series," manual, http://www.maxbotix.com/documents/I2CXL-MaxSonar-WR_Datasheet.pdf, retrieved on 18-06-2014.

[14] Klees, R. and Dwight, R. P., *Applied Numerical Analysis*, June 2012.

[15] Fiedler, G., "Integration basics for game physics," September 2006, http://gafferongames.com/game-physics/integration-basics/, retrieved on 17-06-2014.

[16] Fourment, M. and Gillings, M., "A comparison of common programming languages used in bioinformatics," *BMC Bioinformatics*, Vol. 9, No. 1, 2008, pp. 82.

[17] Prechelt, L., "An empirical comparison of seven programming languages," *Computer*, Vol. 33, No. 10, Oct 2000, pp. 23–29.

[18] Pemmaraju, V., "The Three Simple Rules of Flocking Behaviors: Alignment, Cohesion, and Separation," January 2013, http://gamedevelopment.tutsplus.com/tutorials/the-three-simple-rules-of-flocking-behaviors-alignment-cohesion-and-separation--gamedev-3444, retrieved on 20-06-2014.

[19] Djexplo, "Illustration of geographic latitude and longitude of the earth," May 2011, Wikimedia Commons.

[20] Kühn, S., "a Mercator projection map with Tissot's indicatrices," December 2004, Wikimedia Commons.

[21] Gale, G., "The Greenland Problem And Playing With Mercator's Map," January 2013, http://www.vicchi.org/2013/01/31/the-greenland-problem-and-playing-with-mercators-map/, retrieved on 11-06-2014.

[22] OpenStreetMap, "Slippy Map," September 2013, http://wiki.openstreetmap.org/wiki/Slippy_Map, retrieved on 17-06-2014.

[23] Microsoft, "Bing Maps Tile System," February 2009, http://msdn.microsoft.com/en-us/library/bb259689.aspx, retrieved on 15-06-2014.

[24] Robers, A., "By the numbers: Drones," May 2013, http://edition.cnn.com/2013/04/05/politics/drones-btn/, retrieved on 16-06-2014.

[25] AERONAUTICS, "Orbiter 2 Mini UAS," 2013, http://www.aeronautics-sys.com/_Uploads/dbsAttachedFiles/OrbiterBrochure_2013A.pdf, retrieved on 20-05-2014.

[26] Eli Military Simulations, "Unmanned Aerial System SWAN III," 2012, http://www.eli.ee/products/7/unmanned-aerial-system-swan-ii, retrieved on 20-05-2014.

[27] AeroVironment, "UAS: RQ-20A Puma AE," 2014, http://www.avinc.com/uas/small_uas/puma/, retrieved on 20-05-2014.

[28] Zolfagharifard, E., "Is this the ultimate bird of prey?" http://www.dailymail.co.uk/sciencetech/article-2335600/Robotic-bird-used-future-war-agent-Robo-Ravens-extreme-aerobatics-fool-real-birds-prey.html, retrieved on 23-06-2014.

[29] Festo, "An interview with the engineer behind the man-made Smartbird," http://blog.grabcad.com/blog/2011/06/14/festo-smartbird/, retrieved on 23-06-2014.

[30] Stoll, W., "SmartBird, Aerodynamic lightweight design with active torsion," Esslingen, Germany, 2011.

[31] Clear Flight Solutions, "Robird," http://clearflightsolutions.com/.

[32] RoboRaven official blog, "Roboraven," http://unorthodoxideas.blogspot.nl/search?q=robo+raven, retrieved on 16-05-2014.

[33] Lucintel Corporate Briefing, "Growth Opportunity in Global UAV Market," March 2011, http://www.lucintel.com/LucintelBrief/UAVMarketOpportunity.pdf, retrieved on 12-05-2014.

[34] UPI, "Finland picks Israeli UAV," May 2012, http://www.upi.com/Business_News/Security-Industry/2012/05/04/Finland-picks-Israeli-UAV/UPI-45751336129911/, retrieved on 19-06-2014.

[35] Business Week, "Volkswagen Pockets $23,000 When You Buy That New Porsche," March 2014, http://www.businessweek.com/articles/2014-03-13/volkswagen-pockets-23-000-when-you-buy-that-new-porsche, retrieved 19-06-2014.

[36] Gill, E., "Systems Engineering Methods lecture slides," February 2012.

[37] Ho, S. et al., "Unsteady aerodynamics and flow control for flapping wing flyers," *Progress in Aerospace Sciences*, Vol. 39, No. 8, 2003, pp. 635 – 681.

[38] Räbiger, H., *Wie Ornithopter Fliegen, Aerodynamik und Dynamik grosser Schlagflügelmodelle*, 2011, www.ornithopter.de, retrieved on 15-05-2014.

[39] Liu, T., "Avian Wings," *AIAA*, Vol. 24, No. 1, July 2004.

[40] Thomas, A. and Taylor, G., "Animal Flight Dynamics I. Stability in Gliding Flight," *Journal of Theoretical Biology*, Vol. 212, 2001, pp. 399–424.

[41] Thomas, A. and Taylor, G., "Animal Flight Dynamics II. Longitudinal Stability in Flapping Flight," *Journal of Theoretical Biology*, Vol. 214, 2002, pp. 351–370.

[42] Mulder, J. et al., "Flight Dynamics - Lecture Notes," March 2013.

[43] Nelson, R. C., *Flight Stability and Automatic Control*, McGRAW-Hill, 2nd ed., 1998.

[44] Sachs, G., "Why Birds and Miniscale Airplanes Need No Vertical Tail," *Journal of Aircraft*, Vol. 44, No. 4, August 2007.

[45] Taylor, G. K. and Thomas, A., *Evolutionary Biomechanics*, January 2014.

[46] Caughey, D. A., "Introduction to Aircraft Stability and Control - Course Notes for M&AE 5070," 2011, https://courses.cit.cornell.edu/mae5070/Caughey_2011_04.pdf, retrieved on 12-06-2014.

[47] BBC, "Earthflight," 2011, http://www.youtube.com/watch?v=uk_20kKvGrA, retrieved on 30-6-2014.

[48] Hakola, A., "Barnacle Goose, Branta Leucopsis," April 2011, http://500px.com/photo/63259953/barnacle-goose-branta-leucopsis-by-arto-hakola, retrieved on 10-06-2014.

[49] Townsend, C. W., *The Position of Birds' Feet in Flight*, Vol. 26, April 1909.

[50] Pennycuick, C. J., "A Wind-Tunnel Study of Gliding Flight in the Pigeon Columba Livia," *The Journal of Experimental Biology*, Vol. 49, April 1968, pp. 509–526, http://jeb.biologists.org/content/49/3/509.short, retrieved on 11-06-2014.

[51] Carbonwinkel, http://www.carbonwinkel.nl/nl/carbon-producten/55444563-carbon-buis-gewikkeld-vinylester.html, retrieved on 18-06-2014.

[52] Prajer, M. et al., "Compartmented fibres: the concept of multiple self-healing in advanced fibre composites," *ICSHM2013*, Vol. 4, 2 2013.

[53] Leibler, L. et al., "Self-healing and thermoreversible rubber from supramolecular assembly," *Nature*, Vol. 451, 1 2008, pp. 977–980.

[54] Hacker, "A20-12 XL EVO," http://www.hacker-motor-shop.com/e-vendo.php?shop=hacker_e&SessionId=&a=article&ProdNr=97800010&t=3&c=5396&p=5396, retrieved on 20-06-2014.

[55] Micromo Electronics, "DC Motor Calculations," http://www.micromo.com/motor-calculations, retrieved on 20-06-2014.

[56] Hacker, "Speed Controller X-30 Pro with BEC," http://www.hacker-motor-shop.com/e-vendo.php?shop=hacker_e&SessionId=&a=article&ProdNr=87100003&t=7&c=46&p=46,retrieved on 20-06-2014.

[57] Blue Bird Technology, "Bluebird Midi-Servo BMS-390," http://www.conrad.de/ce/de/product/275487/Bluebird-Midi-Servo-BMS-390-DMH-Doppelt-kugelgelagert-Getriebe-Metall-JR,retrieved on 20-06-2014.

[58] Robotship, "HS-35HD Micro Servo Motor," http://www.robotshop.com/en/hitec-hs-35d-micro-servo-motor.html, retrieved on 20-06-2014.

[59] Song, M. et al., "A Long-Life, High-Rate Lithium/Sulfur Cell: A Multifaceted Approach to Enhancing Cell Performance," Tech. rep., Lawrence Berkeley National Laboratory, November 2013.

[60] Zhang, Y. et al., "Graphene Oxide Sulfur Nanocomposite Cathode for High-Energy, Low-Weight Lithium Sulfur Batteries," Tech. rep., University of California-Berkeley, 2012, http://ei.haas.berkeley.edu/c2m/pdf/MarketReports/2012/Lithium%20Sulfur%20Battery.pdf, retrieved on 23-05-2014.

[61] Allegro Microsystems, "ACS761 Datasheet," http://www.allegromicro.com/en/Products/Current-Sensor-ICs/High-Side-Hot-Swap-Hall-Effect-Based-Current-Monitor-IC/ACS761.aspx, retrieved on 20-05-2014.

[62] ImmersionRC, "Long-range FPV," http://www.immersionrc.com/, retrieved on 18-06-2014.

[63] 4Gdekking.nl, "Vergelijk 4G dekking van alle providers," http://www.4gdekking.nl/, retrieved on 18-06-2014.

[64] Libeliul, "3G Shield," http://www.cooking-hacks.com/documentation/tutorials/arduino-3g-gprs-gsm-gps, retrieved on 18-06-2014.

[65] Dokter, A. et al., "Bird detection by operational weather radar," Vol. WR 2009-06, 2009, Scientific report.

[66] MARSHALL-ELECTRONICS, "2 Megapixel HD-SDI 1/3" CMOS Board Camera," http://www.marshall-usa.com/optical/cameras/board_color/V-1290.php, retrieved on 16-06-2014.

[67] MARSHALL-ELECTRONICS, "2 MP VISIBLE - IR corrected miniature lense," http://www.marshall-usa.com/optical/lenses/IR-corrected/pdf/V-4702_9-2MP-VIS-IR_DWG.pdf, retrieved on 16-06-2014.

[68] Richards, A., "Cooled versus uncooled cameras for long range surveillance," *Technical Note - FLIR Commercial Vision Systems*, 2009.

[69] FLIR, "Quark 2 Uncooled Long-Wavelength Infrared (LWIR) Camera Cores," http://www.flir.com/cvs/cores/view/?id=51266&collectionid=549&col=51275, retrieved on 16-06-2014.

[70] DIYDRONES, "Fiberglass Pan-Tilt Camera Mount for FPV," http://diydrones.com/profiles/blogs/hobby-king-has-a-new, retrieved on 16-06-2014.

[71] MARSHALL-ELECTRONICS, "Single Chip Color CMOS Video Cameras With 251K Active Pixels," http://www.marshall-usa.com/optical/cameras/cmos/v-xa095.php, retrieved on 17-06-2014.

[72] ZTEX, "USB-FPGA Module 2.16: Artix 7 XC7A200T FPGA Board with USB 2.0," http://www.ztex.de/usb-fpga-2/usb-fpga-2.16.e.html, retrieved on 17-06-2014.

[73] Zarandy, A. et al., "A five camera vision system for UAV visual attitude calculation and collision warning," http://workshops.acin.tuwien.ac.at/ICVS/downloads/Oral5_49_camera_vision_system_Akos_Zarandy.pdf, retrieved on 17-06-2014.

[74] Godbehere, A., "Visual Tracking of Human Visitors under Variable-Lighting Conditions for a Responsive Audio Art Installation," *American Control Conference (ACC)*, June 2012, pp. 4305 – 4312.

[75] Bradski, G., editor, *Real time face and object tracking as a component of a perceptual user interface*, No. 19-21. Fourth IEEE Workshop on Applications of Computer Vision, Oct 1998, pp.214,219.

[76] Kolsch, M., *Vision based hand gesture interfaces for wearable computing and virtual environments,* 1st ed., August 2004, Doctoral Dissertation, University of California.

[77] Gonzalez, R., *Digital Image Processing*, 3rd ed., August 2007.

[78] Viola, P. and Jones, M., "Visual Tracking of Human Visitors under Variable-Lighting Conditions for a Responsive Audio Art Installation," *Computer Vision and Pattern Recognition*, Vol. 1, 2001, pp. I–511–I–518.

[79] Lieb, D., "Tracking Multiple Moving Objects from an Autonomous Helicopter," *Stanford Artificial Intelligence Laboratory*, 2004.

[80] Bouguet, J., "Pyramidal Implementation of the Affine Lucas Kanade Feature Tracker," *Stanford Microprocessor Reasearch Labs*, 2001.

[81] Bouguet, J., "Two-Frame Motion Estimation Based on Polynomial Expansion," *13th Scandinavian Conference, SCIA 2003 Halmstad,* June 2003, pp. 363–370.

[82] Mrovlje, J., "Distance measuring based on stereoscopic pictures," *9th International PhD Workshop on Systems and Control: Young Generation Viewpoint*, October 2008, pp. 127–132.

[83] Astrom, K. J. et al., *Feedback Systems: an Introduction for Scientists and Engineers*, Princeton University Press, 2012, Version v2.11b.

[84] Paparazzi UAV, "Theory of Operation," `http://wiki.paparazziuav.org/wiki/Theory_of_Operation`, retrieved on 18-06-2014.

[85] Lim, H. et al., "Build your own quadropter," *IEEE ROBOTICS & AUTOMATION MAGAZINE*, September 2012.

[86] Paparazzi UAV, "Control loops," `http://wiki.paparazziuav.org/wiki/Control_Loops`, retrieved on 18-06-2014.

[87] Mathworks, "Control tutorial - Introduction: PID Controller Design," `http://ctms.engin.umich.edu/CTMS/index.php?example=Introduction&section=ControlPID`.

[88] de l'Aviation Civile, E. N., *Excerpt from Intelligent Surveillance with MAVs R&D 1042-AM-01 Paparazzi User's manual*, Paparazzi UAV, February 2008.

[89] Paparazzi UAV, "INS subsystem," `https://wiki.paparazziuav.org/wiki/Subsystem/ins`, retrieved on 25-06-2014.

[90] Paparazzi UAV, "AHRS subsystem," `https://wiki.paparazziuav.org/wiki/Subsystem/ahrs`, retrieved on 25-06-2014.

[91] Higgins, "A Comparison of Complementary and Kalman Filtering," *IEEE TRANACTIONS ON AEROSPACE AND ELECTRONIC SYSTEMS*, 1975.

[92] Butterworth, "On the Theory of Filter Amplifiers," *Wireless Engineer*, Vol. 7, 1930.

[93] Baek, S. S., *Autonomous Ornithopter Flight with Sensor-Based Behavior*, Ph.D. thesis, University of California at Berkeley, May 2011.

[94] UAV, P., "Data Logger," `http://wiki.paparazziuav.org/wiki/Data_Logger`, retrieved on 23-06-2014.

[95] Fyetech, "Manual - FY-41AP Autopilot System," `http://shop.fyetech.com/dl/fy41ap1.pdf`, retrieved on 15-05-2014.

[96] OpenAltimeter, "Small scale pressure altimeter," `http://openaltimeter.org/`, retrieved on 15-05-2014.

[97] Famosa Studio, "DHT22 - temperature and humidty sensor," `http://www.famosastudio.com/download/datasheet/DHT22.pdf`, retrieved on 15-05-2014.

[98] NATIONAL CONTROL DEVICES, LLC, "CdS Photoconductive Photocells," `http://www.controlanything.com/Relay/Device/PDV-P8001`, retrieved on 15-05-2014.

[99] van der Burgt, J. S., Hameeteman, K. J. M., Harms, J., Lee, S. H., Mikoyan, I. A., Risseeuw, D., Schoneveld, W. J., Telgen, B., Voogt, N. A., and Westbroek, W., *BirdPlane Baseline Report*, May 2014.

[100] *IEEE Standard Computer Dictionary*, Vol. 610, 1990, The Institute of Electrical and Electronics Engineers.

[101] Roland, H. and Moriarty, B., *System Safety Engineering and Management*, 2nd ed., November 1990, John Wiley & Sons.

[102] ITEM Software, "Reliability Prediction Basics," 2007, `http://www.reliabilityeducation.com/ReliabilityPredictionBasics.pdf`, retrieved on 21-05-2014.

[103] Eberhard Gill, T. H., "Verification and Validation for the Attitude and Orbit Control System," 2 2014, Lecture Notes.